Intergovernmental Oceanographic Commission

Workshop Report No. 58 - Supplement

Second International Tsunami Workshop on the Technical Aspects of Tsunami Warning Systems, Tsunami Analysis, Preparedness, Observation and Instrumentation

Novosibirsk, USSR, 4-5 August 1989

Submitted Papers

UNESCO

IOC Workshop Reports

The Scientific Workshops of the Intergovernmental Oceanographic Commission are sometimes jointly sponsored with other intergovernmental or non-governmental bodies. In most cases, IOC assumes responsibility for printing, and copies may be requested from:

Intergovernmental Oceanographic Commission - UNESCO
Place de Fontenoy, 75700 Paris, France.

No.	Title	Languages
1	CCOP-IOC, 1974, Metallogenesis, Hydrocarbons and Tectonic Patterns in Eastern Asia (Report of the IDOE Workshop on); Bangkok, Thailand, 24-29 September 1973 UNDP (CCOP), 138 pp.	E (out of stock)
2	CICAR Ichthyoplankton Workshop, Mexico City, 16-27 July 1974 (UNESCO Technical Paper in Marine Sciences, No. 20).	E (out of stock) S (out of stock)
3	Report of the IOC/GFCM/ICSEM International Workshop on Marine Pollution in the Mediterranean, Monte Carlo, 9-14 September 1974.	E, F, S (out of stock)
4	Report of the Workshop on the Phenomenon known as "El Niño", Guayaquil, Ecuador, 4-12 December 1974.	E (out of stock) S (out of stock)
5	IDOE International Workshop on Marine Geology and Geophysics of the Caribbean Region and its Resources, Kingston, Jamaica, 17-22 February 1975.	E (out of stock) S
6	Report of the CCOP/SOPAC-IOC IDOE International Workshop on Geology, Mineral Resources and Geophysics of the South Pacific, Suva, Fiji, 1-6 September 1975.	E
7	Report of the Scientific Workshop to Initiate Planning for a Co-operative Investigation in the North and Central Western Indian Ocean, organized within the IDOE under the sponsorship of IOC/FAO(IOFC)/UNESCO/EAC, Nairobi, Kenya, 25 March-2 April 1976.	E, F, S, R
8	Joint IOC/FAO (IPFC)/UNEP International Workshop on Marine Pollution in East Asian Waters, Penang, 7-13 April 1976.	E (out of stock)
9	IOC/CMG/SCOR Second International Workshop on Marine Geoscience, Mauritius, 9-13 August 1976.	E, F, S, R
10	IOC/WMO Second Workshop on Marine Pollution (Petroleum) Monitoring, Monaco, 14-18 June 1976.	E, F, S (out of stock) R
11	Report of the IOC/FAO/UNEP International Workshop on Marine Pollution in the Caribbean and Adjacent Regions, Port of Spain, Trinidad, 13-17 December 1976.	E, S (out of stock)
11 Suppl.	Collected contributions of invited lecturers and authors to the IOC/FAO/UNEP International Workshop on Marine Pollution in the Caribbean and Adjacent Regions, Port of Spain, Trinidad, 13-17 December 1976.	E (out of stock), S
12	Report of the IOCARIBE Interdisciplinary Workshop on Scientific Programmes in Support of Fisheries Projects, Fort-de-France, Martinique, 28 November-2 December 1977.	E, F, S
13	Report of the IOCARIBE Workshop on Environmental Geology of the Caribbean Coastal Area, Port of Spain, Trinidad, 16-18 January 1978.	E, S
14	IOC/FAO/WHO/UNEP International Workshop on Marine Pollution in the Gulf of Guinea and Adjacent Areas, Abidjan, Ivory Coast, 2-9 May 1978.	E, F
15	CPPS/FAO/IOC/UNEP International Workshop on Marine Pollution in the South-East Pacific, Santiago de Chile, 6-10 November 1978.	E (out of stock)
16	Workshop on the Western Pacific, Tokyo, 19-20 February 1979.	E, F, R
17	Joint IOC/WMO Workshop on Oceanographic Products and the IGOSS Data Processing and Services System (IDPSS), Moscow, 9-11 April 1979.	E
17 Suppl.	Papers submitted to the Joint IOC/WMO Seminar on Oceanographic Products and the IGOSS Data Processing and Services System, Moscow, 2-6 April 1979.	E
18	IOC/UNESCO Workshop on Syllabus for Training Marine Technicians, Miami, 22-26 May 1978 (UNESCO reports in marine sciences, No. 4, published by the Division of Marine Sciences, UNESCO)	E (out of stock), F, S (out of stock), R
19	IOC Workshop on Marine Science Syllabus for Secondary Schools, Llantwit Major, Wales, U.K., 5-9 June 1978 (UNESCO reports in marine sciences, No. 5, published by the Division of Marine Sciences, UNESCO).	E (out of stock), F, S, R, Ar
20	Second CCOP-IOC Workshop on IDOE Studies of East Asia Tectonics and Resources, Bandung, Indonesia, 17-21 October 1978.	E
21	Second IDOE Symposium on Turbulence in the Ocean, Liège, Belgium, 7-18 May 1979.	E, F, S, R
22	Third IOC/WMO Workshop on Marine Pollution Monitoring, New Delhi, 11-15 February 1980.	E, F, S, R
23	WESTPAC Workshop on the Marine Geology and Geophysics of the North-West Pacific, Tokyo, 27-31 March 1980.	E, R
24	WESTPAC Workshop on Coastal Transport of Pollutants, Tokyo, 27-31 March 1980.	E (out of stock)
25	Workshop on the Intercalibration of Sampling Procedures of the IOC/WMO UNEP Pilot Project on Monitoring Background Levels of Selected Pollutants in Open-Ocean Waters, Bermuda, 11-26 January 1980.	E (superseded by IOC Technical Series No. 22)
26	IOC Workshop on Coastal Area Management in the Caribbean Region, Mexico City, 24 September-5 October 1979.	E, S
27	CCOP/SOPAC-IOC Second International Workshop on Geology, Mineral Resources and Geophysics of the South Pacific, Nouméa, New Caledonia, 9-15 October 1980.	E
28	FAO/IOC Workshop on the effects of environmental variation on the survival of larval pelagic fishes, Lima, 20 April-5 May 1980.	E
29	WESTPAC Workshop on Marine biological methodology, Tokyo, 9-14 February 1981.	E
30	International Workshop on Marine Pollution in the South-West Atlantic Montevideo, 10-14 November 1980.	E (out of stock) S
31	Third International Workshop on Marine Geoscience, Heidelberg, 19-24 July 1982	E, F, S
32	UNU/IOC/UNESCO Workshop on International Co-operation in the Development of Marine Science and the Transfer of Technology in the context of the New Ocean Regime Paris, 27 September - 1 October 1982	E, F, S
32 Suppl.	Papers submitted to the UNU/IOC/UNESCO Workshop on International Co-operation in the Development of Marine Science and the Transfer of Technology in the Context of the New Ocean Regime Paris, 27 September-1 October 1982	E
33	Workshop on the IREP Component of the IOC Programme on Ocean Science in Relation to Living Resources (OSLR) Halifax, 26-30 September 1983	E
34	IOC Workshop on Regional Co-operation in Marine Science in the Central Eastern Atlantic (Western Africa) Tenerife 12-17 December 1983	E, F, S
35	CCOP/SOPAC-IOC-UNU Workshop on Basic Geo-scientific Marine Research Required for Assessment of Minerals and Hydrocarbons in the South Pacific Suva, Fiji, 3-7 October 1983	E
36	IOC/FAO Workshop on the Improved Uses of Research Vessels Lisbon, 28 May - 2 June 1984	E
36 Suppl.	Papers submitted to the IOC-FAO Workshop on Inproved Uses of Research Vessels, Lisbon, 28 May-2 June 1984	E
37	IOC/UNESCO Workshop on Regional Co-operation in Marine Science in the Central Indian Ocean and Adjacent Seas and Gulfs, Colombo, 8-13 July 1985	E
38	IOC/ROPME/UNEP Symposium on Fate and Fluxes of Oil Pollutants in the Kuwait Action Plan Region, Basrah, Iraq, 8-12 January 1984	E
39	CCOP (SOPAC)-IOC-IFREMER-ORSTOM Workshop on the Uses of Submersibles and Remotely Operated Vehicles in the South Pacific, Suva, Fiji, 24-29 September 1985	E
40	IOC Workshop on the Technical Aspects of Tsunami Analyses, Prediction and Communications, Sidney, B.C., Canada, 29-31 July 1985	E
40 Suppl.	IOC Workshop on the Technical Aspects of Tsunami Analyses, Prediction and Communications, *Submitted Papers* Sidney, B.C., Canada, 29-31 July 1985	E
41	First Workshop of Participants in the Joint FAO/IOC/WHO/IAEA/UNEP Project on Monitoring of Pollution in the Marine Environment of the West and Central African Region (WACAF/2) Dakar, Senegal, 28 October - 1 November 1985	E
43	IOC Workshop on the Results of MEDALPEX and Future Oceanographic Programmes in the Western Mediterranean Venice, Italy, 23-25 October 1985	E
44	IOC/FAO Workshop on Recruitment in Tropical Coastal Demersal Communities Ciudad del Carmen, Campeche, Mexico, 21-25 April 1986	E (out of stock), S
44 Suppl.	IOC/FAO Workshop on Recruitment in Tropical Coastal Demersal Communities *Submitted Papers*, Ciudad del Carmen, Campeche, Mexico, 21-25 April 1986	E
45	IOCARIBE Workshop on Physical Oceanography and Climate Cartagena, Colombia, 19-22 August 1986	E
46	Reunión de Trabajo para Desarrollo del Programa «Ciencia Oceanica en Relación a los Recursos No vivos en la Región del Atlantico Sudoccidental, Porto Alegre, Brazil, 7-11 de Abril de 1986	S
47	IOC Symposium on Marine Science in the Western Pacific: The Indo-Pacific Convergence Townsville, 1-6 December 1986	E
48	IOCARIBE Mini-Symposium for the Regional Development of the IOC-UN (OETB) Programme on "Ocean Science in Relation to Non-Living Resources (OSNLR)" Havana, Cuba, 4-7 December 1986	E, S
49	AGU-IOC-WMO-CPPS Chapman Conference: An International Symposium on "El Niño" Guyaquil, Ecuador, 27-31 October 1986	E
50	CCAMLR-IOC Scientific Seminar on Antarctic Ocean Variability and its Influence on Marine Living Resources, particularly Krill (organized in collaboration with SCAR and SCOR) Paris, France, 2-6 June 1987	E
51	CCOP/SOPAC-IOC Workshop on Coastal Processes in the South Pacific Island Nations, Lae, Papua-New Guinea, 1-8 October 1987	E
52	SCOR-IOC-UNESCO Symposium on Vertical Motion in the Equatorial Upper Ocean and its Effects upon Living Resources and the Atmosphere, Paris, 6-10 May 1985	E
53	IOC Workshop on the Biological Effects of Pollutants, Oslo, 11-29 August 1986	E
54	Workshop on Sea-level Measurements in Hostile Conditions, Bidston, UK, 28-31 March 1988	E
55	IBCCA Workshop on Data Sources and Compilation, Boulder, Colorado, 18-19 July 1988	E
56	IOC/FAO Workshop on Recruitment of Penaeid Prawns in the Indo-West Pacific Region (PREP) Cleveland, Australia, 24-30 July 1988	E
57	IOC Workshop on International Co-operation in the Study of Red Tides and Ocean Blooms Takamatsu, Japan, 16-17 November 1987	E
58	International Workshop on the Technical Aspects of the Tsunami Warning System. Novosibirsk, USSR, 4-5 August 1989	E
58 Suppl.	Second International Workshop on the Technical Aspects of Tsunami Warning Systems, Tsunami Analysis, Preparedness, Observation and Instrumentation. *Submitted Papers* Novosibirsk, USSR, 4-5 August 1989	E
59	IOC-UNEP Regional Workshop to Review Priorities for Marine Pollution Monitoring Research, Control and Abatement in the Wider Caribbean. San José, Costa Rica, 24-30 August 1989	E, R, S
60	IOC Workshop to Define IOCARIBE-TRODERP Proposals. Caracas, Venezuela, 12-16 September 1989	E
61	Second IOC Workshop on the Biological Effects of Pollutants, Bermuda, 10 September - 2 October 1988	E
62	Second Workshop of Participants in the Joint FAO-IOC-WHO-IAEA-UNEP Project on Monitoring of Pollution in the Marine Environment of the West and Central African Region, Accra, Ghana, 13-17 June 1988	E
63	IOC/WESTPAC Workshop on Co-operative Study of the Continental Shelf Circulation in the Western Pacific, Bangkok, Thailand, 31 October - 3 November 1989	E

PREFACE

The Second Workshop on the Technical Aspects of Tsunami Warning Systems, Tsunami Analysis, Preparedness, Observation, and Instrumentation, sponsored and convened by the Intergovernmental Oceanographic Commission (IOC), was held on 1-2 August 1989, in the modern and attractive research town of Academgorodok, which is located 20 km south from downtown Novosibirsk, the capital of Siberia, USSR. The USSR Academy of Sciences and the Computing Center of its Siberian Division, hosted the TSUNAMI 89 Conference and this Second International Tsunami Workshop.

The First International Tsunami Workshop on the Technical Aspects of Tsunami Analyses, Prediction and Communications, was held in 1985 at the Institute of Ocean Sciences in Sidney, British Colombia, Canada.

Four years elapsed since the First International Tsunami Workshop. During this time interval, the technology in communications, computer hardware and software, and instrumentation has greatly changed. Therefore, the purpose of the Second International Tsunami Workshop was to bridge the gap of four years of independent developments in the Tsunami Warning System and to bring together tsunami specialists from different countries to improve their knowledge of the tsunami phenomenon and to help find practical solutions to the improvement of Tsunami Warning System for the mitigation of the tsunami hazard. As with the first Workshop, the second Workshop was held right after the International Union of Geodesy and Geophysics (IUGG) Tsunami Conference, and just prior to the XII Session of the International Coordination Group for the Tsunami Warning System in the Pacific (ICG/ITSU), as to maximize participation and minimize costs. Because of the collocation of these meetings, attendance at the Tsunami Workshop was excellent. Approximately 100 people from fourteen countries participated to make the Second Tsunami 89 Conference and the International Tsunami Workshop a great success.

The International Tsunami Information Center (ITIC), in close consultation with the IOC Secretariat and the Chairman of ICG/ITSU, developed a curriculum for the training of officials involved in the Tsunami Warning System as this is an important part of the overall educational requirements of ITSU member countries. These officials are, in turn, responsible for operational improvements in their own countries and for a program of general public education. In accordance to these guidelines, ITIC developed the program of the Second Tsunami Workshop and invited lecturers. Thus, all presentations made at the Workshop were by invitation.

The Program was arranged in eight major areas of interest covering the following: Opening and Introduction; Survey of Existing Tsunami Warning Centers - present status, results of work, plans for future development; Survey of some existing seismic data processing systems and future projects; Methods for fast evaluation of Tsunami potential and perspectives of their implementation; Tsunami data bases; Tsunami instrumentation and observations; Tsunami preparedness; and finally, a general discussion and adoption of recommendations.

A total of 29 presentations were made. Six presentations were deleted from the original program as the lecturers were unable to attend. Three new presentations not included in the original program were given. These were on the "Tsunami Watch and Warning in Fiji," by G. Prasad, the "Tsunami Threat in the Eastern Mediterranean Sea," by S. Tinti, and on the "Development of Numerical Simulation of Tsunami Waves at the Computing Center at Krasnoyarsk," by Yu.I. Shokin, L.B. Chubarov, V.A. Novikov, A.N. Sudakov and K.V. Simonov.

The Workshop presentations not only addressed the conceptual improvements that have been made, but focused on the inner workings of the Tsunami Warning System, as well, including computer applications, on-line processing and numerical modelling. Furthermore, presentations reported on progress has been made in the last few years on data telemetry, instrumentation and communications. Emphasis was placed on new concepts and their application into operational techniques that can result in improvements in data collection, rapid processing of the data, in analysis and prediction.

The Workshop was concluded with a general discussion and evaluation of its significance for future direction. A total of three recommendations were drafted, discussed and adopted, dealing with needed cooperation between international organizations, such as IUGG Tsunami Commission and IOC/ITSU; the need for cooperation between ITSU and the Federation of Digital Broadband Seismograph Networks (FDBSN) for support of the Tsunami Warning System; and finally, with the establishment of Tsunami Warning Systems in other regions exposed to this natural disaster.

A Summary Report on the Second International Tsunami Workshop, containing abstracted and annotated proceedings has been published as a separate report. The present Report is a Supplement to the Summary Report and contains the full text of the papers presented at this Workshop.

George Pararas-Carayannis
Workshop Chairman
Editor of the Proceedings

TABLE OF CONTENTS

1. International Cooperation in the Field of Tsunami Research and Warning

George Pararas-Carayannis
International Tsunami Information Center

Introduction

Tsunami disasters have posed a major threat to the coastal populations of the Pacific and of inland seas. In the past four decades alone, tsunamis have been responsible for the loss of thousands of lives and of millions in property damage (Pararas-Carayannis, 1982). Although advances have been made in our understanding of the tsunami phenomenon and we have established effective international cooperation in warning systems, these advances have been offset by population growth in the different countries particularly because of the development of the coastal zones. Thus, the tsunami risk and vulnerability of the people living in the coastal areas have increased and will continue to increase. More than ever, international cooperation is needed to mitigate the effects of the tsunami disaster.

Recently, as most of you know, the United Nations passed a resolution designating the 1990's as the Decade, during which the international community will enhance cooperation in natural disaster mitigation. The objective of the Decade is to reduce loss of life, property damage and the social and economic disruption associated with natural disasters. The goal of the Decade is to improve the capability to mitigate the impact of natural disasters, particularly through the use of early warning systems, through proper training and education, through dissemination and application of existing knowledge and information, and through proper scientific and engineering research. It is recognized that these goals can be achieved by the concerted action of nations, and will require international programs of cooperation and assistance to acquire the necessary knowledge and to apply the results.

Of all the natural disasters, the tsunami disaster has probably received more attention in the mitigation of its effects. This is because, in contrast to other natural disasters which have localized effects, tsunamis have affected adversely the coastal regions of many nations far away from the region of their origin.

The Tsunami Warning System in the Pacific is an example of how the tsunami disaster can be mitigated through international cooperation, concerted research, the sharing of knowledge and information, and meetings and workshops such as these. We should take pride in knowing that our international cooperative efforts to mitigate the tsunami

disaster started over 25 years ago, long before the Decade was proclaimed, and that tsunami is probably the only disaster that has been dealt so effectively on an international scale. This has been made possible through the leadership of IOC in forming the ITSU Group, and the generosity of the member nations in contributing their resources and sharing their knowledge and information (Pararas-Carayannis, 1988b).

Let us take a look of how the tsunami disaster can be mitigated further through continued international cooperation. International cooperation will be necessary in many areas. More specifically in:

Scientific and Engineering Research
Evaluation and Prediction Capability
Development of the Pacific and Regional Warning Systems
Development of Operational and Emergency Preparedness
Development of Planning and Zoning Criteria
Public Education and Awareness

Scientific and Engineering Research

Central to the successful implementation of the principles of the International Decade in the reduction of the effects of the tsunami disaster is the undertaking of appropriate applied-type of scientific and engineering research. Note that I use the word applied. Theoretical type of research is useful in understanding the phenomenon itself, but it does not result in hazard mitigation. Our goal should be to define and segregate an appropriate applied-type of research program and to develop engineering standards. It will be necessary to choose study topics that focus attention on specific remaining problems.

International cooperation, through a group such as ours, will be needed to identify such problems and allow an interdisciplinary approach to this solution without unnecessary overlap or dispersion of effort. Furthermore, through international cooperation the results of such studies would be shared and applied uniformly for the common good.

For example, the suggestion was made at the beginning of the Tsunami Symposium that we standardize the methodology of determining the tsunami risk and that we apply standardized methods of determining tsunami inundation and the delineation of evacuation zones. This can be done through the use of appropriate numerical modelling and standardization of engineering criteria. Through such standardization and international cooperation, nations threatened by tsunamis could develop proper coastal management policies.

Evaluation and Prediction Capability

An area where international cooperation will prove to be most valuable will be in the further development of tsunami evaluation and prediction capability using current technology of satellite data telemetry and communications, and use of microcomputers. Adequate state of the art seismic and water level instrumentation, rapid telemetry and telecommunications are needed, both for data acquisition and for warning dissemination. These are the most important components for an effective national or regional Tsunami Warning System. The Pacific Tsunami Warning System presently makes use of an extensive seismic and water level instrumentation network that has been made possible through the generous support of member nations of ITSU, through cooperative programs between many agencies and national governments, and through programs such as the International Tropical Ocean Global Atmosphere (TOGA) Sea Level Program (Pararas-Carayannis, 1988b).

Continuous international cooperation will be needed to enhance the Pacific Warning System's capability, and that of regional warning systems. Furthermore, international cooperation will be needed for sharing the knowledge on operational procedures of assessment and evaluation that are being developed, as for example, in French Polynesia, Japan, Soviet Union, and the United States. We heard some very good papers in the last few days on new techniques of evaluation and prediction that can be used by the international community.

Development of Pacific and Regional Warning Systems

The Pacific Tsunami Warning System and other regional and national tsunami warning systems continue to develop their capabilities utilizing computers and new communications technology. However, high tsunami risk regions exist in the world where tsunami warnings cannot be issued in time to be of any usefulness. At least six hazardous tsunamis have occurred since 1976, with great loss of life and property, in areas where warnings could not be issued promptly. If appropriate regional systems existed, warning information could (Pararas-Carayannis, 1982) have been released to the public within minutes permitting evacuation of most of the coastal population to safer places. Such regional systems, equipped with proper instrumentation, can reduce the time needed to evaluate the tsunami hazard, make decisions, and disseminate the warnings on a regional basis. Thus, many lives can be saved and damage to property can be reduced. During the last few years, new operational concepts have been developed that can improve the performance of a regional tsunami warning system. These concepts

utilize modern technology, computers, and instrumentation, including shore-based seismic and tidal sensors, and real time telemetry. There is a need for regional tsunami warning systems, in the South-West Pacific, in South America, and in the Eastern Mediterranean Sea. Considering the regional nature and complex content of such proposed regional tsunami warning systemns, international financial assistance and expertise are required to implement them. Such support can only come from international organizations and need the endorsement and counterpart contributions of national governments. Such regional projects would have considerable benefits for the countries involved, and such efforts would be well within the scope and intent of the International Decade for Natural Disaster Reduction (IDNDR).

Development of Operational and Emergency Preparedness

The key element to tsunami hazard mitigation is a tsunami warning system. But regardless of how sophisticated a warning system may be, all it can do is issue a warning. The effectiveness of the system is judged by what Civil Defense Agencies do with a warning. These agencies must have an effective Operational and Emergency Preparedness Plan to act on the warning and disseminate it rapidly and effectively to the public. This can be done only if there is an established operating plan designating infrastructural communications and responsibilities. Furthermore, it is Civil Defense Agencies and not the Tsunami Warning Centers, that are responsible for establishing plans for evacuation or other preventative measures to be taken before a tsunami strikes. Also they have the responsibility for training their own people by holding frequent exercises and by educating the public on a continuous basis (Pararas-Carayannis, 1988a).

Most of the countries that are members of the TWS have developed such Operational and Emergency Preparedness. However, others have not developed or coordinated adequately their organizational infrastructure so they can deal effectively with an emergency situation. Obviously, international cooperation and assistance are required in assisting such countries with the formulation of a standard emergency operational plan, with the conduct of Tsunami exercises, and with training of government officials. This workshop is an example of such international cooperation but, obviously, it is not sufficient. Efforts should be made by a Group such as ours, to establish more frequent training programs and of longer duration, particularly for developing countries or for countries that have recently decided to do something about planning for their tsunami hazard. Manuals and exercise scenarios can be prepared to assist with training for operational and emergency preparedness.

Development of Planning and Zoning Criteria

The tsunami risk is not evenly distributed along a threatened coastline. Because of the extreme selective nature of tsunami destruction along given coastlines, the development of planning and zoning criteria is required for proper coastal management and for population evacuation during tsunami warnings. Furthermore, the high cost of coastal land in many areas, dictates an accurate assessment of the tsunami risk, rather than arbitrary conservative zonation. Thus there is a need to establish the total risk at any point along a threatened coastline, as well as the probability of occurrence, for insurance purposes. A microzonation map of the tsunami hazard may be required which will be of great usefulness in developing proper coastal management criteria. For critical areas it may be necessary to perform detailed numerical modelling studies which indicate the spatial variation of the tsunami hazard along a given coastline, where expected tsunami height can be quantified and evacuation limits designated (Pararas-Carayannis, 1988a). What I propose is international cooperation in this area and endorsement of a standardized technique for doing this, by an international group such as ours. This would be consistent with the scope of IDNDR for the reduction of the tsunami disaster.

Public Education and Awareness

It is obvious that the best way of mitigating the tsunami hazard is with a program of public education and awareness. Because of the infrequency of tsunamis, the public must be constantly reminded of the potential hazard. Public informational activities must be sponsored by governmental authorities on a regular and continuous basis to assure awareness and public response when a tsunami warning is issued. Development of appropriate educational materials, such as brochures, pamphlets and audiovisual materials are necessary to implement a program of tsunami disaster mitigation. Such educational materials can be best developed with national and international support consistent with the objectives of the IDNDR.

References

Pararas-Carayannis, George, 1982, "The Effects of Tsunami on Society," Impact of Science on Society, Vol. 32, No. 1.

Pararas-Carayannis, George, 1988a, "Risk Assessment of the Tsunami Hazard," Natural and Man-Made Hazards, 183-191, D. Reidel Publishing Company.

Pararas-Carayannis, George, 1988b, "
Tsunami Warning System in the Pacific: An Example of International Cooperation,"
Natural and Man-Made Hazards, 773-780, D. Reidel Publishing Company.

2. SURVEY OF EXISTING TSUNAMI WARNING CENTERS - PRESENT STATUS, RESULTS OF WORK, PLANS FOR FUTURE DEVELOPMENT

PACIFIC TSUNAMI WARNING CENTER

Gordon D. Burton
Pacific Tsunami Warning Center

The Pacific Tsunami Warning Center (PTWC) continues to function as the operational center for the Tsunami Warning System of the Pacific (TWS). PTWC also functions as the National Tsunami Warning Center for the United States and as the Regional Tsunami Warning Center for the State of Hawaii. PTWC is physically located on a 175 acre tract of land in Ewa Beach, Oahu, Hawaii. Personnel consist of five watchstanders who live on site and three electronic technicians who maintain all equipment and instrumentation. PTWC is administered as a field office of the Pacific Region of the National Weather Service. In addition to the primary duties as a Tsunami Warning Center, PTWC also functions as a geomagnetic observatory and as the Hawaii station of the World Wide Standard Seismograph Network (WWSSN).

Any Tsunami Warning Center basically functions on the interaction of three operational parameters: 1.) the acquisition and evaluation of seismic data for event detection and evaluation of tsunamigenic probability; 2.) the acquisition and analysis of sea level data for tsunami confirmation and evaluation; and 3.) a communications system for data exchange and information dissemination. In this context, this paper is intended to provide a review of present capabilities and recent improvements at PTWC in the areas of computer automation, seismic data acquisition, sea level data acquisition, communications, and improvement of tsunami warning services provided to TWS participants.

A. Computer Automation:
Computer automation is applicable to all phases of PTWC's operations, including data acquisition, evaluation, and information dissemination. After more than a two year effort, PTWC has taken delivery of a new minicomputer, a Concurrent/Masscomp 6600. Using a UNIX operating system, the 6600 has two 33 MHZ CPU's, with the option of upgrading to a third CPU. The 32 MB memory is expandable to 128 MB. Each CPU has a Floating Point Processor and a Floating Point Accelerator to maximize performance. Storage consists of two 568 MB hard disks, a 150 MB tape unit, and a floppy disk drive. The floppy disk is capable of reading MS-DOS generated disks for ease of data transfer with microcomputers. Two graphics work stations, each with 1 MB memory, provide a strong graphics capability. A Local Area Network (LAN) is included for interfacing to PTWC's microcomputers, consisting of three 386 PC's, a 286 PC, and two IBM XT's. The 6600 uses a modular architecture to emphasize real-time data processing and real-time communications.

As of December 1989, all of PTWC's operational software has been converted from the old Data General S/230 minicomputer to the Concurrent 6600. The 6600 has now become PTWC's primary operational minicomputer, with the Data General S/230 serving as a backup system. Efforts at PTWC are presently concentrating on development of improved operational software to utilize the state-of-the-art technology now provided by the Concurrent 6600.

B. Seismic Data Acquisition:
PTWC continues to maintain a dedicated data circuit to the USGS/National Earthquake Information Center (USGS/NEIC) in Golden, Colorado, for exchange of real-time seismic data. Data from seismic stations extending from the East Coast of the U.S. to the Western Aleutians are received at PTWC in real-time (Figure 1.), with alarm systems configured for two stations in Alaska and two stations on the U.S. mainland.

The PTWC-NEIC data circuit recently has been upgraded from 2400 Baud to 9600 Baud. In addition to continuation of the present real-time data exchange, the capability now exists to connect PTWC's new 6600 minicomputer with the USGS/NEIC computer for direct communications and file transfer. The operational benefits to PTWC are significant as PTWC will have direct access to the continuing expansion of USGS/NEIC's seismic data acquisition program. In addition to implementation of the new U.S. National Seismic Network, USGS/NEIC is also expanding their acquisition of real-time data from international seismic stations.

PTWC is also working jointly with USGS/NEIC in development of a network of seismic stations with data to be transmitted via NOAA's Geostationary Operational Environmental Satellite (GOES). Front-end processors will be utilized for P-picking and storing of wave-phase data, with a Data Collection Platform (DCP) used for GOES transmission. Procurement of initial system components is underway, with field deployment of some stations anticipated by mid-1990. This satellite seismic network will be interfaced to the existing Pacific Satellite Sea Level Network whenever possible. USGS/NEIC has already installed a ground station to receive data directly from both GOES East and GOES West on a real-time basis. The operational goal for both PTWC and USGS/NEIC is to detect and locate earthquakes in the Pacific within 10 minutes of origin.

C. Sea Level Data Acquisition:
The Pacific Satellite Sea Level Network (Figure 2.) continues to expand and presently includes 32 stations in South America, the South and Central Pacific, and Alaska. Sea Level data from these stations are transmitted via GOES and relayed to PTWC in near real-time within 3-5 minutes of transmission. In addition, PTWC is now receiving sea level data from NOAA's National Ocean

Figure 1. PTWC Real-Time Seismic Network

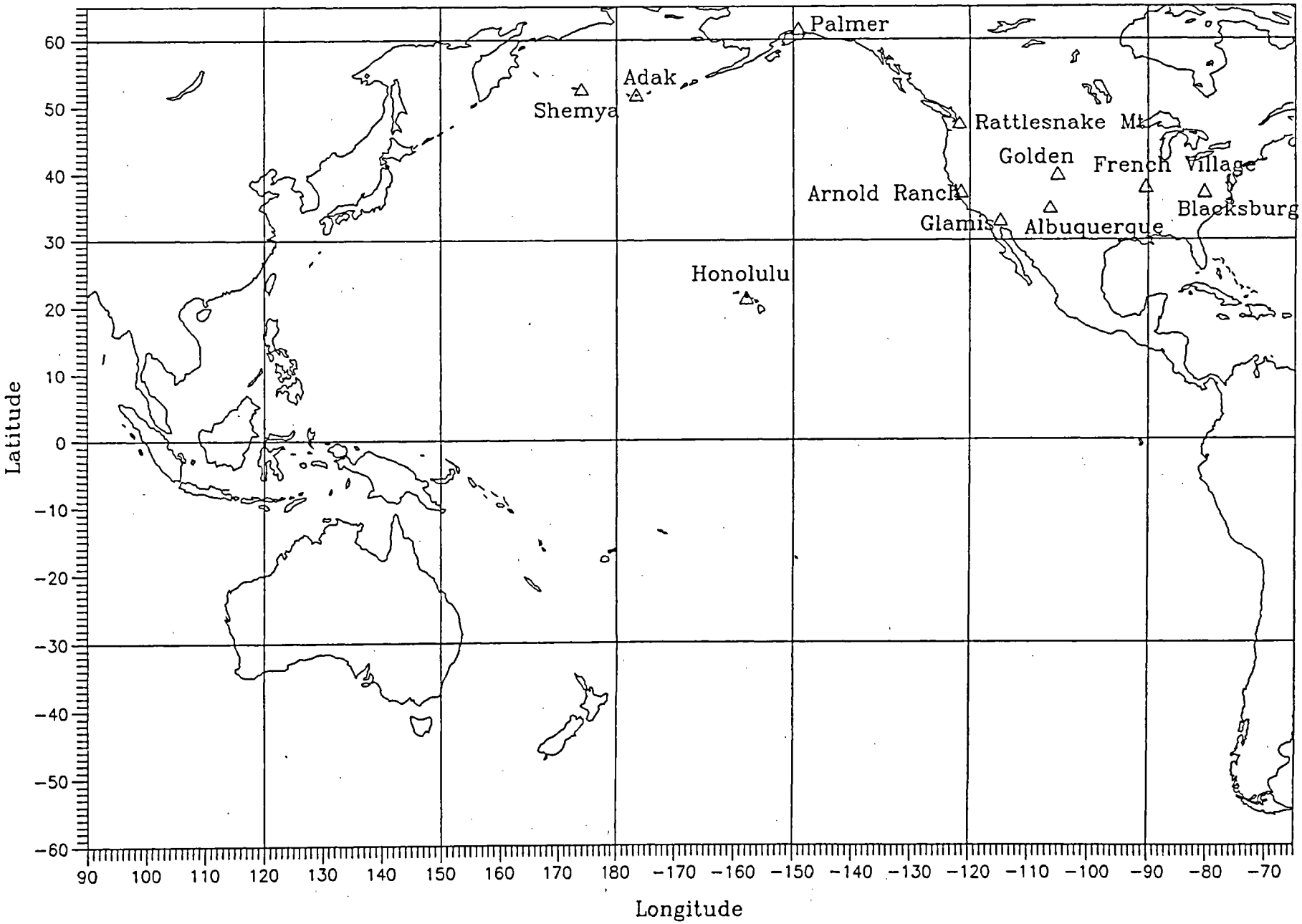

Figure 2. Pacific Satellite Sea Level Network

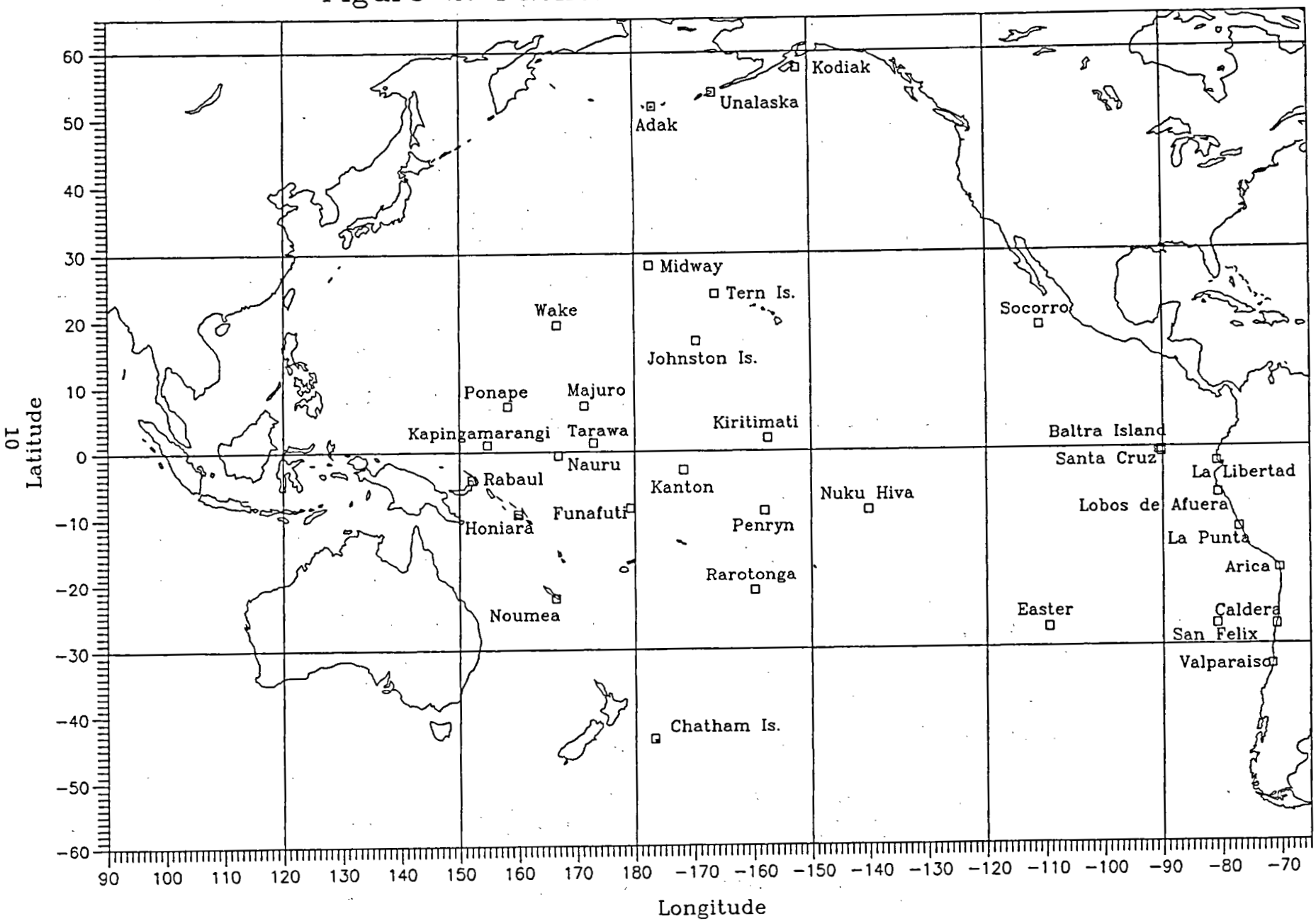

Service stations instrumented with the Next Generation Water Level Measurement System (NGWLMS) and transmitting via GOES. These NGWLMS units are primarily located along the U.S. West Coast, and in Hawaii and Alaska, but units are also installed at some island locations in the Southwestern Pacific. As additional installations are completed by NOS, the data will be available to PTWC via GOES relay.

The coordination of the Pacific Satellite Sea Level Network with TOGA, the University of Hawaii, the National Ocean Service, and TWS participating nations has resulted in a very successful and automated sea level program for the Tsunami Warning System.

D. Communications:
With the installation of the Concurrent/Masscomp 6600 minicomputer, PTWC now has the capability for real-time automation of all communications. Hardware interfaces have already been completed for each of PTWC's teletype circuits to connect directly to a computer port. Software modifications have been implemented so that all PTWC bulletins are transmitted simultaneously for their respective circuits, where previous operations using the Data General S/230 required the sequential transmission of message traffic. The software development effort is continuing so that PTWC will be able to automatically monitor and analyse incoming message traffic on all teletype circuits.

E. Operational Procedures:
In June 1989, PTWC began to fully implement operational procedures set forth in ICG/ITSU Resolution VIII.3 for the immediate issuance of Tsunami Warnings for a restricted area based only on seismic data evaluation. The intent is to provide improved tsunami warning services addressing the near-source tsunami threat. ITSU VIII.3 called for issuing a Warning to all areas within the first 3 hours tsunami travel-time, with a Watch extended for an additional 3 hours travel-time. Full implementation of ITSU VIII.3 was possible only due to recent improvements in PTWC's seismic and sea level data acquisition and in automation of communications.

To assist in operational implementation of Regional Warnings, PTWC staff are continuing historical studies on an area-by-area basis to better evaluate the potential for tsunami generation. The general approach is to analyze the earthquake and tsunami history and potential for specific areas, review present PTWC operational procedures for applicability, and implement improvements where needed. As these studies have significant implication for PTWC's operations, a brief discussion is provided of the approach being used.

The recent work of Dr. Stuart Nishenko of USGS/NEIC on Circum-Pacific Seismic Potential, 1988-1999, is used as the basis for defining specific tectonic units for study. Dr. Nishenko's

methodology is documented in USGS Open File Report 89-86, with an analysis and evaluation being provided for approximately 122 tectonic areas.

Using these areas as a basis for evaluation of tsunami potential, the PTWC studies use the USGS/NEIC digital historical data to analyze the occurrence and distribution of historical earthquakes with regard to both location and magnitude. First-motion focal mechanisms are included in the earthquake analysis. The local and regional tectonics of the area are studied, with emphasis on the possible occurrence of various tsunami source mechanisms, such as volcanic related or sediment displacement. The next phase is documentation of historical tsunamis, using all available catalogs and source material. In order to provide a quantitative evaluation of the tsunami threat, each historical tsunami is rated using a modification of the Imamura-Iida scale used by the Japan Meteorological Agency. The emphasis is to categorize historical tsunamis as having been no threat, having been only a near-source threat, or having been a far-field threat as well as a near-source threat, with the modified Imamura-Iida scale providing a quantitative measure of the coastal runup. This categorization of historical tsunamis is then integrated with the earthquake data for analysis of the relationship between tsunami generation, earthquake size, and the present threshold being used by PTWC for the issuance of Warnings.

These historical area-by-area studies are proving invaluable in providing PTWC staff with a preliminary evaluation of the tsunami potential for any area. In the process, guidelines are being developed for operational implementation of ICG/ITSU-VIII.3 procedures as well as identification of improved procedures for future development.

F. Summary:
The Tsunami Warning System of the Pacific exists as an example of participatory coordination between ICG/ITSU member nations throughout the Pacific Basin. The involvement and participation by many nations has continued to result in significant improvements in the TWS. Although recent operational improvements at PTWC have resulted in the provision of enhanced tsunami warning services, even greater improvements are anticipated over the coming year as PTWC implements the improved automation technology provided by the Concurrent/Masscomp 6600 minicomputer, increased coverage for both seismic and sea level data, improved tsunami evaluation techniques, and increased participation by ICG/ITSU participants.

HAWAII REGIONAL TSUNAMI WARNING CENTER

Gordon D. Burton
Pacific Tsunami Warning Center

In addition to functioning as the operational center for the Tsunami Warning System of the Pacific and as the National Tsunami Warning Center for the United States, the Pacific Tsunami Warning Center (PTWC) continues to serve as the Regional Tsunami Warning Center for Hawaii. The operational emphasis is to provide tsunami warning services for the near-source threat. Warnings are issued in the shortest time possible, using only seismic information, as sea level data are generally not available in a timely manner. To mitigate the risk of issuing false Warnings, only a restricted geographic area is placed in Warning status. A rapid evaluation of the event then permits cancellation or expansion of the Warning as necessary.

The Hawaiian Islands extend as a chain reaching from Midway to the Island of Hawaii (the Big Island), and were created as the result of the northwestern movement of the Pacific Plate over the underlying Hawaii Hotspot. The major seismic activity is concentrated in and around the Big Island at the southeastern end of the island chain. Lesser seismic activity occurs in the vicinity of the central islands (Oahu, Molokai, and Maui) related to the intersection of the Molokai Fracture Zone with the Hawaii Ridge. However, the southeastern coast of the Big Island is the major concern as a source region for tsunami generation.

PTWC has an operational commitment to Hawaii Civil Defense to provide Regional Tsunami Warnings within 10 minutes or less. Issuance of a Regional Warning will result in immediate coastal evacuation procedures being implemented by Civil Defense through the sounding of coastal sirens combined with radio and television announcements using the Emergency Broadcast System. As a Regional Tsunami Warning Center, PTWC essentially makes a decision within minutes as to whether a tsunami threat exists for which evacuation is required. Regional Warnings are issued on an island-by-island basis to minimize any unnecessary evacuation. Over the past 15 years, no false Warnings have been issued.

Over the past year, information was provided for all local earthquakes within less than 10 minutes, with information being provided within less than 5 minutes for 60% of all events. The minimal response time has been within 3 minutes of earthquake origin. This also corresponds to the minimal timeframe for which sufficient data are available for decision making. Immediate voice communication is provided to Civil Defense via the Hawaii Warning System (HAWAS), which is a "hotline" voice circuit connecting PTWC with all State and County Civil Defense units in Hawaii. Hardcopy messages are sent via the Inter-island Civil

Defense circuit, a 2400 Baud digital circuit linking to all Civil Defense units.

For early event detection, PTWC has alarm systems set to two remote seismic stations on the Big Island as well as on both long-period and short-period seismometers at PTWC. A preliminary location is determined by S-P measurements for PTWC's short-period seismometers combined with initial arrival sequence of seismic P-phases at remote stations. A preliminary magnitude is determined by rapid calculation of the local magnitude (Ml) using surface wave deflections measured on PTWC's short-period seismogram. Both location and magnitude are further refined through additional computer calculation and through data exchange with the USGS/Hawaii Volcano Observatory and the USGS/NEIC.

To improve tsunami warning services for Hawaii, PTWC has worked in close cooperation with Hawaii Civil Defense for submission and approval of two House Bills totalling $190,000 and funded by the State Legislature. The first, funded for $90,000, provided for updating of potential tsunami inundation charts for all the Islands, preparation of prototype signs to designate tsunami evacuation areas, and preparation of a prototype public education program. The second, funded for $100,000, provided for installation of additional tide gauges within the Islands combined with an improved data information system.

Through coordination with PTWC, Hawaii Civil Defense purchased instrumentation for nine additional tide gauges in addition to the previous five gauges used for the Hawaii Regional Tsunami Warning Network. The newly installed gauges consist of float-wells with floats connected through a digital encremental encoder to a Limited Automated Remote Collector (LARC). The LARC is a microprocessor data collection platform capable of transmitting data via telephone circuit either on remote query or as a result of exceeding an internally programmed threshold. As such, it is a relatively inexpensive means of obtaining near real-time data without incurring the cost of a dedicated data circuit. In addition to the installation of nine LARC's, a set of 386 microcomputers and TeleFax units were purchased for each of the County Civil Defense Agencies. PTWC developed the microcomputer software so that each Civil Defense unit can independently query and plot the sea level data from their respective gauges. This has proven to be a most successful enterprise. In addition to providing sea level data to monitor tsunami activity, the LARC's are also being used to monitor high surf (Figure 1.).

A summary of PTWC's operational capability as a Regional Tsunami Warning Center is best illustrated by the earthquake and tsunami of 26 June 1989. A strong earthquake having a Richter magnitude of 6.1 occurred off the southeast coast of the Island of Hawaii. PTWC's alarm system was activated within 15 seconds of earthquake origin, with two watchstanders coming to the office from their

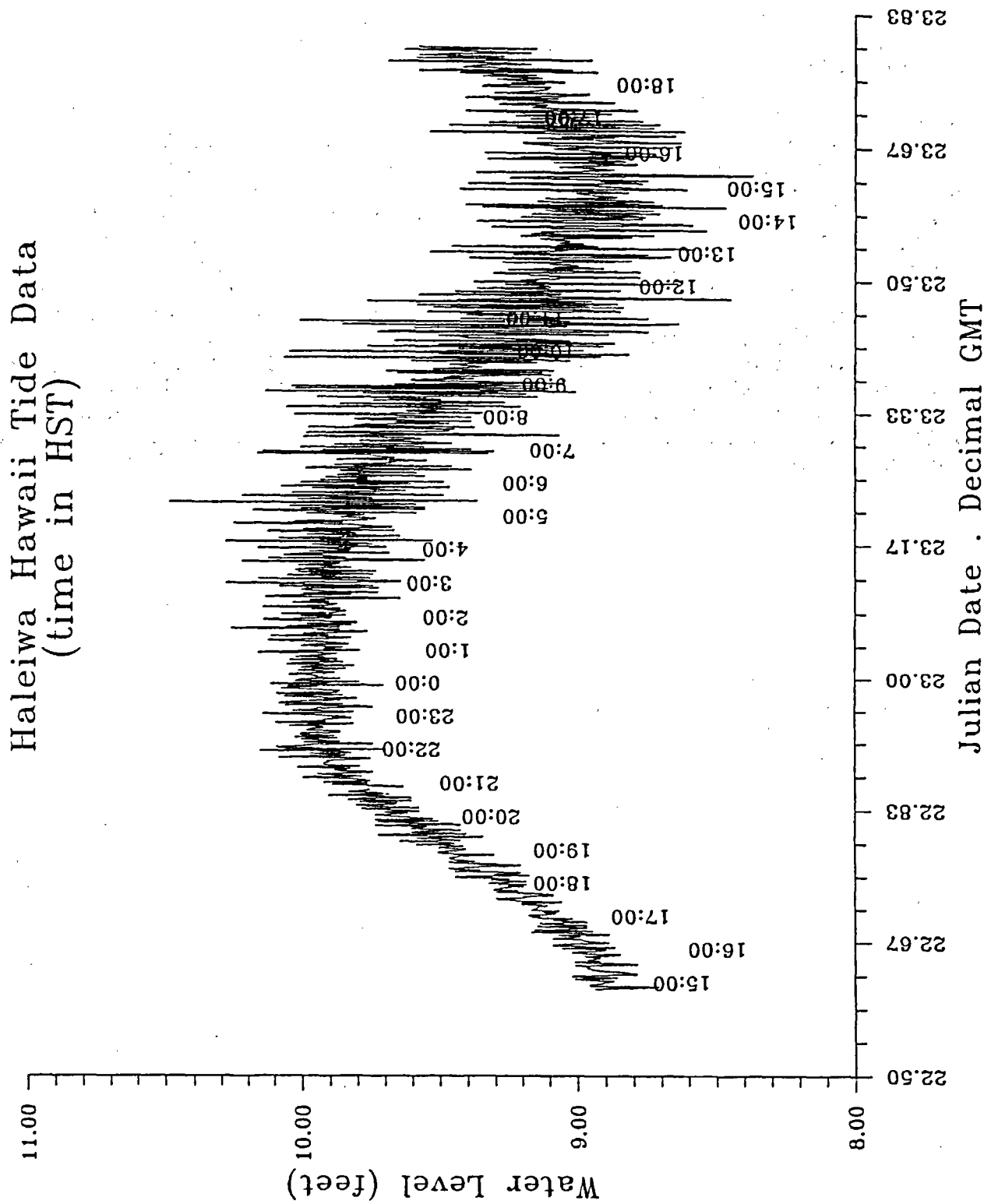

Figure 1. High Surf Recorded by LARC

nearby homes within 2 minutes. A preliminary location off the coast and a preliminary magnitude were determined within 4 minutes of origin. The initial evaluation was not to issue a Warning, with that information being provided to Hawaii Civil Defense via HAWAS within 5 minutes of origin.

However, real-time sea level data from a nearby coastal tide gauge showed indication of tsunami activity. Initial wave activity was about 57 cm peak to trough, but with the tsunami source region being located between the tide gauge and Hilo, there was some uncertainty as to a possible threat to Hilo. Fortunately, a LARC installation had been completed which provided data coverage between Hilo and the tsunami source region. A remote query from PTWC via microcomputer confirmed within three minutes not only the generation of a tsunami, but also that the maximum amplitude was 21 cm, with no threat posed to Hilo or other coastal areas (Figure 2.). The addition of new technology to the Tsunami Warning System provided critical sea level data that prevented possible issuance of a false Warning with resultant coastal evacuation at Hilo and along the coast of the Big Island.

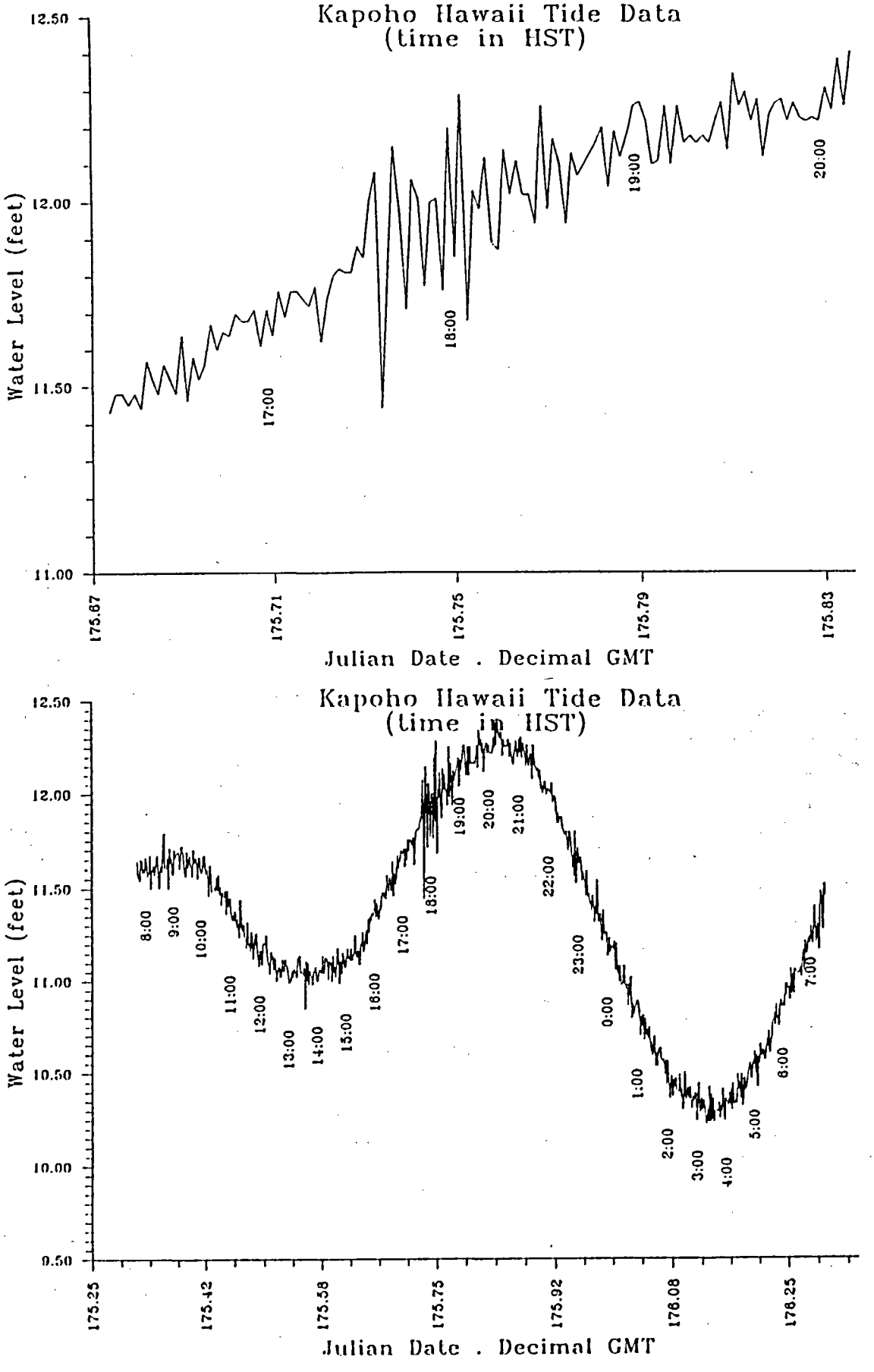

Figure 2. Tsunami Recorded by LARC

THE TSUNAMI WARNING CENTER IN ALASKA

Thomas J. Sokolowski

Alaska Tsunami Warning Center, Palmer, Alaska, USA

ABSTRACT

The Alaska Tsunami Warning Center (ATWC) has implemented many major changes in order to provide timely and effective tsunami warning services for coastal populations in Alaska, and the west coasts of Canada and the lower 48 States. The basis for these improvements was the integration of computers and associated developments into the ATWC's operations. New concepts, technique developments, procedures, computers, and equipment were implemented which resulted in a highly automated warning system which analyzes data from potential tsunamigenic earthquakes in real-time, and immediately disseminates necessary critical information to affected coastal populations. These advancements are leading toward an automated expert system. The present system has been exercised for seven recent potential tsunamigenic earthquakes and has proven to be very timely with tsunami warnings being issued in an average of 11 minutes after the origin time of an earthquake.

Seismic and tide data networks have been enlarged to improve the accuracy and timeliness in locating and sizing earthquakes, and for confirming the existence of a tsunami. New techniques and equipment are being implemented to collect, analyze and process tide data via micro computers. All critical warning and watch information messages are generated by computers which are linked to a satellite and high speed teletypewriter communication systems for rapid dissemination of information. The ATWC's community preparedness efforts has been expanded to aid those individuals who may be caught in the immediate vicinity of a violent earthquake and its subsequent tsunami.

1. Introduction

The Alaska Tsunami Warning System was established in Palmer, Alaska in 1967 as a result of the great earthquake that occurred in the Prince William Sound area on March 27, 1964. This earthquake alerted State and Federal officials to the need for a facility to provide timely and effective earthquake and tsunami information for Alaska and the northern Pacific. The city of Palmer, located 40 miles north of Anchorage, was selected as the site for a primary Center. Two other Centers, located at Sitka and Adak, were incorporated into the system. After an extensive real-time data telemetry network was established, the ATWC became operational using manual methods to fulfill its missions.

Initially, the tsunami watch and warning responsibility for Alaska was shared by the three Centers located at Adak, Sitka and Palmer. In later years, the responsibility to provide all tsunami warning servic-

es for Alaska was transferred to the Palmer Center. In 1973, the ATWC was transferred to the National Weather Service's Alaska Region. In 1982, the responsibility for issuing tsunami watches and warnings to the U.S. west coast and Canada, for earthquakes occurring in those areas, was transferred to the ATWC from the Pacific Tsunami Warning Center (PTWC) in Hawaii. This additional responsibility made the ATWC the largest regional tsunami warning center in the Pacific Basin, covering more than 4300 linear miles of coast line in Alaska, Canada, Washington, Oregon, and California.

To improve the ATWC's tsunami warning services, it became necessary to integrate computers into the ATWC operations and to design an expert automated system. In general, an expert system in the tsunami warning system is one which can rapidly determine a potential tsunami threat from a source for immediate use by intended recipients. Further, for a warning system to be effective, it must address at least the following three main parts: obtain data; analyze the data; and disseminate data/information to intended recipients. If one part fails, the warning system has failed. The initial areas that were identified for improvement concerned: (1) automatic detection and analysis of seismic data in real-time; (2) immediate dissemination of critical earthquake and tsunami information; (3) automatic detection and analysis of tidal data in real-time or near real-time; (4) rapid discrimination of tsunamigenic from non-tsunamigenic earthquakes; and (5) reasonable estimates of probable tsunami wave heights and areas of inundation in the path of a tsunami.

Since regional tsunami warnings are based upon seismic data alone, (1) and (2) became primary concurrent goals. Previous computer concepts by Sokolowski and Miller (1967), Sokolowski (1974), and Sokolowski (1978) began to be implemented at the ATWC. During the early 1980's, many operational changes began to replace the highly dependent manual methods with more sophisticated ones which used a mini computer to automatically collect seismic data to determine an earthquake's location and magnitude in real-time, and to immediately disseminate critical earthquake and tsunami information (Sokolowski et al., 1983). To further improve the ATWC, the mini computer system concept was replaced with a distributed micro computer concept by Sokolowski (1985). During the remainder 1980's, the ATWC continued to become highly automated (Sokolowski et al., 1989) with warnings issued in an average time of 11 minutes from an earthquake's origin time. These new approaches reduced the time to issue a warning by more than 50%. Also, they standardized procedures and increased the quality and quantity of data processed and information disseminated. During the latter part of 1989, the communication part of the system was enhanced with the installation of a satellite communication system for immediate dissemination of critical information to the Tsunami Warning System (TWS) recipients. This paper discusses some of the operational areas in the Alaska Tsunami Warning Center in more detail.

2. Missions

The primary mission of the Alaska Tsunami Warning Center is to provide

timely tsunami watches and warnings for Alaska, California, Oregon, Washington, and British Columbia in Canada, for potentially tsunamigenic earthquakes that occur in those regions. For non-tsunamigenic earthquakes, or earthquakes outside of the ATWC's areas of responsibility, earthquake parameters and other associated information are appropriately disseminated to: Alaska Division of Emergency Services; Alaska Air Command; National Earthquake Information Center in Colorado (NEIC); PTWC in Hawaii; USGS-Menlo Park Research Center in California; University of Alaska's Geophysical Institute in Fairbanks; Japan Meteorological Agency, Tokyo; Royal Observatory, Hong Kong; appropriate agencies in Canada; news media; and to many other recipients including both State and Federal disaster preparedness agencies. Although numerous non-tsunamigenic earthquakes are automatically detected and processed each month, only a small number of these earthquakes are released to officials and the public.

This service is provided on a 24 hour basis, for each day of the year, by two duty personnel. During those times that the Center is not manned, the duty personnel are in a paid standby duty status which requires that they respond to the Center within 5 minutes after being alerted that a significant earthquake has occurred. To ensure a rapid response to earthquakes occurring at night, weekends, or holidays, all personnel are required to live within 5 minutes travel time to the Center. They are notified of the occurrence of an earthquake, or irregularities in the Center's operations, by a sophisticated radio-alarm system.

In addition to the above primary and secondary missions, the ATWC personnel: process and disseminate collected data; participate in fulfilling interagency cooperative agreements; create and implement software; and, conduct technique and equipment development to improve the present system. These improvements involve both the reactive and predictive areas of the ATWC's operational system. The reactive part concerns minimizing the response time between the occurrence of a tsunamigenic earthquake and the issuance of a tsunami warning to people in coastal areas. Specifically, this part seeks improvements in: communications; present techniques and development of advanced ones; equipment and instruments; software development and/or modifications; community preparedness; and, operational procedures. The predictive part involves both in-house and cooperative work efforts with other experts and/or agencies concerning areas, such as, tsunamigenic earthquakes and zones, source mechanisms, and tsunami formation, propagation, run-up, and interaction with coastal shores.

The ATWC has both formal and informal cooperative agreements with many agencies and institutions. The agreements concern telemetry of seismic and tide data; seismic and tide site installations; cooperative technique and equipment developments; communications; equipment maintenance; and the exchange and analysis of data. Some of these agreements involve daily collecting, processing, and archiving data forappropriate agencies. Additionally, past recorded data from the ATWC network are archived at the ATWC and made available to visiting scientists to assist them in their work projects.

3. Seismic and Tide Networks

The ATWC is a large geophysical data acquisition Center which consists of 4 subnetworks owned and maintained by the ATWC, U.S. Geological Survey at Menlo Park (USGS-Menlo), National Earthquake Information Center (NEIC), and the University of Alaska at Fairbanks. Figure 1 shows the geographical locations of stations used by the ATWC.

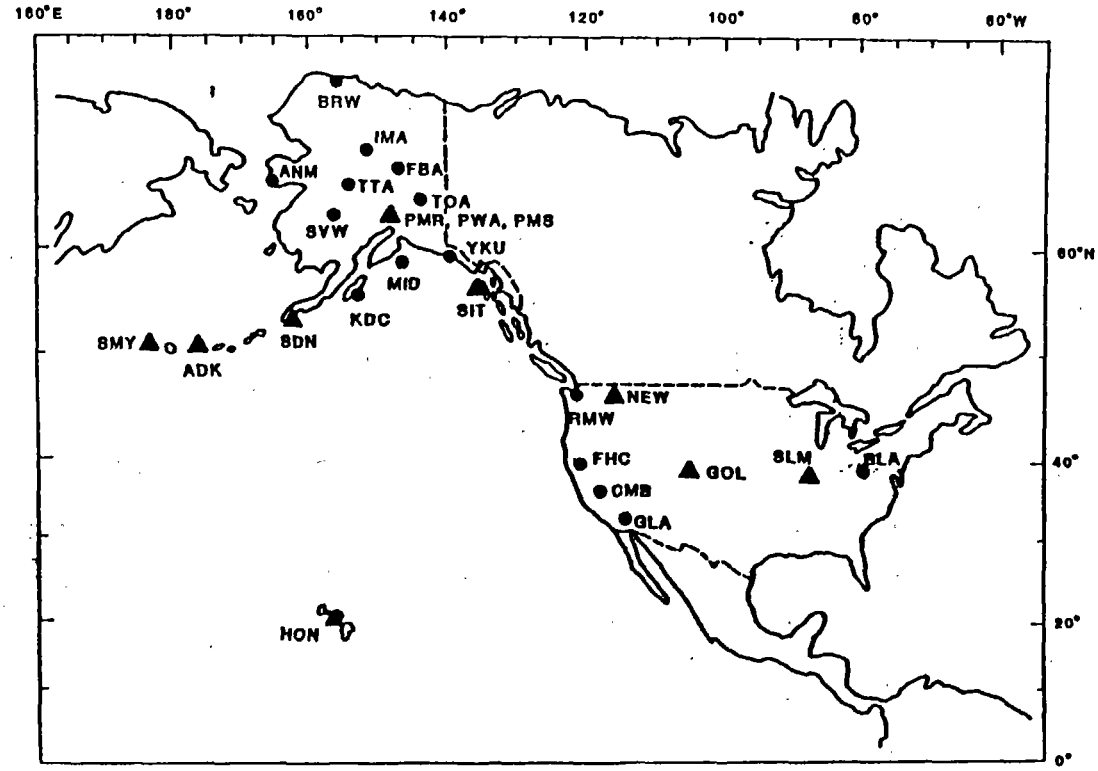

Fig. 1. Map showing seismic site locations that are telemetered to the ATWC in real-time. The filled circles show the short period seismic sites. The triangles show sites that have collocated short and long period instruments.

The ATWC's network consists of 16 seismic sites located at remote places throughout Alaska ranging from the far western Aleutians to Sitka, Alaska. The data are telemetered in real-time by satellite and microwave with very little interruption of data flow from the remote sites. The data are archived on various types of recorders, computer disks and magnetic tapes. In addition to the 16 short period seismometers, long period seismometers are collocated at Shemya, Adak, Sand Point, Sitka, and Palmer sites. Through an interagency agreement with NEIC, the ATWC telemeters 14 channels of data to the NEIC in Golden, Colorado. In return, the ATWC receives 14 channels of real-time seismic data telemetered from NEIC's network from California to the east coast of the U.S. The ATWC also records real-time short period data from networks operated by the USGS-Menlo and the University of Alaska.

Long period data are also telemetered to the ATWC via NEIC from a PTWC seismic site in Hawaii. From this accumulation of data, 23 short period and 9 long period sites' data are routed into the ATWC's computer for real-time processing to determine earthquake parameters, and for immediate information dissemination to the appropriate disaster agencies and other hazard Centers. From time to time, data from different seismic stations are used to ensure a continuous flow of quality data to the ATWC.

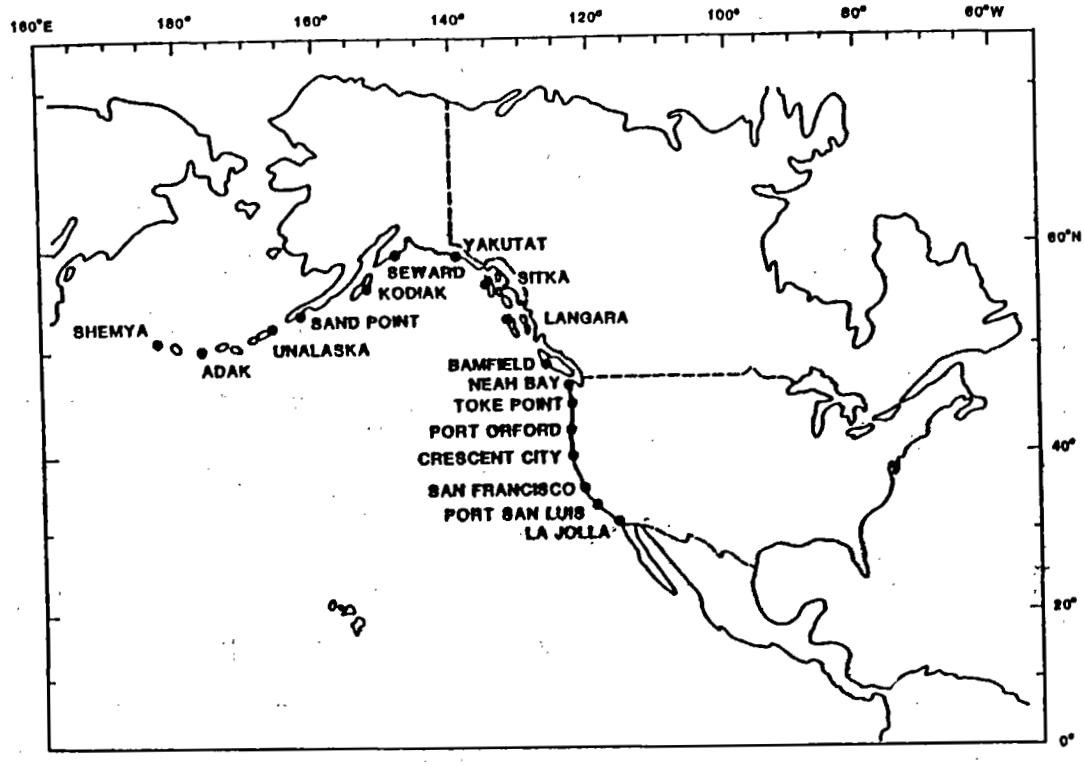

Fig. 2. Map showing the tide site locations near the coastal areas of Alaska, and the west coasts of Canada and the lower 48 States.

The ATWC has access to data from more than 15 tide sites that are owned and maintained by NOAA's National Ocean Survey (NOS) and Canada. Figure 2 shows tide site locations near the coastal areas of Alaska and the west coasts of Canada and the lower 48 States. Through a cooperative agreement with the NOS, the ATWC has transmitters at each of the 8 NOS sites in Alaska for telemetering data to the Center in real-time. The data are transmitted via satellite for immediate confirmation of the existence or nonexistence of a tsunami. Tide data are obtained from the west coast of the U.S. and Canada via teletypewriter, telephone, and micro computer. All U.S. tide sites are owned and operated by the NOS, except for Shemya which is maintained and operated by the ATWC. The ATWC continues to access near real-time data from the NOS's water level telemetry systems (WLTS) which are located along

the U.S. west coast. This access uses computer-to-computer linking for transmitting selected windows of time periods of tide/tsunami data to an ATWC micro computer for analysis.

4. Preventative Maintenance and Equipment Upgrades

Equipment maintenance, additions, calibrations, and replacements are critical ongoing functions at the ATWC's field sites and the Center. All field sites are visited by ATWC personnel each year, or as soon as possible after equipment failure. These visitations include the seismic network throughout Alaska, Shemya tide site, and ATWC's transmitters at each of the NOS tide sites in Alaska. All of the ATWC's seismometers have automatic sine wave calibrations which are transmitted along with the seismic data so that the computer can automatically monitor and update an instrument's sensitivity. this occurs twice daily for each of the short period seismometers. The calibrations of the long period instruments are checked interactively every week. Tide site visitations are coordinated with the NOS field personnel to minimize cost and maximize aid to each other. At the Center, the incoming seismic and tide data are recorded on multiple gain helicorders, tide recorders, and in micro computer systems. The equipment and systems are monitored daily by personnel and by other electronic equipment, to ensure a continuous data flow to the Center. This preventative program has resulted in very little down time and a continuous flow of high quality data to the Center.

To keep abreast of changes in new equipment and electronics, the ATWC receives many catalogs, brochures, and specifications of equipment and hardware which are continually researched for improving existing equipment. As funding becomes available, the equipment is enhanced or replaced. In some instances, new equipment is loaned to the ATWC for testing, prior to procurement, to ensure compatibility with existing equipment and computer systems.

5. Radio-Alarm System

The Center's standby duty is a critical element of the ATWC's operations where an immediate response is required of the personnel when the office is not manned, e.g. during evenings, nights, weekends, and holidays. The standby duty personnel are alerted to large earthquakes, or equipment failure, by a sophisticated radio-alarm system (RAS) which is interfaced to the Center's computer system. This state-of-the-art RAS system replaces the previous RAS system described by Sokolowski (1985). The new system permits local, regional, or world wide earthquake information to be immediately transmitted to, and received by, the standby duty personnel to let them know the urgency of the situation, or whether it is a false alarm, telephone call, or equipment malfunction. The RAS system consists of a transmitter, a radio-alarm alphanumeric pager unit with an associated printer (RU), and computer interfacing equipment. The unit can fit in the palm of one's hand and has a LCD display area to view messages received from the ATWC's computer system. Hard copies of the messages are displayed on the printer. The new RAS system uses the previous RAS threshold method as a backup system.

As soon as an earthquake is automatically located and sized by the ATWC's computer system, the computer transmits selected earthquake parameters to remote alphanumeric pagers which are carried by standby duty personnel. A short 80 character message, which contains a literal location, latitude, longitude, magnitude, origin time, average residual, and azimuthal control, is telemetered to pager units and the RU's printer. This provides the duty personnel with immediate knowledge of an earthquake's parameters, thus the urgency of the situation. The RU receives other messages from the computer concerning other equipment that is being monitored by the computer, and which alarm was activated. With a push of a button, the standby duty personnel can immediately view an earthquake's parameters which are displayed on the unit's LCD. A beeper tone is activated in the RU as each message is received and stored by the RU unit. The unit can store 16 messages for about a total of 1300 characters which can be scrolled, reviewed, and deleted.

6. Automatic and Interactive Earthquake Processing System

Since the early 1980's, the ATWC has been processing earthquakes automatically and interactively using a mini computer system, graphics subsystem, and related peripherals (Sokolowski et. al., 1983). Due to the advances in micro computer hardware and software, the mini computer system was replaced with a Digital Equipment Corporation (DEC) Micro VaxII computer system (Sokolowski et al., 1989). Although the present automatic earthquake processing system is more enhanced than the previous system, many of the key elements were converted to the DEC system. The enhancements concentrated on those elements that would improve the ATWC's performance in its missions. A summary of the automatic and interactive processes are given below.

For the automatic processes, thirty-two channels of real-time seismic data are continually monitored in the DEC system. Twenty-three are used for short period data (T_o=1s) and 9 for long period data (T_o=20s). Figure 1 shows the array of stations providing seismic data for processing. Each station's data are sampled at 25 samples/second, however, the long period data are later resampled at 1 sample/second. As the analog signals are sampled by the A/D cards, their data are automatically stored in memory and evaluated for the occurrence of a local, regional, or teleseismic earthquake. Once detected, the onset of the P wave times (P-picks) are determined along with periods and amplitudes of the P waves and Lg waves for appropriate mb or Ml magnitude computations (Sindorf, 1972). The P-pick algorithm used was described by Sokolowski et al., (1983). After a P-pick has been declared, 8 seconds of pre-earthquake and 10 seconds of post-earthquake wave form data are displayed on a graphics terminal for viewing. The computer determined P-pick is distinctly marked on the displayed trace and can be easily changed using a mouse. If 3.5 minutes have elapsed with no P-pick declared on any other channel, the wave form data that have been temporarily saved on disk are deleted. If 5 channels successively declare P-picks with time intervals between P-picks of less then 3.5 minutes, an earthquake is declared and the 5 P-pick times are used in a location algorithm to determine an earthquake's parameters. This includes parameters, such as, latitude, longi-

tude, origin time, depth, literal location, and magnitude which are listed on a printer and displayed on video display monitors (VDM's). Associated with the earthquake parameters are the seismic station names, P-pick times, distances, azimuths, residuals, etc. The depth for all automatic locations is fixed at 33km. The major parts of the location program to process earthquakes automatically (Sokolowski et al., 1983) are used in the DEC system. During output processing, incoming signals continue to be evaluated on other channels which have not declared a P-pick. After 7 P-picks have been recorded, and again after 9 P-picks, the earthquake's parameters are recomputed. Additional stations' data continue to be processed unless a user interactively stops the process, or 3.5 minutes have elapsed after the last P-pick. In either case, a final computation is performed which includes a full magnitude summary in addition to the parameters listed above.

If the location program yields high residuals, the P-pick data are assumed to be erroneous or associated with another earthquake. Each P-pick is successively removed from additional recomputations and the residuals retained. The recomputation with the lowest acceptable residuals is saved and printed. If the computation has unacceptable residuals and there are more than 5 P-times, 2 P-picks are removed and recomputations performed as above. Each of these computational results are available within seconds after the appropriate number of P-picks are available for computations in the location program.

Following an acceptable earthquake location, magnitudes are computed using short period amplitudes that were determined earlier. If an epicenter is within 9 degrees of the station, the Lg data are used for Ml computations; if the distance is 15 degrees or more, the P data are used for Mb computations.

Immediately after an earthquake's parameters and associated data are printed, the information is transmitted to the RAS system to provide the duty personnel with immediate knowledge of an earthquake's parameters. To facilitate operational procedures and the dissemination of critical information, several wall-mounted VDM's are used to show an earthquake's parameters, the epicenter superimposed upon an appropriate map, and specific procedures in conducting an earthquake/tsunami investigation.

Automatic processing of long period data begins after the final automatic location for teleseismic earthquakes of magnitude greater than or equal to 5.5, and for local earthquakes with an Ml greater than 5.0. The long period wave form data are processed at 10 seconds before to 30 seconds after the expected P arrival for a MB magnitude computation. Similarly, this same wave form data are processed for the interval of 1 minute before to 10 minutes after the expected Rayleigh wave arrival time. A summary of the MS and MB magnitudes is printed. The wave forms from which each MB and MS is computed are displayed on another graphics terminal along with the MB and MS values. As broadband equipment becomes available to the ATWC, its data and the techniques as suggested by Kanamori (1985), and Okal and Talandier (1989), are intended to be implemented for automatic processing.

The interactive processing software has been in use at the ATWC since the early 1980's with enhancements added as needed to improve the ATWC operations. It is menu driven and collocated with the automatic software in the DEC system. Also, this same interactive software is used in a separate IBM 386 micro computer which functions as a backup for the DEC micro system. Except for the P-pick processing algorithm, all major algorithms and processes in the automatic software are also in the interactive software. Access to execute this software is via a dedicated video display terminal (VDT).

The interactive software is used to produce all warning and other critical messages, whether disseminated by voice, teletypewriter, or satellite communication systems. It is also used for generating procedural aids for duty personnel, routine communication messages, and for daily earthquake processing. The major parts of the location program which exist in the automatic system is also in the interactive system. From a menu, an operator can select to: transfer data from the automatic system for concurrent recomputation of an earthquake and/or refinement; transfer results from the automatic system; independently compute an earthquake's parameters via interactive seismic data input; fix or float an earthquake's depth; eliminate erroneous P times; produce many procedural aids for duty personnel; determine water wave travel times; eliminate or add P-times; compute magnitudes (mb,Ml,MB,MS,Mw) interactively; compute epicentral distances and Rayleigh wave arrival times; compute depth from pP phase data; recompute magnitudes from the automatic system with an updated earthquake location; and display an epicenter superimposed on an appropriate map on a VDM.

Once an earthquake's parameters are determined, a variety of critical messages can be generated which include warnings, watches, press releases, and tide queries. These messages are disseminated over a teletypewriter system, National Warning System, and over the National Weather Service weather wire to appropriate agencies. For a tsunami warning and watch messages, the warning and watch areas are taken from a table for the particular epicentral region and magnitude. Estimated tsunami times of arrival for various locations in Alaska, British Columbia, and the West Coast are integrated into these messages.

7. Earthquake/Tsunami Investigations

Every earthquake that activates the ATWC's RAS initiates an earthquake/ tsunami investigation (ET) which culminates in processing the earthquake routinely or in the issuance of a watch/warning (WW). The first procedural steps for any ET is to determine an earthquake's location and magnitude. A WW is issued when the magnitude of an earthquake has exceeded a predetermined threshold, and the earthquake's location is near a coastal area from Kamchatka through southern California. The minimum threshold magnitudes for issuing a tsunami warning are dependent upon an area, and currently range from 6.75 to 7.1. When an earthquake's magnitude has exceeded an area's threshold, a limited geographical area is placed in a warning status. Other geographical

areas, outside the warned area, are placed in a watch status. As techniques and developments become more definitive and accurate, magnitude thresholds and the areas subjected to watches and warnings will be modified to minimize evacuations of coastal inhabitants.

After the initiation of a WW, tide site's data that are nearest the epicenter are monitored for the existence of a tsunami. Upon confirmation that a significant tsunami has been generated, the previously designated watch areas are upgraded to a warning which could be expanded. The WW is cancelled if an insignificant or no tsunami has been generated. Earthquakes that are smaller than threshold, and important to hazard officials, are processed on a routine basis and the information disseminated to appropriate officials.

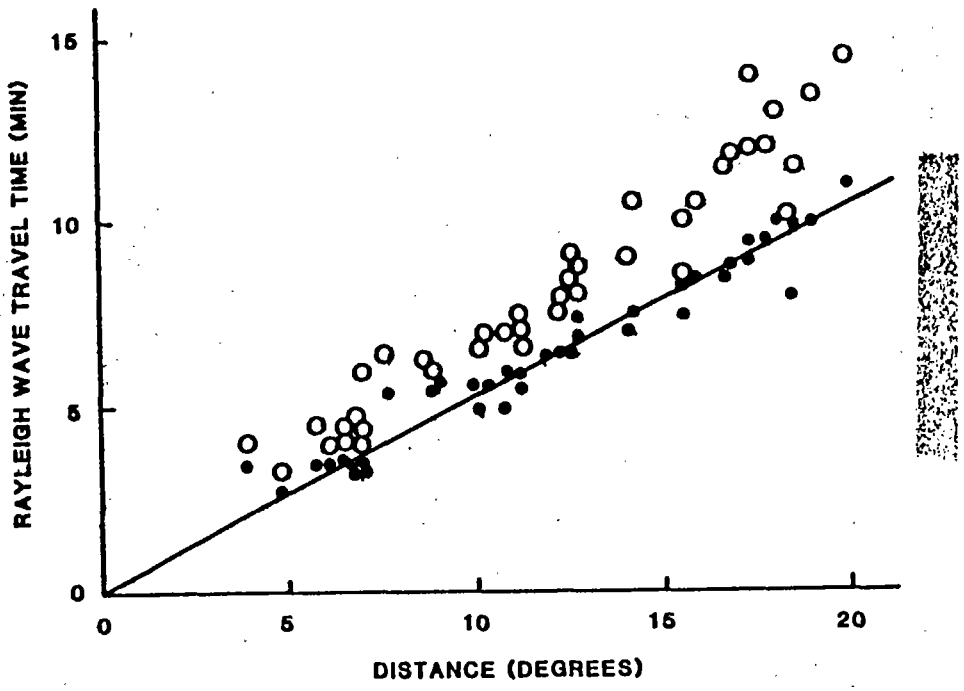

Fig. 3. Graph showing the Rayleigh wave travel time plotted as a function of distance. Dots indicate the wave travel time for various distances. Circles indicate the minimum time for the Rayleigh wave (18-22 seconds) to develop to a maximum for use in determining MS magnitudes (issue a warning).

Due to the ATWC's automation, an earthquake's location is available within seconds after 5 or more seismic stations receive data from a large earthquake. The main delay introduced in locating an earthquake is due to the P wave travel time from the hypocenter to the network of seismic sites. Earthquake locations for earthquakes in Alaska, and the west coasts of Canada and the U.S. are available within 1 to 6 minutes after the origin time. A WW is issued for an earthquake based upon the Richter MS magnitudes or the ATWC's regional magnitudes (Whitmore and Sokolowski, 1987). The travel time of the Rayleigh wave introduces a

delay in sizing an earthquake. This delay is dependent upon the distance of a long period site from an earthquake source. Therefore, to decrease the delay time for determining MS magnitudes to within 15 minutes, the ATWC has established long period Alaskan sites at Shemya, Adak, Sand Point, Palmer, and Sitka, and uses a few of NEIC's long period sites in the lower 48 states. Figure 3 shows the minimum time (circles) required to determine an MS magnitude (issue a warning) using long period sites between 5 to 20 degrees from a source. If a long period instrument is further than 20 degrees away, the time delay will be more than 15 minutes.

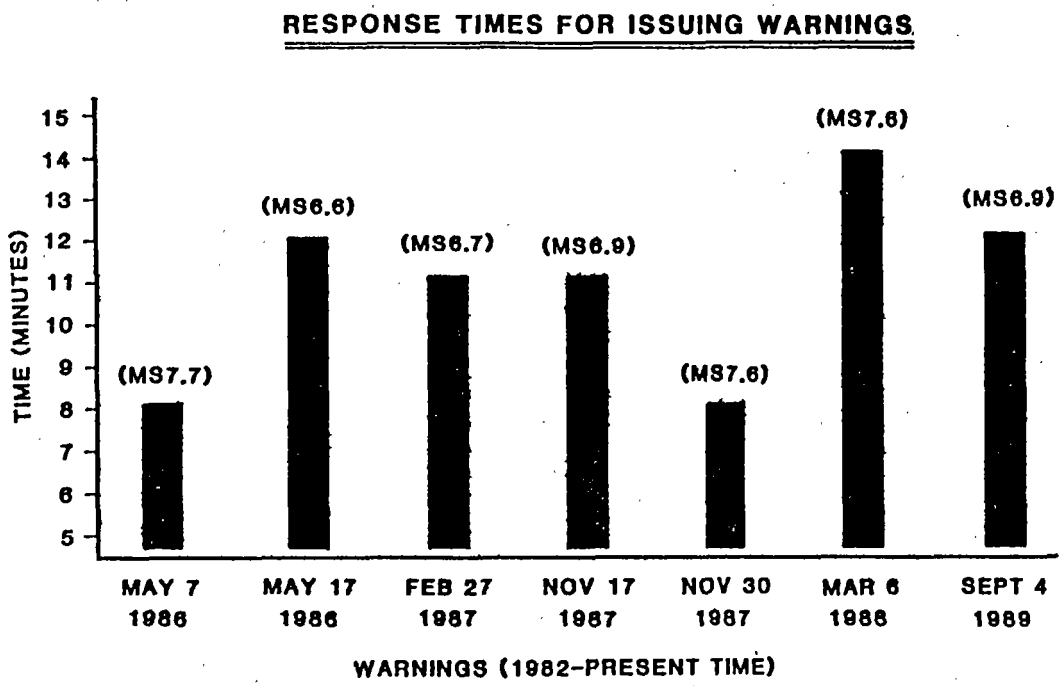

Fig. 4. Graph showing the response times to issue warnings from the earthquake origin time during the period from 1982 to the present time.

8. Tsunami Warnings

Since inception to the present time, 14 warnings have been issued by the ATWC with seven occurring during the period from 1986 through 1989. Two of the earthquakes (MS=7.7, 6.6) occurred about the Adak area in 1986 on May 7 and 17, and one (MS=6.7) in the Unalaska area on February 27, 1987. Three of the earthquakes (MS=6.9, 7.6, 7.6) occurred on the Pacific Plate, just south of the Yakataga seismic gap on November 17 and 30, 1987, and March 6, 1988. The remaining earthquake (MS=6.9) occurred on September 4, 1989 east of the Shumagin Is. Figure 4 shows the actual response time, in minutes, to issue warnings from the origin time of the earthquakes. Five of the past seven earthquakes for which tsunami warnings were issued occurred during standby duty hours, i.e. when the duty personnel are not in the Center. Only the May 7, 1986 and Nov 30, 1987 earthquakes occurred during office hours.

9. Historical Earthquake/Tsunami Data Base

The ATWC maintains a historical tsunami and earthquake data bases that were obtained from the National Geophysical Data Center (Lander and Lockridge, 1986) and from the National Earthquake Information Center. Menu-driven software was created to search the data bases for requested data and lists these on a printer. Figure 5 shows a block diagram to retrieve historical data. The tsunami data base is used during all warnings to determine past hazard occurrences in and about an earthquake source to facilitate decision- making. The earthquake data base contains more than 7000 earthquakes of magnitude 6.0 or greater that have occurred in the Pacific Basin. Earthquake information can be retrieved by year, latitude/longitude, or by Flinn-Engdahl region numbers. The earthquake data base is cross referenced to the tsunami data base which contains more than 1100 historical tsunamis that have occurred
in the Pacific Basin. The tsunami information (wave heights, damage, etc.) can be retrieved by year, latitude/longitude, and area. This information can be in summary (condensed) or detailed (expanded) form.

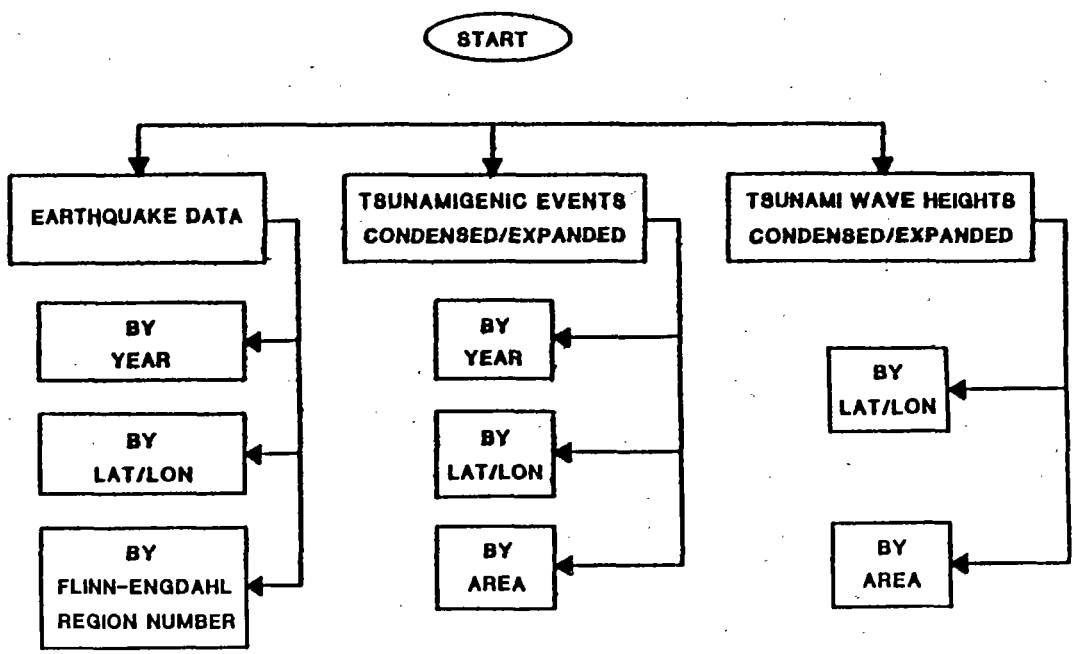

Fig. 5. Block diagram showing different methods to retrieve historical earthquake and tsunami data.

10. Communications

The main methods for disseminating emergency and routine information (U.S. Department of Commerce, 1987) are by the National Warning System (NAWAS), Alaska Warning System (AKWAS), National Weather Wire Satellite System (NWWS), commercial telephones, Alaska Division of Emergen-

cy Services, VHF radio system, high speed teletypewriter system (TTY), VHF Weather Radio, HF Marine Weather Radio, Emergency Broadcast System (EBS) through the National Weather Service, and EBS and HF via the Coast Guard. The NAWAS, a voice disseminating system, is the primary one used to alert disaster officials in the U.S. and Canada of large earthquakes. The AKWAS, which is the State side of NAWAS, permits immediate voice communication with Alaska disaster officials. The NWWS and high speed VDT teletype system provide recipients with hard copies of watch/warning and other information. All of these systems are monitored and tested very frequently to ensure that they are operational.

Communication transmissions to the ATWC that concern incoming real-time data communication circuits are checked on a daily basis with immediate corrective actions implemented as problems surface. The computer systems, which are interfaced with the teletype VDT for dissemination of warnings, are checked daily. As problems surface, actions are taken immediately to correct the problem or improve the equipment. Additionally, the ATWC maintains a list of critical telephone numbers that are frequently checked for validity to ensure contact with primary hazard officials during warning situations.

The NWWS is expected to be operational in 1989 for disseminating tsunami watches, warnings, and other information via satellite to recipients in Alaska, Washington, Oregon, and California. One of the two satellite dishes installed at the ATWC will permit information to be transmitted and received, while the other will have only receiving capability. This satellite ground station at the ATWC will also function as a backup system for the Alaska Region's ground station located in Anchorage.

11. Community Preparedness

The ability of any warning system to successfully save lives and reduce property damage depends upon getting the information to the public and getting them to respond to the emergency. To maximize the effectiveness of the community preparedness efforts, the ATWC cooperates with the Alaska Department of Emergency Services (ADES) and many other hazard officials on the west coasts of the U.S. and Canada, and the far western Aleutian Is. The aim of this program is to educate the public to help themselves if they are caught in the middle of a violent earthquake and/or tsunami, and to be aware of safety procedures, safe areas, and the limitations of the Tsunami Warning System. In general, the community preparedness presentations include: a slide show concerning earthquake/tsunami effects; discussions concerning earthquakes and tsunamis; a community's particular hazard potential (Carte, 1984) and their expected response; and the ATWC operations, missions, and capabilities.

All professional staff members participate in providing a three part community preparedness program which includes: visits to distant coastal communities from Adak to southern California; visits to local group facilities and schools that are within commuting distance of the ATWC; and tours through the ATWC's facilities. Frequent visitations are made

to those areas that are within reasonable driving distance from the Center, and visitations to outlying communities are made each year. Groups, such as schools, are encouraged to video tape the ATWC presentations for later use. Community preparedness is also done via telephone for special requests and projects that are received throughout the year. In addition to the outside visitations and presentations, the ATWC facilities are open to the public each Friday from 1 to 3 in the afternoon for local and other visitors. During these visits to the Center, the staff conducts a tour of the facilities with presentations concerning the TWS.

In addition to this ongoing program, special visitations are made by the ATWC staff to the communities that were evacuated during an actual tsunami warning and no significant wave action materialized. The purpose of these visitations is to explain the warning actions to the public and to stress the continued need to respond to emergency tsunami warnings.

12. Micro Computer Concept Leading to an Automated Expert System

Another ongoing effort at the ATWC is to seek improvements in the performance of all its missions by creating and implementing new concepts, initiatives, and equipment, and to enhance the effectiveness and efficiency of previous implementations. As a result of a feasibility study, a micro computer concept was introduced by Sokolowski (1985). This concept envisioned the use of several micro computers to address the initial ATWC improvement areas that were stated earlier in leading toward an expert system. The concept is evolutionary in that future tasks and additional micro systems can be integrated into the ATWC operations to enhance both the reactive and predictive parts of the operation. The micro systems are intended to communicate with each other via a local area network (LAN), or function independently, to perform both operational and administrative tasks.

Some initial advantages in using micro computers concern cost effectiveness, equipment, and personnel tasks. For cost effectiveness, there are significant savings in computer replacement costs, peripherals, and supplies which are available from many sources; computer maintenance; and power and space requirements. The hardware is constantly improving in its capabilities and can function as backups for critical units. The micros can be networked and modular, so that selective units can be replaced, upgraded, or added as growth dictates The units can be distributed in different work areas, thus maximizing aid for personnel and minimizing procedural response times in routine or emergency situations. Modular units permit a more effective use of personnel in performing their duties and technique developments.

Figure 6 shows the current micro computer concept which envisions 5 separate micro computer systems which are networked via a LAN system to perform their various functions. Several functions are duplicated due to the critical nature of the task, or to facilitate personnel duties and technique developments. The future micro computers are expected to use CPU's of the 386/486/586 variety, and make maximum use

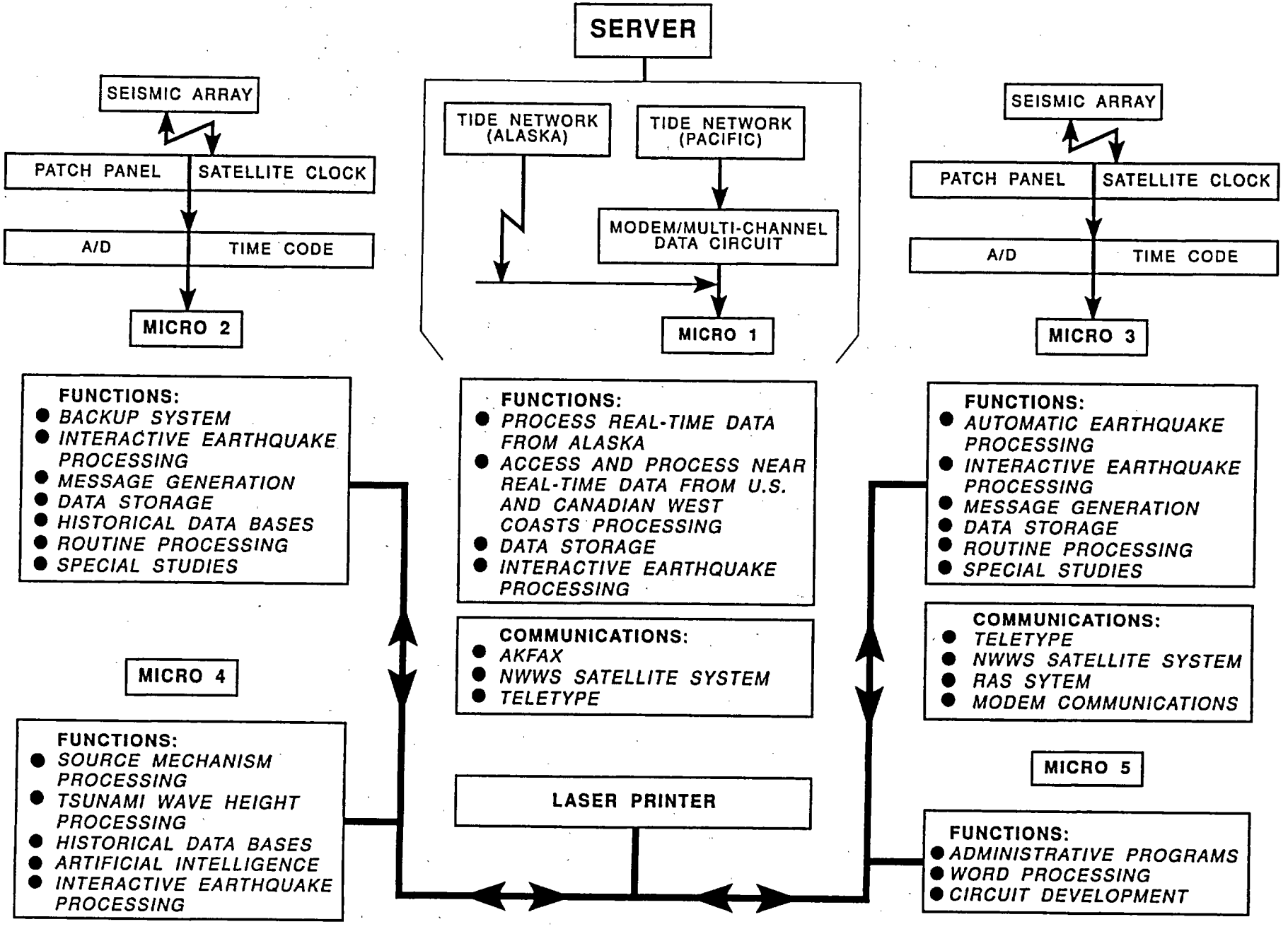

Fig. 6. Block diagram showing a distribution of micro computers which are networked via a LAN system to perform their indicated fuctions.

of common peripherals and equipment for printing, storage, etc. They will also have access to appropriate data bases. For redundancy, the micros will also have access to the major communication systems, such as the NWWS and TTY systems for disseminating/receiving critical data and information. The micros and associated equipment will be implemented as funding becomes available, and techniques are developed or become available to the ATWC. As additional task requirements evolve, additional micros can be added to the LAN or specific micro(s) can be upgraded. This provides a mechanism for keeping abreast of state-of-the-art equipment and for future technique developments and growth. Given below are summaries of some key functions of the 5 micro computers and associated equipment.

Micro 1 will be used as both a server (supervisor) of a LAN system, and for concurrent processing and analysis of tidal data from Alaska, and the west coasts of Canada and the U.S. The data are available to the ATWC in several ways. First, the NOS's water level telemetry systems have the capability of transmitting data directly to the ATWC in real-time from sites in Alaska. They can also transmit tsunami data from the Pacific Basin, via satellite, to the U.S. east coast. These data are available to the ATWC in near real-time through a dedicated circuit from the east coast to the ATWC for processing and analysis by this micro computer. Finally, this computer will also be capable of receiving tidal data in near real-time via a modem interface to the NOS Pacific sites. The tide station's data will be stored for rapid retrieval, analysis, and archiving. Micro 1, like the other micros, will have access to the the AKFAX, NWWS, TTY, storage devices, and printers.

Micro 3 is the current automatic real-time and interactive system which has been described earlier. It is the primary system for providing tsunami warning services to ATWC's areas of responsibilities. Since this micro has recently been placed into service, its future successor will be of a CPU type given above and does not have a high priority for replacement at this time. For redundancy, this micro has separate interfaces to the TTY, NWWS, RAS, and modem communication systems.

Micro 2 will function as a backup system to Micro 3, for routine processing and special studies. The same seismic array data that are routed to Micro 3 will be monitored and processed by this computer. Its CPU is a 386 type which has an additional CPU for receiving real-time data for subsequent signal processing in real-time. The key algorithms used in the automatic and interactive processing systems have been converted to run on this system. As development progresses, this system (or its successor) will eventually replace the DEC micro computer system.

Micro 4 will be used for source mechanism and tsunami wave height processing, and other topics which will involve artificial intelligence (AI) applications. The input for AI evaluation could include such knowledge as, earthquake parameters and source mechanism; actual tide heights at various locations; reasonable estimates of

expected tsunami wave heights at various locations; reasonable estimates of expected tsunami inundation from predicted tsunami wave heights, flood data, etc.; historical tsunami data, damage, and other information from various source regions; and, historical earthquake data from various source regions. In the near future, an initial AI study will begin using some accomplished results and existing data bases. This study will be continually enhanced to include other results and data as they are developed or become available to the ATWC.

The remaining micro will be used for administrative programs and routine staff functions. It is also used by the electronic personnel for designing circuitry and generating seismic response curves.

13. Conclusion

The ATWC continues to improve both the reactive and predictive areas of its operations. Since the early 1980's, numerous changes have taken place in areas, such as, operational concepts and procedures - especially in response to emergency situations; micro computer concepts; computers, peripherals and associated equipment; expanded area responsibility; seismic and tide networks; technique developments; community preparedness; and communications for disseminating critical information. The ATWC system is designed for speed, effectiveness, and efficiency. The integration of micro computers and developments have already made a considerable improvement in performing ATWC's missions. The ATWC continues to maximize its efforts toward an expert system that will be able to: (1) automatically detect and analyze seismic data in real-time; (2) immediately disseminate critical earthquake and tsunami information; (3) automatically detect and analyze tidal data in real-time or near real-time; (4) rapidly discriminate tsunamigenic from non-tsunamigenic earthquakes; and (5) determine reasonable estimates of probable tsunami wave heights and areas of inundation in the path of a tsunami. Due to the accomplishments in (1) and (2) above, the average response time to issue a warning has been reduced by more than 50%. In addition to timeliness, procedures have been considerably simplified and standardized.

Local, regional, and teleseismic earthquakes parameters are automatically computed and sized (mb,Ml) within tens of seconds after receiving appropriate data at real-time seismic sites distributed throughout Alaska and the lower 48 states. The automatic determination of an earthquake's parameters, plus the resident historical data bases has enhanced the accuracy and quantity of parametric data and the resulting information disseminated to the TWS recipients. Long period seismic instruments have been established at strategic coastal locations in Alaska to decrease the response time in computing magnitudes. The real-time data are automatically sized (MS), cycle by cycle, by the computer. Earthquake parameters are immediately available at the Center, and/or transmitted by a computer and RAS system to the ATWC staff for an immediate response. The new RAS system for alerting standby duty personnel has considerably improved the effectiveness of the ATWC personnel in performing their missions.

Tidal data are accessed and analyzed via micro computer in near real-time for Canada and the U.S. West Coast. New NOS tide equipment, and communications via new circuits, satellite, and micro computers will be used in the near future to access and analyze pacific tidal data in real-time and near real-time. A new satellite system with dishes established at the Center will enhance the ATWC's capabilities to immediately disseminate critical information to numerous areas. Getting the public to respond to critical earthquake/tsunami information is a vital part of the ATWC efforts and necessitates a continued and expanded educational community preparedness program. This program covers selected areas in large geographical areas, and in cooperation with other agencies and hazard officials. All professional staff members participate in this important part of the ATWC.

The integration of micro computers and ongoing technique developments are critical to the ATWC's momentum in improving its tsunami warning services to the coastal inhabitants for potential tsunamigenic earthquakes. These continual efforts involve the implementation of new concepts, additional computers, technique developments, and sophisticated equipment. Future efforts are expected to continue in the areas given above, and in other evolving areas such as, AI applications.

14. Acknowledgments

The author thanks the National Weather Service (NWS) and the Alaska Regional Headquarters for its continued support in automating the Alaska Tsunami Warning Center. The author also thanks those many past and present ATWC Staff members who have made important contributions over the years in various parts of automation projects. Lastly, the author especially thanks Mr. Stuart G. Bigler (former NWS Director of the Alaska Region) for his past significant support in ATWC projects that are now being realized.

15. References

Carte, G., 1984. A tsunami preparedness assessment for Alaska, Sci. Tsunami Haz., 2, P. 119-126.

Kanamori, H., A numerical experiment on seismic tsunami warning network for Alaska and the Aleutians, Proceedings of the International Tsunami Symposium, IUGG, 1985, edited by T.S. Murty and W.J. Rapatz, P. 30-39.

Lander, J.F. and Lockridge, P.A., National Geophysical Data Center's Tsunami Data Base (Personal Contact, 1986) National Geophysical Data Center, Boulder, Colorado.

Okal, E.A. and Talandier, J., 1989. Mm: A variable-period mantle magnitude, J. Geophys. Res., 94, P. 4169-4193.

Sindorf, J. G., 1972. Determining magnitude values from the Lg phase from short period vertical seismographs, Earthquake Notes, Seismol. Soc. Am., 3, P. 5-8.

Sokolowski, T.J. and Miller, G.R., 1967. Automatic epicenter locations from a quadripartite array. Bull. Seismol. Soc. Am., 57, P. 269-275.

Sokolowski, T.J., 1974. Feasibility Proposal for the Initial Automation of the Tsunami Warning System. National Weather Service, Pacific Region Report. 22pp.

Sokolowski, T.J., 1978. Initial Automation of the Pacific Tsunami Warning Center. (unpublished) 11pp.

Sokolowski, T.J., Fuller, G.W., Blackford, M.E. and Jorgensen, W.J., 1983. The Alaska Tsunami Warning Center's automatic earthquake processing system, Proceedings of the International Tsunami Symposium, IUGG, 1983, edited by E.N. Bernard, P. 131-148.

Sokolowski, T.J., 1985. The Alaska Tsunami Warning Center's Responsibilities and Operations. Sci. Tsunami Haz., 1, P. 23-33.

Sokolowski, T.J., 1985, Mini and micro computer applications at the Alaska Tsunami Warning Center. Proceedings of the International Tsunami Symposium, IUGG, 1985, edited by T.S. Murty and W.J. Rapatz, P. 174-181.

Sokolowski, T.J., and Whitmore, P.M., and Jorgensen, W.J., 1989, The Alaska Tsunami Warning Center's automatic and interactive earthquake processing system, 1989. Presented at the Tsunami Symposium in Novosibirsk, USSR, August 1989. Submitted for publication in Proceedings of the International Tsunami Symposium, IUGG, 1989.

U.S. Department of Commerce, 1988, National Oceanic and Atmospheric Administration, National Weather Service, Communication Plan for the Tsunami Warning System, Eleventh Edition. 123 pp.

Whitmore, P.M. and Sokolowski, T.J., 1987. Rapid Sizing of Potentially Tsunamigenic earthquakes at Regional Distances in Alaska, Sci. Tsunami Haz., 2, P. 67-76.

JAPAN TSUNAMI WARNING SYSTEM

N. Hamada
Earthquake and Tsunami Observation Division
Japan Meteorological Agency
Tokyo, Japan

1. Tsunami Warning Service in Japan

The Japan Meteorological Agency (JMA) is responsible the for Tsunami Warning Service in Japan since 1952.

Tsunami warnings and advisories are handled by the Earthquake and Tsunami Observation (ETO) Division of the Seismological and Volcanological Department of JMA. Because of the localized nature of earthquakes and tsunamis, the Japanese archipelago is divided into six regions covered by local centers located in 6 key cities; Sapporo, Sendai, Tokyo, Osaka, Fukuoka and Naha. These local centers are operated by the District Meteorological Observatories under JMA except for the Tokyo Center.

An individual local center issues warnings and advisories for tsunamis generated by earthquakes in the responsible areas, within 600 km from the designated stretch of the coastline. For the areas outside the 600 km zone, the ETO Division, serving both as the local center for the Tokyo region and as the national center, assumes responsibility, relying much on information from the Pacific Tsunami Warning Center (PTWC) in Honolulu.

2. Present Status of Tsunami Warning Operation

A modern seismological data acquisition and processing system which is called Earthquake Phenomena Observation System (EPOS) was developed and is in operation since March, 1987 in the Headquarters of JMA. EPOS is composed of a group of super mini-computers, telecommunication links and telemetering facilities which are connected with more than 60 seismological stations, including two Permanent Ocean Bottom Seismograph (POBS) systems.

EPOS uses an automatic event detection and identification algorithm for picking P and S wave arrivals in the telemetered seismic signals by use of the AR (Auto-Regressive) stochastic model. The hypocenter location and estimation of magnitude are automatically executed. If the size and location of an earthquake satisfies some criterion for tsunami

generation, the warning service is successively conducted by the System. Based on the above analyses including some interactive process for verifying the analyses, the duty officer makes a final decision and tsunami messages are automatically generated by and issued through the System to field offices of JMA, relevant governmental bodies which are concerned with disaster mitigation, and the media, including radio and TV stations. The time required for the service, from detection of earthquake to dissemination of Tsunami warning, has been shortened to 8 minutes in average.

At other local centers, a somewhat older computer-oriented meteorological and seismological data acquisition system called L-ADESS (Local Automated Meteorological Data Editing and Switching System) is used for tsunami warning services. Seismic signals exceeding a threshold value activate a disk drive, chart recorders and an alert buzzer. From the chart recorder's traces the duty officer inputs P and S arrival times and amplitudes of seismic waves into the computer by using an X-Y digitizer. Under the supervision of the duty officer, the computer determines hypocenter and magnitude, the possibility of tsunami occurrence, the warning level, and then produces wording of warning and/or advisory. A touch of a button transmits the warning messages to various concerned organizations. The average time needed to issue the warning by this system is about 13 minutes presently. Next March, L-ADESS in Sendai District Meteorological Observatory is to be upgraded to the new system which is equivalent to EPOS to its function for tsunami warning services.

3. Emergency Warning System

A system designed to turn radio and television receivers on automatically in response to signals sent from broadcasting stations was developed and is in operation since 1985. This new system called Emergency Warning System (EWS) requires a special dedicated receiver. The EWS is used in cases where information about disasters must be disseminated urgently and widely by broadcasting. These cases include: (1) Earthquake Warning Statement issued by the Prime Minister according to the provisions of the Large-scale Earthquake Countermeasures Act (for the Tokai Earthquake); (2) Tsunami warning; and (3) Legal measure requested by a prefectural governor. Leading and regional 44 TV and radio broadcasting stations already joined the EWS for the rapid dissemination of tsunami warnings.

TSUNAMI WARNING SYSTEM IN THE USSR

Boris A. Kouznetsov
Yuzhno-Sakhalinsk, USSR

The disastrous tsunami of November, 1952, practically wiped away the town of Severo-Kurilsk. Many of its residents perished by it. The catastrophe, among other things, was responsible for the creation, in 1956-1958, of the Tsunami Warning System (SPTS is the Russian acronym) in coastal regions of the Soviet Far-East. The system serves a territory which stretches for nearly 4500 kilometers, and which is seismically highly active. In fact, it is one of the most active on our planet with nearly 80% of all earthquakes in our country occurring here, as well as pratically all of the tsunamis. The epicenters of potential tsunamigenic earthquakes are located in the immediate proximity of the region, and travel times of generated tsunami waves to the closest settlements vary from 15 or 20 minutes up to an hour.

These factors and the absence of necessary communications account for the system's structure and its specific characteristics. The basic system comprises of tsunami stations at Petropavlovsk-Kamchatsky, Yuzhno-Sakhalinsk and Kurilsk. Each of these stations functions independently, issuing warnings of possible tsunamis, based on seismic information alone for a fixed area.

The basic principles of the system's operation have remained the same until now, although some expansion and equipment updating have taken place.

Presently, five seismic stations provide seismological data for the USSR Academy of Sciences. They are located at Petropavlovsk-Kamchatsky, Yuzhno-Sakhalinsk, Severo-Kurilsk, Kurilsk, and at Shikotan Island. Until now the tsunami warnings are issued by seismologists at these stations on the basis of seismograms, and partially processed by hand, using special nomograms. In doing it that way, up to 10 minutes of time may be lost since the beginning of earthquake registration. The precision of the computation depends on personal skills of the seismologist on duty with errors of 100 km for epicenter coordinates and up to about 0.2 for earthquake magnitudes. Such errors combined with the conditional character of adopted alarm thresholds related to earthquake magnitudes, result in a number of false alarms. On the average 3 out of 4 of all alarms are false. Furthermore, sometimes major tsunamis occur without detection as those of June 10, 1975 and of May 26, 1983.

The system's operation was somewhat improved when the boundaries of the tsunamigenic zones were defined more precisely, when the magnitude thresholds were made more exact, and when the earthquake focus depth was taken into account. At the same time more attention was given to issuing warnings of tsunamis generated from local Kurile-Kamchatka earthquakes. Notwithstanding its regional character, the USSR Tsunami Warning System is constantly busy monitoring seismic activity throughout the entire Pacific basin.

Among the basic flaws of the tsunami warning service is the absence of operational communications between the seismic stations which make impossible the collective processing of data and the correction of errors of individual seismologists. The Ministry of Communications is responsible for providing communications to the Tsunami Service. Also, communications of the USSR Ministry of the Merchant Marine, of the Ministry of Fisheries, and of the State Committee for Hydrometeorology (Goscomgydromet in Russian), among others are used. However, until recently the tsunami information was transmitted through public channels, which were rather unreliable and inefficient.

The Automated Tsunami Warning System in Kamchatka district became in 1977 the first experimental action taken to improve tsunami warning communications. The system ensures transmissions within 1 minute with probability of no less than 0.995. A broadcasting radio station is used for transmissions of signals, then the information is disseminated to local authorities and the population via telephones, sirens and internal communications. Three types of messages are provided: warning about a local earthquake; tsunami warning; and cancellation of tsunami warning.
The messages are tape recorded at the local post offices.

Among the drawbacks of this system is the limited character of the types of transmitted messages as compared with the power of equipment, and the absence of simple individual receivers.

A hydrophysical subsystem belonging to Goscomgydromet is responsible for issuance of warnings for tsunamigenic earthquakes at distant regions of the Pacific. Also, Goscomgydromet is responsible for the overall coordination of activities among concerned Ministries and departments in organizing the timely tsunami warning for the coastal areas of the Far East, in the supervision of these activities; and in the operative interaction with foreign centers.

The hydrophysical subsystem is dependent on the already existing hydrometeorologic stations, in the Kamchatka and Sakhalin regions, and in the Maritime territory. Since

the tide gauge recording system was not originally intended for tsunami observations, these recorders are of limited range. The recorders may ensure sea level observations of only 2 or 3 meters higher than the maximum tide level, while the estimated height of a tsunami wave could be as much as 20 meters. Thus, tsunami observations are carried out visually, taking the observer's security into consideration.

Organizing the evacuation of population is the responsibility of the Civil Defense, local authorities and departments. Until 1989, it took from 20 to 30 minutes from the moment when a tsunami was observed to begin evacuation. Often 20 or 30 minutes proved unacceptable.

Historically most damaging tsunamis have occurred in actively developed territories. This is because residential development has taken place near industrial centers. In case of a tsunami, evacuation is extremely difficult depending on the hour of the day or night and on climatic conditions particularly in the Kuriles, and particularly in winter. Measures are being taken to remove such development out of the tsunamigenic zones.

Recreational and vacation areas usually visited by thousands of people must be protected also. Other popular areas such as beaches and popular off-shore ice fishing sites especially vulnerable to tsunamis, must be protected.

Most of the cities, towns and other settlements are situated in the coastal zones. In developing the Far-Eastern region of our country, and bearing in mind the importance of the security of population in these areas from tsunamis, the USSR government issued a Decree setting up an Atuomated System of observing the tsunami origin and propagation and the tsunami warning (Russian acronym - EASTS), which must be made part of the presently operating Tsunami Warning System. The new system must provide maximum automation for collecting and processing seismic and tidal data, and issuing appropriate warning messages to areas where tsunami impact is expected. The first phase of the proposed operational system is planned for 1990.

The catastrophic earthquakes in Armenia and Tadjikistan together with the increase in seismic activity in USSR established the need for additional measures to upgrade efficiency of the present system. To accomplish this a department was established, technically equipped, and with an updated library of tsunami literature within the operational Tsunami Warning Center in Yuzhno-Sakhalinsk.

A system of automated issuance of tsunami information was initiated which includes teletype messages, and which has made it possible for scientists on duty to transmit domestic and foreign information at the same time.

A direct telephone connection has been installed with the Civil Defense, as well as with the Central Telegraphic Office, and other important organizations.

Presently the transmissions of the tsunami watch to threatened regions are conducted through a telephone system of higher reliability. Now it takes 1 minute to transmit a message instead of 15 or 20 minutes as before. Also, the automated system provides immediate activation of sirens, street loud-speakers, house intercoms and simultaneous transmissions of information over telephones. With proper public education and preparedness, urgent evacuation of threatened areas is possible. Experience shows that it is easier to address technical matters than to organize preparedness and training. For this reason the dissemination of educational tsunami booklets has been recently initiated. Preparedness includes now media coverage and appropriate lectures of interested groups. In spite of such action the high number of false alarms creates mistrust among the population who ignore directives of evacuation. Also, it should be pointed out that the residents of the Kurile Islands have grown accustomed to volcanic eruptions, typhoons, frequent earthquakes, and other natural disasters. The situation is especially complex in winter, when the snow storms, tempestuous winds and resulting impassibility of roads make evacuation extremely difficult. For example, in the town of Severo-Kurilsk snow drifts of many meters of height are in the streets as late as May, and sometimes even in June. Therefore, it is urgent to forbid residential development in tsunamigenic zones. Such measure may be regarded as one of the most efficient in terms of preventing disastrous tsunami effects.

The combination of a potentially dangerous tsunami and difficult climatic conditions puts our service into especially complicated circumstances as compared with similar services elsewhere. Once more, it explains why greater efforts should be undertaken in improving the system's operation.

Presently, scientists work independently at the centers of Petropavlovsk-Kamchatsky and Yuzhno-Sakhalinsk. In Vladivostok there is only a group of oceanologists. In Yuzhno-Sakhalinsk, it is the seismologists who provide seismic service for the area of Vladivostok and of the Maritime territory. These groups are now communicating by means of direct telegraphic lines. However, the data is not processed collectively so far. It will not be until the year 1991 that we will be able to produce all the elements of the automated system.

It will be economically and technologically reasonable when similar technical means as those used by tsunami services abroad including communications and technology, are applied in our system.

We are taking measures to introduce modern computers and technology into the present system. It is important for us because we are located near potentially destructive tsunamigenic sources. Presently, we cannot issue tsunami warnings in a shorter period.

The application of computers will enable us to improve the scientific and methodological grounds of the service. Presently tsunami travel charts have been prepared for all the threatened areas in the coastal zones. The operational manuals are being written and scientific and methodological literature is being prepared.

We follow closely the achivements and trends in all aspects of development of our foreign counterparts, especially the Japanese ones. Our close proximity accounts for the fact that we share concerns and priorities.

As mentioned earlier, the department of the operational tsunami warning within the Yuzhno-Sakhalinsk Tsunami Center was set up recently. Unfortunately there are no specialists among our employees who might be knowledgeable in several disciplines, or possess certain managerial talents. This is why we are very much interested in extending ties of cooperation with tsunami specialists of other countries.

FRENCH POLYNESIA TSUNAMI WARNING CENTER (CPPT)

J. TALANDIER

Laboratoire de Géophysique, Commissariat à l'Energie Atomique,
Centre Polynésien de Prévention des Tsunamis,
Boîte Postale 640, Papeete, Tahiti, French Polynesia.

Abstract

Since 1964, the Geophysical Laboratory has been charged of Tsunami Warning. But this research laboratory is also designed to other missions. One of whom is the study and oversee seismicity and volcanism of South Central Pacific. For this activity the Geophysical Laboratory, which is also the French Polynesia Tsunami Warning Center (Centre Polynésien de Prévention des Tsunamis - CPPT) disposes of the data recorded by the Polynesian Seismic Network which includes 21 short-period stations, 4 broad-band three components long period stations and 2 tide gauge stations. This stations are, for the most, telemetred toward the CPPT in Tahiti which is equiped with data processing means.

The data acquisition is performed on optic discs, tape drive recordings and graphic recordings.

In the CPPT, the Tsunami Warning is based on the measurements of the Seismic Moment through the mantle magnitude Mm and the proportionality of observed tsunami height to this seismic moment.

The new mantle magnitude scale, Mm used the measurement of the mantle Rayleigh and Love wave energy in the 50-300 s. period range and is directly related to the seismic moment through Mm = log Mo - 20. The knowledge of the seismic moment allows computation of an estimate of the high-seas amplitude of a range of expectable tsunami heights.

The formula estimating the tsunami height according to seismic moment is justified on the basis of normal mode tsunami theory but also fits a dataset of 17 tsunamis recorded at Papeete (PPT) since 1958.

In establishing seismic thresholds for tsunami warning, we assume that tsunami risk is substantial when the upper found on the amplitude predicted at PPT reach 1 m. On this basis, the risk levels have been identified as a function of the magnitude Mm. For the Polynesian Islands the destructive tsunami danger would subsequently exist for Mm $\geq$ 8.7 (Mo $\geq$ 5 X 10^{28} dyn-cm), in the case of epicenters in Samoa, Tonga, Kermadec and Mm $\geq$ 9.0 (Mo $\geq 10^{29}$ dyn-cm) for other farther epicenters.

This procedure is fully automatic : One computer detects, locates and estimates the seismic moment through the Mm magnitude and, in terms of moment, gives an amplitude window of the expected tsunami. This different operations are executed in real time. In addition, the operator can use the historic references and, if necesary, the acoustic T waves.

This method with its automatic procedure, which operates at the CPPT since 1986, is certainly transposable and applicable to other teleseismic warning centers.

Introduction

Following the major 1964 Alaska Earthquake the Geophysical Laboratory has been charged of Tsunami Warning. However, this Laboratory is a Research Center in Geophysics, also designed to others activities. One of whom is the study and oversee of seismicity and volcanism in South Central Pacific (There are 5 active volcanoes in this area, the Mac-Donald and the volcanoes related to the Mehetia hot spot). Broadly speaking the Geophysical Laboratory is charged of the survey of the physical environment of this area.

Concerning the means as well as the equipment, those different tasks can't be dissociated. In order to carry out its missions,the Geophysical Laboratory disposes of the data recorded by the Polynesian Seismic Network (Réseau Sismique Polynésien : RSP) which was created at the early sixties and includes 21 short-period stations, 4 long-period broad band stations and 2 tide gauge stations. The RSP also deals with different measures recorded at the main Laboratory in Tahiti. Situated near the city of Papeete, this Laboratory is a Research Center equiped with data processing means. It includes also the French Polynesia Tsunami Warning Center (Centre Polynésien de Prévention des Tsunamis CPPT).

Polynesian Seismic Network

The Polynesian Seismic Network is situated in a huge approximately triangular area which extreme distances are 1.000 km between Rangiroa and Tubuai, and 1.800 km between Tahiti and Rikitea. Figure 1 shows the geographical locations of stations used by the CPPT.

It includes 21 short-periods divided in telemetred sub-networks and in two single stations in Tubuai (Austral Islands) and Rikitea (Gambier Islands). Distant from 350 km, the sub-networks of Tahiti, Moorea, Tetiaroa, Mehetia (8 stations) and Rangiroa (4 stations), are telemetred in real-time to the CPPT (figure 2). Eventually the sismogram of Tubuai and Rikitea are transmit by satellite connection.

The 4 central stations of the Tahiti, Rangiroa sub-networks , Tubuai and Rikitea, are equiped with broad-band 3 components long-period instruments. Tahiti is also a part of the Geoscope Network. Finally, Rikitea and Papeete are equiped with tide gauges, the last one telemetred to the CPPT.

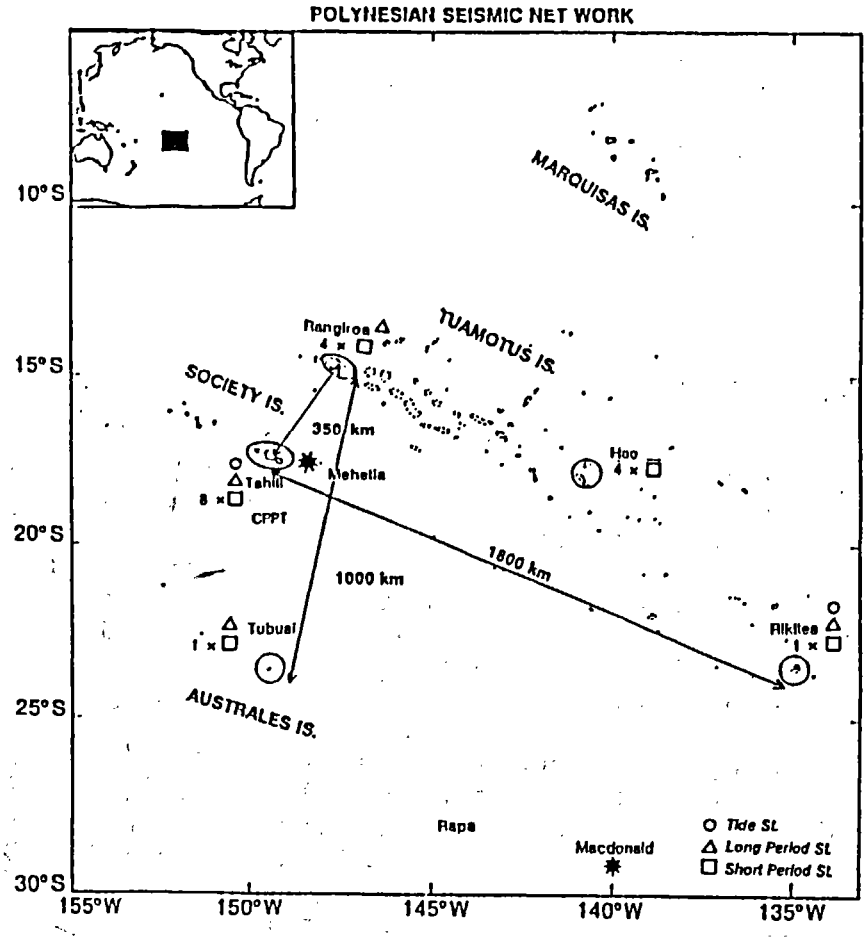

Figure 1

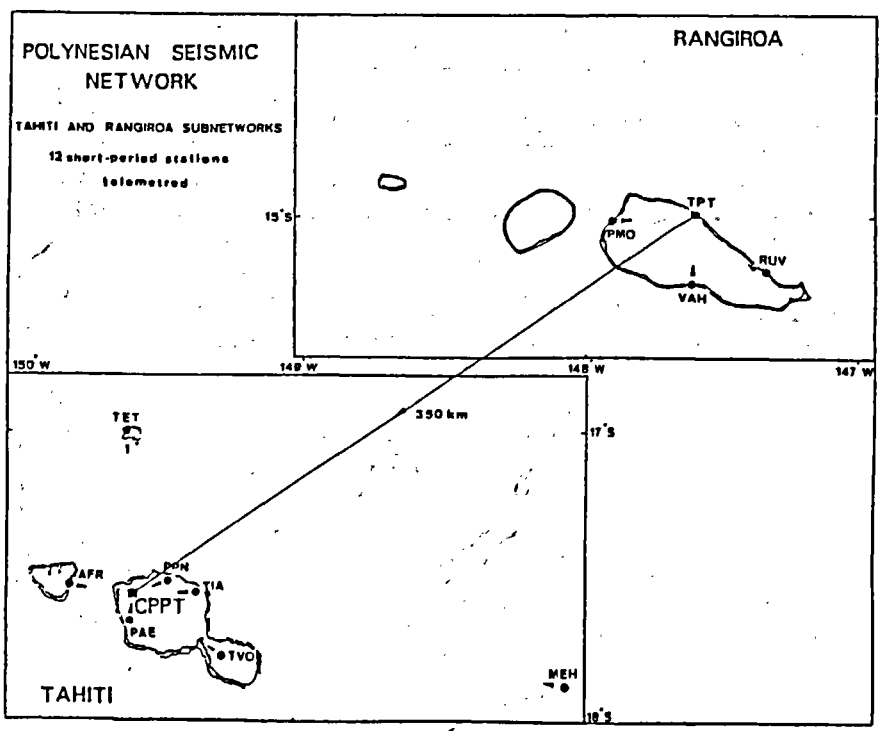

Figure 2

In order to exchange fast information independently of the real-time telemeasures, a phonic transmission links each sub-network including Tubuai and Rikitea to the CPPT in Tahiti.

EQUIPMENT

1 - Data Acquisition :

The acquisition of all data centralized at the Geophysical Laboratory, and therefore at CPPT in Tahiti, is carried out by a Hewlett-Packard computer 9000/400 (24 Mb of memory) with two optic discs of 650 Mb and a hard disc of 670 Mb. This computer executes also the real-time processing to determine earthquake parameters (Detection, location, Mm and Mo calculations etc...for tsunami warning and others missions - see next section).

The computer digitizes continuously 40 channels sampled at 50 samples/second and 40 channels sampled at 5 samples/second, and conditioned with anti alias filters.

This acquisition processing and analysis system covers the entire spectrum of the seismic waves between 24 hours of period (Earth Tide) and 20 hertz. The recording is on scale for very small local earthquakes, large regional earthquakes and major teleseisms such as the Chili earthquake of May 22, 1960 of 4 X 10^{30} dyne-cm. The dynamic range is 117 db in short periods and 152 dB in long periods.

This system is connected by an Ethernet line with the main computer system for further off-line analysis.

A HP 9000/320 computer equiped with an optic disc, tape drive and hard disc carries out the reading of old data recordings for deferred processing and analysing. It is also connected by an Ethernet line to the main computer system.

2 - Computer System Configuration

The main computer system wich is operating at the CPPT (and the Geophysical Laboratory) consists of an other Hewlett-Packard computer, 9000/400 (24 Mb of memory) under UNIX system with a hard disc of 670 Mb, many work stations and personal computers. This system is in network and connected with others magnetic discs, floppy disc drives, tape drive, printers, plotters and graphic terminals.

A personal computer using a 1200 bps Modem is connected to international data bases and research organisms. Finally two old HP computers 9000/520 with their peripherics are still used but are not connected with the main system.

3 - Seismometers

In short periods, the seismometer is a velocity sensor type ZM 500 (Vertical) and HM 500 (Horizontal). LDG/FRANCE.

- Normal frequency : 1 Hz
- Damping factor : 0,7
- Sensitivity : 3200 V/mm at 1 Hz.

In short periods the digital records is directly the transfert function of the sensor.

In long period the seismometer is a broad band feedback sensor type LDG/FRANCE with two electronic integrators to obtain the ground displacement from 1 to 300 seconds or 1 to 1000 seconds for records of high or weak sensitivity.

Note that use of feedback sensor avoid the non linearity effects observed with the velocity sensor for the great displacements.

Others sensors and tiltmeters are used for the very long period.

Figure 3 shows (top) an example of broadband record at PPT station. Note the prominent mantle Rayleigh waves. (Bottom) Frequency response of the broadband system at PPT.

4 - Varied equipment :

A teleprinter directly received the HANDAR-GOES platform data of the Rarotonga (Cook Islands), Christmas, Nuku-Hiva (Marquesas Islands), Easter Islands and, in the near future, Niue Island. This teleprinter is used also to communicate with the other centers of the Pacific, still PTWC and ATWC.

An electronic system detects the seismic waves (DES - Detecteur d'Evenement Sismique) and warns the geophysicist in charge of an important earthquake (From Mm 5,0 or Ms 6,0). Immediate response of the staff in watch is required when the office is not manned, during nights, week-ends and holidays.

This warning system is operating at each main station of the seismic network (Tahiti, Rangiroa, Tubuai, Rikitea). To make assurance double sure, the warning by telephone is doubled.

5 - Graphic Recordings :

The permanent short and long-period graphic recordings cover a large dynamic in many sensitivities and bandwidths.

a) Three magnifications for each of the 21 short period stations : (Figure 4)

- 2×10^6 at 3 Hz
- 125,000 at 1 Hz
- 7,000 at 1 Hz

Rolling speed 2,5 mm/sec.

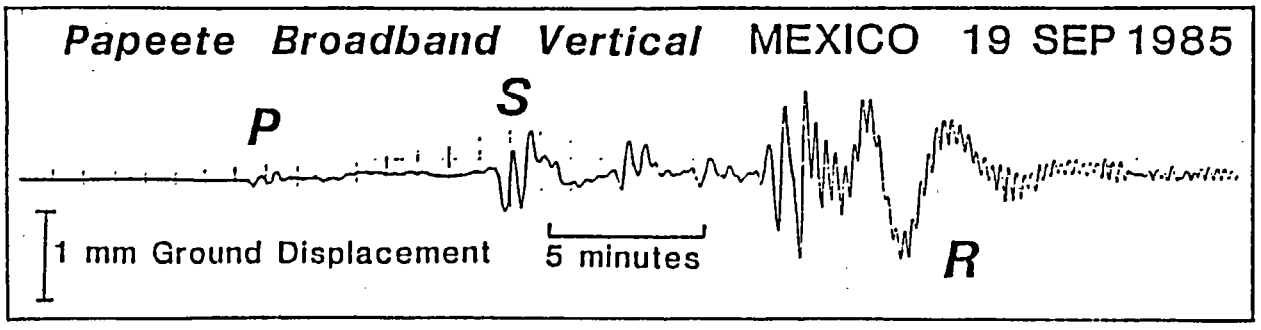
Papeete Broadband Vertical MEXICO 19 SEP 1985
P
S
R
1 mm Ground Displacement
5 minutes

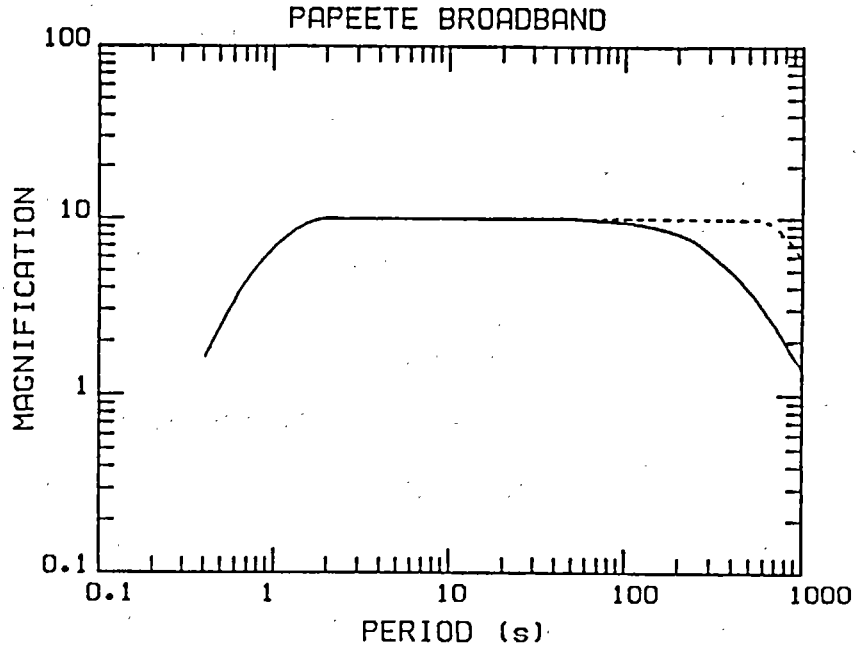
PAPEETE BROADBAND
MAGNIFICATION
100
10
1
0.1
0.1
1
10
100
1000
PERIOD (s)

Figure 3

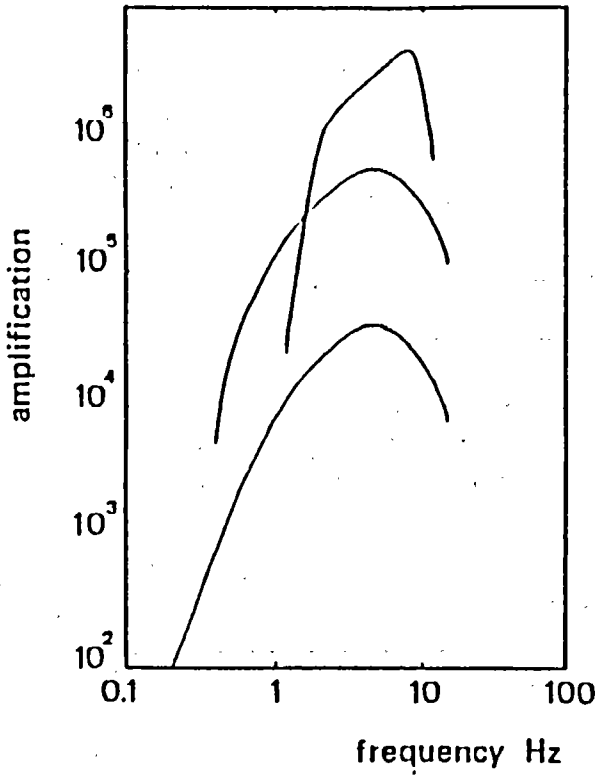

SHORT PERIOD INSTRUMENTAL RESPONSE

OF GRAPHIC RECORD

Figure 4

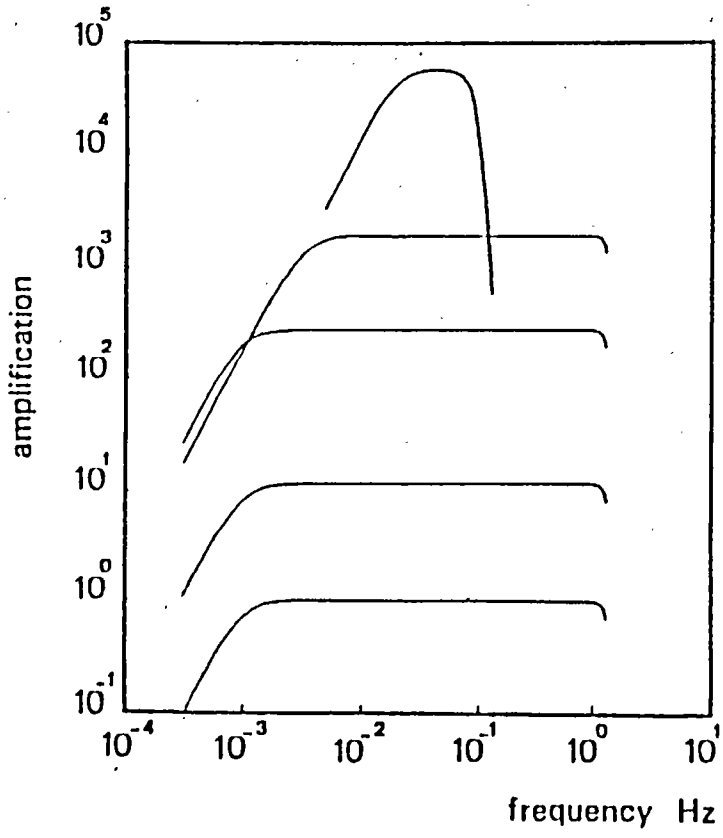

LONG PERIOD INSTRUMENTAL RESPONSE

OF GRAPHIC RECORD

Figure 5

b) Six magnifications with flat displacement response for long-period broad-band 3 components stations of Tahiti. Two magnifications for others 3 stations : (Figure 5)

- 56,000 (12 at 60 sec.) - 2,000 (8 at 60 sec.) - 280 (1 at 300 sec.) - 56 (1 at 1000 sec.) - 12 (1 at 1000 sec.) - 1 (1 at 1000 sec.)	Rolling speed 20 mm/min.

c) Three magnifications with flat acceleration response, for Geoscope VLP, 3 components station of Tahiti :

- 1.3×10^6 - 1.3×10^5 - 1.3×10^4	Rolling speed 5 mm/min.

However, because of the good quality of the on line real time detection and analysis system, some of these graphic recordings should be suppressed at an early date.

METHOD

1 - Tsunami Warning generality :

The ideal answer for tsunami teleseismic warning is the determination of the expected tsunami amplitude in a given place according to the seismic waves features. In this way, the CPPT infers the seismic moment of the Mm magnitude and values the tsunami amplitude according to the experimental relation theoretically justified linking these two parameters.

Now in use and entirely automatic, this method improved in course of time. Nevertheless, from the beginning in 1964, the CPPT applied itself to evaluate the tsunami risk, according to the seismic data it recorded, following the above process :

Detection ⟶ Location ⟶ Risk estimation according to the seismic source size.

At that time and approximately during two decades, the CPPT tsunami risk estimation was based on the acoustic T waves duration length, propagating in the oceanic SOFAR channel. It gives an estimate of the seismic moment Mo which represents the seismic source size and is the main parameter monitoring a tsunami generation. The T train of waves length increases as the rupture length at the source, proportionately to $Mo^{1/3}$. However the generation, propagation and conversion at the arrival on the coast are monitored by the sea bottom bathymetry which complexity escapes our understanding. This induces a heavy dispersion that can't ever be constrained by a regionalization.

Rayleigh waves representing low frequency energy radiated by the event give a better and faster determination of Mo. Unfortunately the Ms magnitude which uses this Rayleigh waves saturates when the rupture length along the fault becomes comparable with the period used for the measure. This saturation, which is due to the destructive interference resulting from the spatio temporal extent of the seismic source, appears on figure 6, which shows the spectrum at the source of that surface wave. Thus for large earthquakes, and in particular those causing tsunami risk, Ms measured at 20 sec., a fortiori mb measured at one sec, loses significance.

2 - Magnitude Mm

Measured on the flat portion of the source spectrum, at a frequency less than the corner frequency, the Mm magnitude avoid this saturation effect.

The development and measurement of Mm are based on the theory of excitations modes and surface waves by seismic source. The effects of propagation and of source excitation are separate. Accordingly, to recover the seismic moment from the amplitude spectrum of rayleigh wave we use this expression, where C_D is a distance correction and C_S a source correction.

$$Mm = \log X(\omega) + C_D + C_S - 0.9 \qquad (1)$$

In order that the usual graphics recordings could be used, Mm can also be determinated in the time domain with this relation where a is the amplitude (zero to peak) and T the period :

$$Mm = \log(a.T) + C_D + C_S - 1.2 \qquad (2)$$

The distance correction C_D reflects the geometrical spreading on the spherical earth and corrects for an anelastic earth regionalized into seven tectonic provinces along a 10° X 10° coordinate grid.

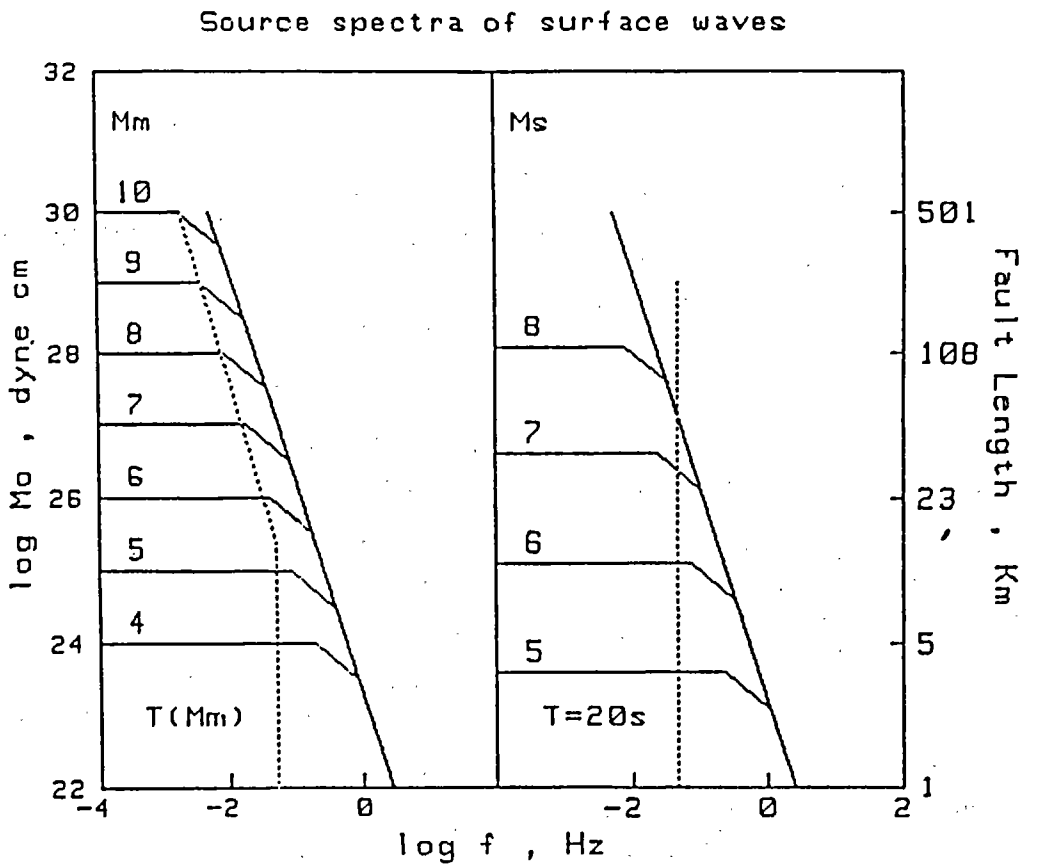
Source spectra of surface waves
Mm
Ms
10
9
8
7
6
5
4
8
7
6
5
T(Mm)
T=20s
log Mo , dyne cm
log f , Hz
Fault Length , Km
32
30
28
26
24
22
501
100
23
5
1
-4
-2
0
-2
0
2

Figure 6

The source correction Cs take into account the excitability of the Rayleigh waves in function of the focal depth and frequency.

Finally Mm is directly linked to the seismic moment by this simple formula :

$$\text{Log Mo} = \text{Mm} + 20 \quad (\text{Mo in dyne-cm}) \qquad (3)$$

In the same way Mm can be calculated with Love waves, in the frequency domain, following the same principle. Tectonics models and source correction are their adapted. The combination of values of Mm obtained by the Rayleigh and Love waves provides an additional safeguard against the problem of a nodal station. (Okal and Talandier, 1990).

Mm is accurate for great distances and multipathing but also for the short distances, at least 3 degrees.

Mm is accurate for small earthquakes, at least 10^{23} dyne-cm and, without upper limit for the great earthquakes.

Therefore, Mm is an universal magnitude scale perfectly adapted to the measurement of large and small earthquakes, and to tsunami risk estimation.

One can refer to Okal and Talandier, 1987 ; 1989 and Talandier and al, 1987 for more precision concerning this magnitude scale Mm.

3 -Seismic Moment and Tsunami Amplitude Relation :

In addition to the real time seismic moment determination, through the Mm magnitude, the fundamental criterium on which is based the prevention method used by the CPPT is the proportionality of observed tsunami height to the seismic moment. This direct relation is justified by the normal mode tsunami theory and is experimentaly verified according to the amplitude of the 17 tsunamis recorded in Papeete harbor since 1958. (Talandier and Okal, 1988 ; 1989). On the figure 7 the amplitude are equalized to a common distance of 90°. The thin solid line is the theoretical relation and the thick line the linear relation best-fitting the dataset under the constraint of a slope of one. We find excellent agreement between the theoretical and expected values. This illustrates the fact that focal geometry plays little role in tsunami excitation. (Okal, 1989).

The two cases in desagreement are the Alaska earthquake of March 1964, resulting from a strong directivity effect at the source and the Tonga earthquake of December 1982, an example of a so-called "Tsunami Earthquake".

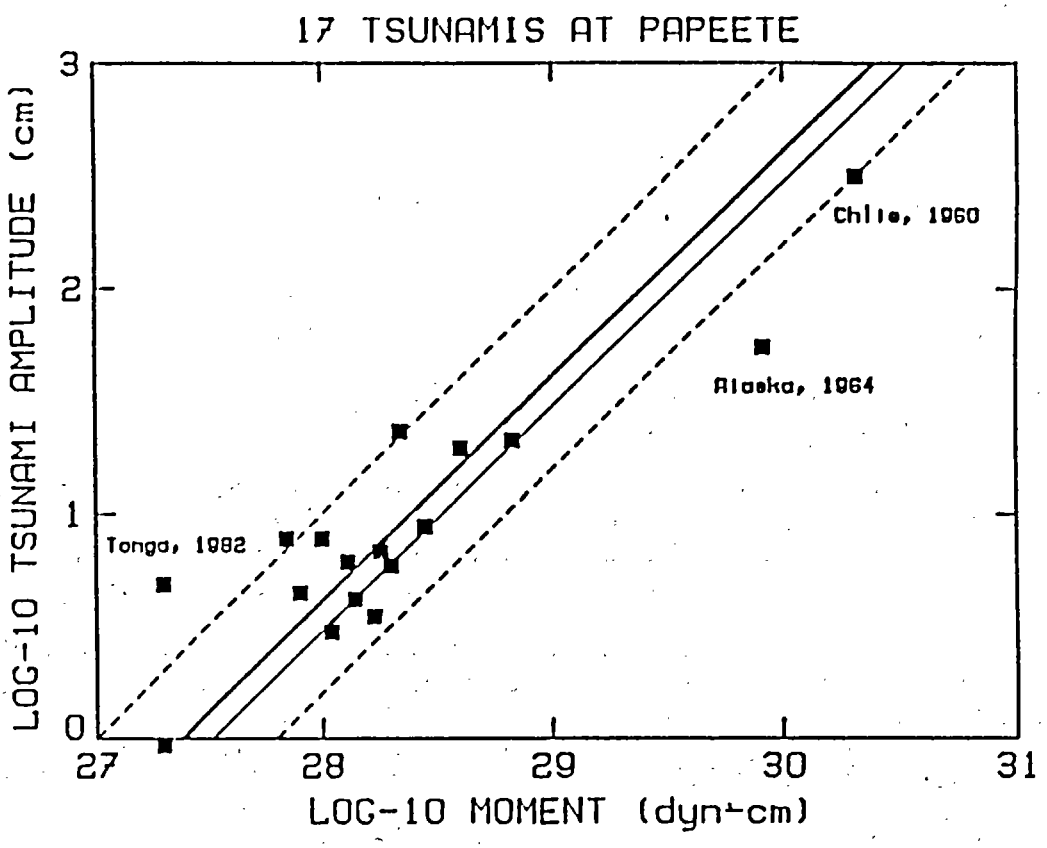
17 TSUNAMIS AT PAPEETE
LOG-10 TSUNAMI AMPLITUDE (cm)
LOG-10 MOMENT (dyn-cm)
Chile, 1960
Alaska, 1964
Tonga, 1982
0
1
2
3
27
28
29
30
31

Figure 7

On the basis of the above dataset, we define a window of expected peak-to-peak tsunami amplitude, as a function of seismic moment and distance :

$$\text{Upper bound : } \log (TS)_{10} = \log_{10} Mo - 0{,}5 \log_{10} (\Delta \sin \Delta) - 26.0 \quad (4)$$

$$\text{Average : } \log (TS)_{10} = \log_{10} Mo - 0{,}5 \log_{10} (\Delta \sin \Delta) - 26.4 \quad (5)$$

$$\text{Lower bound : } \log (TS)_{10} = \log_{10} Mo - 0{,}5 \log_{10} (\Delta \sin \Delta) - 26.8 \quad (6)$$

These must be taken as amplitudes in Papeete harbor that minimizes amplifications and resonance effects. For other receiving sites, local bathymetry entices additonal corrections, which, for example, can reach a factor of 3 to 5 for resonant bays in the Marquesas chain.

Note that the dimensions of Polynesian islands are small compared to wave lenght of the tsunami. Conséquently, the orientation of the shore respectively to the epicenter direction has small or null effect on the tsunami amplitude.

In establishing seismic thresholds for tsunami warning, we assume that tsunami risk is substantial when the upper bound on the peak-to-peak amplitude predicted at PPT (equation 4) reaches 1 m. Data from Figure 7, as well as the compilation of historical references (e.g., Pararas-Carayannis, 1977 ; Solov'iev and Go, 1984), suggests the following criteria for substantial tsunami risk : $Mo \geqslant 5 \times 10^{28}$ dyne-cm for Samoa-Tonga-Kermadec epicenters, and $Mo \geqslant 10^{29}$ dyne-cm for all other epicenters. The former figure, obtained here experimentally, is in agreement with Ward's (1980) theoretical threshold for destructive tsunamis. We treat separately the case of epicenters from the region Samoa-Tonga-Kermadec, which can be as close as 22° from PPT ; for such events, geometrical spreading is significantly reduced, resulting in substantial distance corrections in (4 through 6).

4 - Risk levels :

In this framework, the following risk levels have been identified as a function of the magnitude Mm :

1. $Mm < 7$ ($Mo < 10^{27}$ dyne-cm) : No tsunami risk.

2. $7 \leqslant Mm < 8$ ($10^{27} \leqslant Mo < 10^{28}$ dyne-cm) : The generation of a very large tsunami remains improbable, but a "tsunami earthquake" cannot be totally ruled out. Although it may be improper to describe it in terms of Mm or Mo, the Aleutian earthquake-landslide of 1 April 1946 apparently belonged to this range of seismic measurements (Kanamori, 1972), and yet it created one of the two largest tsunamis in the past 150 yr. Further interpretation, for example of T-wave durations, may be warranted.

3. $8 \leqslant Mm < 8.7$ ($10^{28} \leqslant Mo < 5 \times 10^{28}$ dyne-cm) : A tsunami will probably be generated, but except for the possible case of a tsunami earthquake, should not be catastrophic at teleseismic distances from the epicenter. Interpret T waves.

4. $8.7 \geqslant Mm > 9.3$ ($5 \times 10^{28} \geqslant Mo > 2 \times 10^{29}$ dyne-cm) : Probable generation of a potentially destructive tsunami. Immediate tsunami watch issued if epicenters is in Samoa-Tonga-Kermadec, or otherwise closer than 4000 km.

5. $Mm \geqslant 9.3$ ($Mo \geqslant 2 \times 10^{29}$ dyne-cm) : Generation of a very large, probably very destructive tsunami. Immediate alarm issued for Samoa-Tonga-Kermadec epicenters ; immediate tsunami watch issued for other regions.

The following are definitions of "Tsunami Watch" and "Tsunami Alarm" as they are used by CPPT : A Tsunami Watch is a first-level warning, designed to acquaint Civil Defense authorities of the possibility of a substantial tsunami, in order to allow them to achieve readiness in case of the later issuance of a tsunami alarm. A tsunami watch issued by CPPT includes predicted arrival times of the wave in Polynesia. A Tsunami Alarm warrants immediate action on the part of Civil Defense authorities, in compliance with relevant governmental procedures. In most cases, it will follow a tsunami watch, but could be issued early in the case of close-by epicenters. The tsunami alarm confirms arrival times at Polynesian islands.

Obviously, our estimate of tsunami risk is later updated, taking into account tidal gauge data, as they become available following propagation of the tsunami wave, through retransmission to CPPT by the Pacific Tsunami Warning Center in Honolulu, and from the HANDAR GEOS platforms at Rarotonga (Cook Islands), Christmas, Nuku-Hiva (Marquesas Islands), Easter Island, and, in the near future, Niue Island.

5 - Automation of the measurements :

The tsunamis prevention device used by the CPPT is entirely automatized. A computer detects, locates and evaluates the seismic moment through the Mm magnitude, and, in terms of the moment, gives an amplitude window of the expected tsunami. Those different operations are executed in real time. In addition, the operator can use the historic references and, if necessary, the T waves. But, in practice, these T waves are neither used.

Here is the flow chart of tsunami warning organization at PPT. The thinner traces involving T waves and historical references indicate the complementary nature of these ingredients.

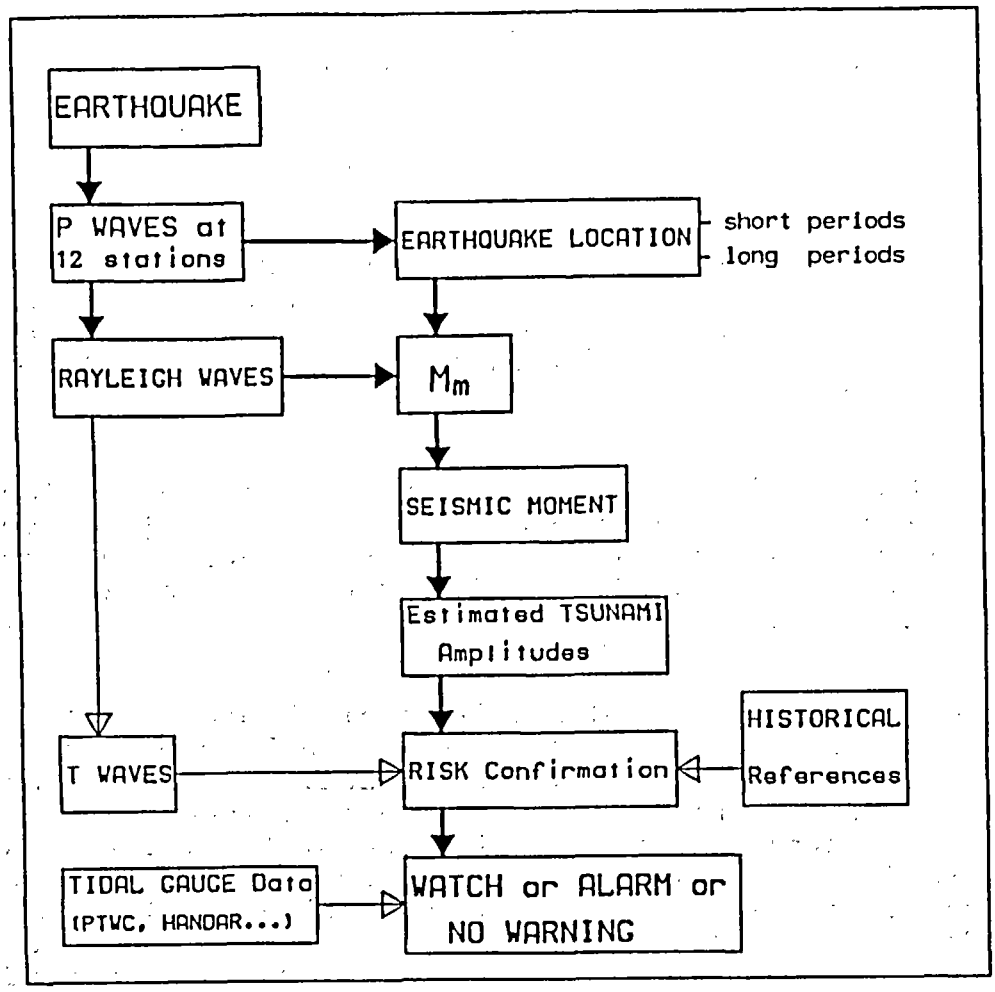

We will see the different steps of this procedure. However, it is necessary of emphasize that this device is also used, with respect to the function of detection, location in short and long period, Mm calculation and acquisition for geophysical researchs and others missions of the Geophysical Laboratory. Consequently this device process the very strongly earthquakes but also the small earthquakes, the far seismicity moreover that near seismicity with the very small earthquakes of volcanic origin from hot-spot of Mehetia.

Detection

Two detection devices work simultaneously in short and long periods.

Short-Period Detection is achieved through a criterion based on the temporal derivative of the energy of ground motion. For telesismic events, a minimum of 4 stations in the Society subarray must exceed a given threshold ; a somewhat different algorithm is used for local earthquakes.

Long-Period Detection is activated by comparison of the low-pass filtered seismic signal with its smoothed long-time average, this difference being required to remain above a given threshold for at least 2.5 s. Long-period detection is also triggered automatically by activation of the short-period detection algorithm.

The detection threshold are adapted according to the seismic noise of the moment. Them middle values are about :

- 0,5 mμ at 10 Hz (Small volcanic near seismicity)
- 20 mμ at 1 Hz (Teleseismic body waves).
- 100 mμ in long period (10< T < 100 sec).

Location

As it is the case for the detection, two locations are independently executed in short and long-periods.

In short periods, the former is based on the P waves in the 12 Tahiti and Rangiroa sub-network stations. Arrival times are defined according to a rather intricate procedure, in order to obtain accurate values whatever the characteristics of the beginning of this P waves are (Impetus or emergence).

For the teleseisms starting epicenter is determined using Husebye's method and the solution refined through Geiger's algorithm. The software allows the elimination of up to 2 stations in the Society subarray, and one on Rangiroa, if their residuals exceed 1.5 s. The program automatically prints the resulting epicentral coordinates, as well as the name of the seismic region.

For near epicenters the location techniques are based on HYPOINVERSE program.

The figures 8 and 9 shows an example of short period location for a near and far earthquake.

In long period, Detection triggers acquisition of an 80 minutes long-period time series, in which an Identifier (based on energy criteria applied to moving windows) recognizes the phases P, S, and R. A long-period estimate of the epicenter is calculated using the S - P time to infer distance and the 3 component polarization of P to obtain the azimuth of arrival.

Mm Magnitude

The Mantle Magnitude of the event (Mm = log Mo - 20) is then determined by isolating a 13 mn stretch of Rayleigh wave on the LP vertical record. In the frequency domain, the spectral amplitude $X(\omega)$ is computed between 3 mHz and 20 mHz, and Mm obtained through.

$$Mm = Log_{10} X(\omega) + C_D + C_S - 0.90$$

where C_D, is a correction for distance and C_S a source correction. The largest value of Mm at the various frequencies is kept.

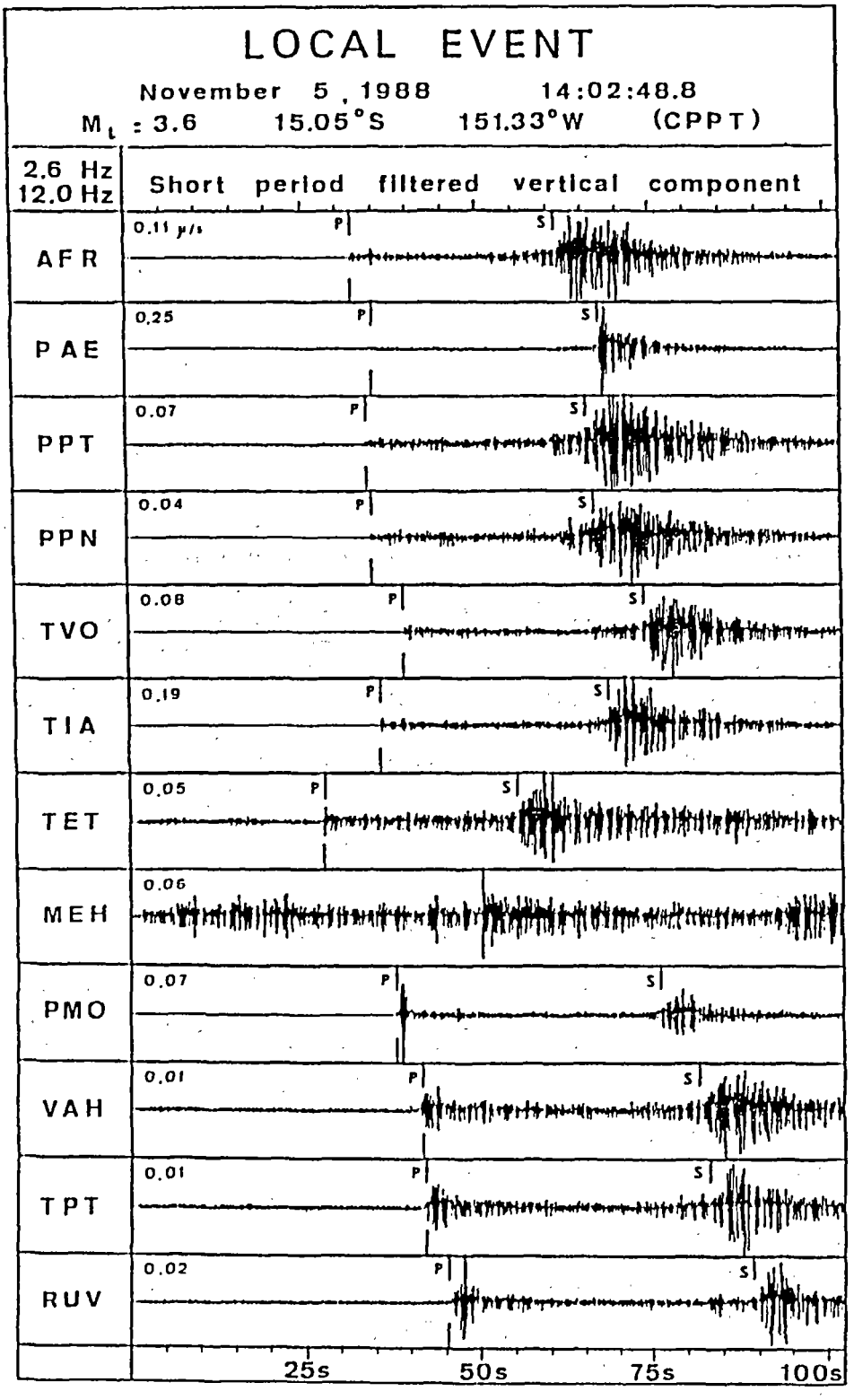
LOCAL EVENT
November 5 , 1988 14:02:48.8
M_L : 3.6 15.05°S 151.33°W (CPPT)
2.6 Hz
12.0 Hz
Short period filtered vertical component
AFR
PAE
PPT
PPN
TVO
TIA
TET
MEH
PMO
VAH
TPT
RUV
P
S
25s
50s
75s
100s

Figure 8

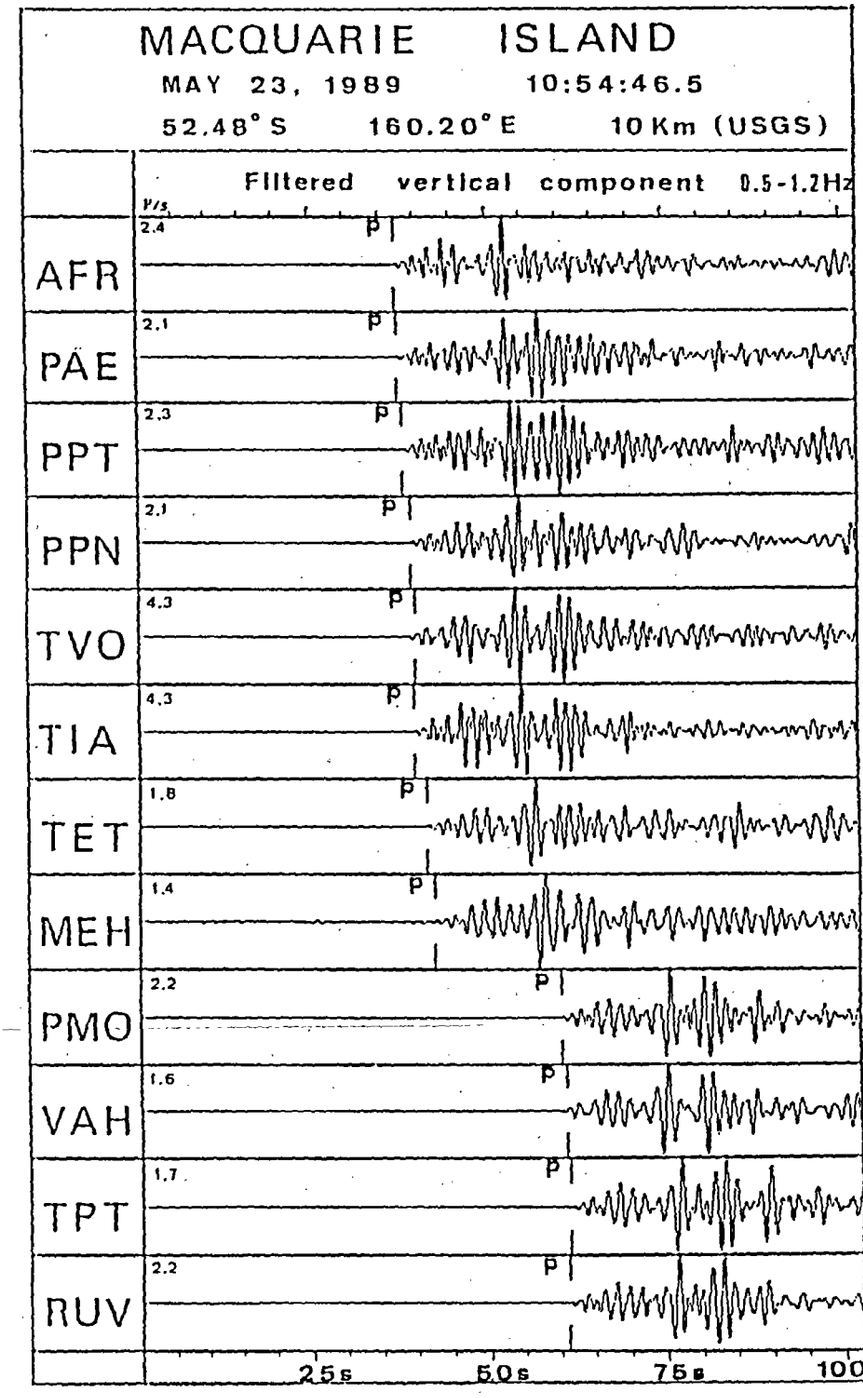

CPPT determination of epicenter :

51.69°S 156.74°E 10:54:35.9

Figure 9

In order, to eliminate the incertitude that may subsist concerning Rayleigh waves radiation connected with the source geometry, Mm magnitude is also determinated with Love waves following an equivalent procedure.

In the time domain, the seismogram is filtered to remove frequencies greater than 20 mHz, peaks and troughs automatically picked, their zero-to-peak amplitudes (a) and apparent periods (T) measured, and the time-domain magnitude obtained through :

$$Mm = Log_{10}(a.T) + C_D + C_S - 1.20$$

with the same corrections ; again the largest value of Mm is retained.

The figures 11 and 12 shows two examples of location with the 3 components polarization of P waves and Mm determination : The Macquaries earthquake on May 23, 1989 and Loma-Prieta earthquake on October 18, 1989. The results obtained in real time at the CPPT are given as well as the delayed values published by USGS and Harvard and Geoscope for the seismic moments.

Once a value of Mm is obtained the computer prints out automatically estimates of tsunami heights and of arrival times at various Polynesian sites.

On the basis of these results and according to the risk level, which has been defined, a geophysicist has the ultimate responsability of issuing a tsunami watch or alarm. If necessary he can used the historical references or, in the difficult case, interpreted the T waves.

The seismic moments obtain in real-time are immediatly sent to Pacific Tsunami Warning Center and Alaska Tsunami Warning Center for the earthquakes of seismic moment from 10^{27} dyne-cm and to National Earthquake Information Center of the USA for alls determinations of Mm, generally from 10^{24} dyne-cm.

It must emphasized that the seismic moments obtained in real-time at the Geophysical Laboratory or CPPT are the first published by the NEIC.

6 - Automatic Device to Estimate the Tsunami Risk

On the base of his experience the Geophysics Laboratory propose an integrated automatic device for estimate the tsunami risk. It would include a long period broad-band three components seismometer linked to a calculator such as an IBM PC. It would carry out in real-time operations of detection, location thanks to the P waves polarization, calculation of the Mm magnitude with the Love an Rayleigh waves, determination of the risk level according to this Mm magnitude and the seismic moment that issues.

MACQUARIE , MAY 23 , 1989

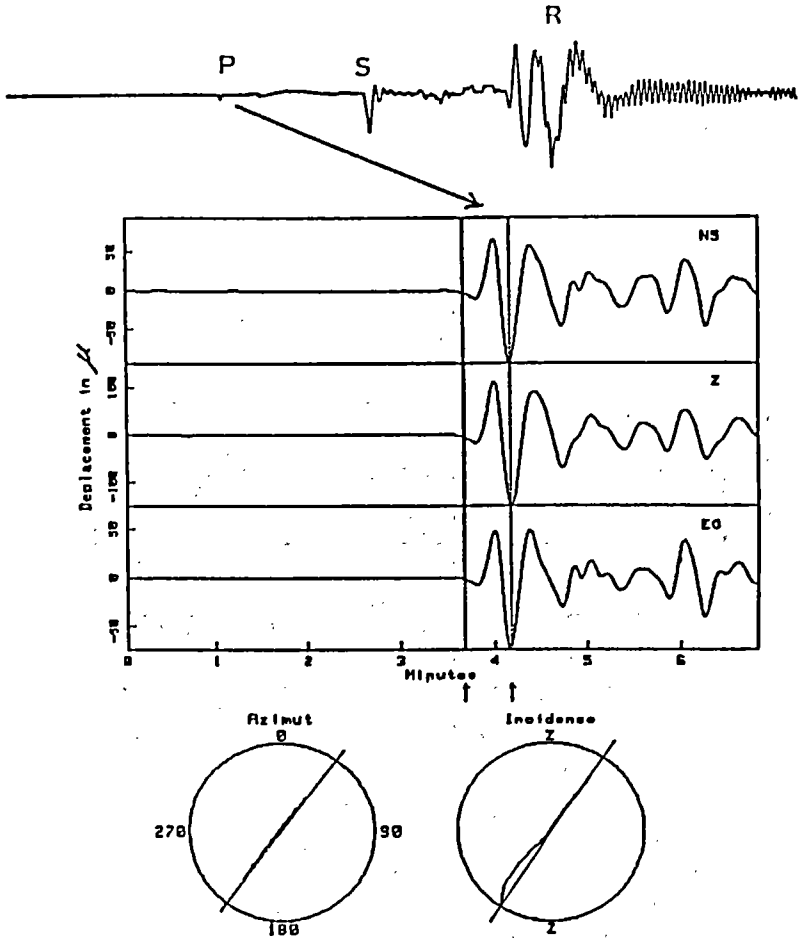

54.0 S - 158.3 E (USGS : 52.5 S - 160.2 E)

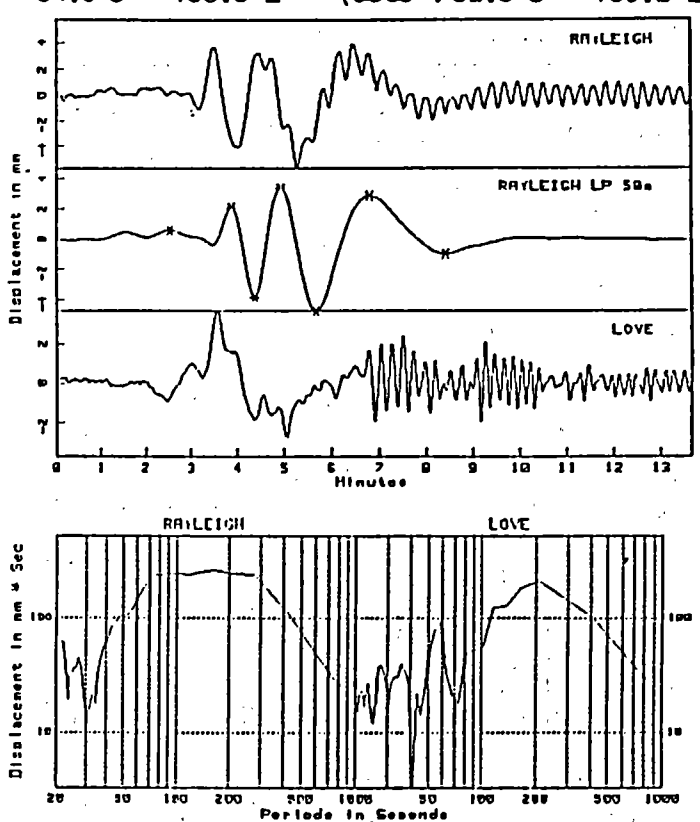

Mn 8.4 Mo 2.5 X 10^{28} dyne-cm

Figure 10

HRV : 1.4 X 10^{28}

GEOS : 2.1 X 10^{28}

SAN FRANCISCO , OCT , 18 , 1989

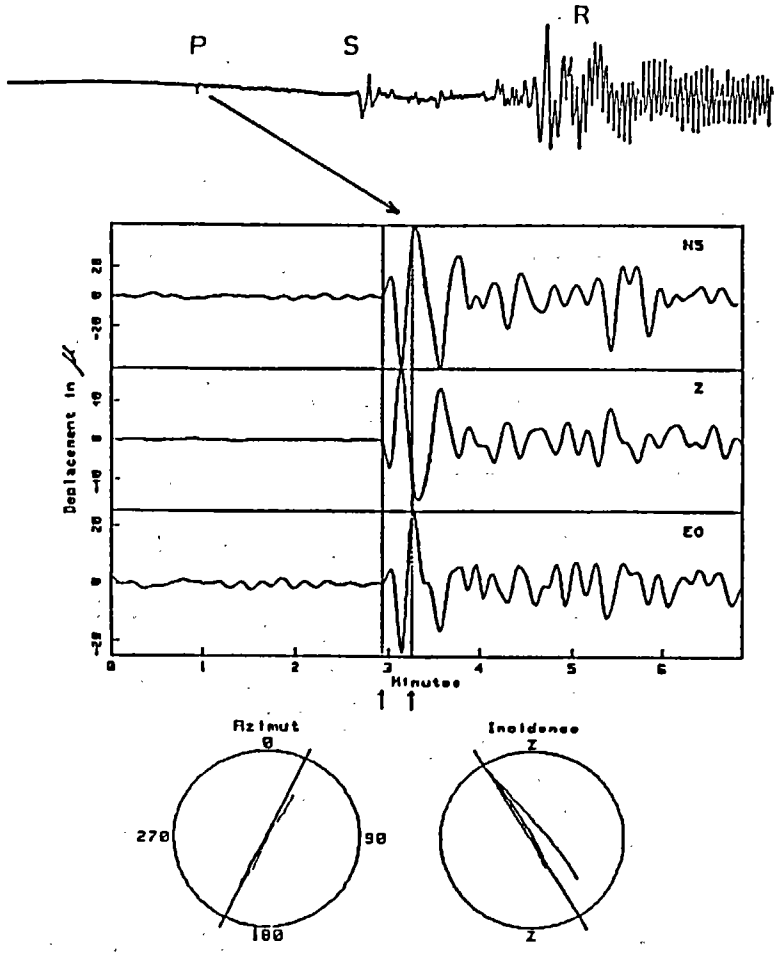

36.5 N - 119.6 E (USGS : 37.0 N - 121.8 W)

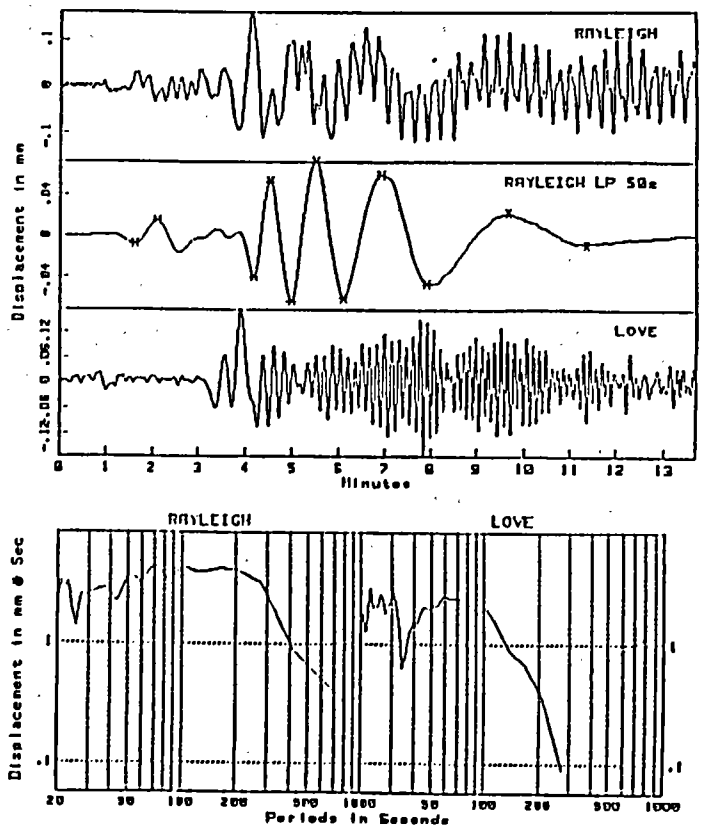

Figure 11

Mm 6.6 Mo 4 X 10^{26} dyne-cm

HRV : 2.5 X 10^{26}

GEOS: 7 X 10^{26}

Risk levels could be those defined by the Geophysical Laboratory and used by the Polynesian Tsunami Warning Center (CPPT), for far field.

Concerning the warning for near field, which does interest several countries, these risk levels should be, of course, adjusted according to seismic regional parameters and shores configuration.

Essentially based on a long period, three components station this device needs a minimum of infrastructure and is much less expensive than a network of short period telemetred stations which, anyway, also needs to use in addition a long period broad-band seismometer.

Independantly of the permanent and entire system which has been described, this simply device is tested since 1989 on the CPPT.

This system which automatically acquires three broad band components, in two sensitivities of dynamic of 96 dB each, is also a seismic station of great quality.

CONCLUSIONS

The method used by the French Polynesia Tsunami Warning Center includes four main stages :

- Detection of seismic wave P
- Location of the epicenter
- Determination of the seismic moment through the Mm Magnitude
- Estimation of the expected tsunami according to the proportionality between tsunami amplitude and seismic moment.

1) Two detection devices in short and long period and with a weak treshold.

2) In order to make assurance double sure, the epicenter location is carry out with two independant devices in short and long period.

3) The mantle magnitude Mm allows recovery of the seismic moment with a standard deviation less than 0.2_{24} unit of magnitude. (0.19 for 300 determinations of Mo between 10^{24} and 4 X 10^{28} dyne-cm, respectively at the published Mo with error of 0,1 on the logarithm).

4) The direct relation between observed tsunami and seismic moment is theoretical justified and experimentaly verified according to the amplitude of the 17 tsunamis recorded in Papeete harbor since 1958.

Used since 1986, this elaborate system etablished on the theoretical and experimental solid basis, has stood the test of time. The method used which the procedure is fully automatic, is certainly transposable and applicable to other warning centers. Based on the same principle, the simplified device we propose, can on account equip a teleseismic an regional warning center.

REFERENCES

OKAL, E. A. (1988). : Seismic parameters controlling far-field tsunami amplitudes : a rewiew, Natural Hazards Journal 1, 69-96.

OKAL,E. A. and J. TALANDIER (1986). : T-wave duration, magnitudes and seismic moment of an earthquake : application to tsunami warning, J. Phys. Earth 34, 19-42.

OKAL, E. A. and J. TALANDIER (1987). Mm : theory of a variable-period mantle magnitude, Geophys. Res. Lett. 14, 836-839.

OKAL, E. A. and J. TALANDIER (1989). Mm : A variable period mantle magnitude, J. Geophys. Res.94 (in press).

OKAL, E. A. and TALANDIER (1990) : Mm : Extension to Love waves of the concept of a variable-period mantle magnitude, Pure Applied Geophys., 134, 355-384.

PARARAS-CARAYANNIS. (G. (1977). Catalogue of Tsunamis in Hawaii, World Data Center, NOAA, Boulder, Colorado, 24-43.

REYMOND, D., O. HYVERNAUD, and J. TALANDIER (1990). Automatic Detection, Location and Quantification of Earthquakes : Application to Tsunami Warning Pure Applied Geophys. (in press).

SOLOV'IEV, S.L. and Ch. N. Go (1984). Catalogue of Tsunamis of the Pacific Ocean, Canadian Translations of Fisheries and Aquatic Sciences 5077-5078, 2 Vol. Sidney, 722 pp.

TALANDIER, J. (1972). Etude et prévision des tsunamis en Polynésie Francaise, Thèse d'Université, Université Pierre-et-Marie Curie, Paris 128 pp.

TALANDIER, J. D. REYMOND, and E.A. OKAL (1987). Mm : Use of a variable-period mantle magnitude for the rapid one-station estimation of teleseismic moments, Geophys. Res. Lett. 14, 840-843.

TALANDIER, J. and E. A. OKAL (1989). An Algorithm for Automated Tsunami Warning in French Polynesia Based on Mantle Magnitude, Bull. Seism, Soc. Am 79, 1177-1193.

TALANDIER, J. and E. A. OKAL (1989). Mm : Correlation between Seismic Moments, Mantle Magnitudes and Amplitudes of Tsunamis in Polynesia, In PACON 88 Proc. Pacific Cong. Mar. Sci. Techno., Edited by Saxena, OSTG/64-OSTG/76.

WARD, S. N. (1980). Relationsships of tsunami generation and an earthquake source, J. Phys. Earth 28, 441-474.

LATE IMPROVEMENTS OF CHILE TSUNAMI WARNING SYSTEM

E. LORCA

INSTITUTO HIDROGRAFICO DE LA ARMADA DE CHILE

ABSTRACT

The instrumentation for the tide stations has been improved with the replacement of the old Ballauf Standard tide gauge by the bubbler type in 15 locations besides the installation of five Handar Data Collection Platforms (DCP) provided by U.S.NOAA.

The existing seismic network is still far from having a good coverage of the country; however, four short period seismometers have been lately installed around the Iquique seismic gap (Latitude 20o S), linked to the Geophysics Institute Office in Santiago, and two THRUST seismic triggers are in operation at Iquique and Valparaíso ports.

Communications with the National Emergency Office has been improved with a HF transmitter which permits linking with all the Regional Emergency Offices along the country.

The Standard Operations Plan in Case of Tsunami has been tested in a tsunami simulation exercise, where some problems arised between different emergency agencies; a revision of the Plan has been adopted.

1. INTRODUCTION

Chile has participated in the tsunami warning system since very early in the history of the Seismic Sea Wave Warning System, namely July 7, 1958. Thanks to this, the big earthquake and tsunami produced in May 1960 could be timely reported to Hawaii.

First steps of the system to send and receive data from the International System, were depending on the existing tide gauges installed since 1940 through a cooperative effort with the U.S.Inter American Geodetic Service; on the existing seismic stations and on the naval telenetwork, besides the NASA ground station facilities.

The improvements and development of the actual system will be summarized in the rest of this paper.

2. THE NATIONAL TSUNAMI WARNING SYSTEM (NTWS).

On July 30, 1964, the National Tsunami Warning System was officially placed under the Chilean Navy's Hydrographic Institute which, at the same time, was designated as the national representative to the International Co-ordination Group for the Tsunami Warning System in the Pacific.

Several other organizations are involved in seismic data collection, warning dissemination and public evacuation (Figure 1) and a comprehensive national emergency plan exists to deal with different types of disasters.

The overall coordination of the NTWS is under IHA, which is the sole agency responsible of the issuance of tsunami watches and warnings in Chile. The National Emergency Office (ONEMI) is the organization that coordinates and executes the necessary activities for the prevention and/or solution of problems resulting from natural or man-made disasters; within the NTWS, is in charge of dissemination, through civil channels, of the tsunami watches and warnings. The Department of Geology and Geophysics of the University of Chile (DGG) is the only organization in the country which can provide seismic parameters (location and magnitude) to IHA and ONEMI.

3. INSTRUMENTATION

3.1 Water Level Gauges

On the Master Plan for the Tsunami Warning System in the Pacific it is stated that: for the confirmation of a tsunami, a well-distributed shore based and offshore water level gauging network is required, which must be equipped with instruments to respond upon interrogation to designated warnings and/or data dissemination and analyses centres.

The Chilean tide gauge network, operated by IHA, is shown in Figure N°2; most of the instruments are of the bubbler type with some of them equipped with Handar Data Collection Platforms(DCP), which store data in a memory module. This data is automatically transmitted to the GOES satellite every 3 or 4 hours, but a self transmit mode is operative if a preset water level is surpassed. The DCP sends air and water temperature besides water level data, except Easter Island which has only a barometric pressure sensor. These units are self-powered and a pair of solar panels provide the necessary charging current for the batteries. A once a year maintenance trip is recommended to keep them in good shape.

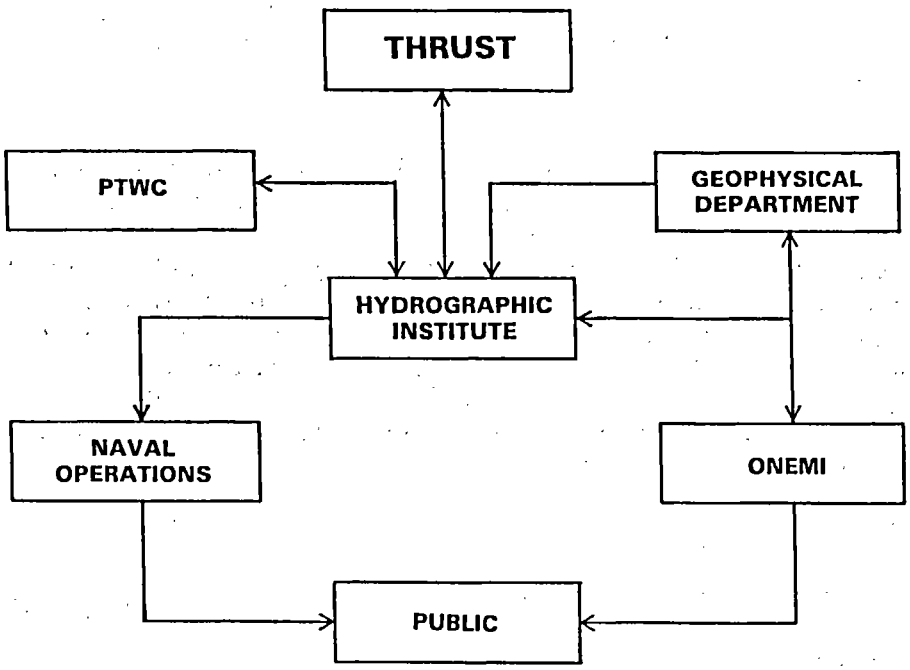

Figure 1.- National tsunami warning system organization.

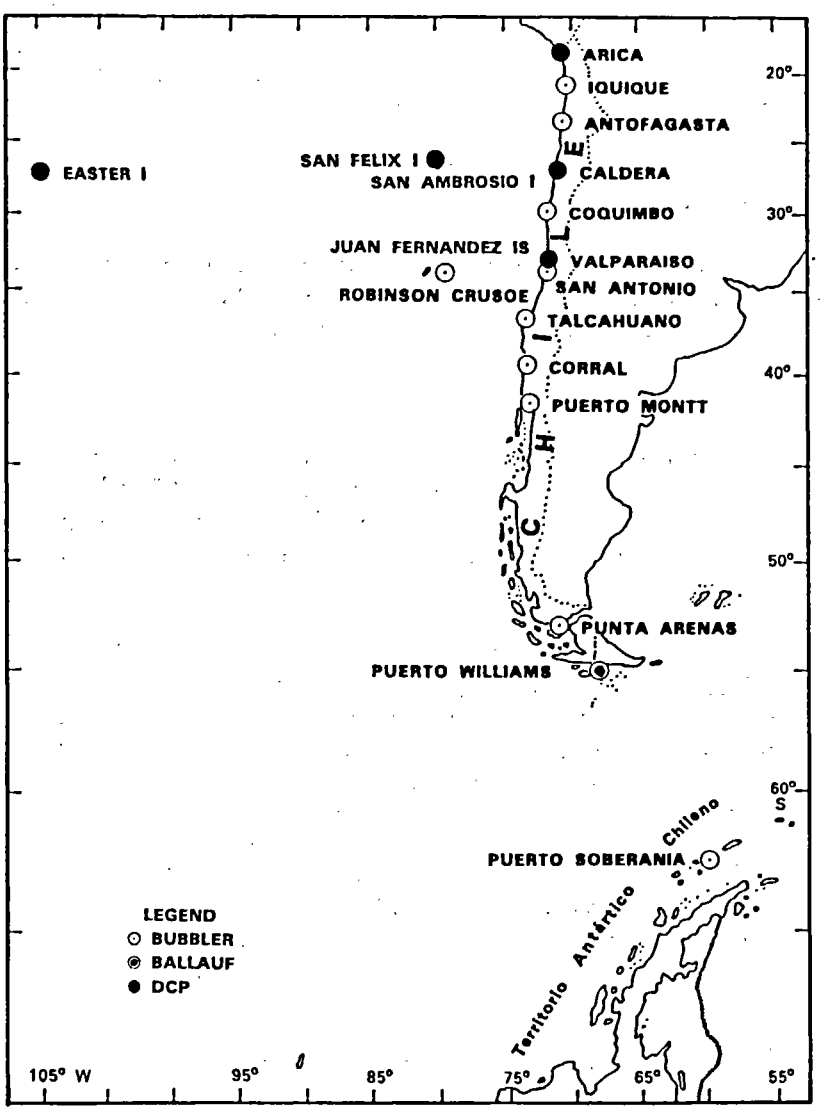

Figure 2.- Tide gauge network.

Water level data from the DCP's consist in a 2 seconds sampling interval, getting a tide level average every 4 minutes for the bubbler and every 15 minutes for the incremental encoder which is connected to a float.

The included bubbler gauge provides also an analog output to a pen recorder which is driven with a clock spring, resulting in a record where direct reading of time and height of the water level can be accomplished. This type of instrument is highly recommended because it does not need an stillig well and power, and its maintenance is simple.

3.2. Seismic network

Seismic stations location is shown in Figure N°3. Several stations in the central and north part of the country send its signals by telemetry to the DGG, where hypocenter and magnitude determination is performed.

A good complement for the warning capabilities of the system is the contribution coming from the THRUST Pilot Project. One of the components of this project is a satellite-based communication system that allows information delivery within minutes after the earthquake.

There are two seismic triggers installed in the country (see Figure N°3) which will be activated in case of a big earthquake located no more than 80 miles from the sensors. THRUST receivers are located at the Hydrographic Institute(IHA) in Valparaíso and at the Pacific Tsunami Warning Center(PTWC) in Hawaii.

Notwithstanding the former, more local networks and a 24 hours a day hipocenter and magnitude determination capability are necessary to fulfill the requirements of a good warning service.

4. COMMUNICATIONS (Figures N°4 & N°5).

4.1 Seismic Data transmission.

No direct link exists from the seismic stations to IHA. There is a low gain short period seismograph in this office, to monitor the high and medium magnitude earthquakes in the country and surrounding areas.

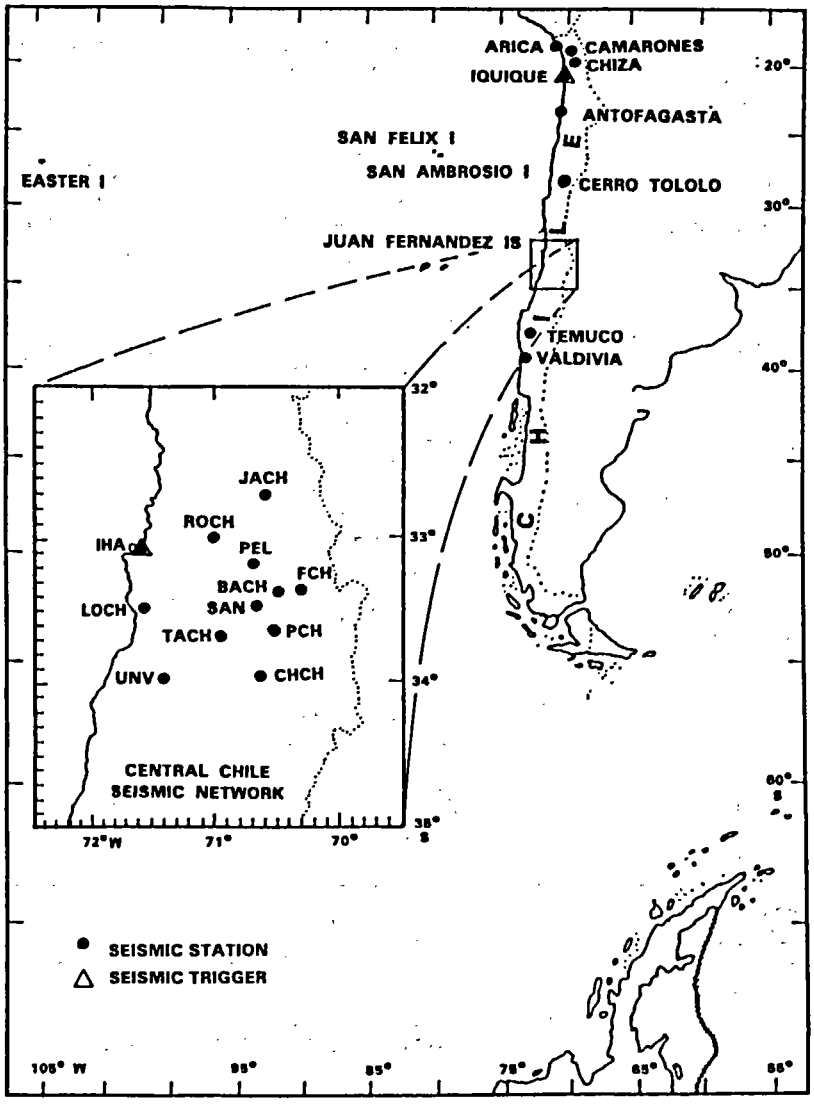

Figure 3.- Seismic stations.

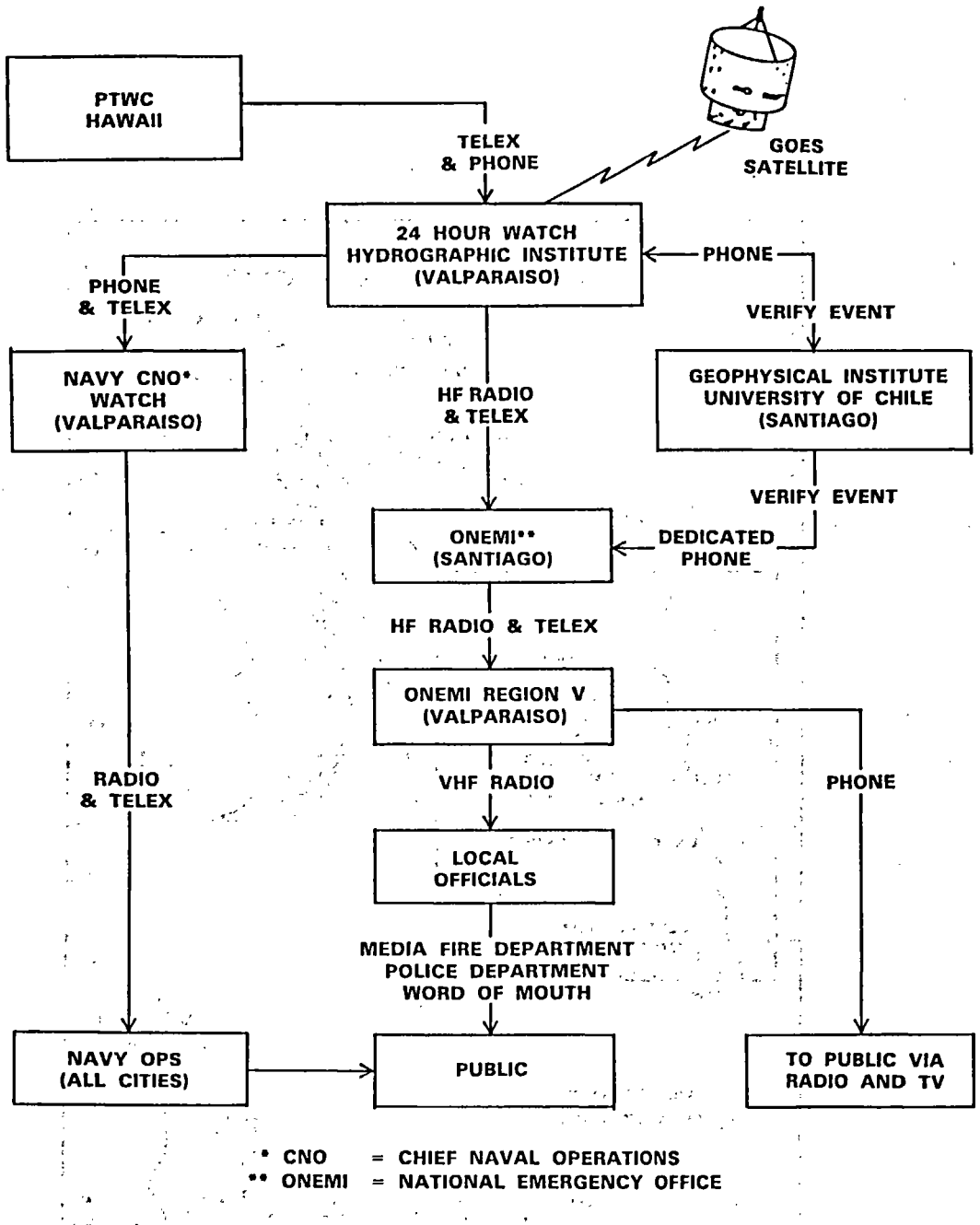

Figure 4.- NTWS communications.

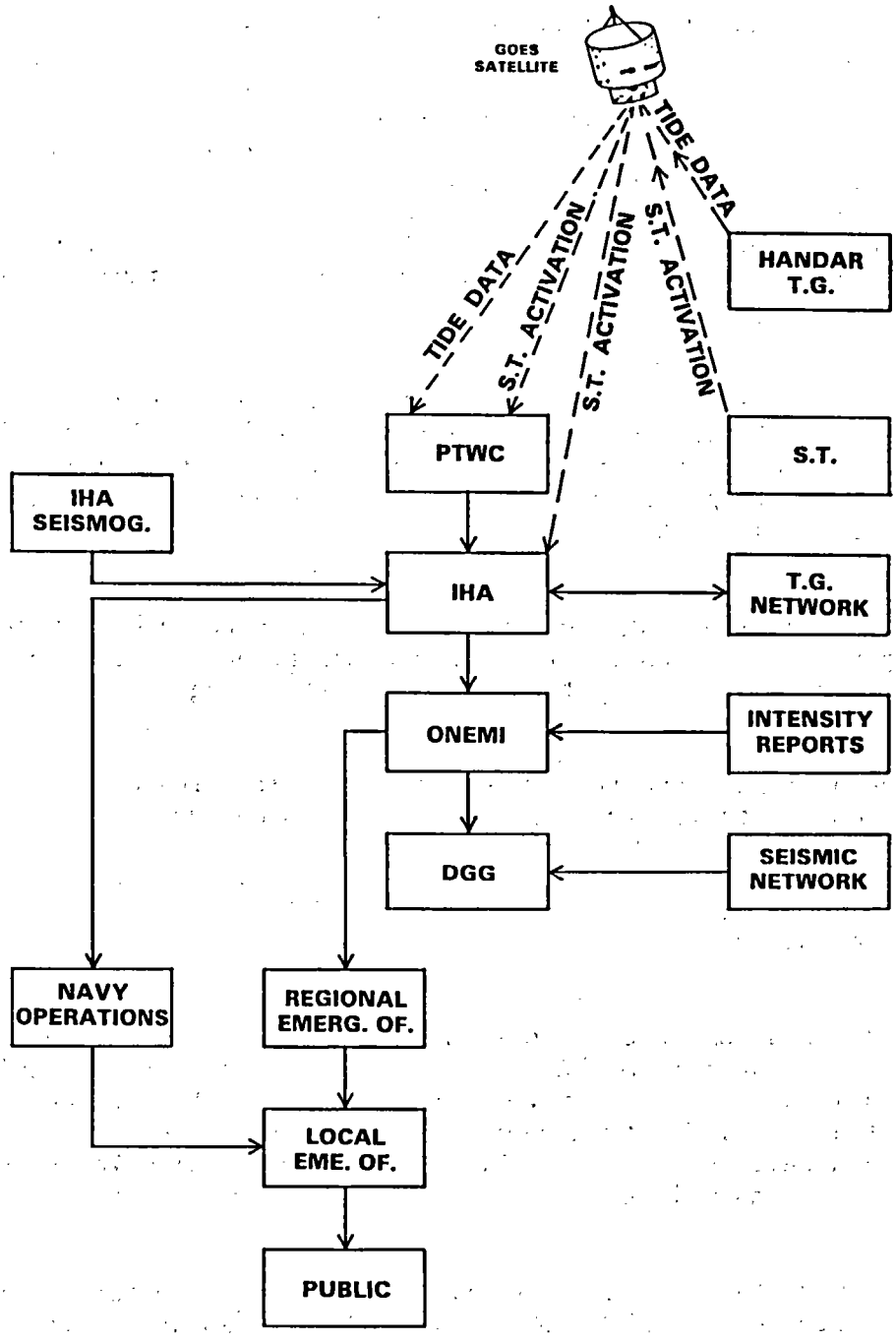

Figure 5.- Tsunami operations data flow.

The main office in charge of the recording and location of earthquakes is the DGG, in Santiago. Hypocenter and magnitude determination are performed off-line and the results are sent via a dedicated telephone line to the National Emergency Office (ONEMI), where is transmited to the IHA by radio and/or by telex.

However, the sparsity of stations in some areas and the lack of a 24 hours a day operation basis of the DGG, prevents the system to rely on this procedure for tsunami warning purposes. In this case IHA sends its seismic readings to PTWC by telex, telephone and/or facsimile within minutes of the occurrence of the earthquake, getting a preliminary result not later than 15 minutes after the origin time of the earthquake.

If a big earthquake occurs close to the THRUST sensors, a signal will be transmitted from the trigger to the GOES satellite, from there the signal will be sent to the Command and Data Acquisition (CDA) facility at Wallops Island, Virginia, to achieve rapid dissemination of the required information.

On receipt of the emergency message at PTWC in Hawaii and at IHA in Valparaiso, via satellite, they simultaneously activate visual and audio alarms and then print a tsunami alert message.

The average response time during the pilot project was 2.5 minutes and the communication reliability rate was about 99 %.

4.2 Tide data transmission.

Tide stations operators send information about a tsunami any time there is a request from IHA, through the navy teletype circuits, or by navy radio link or by navy telephone service. These requests can be originated at PTWC, from where they are sent by telex to IHA. Answer back to Hawaii is performed through the best available communication way (telex, facsimile or telephone).

Another faster and better way to get tsunami water level information is through the HANDAR DCP's (see Figure N°2) which transmit their data by means of the GOES satellite, being received at PTWC almost in real-time. PTWC plots this data and can send the recovered marigram to IHA through the facsimil.

4.3 Tsunami watch and warning dissemination.

Every decision-making taken by IIIA is disseminated to the public through two simultaneos routes:

a) To Navy coastal authorities (Captain of the Port) by navy teletype, navy radio and/or navy telephone.

b) To ONEMI by a HF transmitter or by telex, where is disseminated to the Regional Emergency Offices. From there, VHF links permits the reception of the tsunami watch or warning on any coastal town Major Office, where local emergency procedures states the way to act.

Normal dissemination procedures for small towns are the sounding of Fire Department sirens and the use of loudspeakers. In bigger towns and cities, this is complemented by announcements by radio a TV stations.

5. TSUNAMI EVACUATION PROCEDURES.

5.1 In Valparaíso.

Modelling techniques were selected by the THRUST project(Tsunami Hazard Reduction Utilizing Systems Technology) to estimate local inundation areas and the results of the numerical simulations were used as an aid in disaster planning, whose final result is a "Tsunami Emergency Operations Plan" for Valparaíso.

The Plan identifies emergency resources and tools that must be available on short notice, including hospitals, staging areas, and evacuation routes on simulated inundation maps, combined with baseline topography and street maps (Figure N°6). The maps depicts probable inundation areas, evacuation routes, security areas, hospitals and other important disaster resources.

Main purpose of the plan is to point out the functions and responsibilities of every emergency agency involved in the tsunami operations procedures, securing maximum coordination between them.

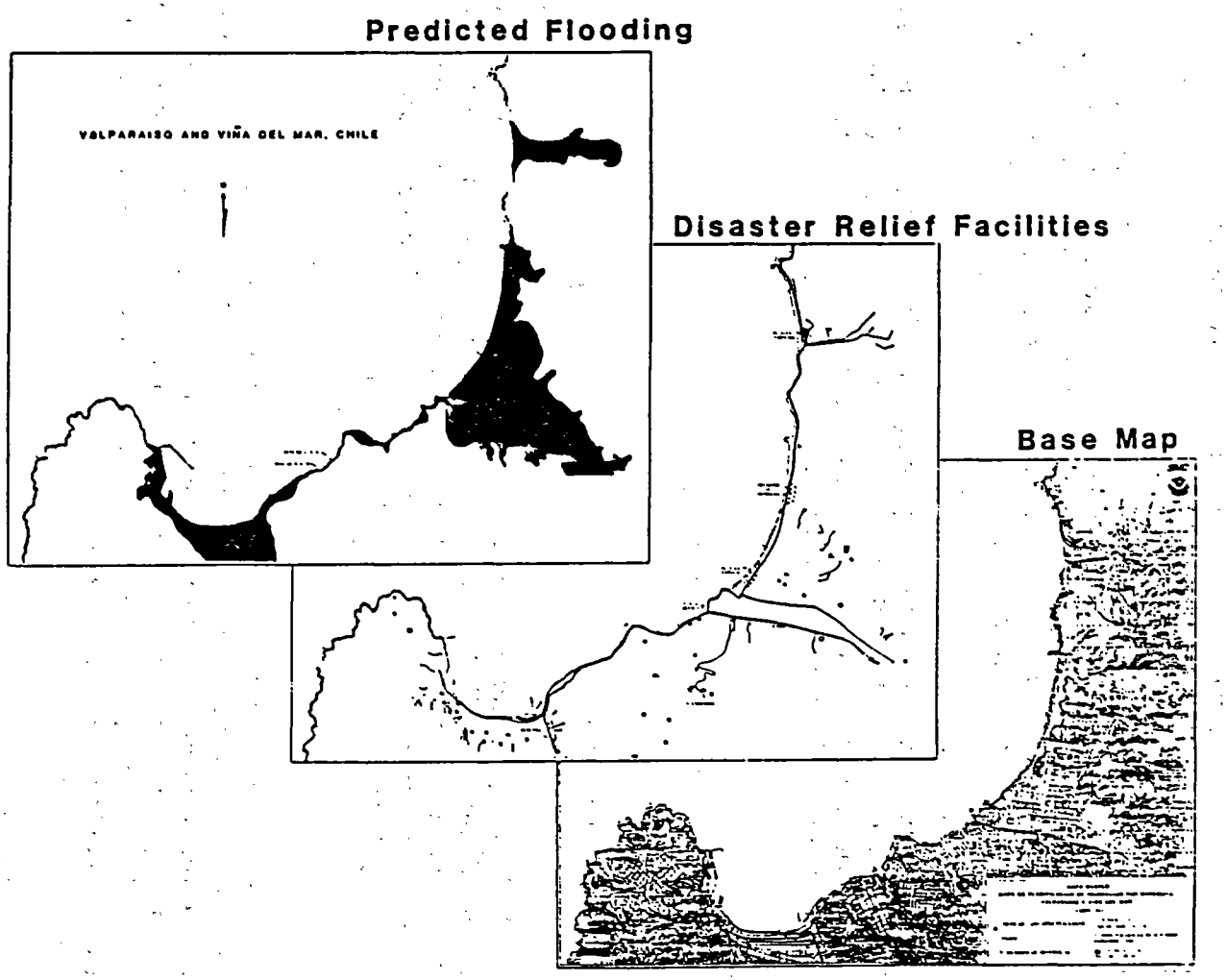

Figure 6.- Tsunami inundation planning.

5.2 In other cities.

Several other cities have already adopted the Standard Tsunami Operations Plan. However, they have to adapt the procedures since no modelling technique has been used in them to estimate flooding. Most of them have fix a maximun inundation level of 25 meters, based on the historical run-up data, determining from there the inundation areas and the corresponding security areas and evacuation routes.

5.3 Simulation Exercises.

The Standard Tsunami Operations Plan was tested in December 1988, in a Simulation Exercise held in Valparaíso, with the participation of every regional organization or agency having a responsability in a tsunami emergency. Several observers from others Regional Emergency Offices attended.

A detailed exercise scenario was used with inputs from a Control Team, generating news or problems to the participants. Lack of coordination between them was one of the main detected problems in the simulated operations resulting from the inputs. A revision of the Plan was performed to solve the problem and modifications were adopted. Another simulation exercise will take place before the end of the year to test the level of tsunami preparedness in Valparaíso.

6. PRESENT RESPONSE OF THE SYSTEM.

The only way to measure the actual response of the whole system is through a real event. No big earthquake and tsunami has occurred since the implementation of the present configuration and procedures of the National Tsunami Warning System; however, some assessment can be deduced from the operation of part of the system during medium size earthquakes.

On August 14, 1988, an earthquake was recorded at the IHA seismograph. Since the estimated magnitude was bigger than 6.5, a series of actions took place. The sequence of events was as follows:

TIME (GMT)	EVENT OR REMARKS
1753	Earthquake occurrence at Lat.27.260°S; Lon.71.092W
1758	Earthquake in progress noticed by IHA watchstander.
1802	Caldera T.O. reports intensity VI.
1804	IHA sends by phone seismograph readings to PTWC.
1819	IHA receives by telex PTWC preliminary information about location and origin time of the earthquake.
1824	IHA starts a query to Caldera T.O.
1832	IHA sends an Earthquake Information Bulletin to ONEMI.
1836	IHA receives PTWC Bulletin with magnitude information (M = 6.8, S-wave).
1837	IHA sends magnitude information to ONEMI.
1838	Alarm triggered at PTWC.
1845	IHA receives by telex PTWC Earthquake Information Bulletin with final hypocenter, magnitude determination and the no tsunami advise.
1848	IHA advise ONEMI about the no tsunami conditions.
1906	IHA receives by telex from PTWC, NEIC information about the earthquake.
1909	IHA sends to ONEMI the NEIC bulletin.
1910	Caldera T.O. reports normal activity.
1921	ONEMI reports intensity data.
1925	IHA closes the tsunami operations.

7. CONCLUSIONS AND RECOMMENDATIONS.

- Big improvements on the tide gauge network has been achieved; however, a direct access to tide data from HANDAR units is desirable.

- The seismic part of the system should be improved with more local seismic networks and a 24 hours a day operation capability.

- Continuous testing of the Standard Operations Plan on a local level is recommended.

- Good communications with the Pacific Tsunami Warning Center are essential for a fast interchange of tsunami data.

****

TSUNAMI WATCH AND WARNING IN FIJI*

by

G. Prasad

Mineral Resources Department, Private Mail Bag, Suva, Fiji.

INTRODUCTION

Fiji is prone to natural disasters such as cyclones, floods, earthquakes and tsunamis. Of these cyclones are most frequently destructive. Earthquakes frequently occur within Fiji, but only two, the 1953 Suva Earthquake and the 1979 Taveuni Earthquake, caused any damage in recent history. Tsunamis in Fiji are less frequent and only one tsunami, resulting from the 1953 Suva Earthquake, is known to have caused serious damage and loss of life. The Emergency Services Committee (EMSEC) is responsible for mitigation of all natural disasters in Fiji.

Tsunamis in Fiji

Fiji is surrounded by coral reefs which protect most of the nation from large tsunami waves reaching the shores. However, small tsunami waves do reach the shores. Eleven tsunamis have been reported in Fiji (Table 1), of which three were produced locally while the others were Pacific-wide tsunamis. The tsunami of 1953 resulted from large underwater slumping of sediments caused by an earthquake near Suva. The first of the waves arrived in Suva about three minutes after the earthquake. The wave heights were estimated to be as much as 15 m on the coral reefs and about 2 m on the nearby shores. The tsunami was reported from as far as 290 km (western Lau) from the epicentre of the earthquake. However, instrument records show that the tsunami reached Pago Pago and Honolulu. This tsunami caused about $50 000 (1953 values) worth of damage to wharf facilities, seawall in Suva and recreational facilities on two small sand cays in Laucala Bay, Suva. It also took five lives, three in Suva and two in Kadavu. It was fortunate that the tsunami occurred at low tide; the damage would have been much greater had the tsunami occurred at a high tide.

A relatively small earthquake (M_S about 5.2) on 17 December 1975 in Kadavu Passage (Fig. 1) produced sea-level fluctuations at Laucala Bay in Suva for about hour and a half and for an unknown period at Kadavu and Ono islands. The wave heights were estimated to be about 0.5 m at Laucala Bay. The possible cause of this tsunami was slumping of underwater sediments. If an earthquake of this magnitude can cause slumping of underwater sediments resulting in a tsunami then there is little doubt that an earthquake of magnitude similar to that of 1953 earthquake offshore from Suva will produce a sediment-slump large enough to generate a damaging tsunami.

The tsunami generated by the 23 May 1960 Chilean earthquake took 13.3 hours to reach Suva and caused minor damage to ships in Walu Bay, Suva and left a few ships temporarily stranded after the sea level dropped. The first of the waves arrived in Suva at about 9:00 pm (Fiji time) on 23 May 1960. The maximum wave height reported was about 1.2 m in Suva. The wave activity continued all night and most of the next day. The tsunami was also reported from Savusavu where the sea is said to have washed in and out all day after the earthquake. No estimate of the wave heights is available from Savusavu, but it is expected to be as high as that in Suva.

---

* Published with the permission of the Director of Mineral Development

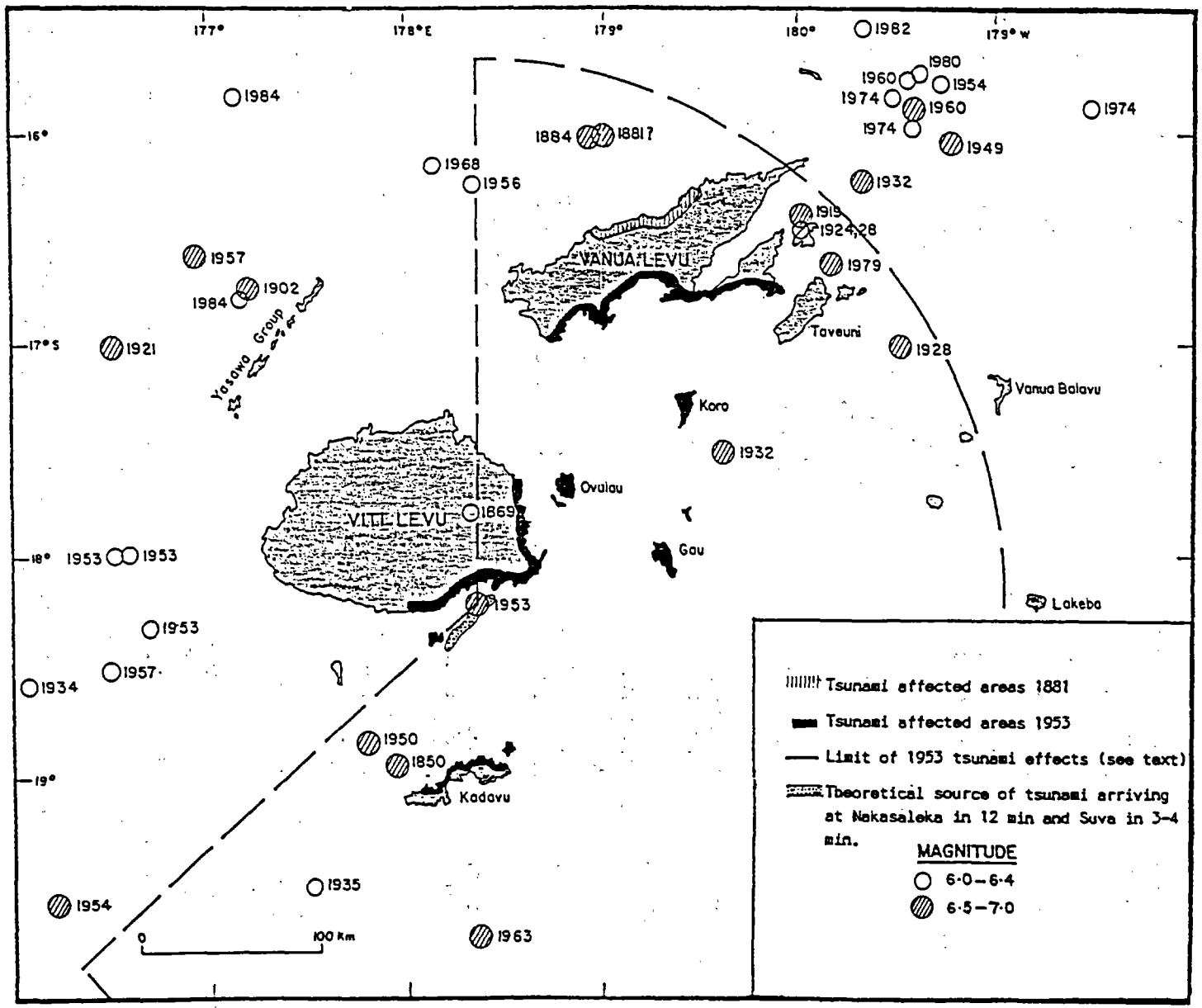

Figure 1. Location of large earthquakes in the Fiji Region and the areas affected by the 1877, 1881 and 1953 tsunamis.

TABLE 1

Tsunamis recorded in Fiji

YEAR	DATE TIME (local)	SOURCE AREA MAGNITUDE	LOCALITY AFFECTED	SHORE HEIGHT (m)	TRAVEL TIME (hr)
1877*	MAY 10 1259	Chile 21.5°S 71°W	Savusavu	2	18
1881?	JUL 12 0530	N of Vanua Levu 16°S 179°E M_S 6.5-7.0	N coast of Vanua Levu Levuka	1.8 0.4	
1953*	SEP 14 1227	SE Viti Levu 18.2°S 178.3°E M_S 6.75	Suva Makuluva Beqa Koro Nakasaleka Honolulu Pagopago	1.8 1.8 1.4 1.4 4.6 0.1 0.2	0.15 0.2 7.3
1960*	MAY 23 0711	Chile 41.0°S 73.5°S M_S 7.2	Suva Savusavu	0.5	13.3
1967	JAN 01 1015	New Hebrides 11.3°S 16°E	Suva	<0.1	
1968	JUL 25 1923	Kermadec Islands 30.8°S 178.4°W M_S 7.2	Suva	0.1	
1975	DEC 17 0902	Kadavu Passage 18.5°S 178.6°E M_S 5.2	Suva Ono (Kadavu)	0.27 0.27	0.3 0.5
1975	DEC 27 0357	Tonga 16.2°S 172.5°W M_S 7.8	Suva	0.08	
1976	JAN 15 0448	Kermadec Islands 29°S 177.4°W M_S 8.0	Suva	0.22	
1977	JUN 23 0008	Tonga 16.8°S 172.0°W M_S 7.2	Suva	0.16	1.4
1977	OCT 10 2354	Kermadec Islands 26.1°S 175.3°W M_S 6.9	Suva	0.02	2.2

* Destructive tsunamis

Although EMSEC is responsible for formulating disaster related laws and oversees the disaster mitigation, other orgainisations are also involved directly or indirectly in tsunami watch and warning in Fiji and these are:

1. Mineral Resources Department (MRD)
2. Fiji Marine Department
3. Fiji Meteorological Service
4. Fiji Police Force
5. Radio Fiji
6. The Red Cross Society of Fiji

Mineral Resources Department

The Seismology Section of MRD operates a network of one long-period and 10 short-period seismograph stations. One more seismograph station at Nadi (NDF) belongs to Pacific Tsunami Warning Center (PTWC) and is being looked after by the Fiji Meteorological Service. In 1984 the number of seismograph stations in Fiji had reached 18, but since then the number has been gradually declining mainly due to financial constraints.

The seismograph station at Nadi is a key station in the Southwest Pacific for obtaining phase data for location of large shallow events in the region for the purpose of tsunami warnings. The excellent communication system at Nadi Meteorological Station and immediate response to queries by PTWC makes it an ideal station in the region. However, the station uses obselete equipment and has not been properly maintained for some time and hence is prone to frequent breakdowns. The station ceased to operate in early December 1988 due to clock failure. The clock was not repairable and a replacement clock could not be obtained so a clock from MRD Seismology Section was modified and installed in March 1989. Simple tests have shown that many other problems exist with the seismograph and may need urgent attention.

The main task of the Seismology Section at present is the collection and distribution of earthquake data to local and international organisations. Phase data of all teleseismic events and local events with magnitude (M_L) greater than 4.0 are sent to USGS. The hardware and the software are available to do routine location of hypocentres. At present the routine location of hypocentres are done on MicroVax II computer of CCOP/SOPAC using HYPO71 and HYPOINVERSE programmes. In the near future HYPO71PC will be installed on Olivetti PC and the locations will be carried out on the PC. Most of the earthquakes occur outside the network resulting in large hypocentre location errors. This problem is partially overcome by use of improved velocity and structural parameters (Everingham, 1988) and station corrections (Prasad, 1988). The section is also actively involved in educating the public on earthquakes and tsunamis and the related dangers.

Fiji Marine Department

The Hydrographic Section of the Marine Department is responsible for operating and maintaining the tide gauge. The old tide gauge was replaced by a new one in late February 1989. This tide gauge, Stevens Digital Recorder number 191-0000, is located at Suva (18.13°S and 178.43°E) and belongs to National Oceanographic Atmospheric Administration (NOAA). The tide gauge records water-level data as a pattern of punched holes in paper tape at intervals of six minutes. Most of the large tsunami waves would break on the outer coral reefs and perhaps smaller waves with shorter wave lengths would reach the shores of Fiji and therefore this sampling rate may not be appropriate for monitoring tsunamis in Fiji. More-frequent sampling, perhaps at a rate of one every minute, will be more appropriate. NOAA is planning to put in a telephone modem so that data could be obtained immediately. Provision for data transmission through Geostationary Operational Environmental Satellite (GOES) is also available.

Fiji Meteorological Services of Fiji

The Fiji Meteorological Service acts as the communication centre for Fiji and is responsible for receiving queries and warnings from PTWC and distributing data to the appropriate agencies. It responds quickly to tsunami dummies and also provides P-wave arrival times to PTWC from the seismograph station (NDF) installed at the weather forecasting office at Nadi.

Fiji Police Force

The Fiji Police Force also acts as a medium for communication. It receives messages from the Meteorological Service, especially after office hours, and relays to authorities responsible for issuing of tsunami warnings in Fiji, e.g. the Director of Mineral Development. The police force together with the security forces of Fiji would carry out essential duties during a disaster such as evacuations or giving help to those who need it.

Radio Fiji

Radio Fiji is the medium through which the public is informed of impending disasters and actions to be taken by the members of the public and also the disaster relief workers.

COMMUNICATIONS PLAN

The communications plan and actions to be taken for earthquake and tsunami disasters are summarised, diagramatically, in Figure 2. The earthquake disasters may be dealt with quite well by this communications and action plan while some difficulties may occur with tsunamis generated locally. This plan of action is most applicable for distant tsunami warnings issued through Pacific Tsunami Warning Center (PTWC). The warnings have to be communicated through the radios, and there is no system of warning developed in the form of alarms such as sirens. This is a step which needs to be taken by the authorities responsible for issuing warnings. Another aspect which has not been tested is whether the plan of action can be put in practice within the required time. A dummy tsunami warning should be issued and response time evaluated.

There may not be enough time to issue warnings for tsunamis generated by nearby earthquakes as was the case for the 1953 Suva tsunami which took only a few minutes to arrive at the coast of Suva. In this case the plan of action becomes ineffective. To combat the tsunamis generated locally we have to educate the public to be aware of the dangers and the action to take in case of a strong earthquake being felt. For this purpose the sub-committee of EMSEC, which was formed for natural disaster awareness and preparedness in 1988, plays an important part. This sub-committee is responsible for developing educational material for disaster awareness and preparedness and for organising national disaster awareness-preparedness week. One such week was organised in April (03-08) 1989. The week proved to be very successful as many hundreds of people visited the displays put up by various organisations. Displays on general information and dangers of earthquakes and tsunamis were put up by the MRD. The Seismology Section of MRD is also visited by schools and other organisations to learn more about earthquakes and tsunamis.

MRD EARTHQUAKE & TSUNAMI PLAN OF ACTION

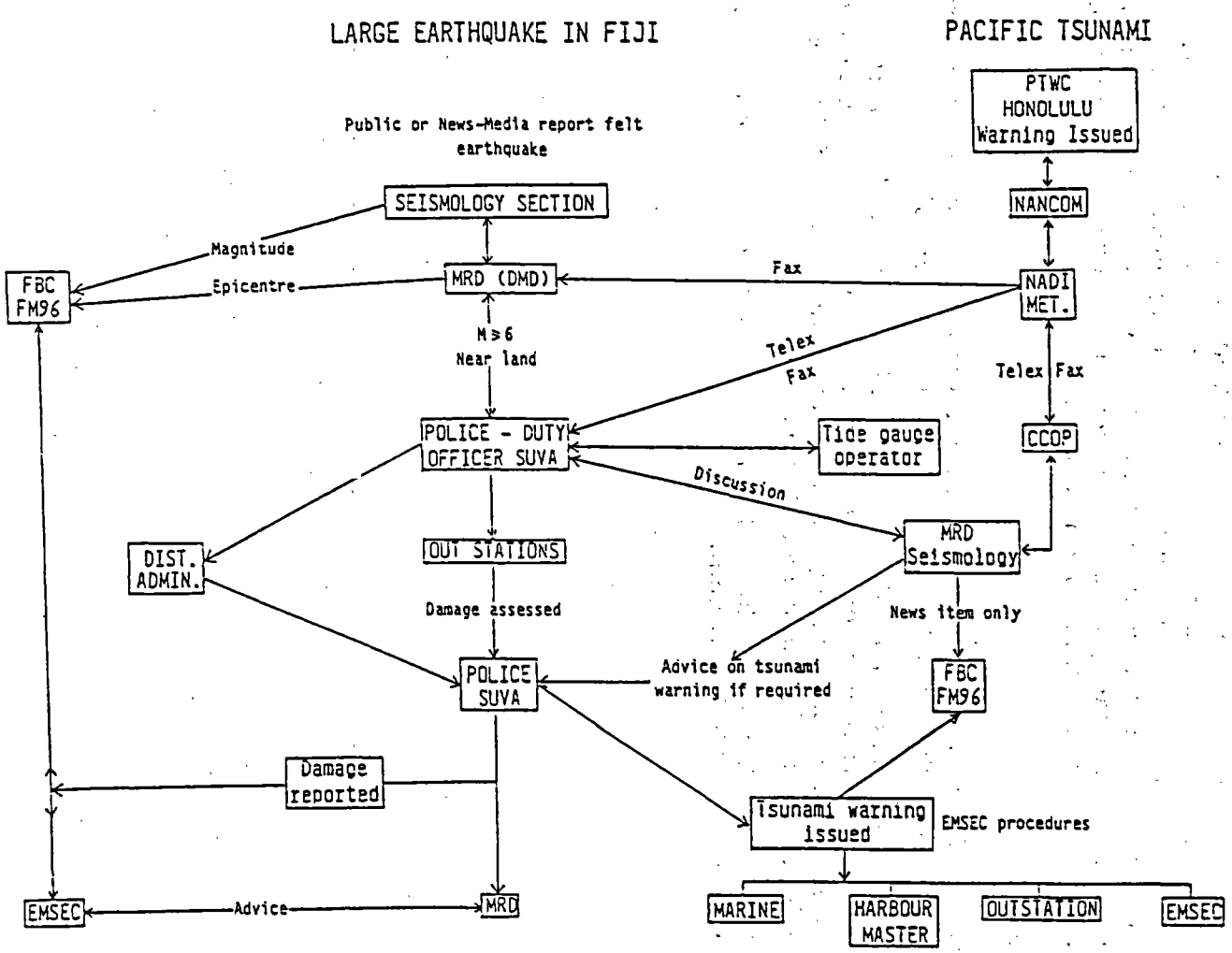

Figure 2. A diagramatic representation of Mineral Resources Department's earthquake and tsunami communication and action plan.

CONCLUSION

The tsunami warning system needs further development in Fiji. The MRD earthquake and tsunami plan of action needs to be tested and appropriate authorities drilled in putting this plan into practice. It also needs to be supplemented with an alarm system such that people near the coasts, especially in built-up areas such as Suva can be made aware of impending tsunami danger. The plan of action becomes virtually ineffective when dealing with locally generated tsunamis and for this we have to rely on public education as it is not yet possible or practical to devise a warning system which can be activated within adequate time.

REFERENCES

Everingham, I.B., (1988). Seismic refraction data and crustal structure for S.E. Viti Levu, *Mineral Resources Department Report* 63.

Prasad, G., (1988). *Relocation of deep and shallow earthquakes in the Tonga-Fiji Region: station corrections for Fijian stations and implications for deep and shallow structures,* MSc. Thesis, University of New England, Armidale, Australia (unpublished) 184pp.

Singh, R., (1987). Tsunamis in Fiji and their effects, *Mineral Resources Department Note* BP27/5 (unpublished).

3. SURVEY OF SOME EXISTING SEISMIC DATA PROCESSING SYSTEMS AND FUTURE PROJECTS

SEISMIC DATA PROCESSING IN THE NEIC AND PLANS FOR THE NEW U.S. NATIONAL SEISMIC NETWORK

J. W. Dewey

U. S. Geological Survey
Stop 967, Federal Center, Box 25046
Denver, Colorado 80225, USA

INTRODUCTION

The NEIC (National Earthquake Information Center, U. S. Geological Survey) is upgrading its recording of seismological data in order to improve the estimation of earthquake parameters and make these parameters more rapidly available to users. The purpose of this paper is to summarize present NEIC capabilities in rapid estimation of earthquake parameters and to discuss improvements in these capabilities that will occur when upgrading of NEIC networks is complete. A more extended review of present and future NEIC activities is given by Massé and Needham (1989).

IMPROVEMENTS TO SEISMOGRAPH NETWORKS RAPIDLY ACCESSED BY THE NEIC

The NEIC presently receives data that are telemetered from stations in the contiguous United States, Alaska, Hawaii, and Canada, and that are recorded in analog format. The initial NEIC epicenter and magnitude are based principally on these telemetered data. Additional vital data are provided to the NEIC by cooperating institutions; these data consist of arrival-times and amplitudes.

The NEIC upgrade will involve installation of new stations, the establishment of satellite-telemetry links to cooperating stations and networks, and a change of recording format from analog to digital. Figures 1, 2, and 3 show planned networks that will be particularly important for the registration of tsunamigenic earthquakes in the Pacific region. All networks will telemeter data to the NEIC via satellite. All networks will be operational in the early 1990's, with installation of the first stations planned for 1990.

The U.S. National Seismic Network will eventually consist of approximately 100 broadband stations in the United States, with additional cooperating stations in Canada and Mexico. Figure 1 shows more than 50 sites for which funds have to date been identified. Each station of the National Seismic Network will have 3-component high-gain and low-gain seismometers; each pair of high- and low-gain seismometers will be on-scale over a dynamic range of 210 db.

The Pacific Satellite Seismograph Network (PSSN), currently being installed by the NEIC in cooperation with the Pacific Tsunami Warning Center, will telemeter automatically determined P-wave arrival times and some P-waveform data from stations located on islands and margins of the Pacific Ocean (Figure 2). These data will be sent from individual stations at phased intervals, with the entire network being sampled in a period of several hours.

The Global Telemetered Seismograph Network (GTSN) will provide automatically detected P-wave arrival times in near real-time from stations in Africa, South America,

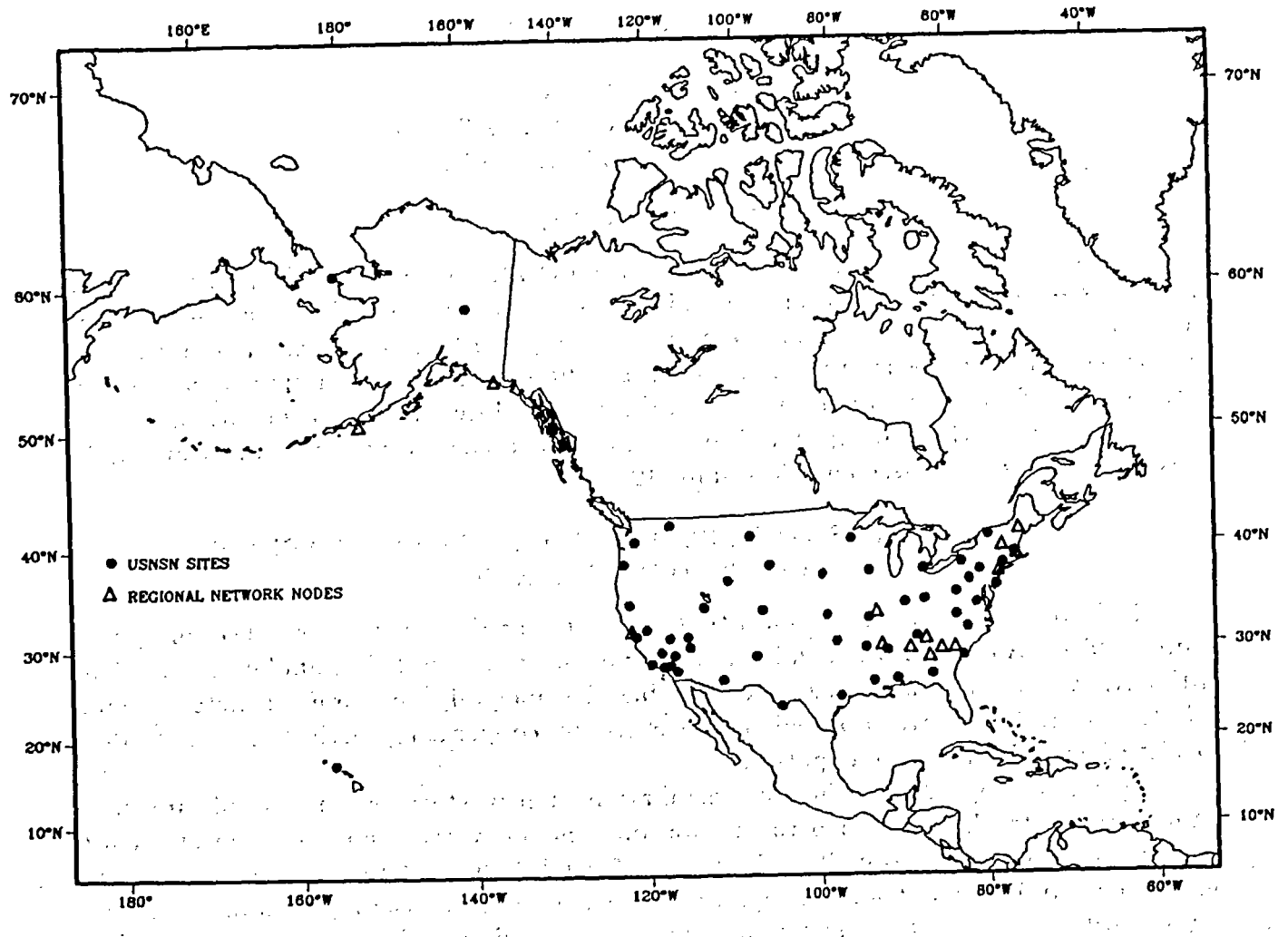

Figure 1. U. S. National Seismograph Network

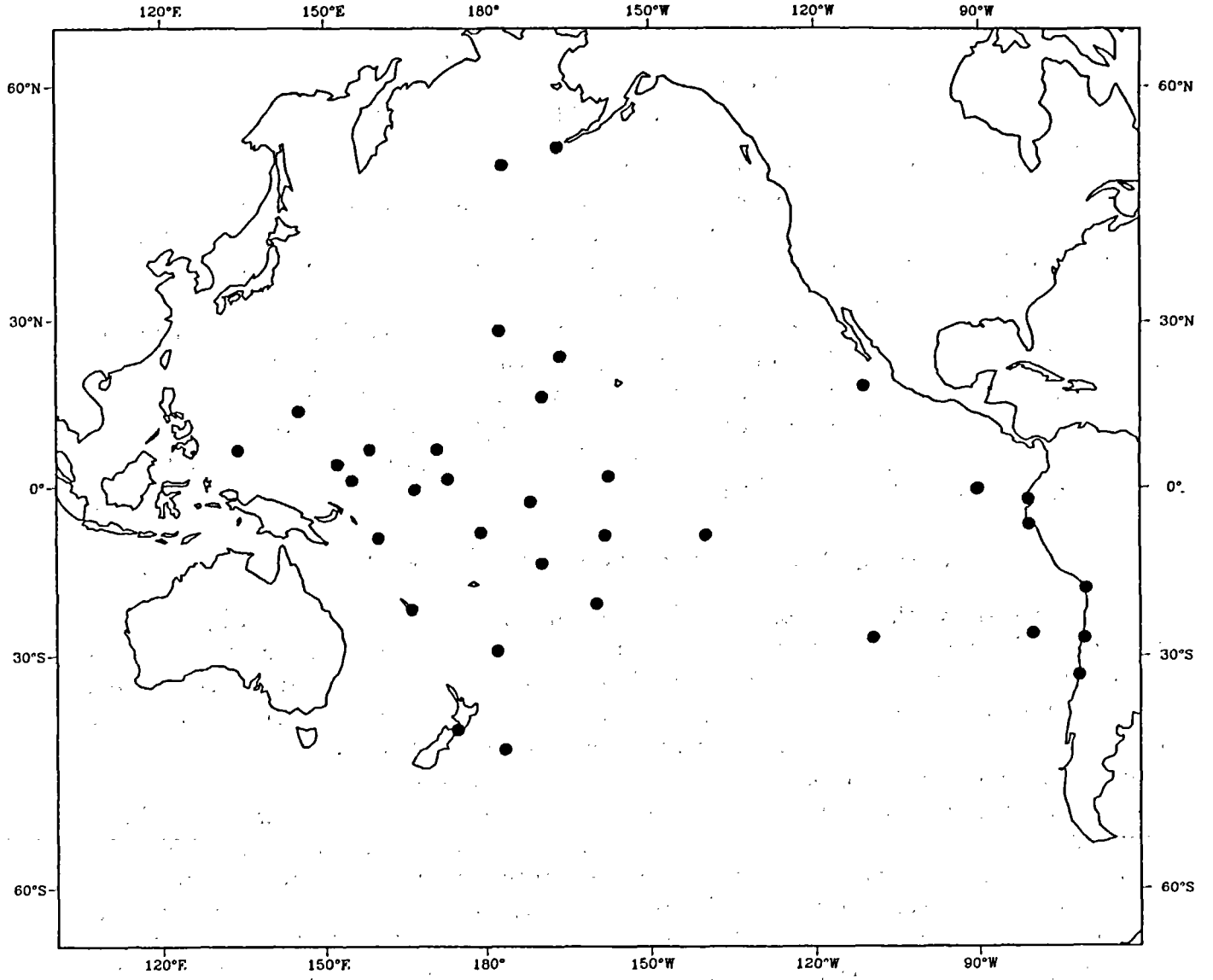

Figure 2. Pacific Satellite Seismograph Network

and Antarctica (Figure 3). It is planned that waveform data from the GTSN will be sent at phased intervals.

CURRENT AND ANTICIPATED TIME-INTERVALS BETWEEN OCCURRENCE OF AN EARTHQUAKE AND DETERMINATION OF EPICENTER AND MAGNITUDE

The initial NEIC location and magnitude of a major earthquake are now usually obtained within one hour following the earthquake. A shortening of the time elapsed between occurrence of an earthquake and issuance of the NEIC location and magnitude will result from the upgrade of NEIC networks, because the digital format will allow automatic event-detection, event-location, and magnitude-calculation. The shortening of time between earthquake occurrence and NEIC report should be particularly significant for earthquakes occurring during non-working hours, when employees must be called from their homes to the NEIC laboratory. With automatic event-location, much of the preliminary analysis will have been accomplished by the time the employees arrive at the laboratory. The digital format will also allow NEIC seismologists to do some analysis and early communication from their homes.

CURRENT AND FUTURE ACCURACY IN EPICENTER DETERMINATION

Figure 4 shows the effect of random errors on epicentral precision for a hypothetical earthquake in the Central Aleutian Islands, near longitude 165°W. Nishenko (1989) estimated that this region had a 44-percent probability for occurrence of a large earthquake in the next ten years. Although the seismic gaps in this region do not have dimensions that are typically associated with great tsunamigenic earthquakes (Nishenko, 1989), disastrous tsunamis have originated from this section of the Aleutian arc.

Shown in Figure 4 are 90-percent confidence ellipses for the epicenters of two hypothetical Aleutian Islands earthquakes. Both ellipses are computed under the assumption that errors in arrival-times have a Gaussian distribution with zero mean and 1 sec^2 variance. The ellipse associated with the "Current" epicenter demonstrates the precision that would be obtained with a typical suite of stations that are rapidly available to the NEIC in current operations. The particular set of stations chosen is the set that the NEIC used to obtain the initial location of the Gulf of Alaska earthquake of 6 March 1988. The "Current + 4 PSSN" epicenter demonstrates the increase of precision that would have resulted with arrival-times from four additional stations optimally distributed around the Pacific Basin at sites of future PSSN stations. Using data from all of the PSSN stations would have made the "Current + 4 PSSN" ellipse slightly smaller.

The implication of Figure 4 is that the present configuration of NEIC stations does a good job for earthquakes in the central Aleutian Islands. The effect of additional stations on location precision will be modest and, with present knowledge of tsunamigenesis, probably not significant for purposes of issuing tsunami warnings. The modest effect for Aleutians' earthquakes of adding new stations to the present network of rapidly responding stations is also demonstrated by comparing epicenters computed by the NEIC within an hour of an earthquake with epicenters ultimately published in the Monthly Listing of Preliminary

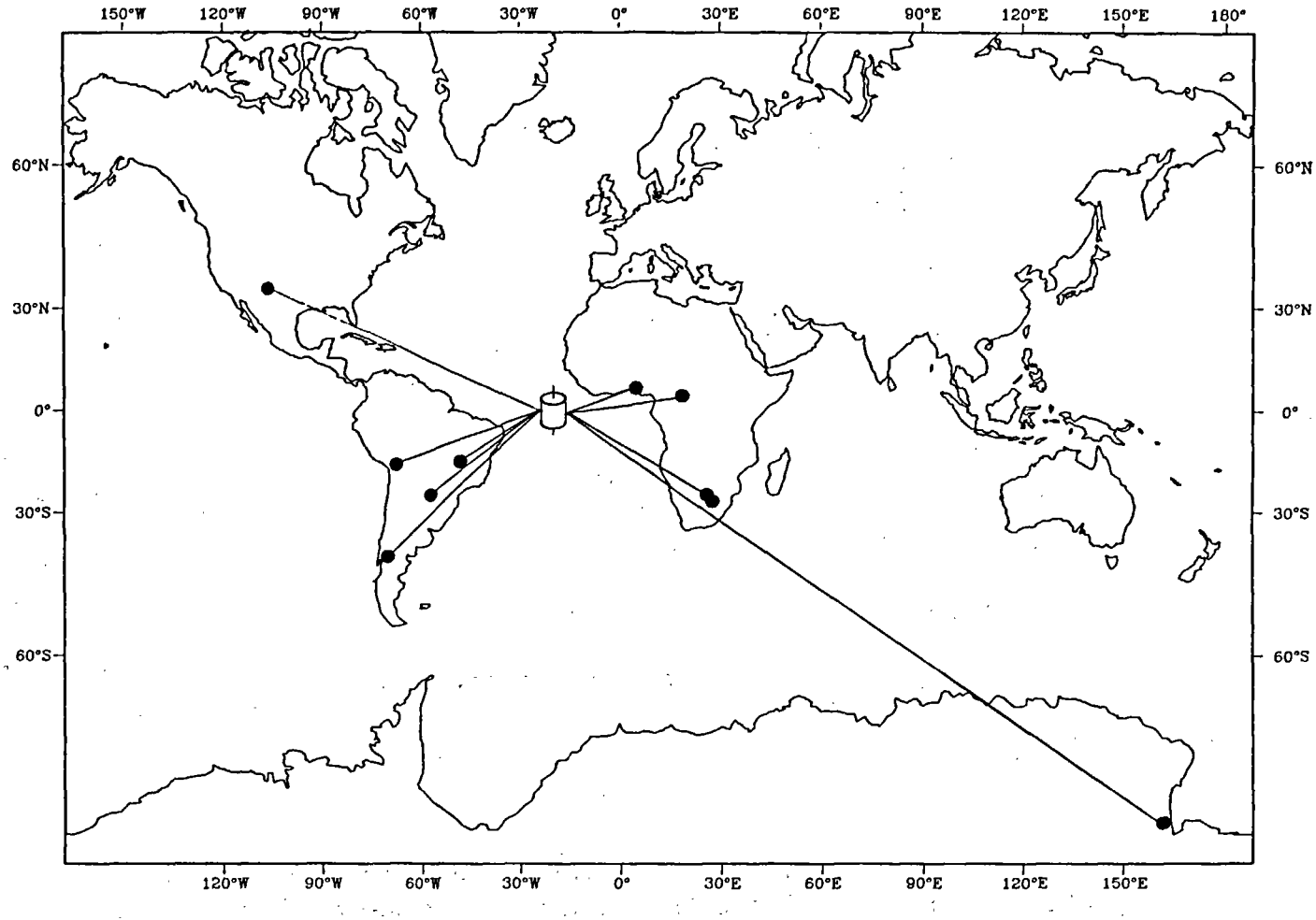

Figure 3. Global Telemetered Seismograph Network

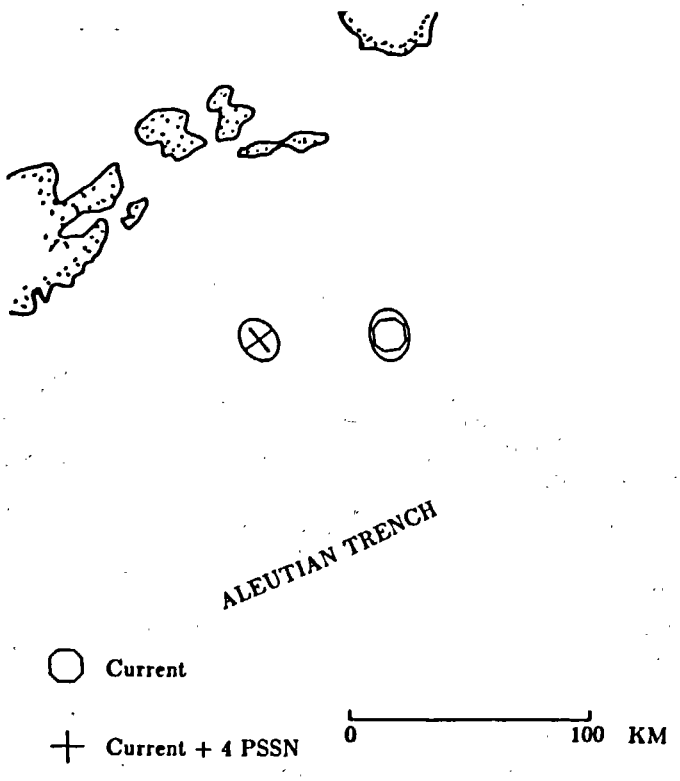

Figure 4. Improvement in epicentral precision from adding stations to the NEIC network, for hypothetical earthquakes in the Aleutian Islands. Arrival-time data assumed to have a variance of 1 sec^2. Epicenter symbols show position of true epicenter, and ellipses are confidence regions that cover the area within which a computed epicenter would fall with a 90 percent level of confidence. See text for explanation of data sets used to compute each ellipse.

Determination of Epicenters (PDE). The first epicenters are in most cases within tens of kilometers of the final epicenters.

The situation is different in other regions about the Pacific. With the present network of stations from which data are quickly available, first NEIC epicenters of earthquakes occurring at some locations on the margins of the southern Pacific may differ by more than 100 km from the final PDE epicenters. Current knowledge of tsunami generation is sufficiently high that a substantial reduction of epicentral uncertainty below the present 100 km might be highly useful in the tsunami warning process. Such a reduction of epicentral uncertainty will occur when data from the PSSN and other networks are received at the NEIC.

Figure 5 illustrates the effect of random errors on epicentral precision for a hypothetical earthquake on the western coast of South America near latitude $20°S$, in the region of the great tsunamigenic earthquake of 9 May 1877. Nishenko (1989) estimates that this region has a 20 percent probability of producing a great earthquake in the upcoming 10 years. Again, we consider precision of the network of stations from which data are rapidly available to the NEIC, and we consider the network as it will be augmented in the future. We assume that the statistical properties of the arrival-time data are the same as we assumed for the Aleutians. For the present network, even small random errors in arrival-time data can produce large errors in the computed position of the epicenter, as is clear from the large size of the ellipse associated with the "Current" epicenter in Figure 5. The set of stations used to compute the ellipse is the set of stations that the NEIC used to compute the initial epicenter of the Peru earthquake of 12 April 1988. The large size of the "Current" ellipse explains why we observe large discrepencies between initial and final PDE epicenters for many real earthquakes along the west coast of South America. These errors are large enough that an earthquake occurring offshore of western South America could be initially mislocated well inland, or an earthquake occurring well inland could be initially mislocated offshore. Including data from the PSSN network will yield a dramatic reduction in the confidence ellipse, corresponding to a dramatic increase in the precision of the earthquake. The ellipse associated with "Current + 4 PSSN", Figure 5, shows the effect of adding 4 optimally distributed PSSN stations to the "Current" suite of stations. Adding data from two GTSN stations in the interior of the South American continent will increase precision still more (ellipse associated with "Current + 4 PSSN + 2 GTSN", Figure 5). Using data from more of the PSSN and GTSN stations would produce even smaller ellipses (not shown).

The foregoing discussion of epicentral precision has not considered location bias resulting from lateral variations in seismic wave velocity. Such bias can in principle be minimized by ray-tracing methods and by relative location methods such as joint hypocenter determination (e.g., Engdahl et al., 1982). The confidence ellipses represent the uncertainty of the epicenters after bias has been removed.

CURRENT AND FUTURE ESTIMATES OF EARTHQUAKE SIZE

Initial magnitudes reported by the NEIC for large, shallow, earthquakes are 20-second surface-wave magnitudes. For the largest earthquakes, there is sometimes a problem that magnitude estimates must be based on data from the relatively few long-period seismo-

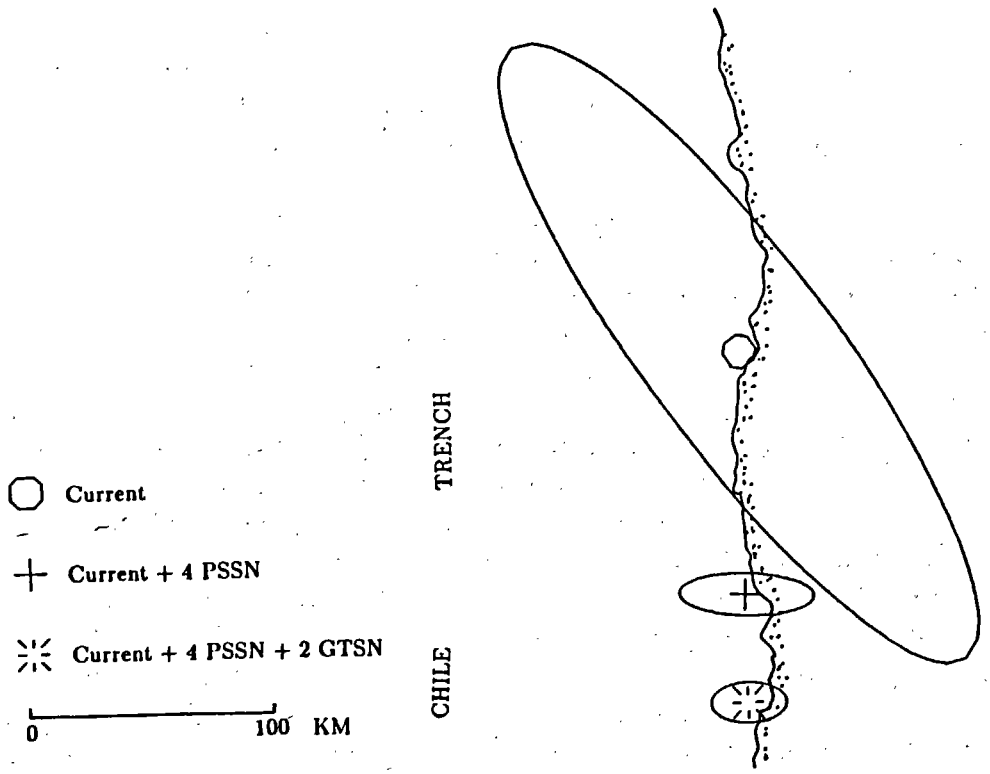

Figure 5. Improvement in epicentral precision from adding stations to the NEIC network, for hypothetical earthquakes on the west coast of South America. Arrival-time data assumed to have a variance of 1 sec^2. Epicenter symbols show position of true epicenter, and ellipses are confidence regions that cover the area within which a computed epicenter would fall with a 90 percent level of confidence. See text for explanation of data sets used to compute each ellipse.

graphs that are not driven off-scale by the earthquakes. Nonetheless, initial magnitudes are usually within about .3 magnitude-units of those later published in the PDE catalogs.

The general reliability of initial NEIC magnitudes notwithstanding, the augmented NEIC network should permit computation of earthquake magnitudes that are ultimately more useful for tsunami-warning purposes than the present 20-second surface-wave magnitudes. The high dynamic-range of the digital seismographs will permit on-scale recording of the largest earthquakes, so that the problem of computing 20-second surface-wave magnitudes from a few on-scale seismograms will disappear. The digital format of the data will also enable easy computation of moment-magnitudes from mantle surface-waves. For the largest earthquakes, moment magnitudes will differ from 20-second surface-wave magnitudes, and they are likely to be better predictors of tsunami potential.

FOCAL DEPTH AND FOCAL MECHANISM

At present, initial focal depths of NEIC hypocenters are estimated from depth-phases visible on analog records; for large shallow-focus earthquakes, initial hypocenters are usually held at 33 km focal depth. Focal mechanisms are not estimated in the first hours following an earthquake. Their estimation is deferred until preparation of the monthly summaries, which are published with a time lag of about six months. In the long-term, we anticipate that the determination of the seismic moment-tensor and focal-depth from P-wave signals (e.g., Sipkin, 1982) will be made automatically from the telemetered data soon enough to be incorporated into the tsunami-warning process.

CONCLUSION

With the installation of new networks of digital seismographs, the NEIC will be able both to improve the precision of the data it contributes to the tsunami-warning process and to shorten the time between earthquake occurrence and transmittal of data.

REFERENCES

Engdahl, E. R., Dewey, J. W., and Fujita, K., 1982, Earthquake location in island arcs: Physics of the Earth and Planetary Interiors, v. 30, p. 145-156

Massé, R. P., and Needham, R. E., 1989, NEIC – The National Earthquake Information Center: Earthquakes and Volcanoes, v. 21, p. 4-44.

Nishenko, S. P., 1989, Circum-Pacific seismic potential 1989-1999: U. S. G. S. Open-File Report 89-86, 126 p.

Sipkin, S. A., 1982, Estimation of earthquake source parameters by the inversion of waveform data; synthetic seismograms: Physics of the Earth and Planetary Interiors, v. 30, p. 242-259.

Figure 1. U. S. National Seismograph Network

Figure 2. Pacific Satellite Seismograph Network

Figure 3. Global Telemetered Seismograph Network

Figure 4. Improvement in epicentral precision from adding stations to the NEIC network, for hypothetical earthquakes in the Aleutian Islands. Arrival-time data assumed to have a variance of 1 sec^2. Epicenter symbols show position of true epicenter, and ellipses are confidence regions that cover the area within which a computed epicenter would fall with a 90 percent level of confidence. See text for explanation of data sets used to compute each ellipse.

Figure 5. Improvement in epicentral precision from adding stations to the NEIC network, for hypothetical earthquakes on the west coast of South America. Arrival-time data assumed to have a variance of 1 sec^2. Epicenter symbols show position of true epicenter, and ellipses are confidence regions that cover the area within which a computed epicenter would fall with a 90 percent level of confidence. See text for explanation of data sets used to compute each ellipse.

POSEIDON PROJECT - ITS APPLICATION TO THE BETTER UNDERSTANDING OF THE NATURE OF INTERPLATE EARTHQUAKES

R. Geller

Department of Geophysics, Faculty of Science, Tokyo University

1 Introduction

As Japan's contribution to research in global seismology, we propose to deploy seismographs in the Western Pacific, and in Eastern and Southeastern Asia. Our proposed project has been named the POSEIDON (Pacific Orient SEIsmic Digital Observation Network) Project. The POSEIDON project will be coordinated with the FDSN and its member countries, to ensure maximum productivity and eliminate duplication of effort.

The POSEIDON seismic array will be operated cooperatively by the participating institutions. Data from the POSEIDON network will be exchanged freely in accordance with procedures to be set up by the FDSN.

Progress in seismological observation and geophysical research is important for the countries in the western Pacific, including Japan, which suffer from seismic, tsunami and volcanic hazards. The POSEIDON project will contribute greatly to the advancement of research in earth science and to the mitigation of natural hazards in all of the countries in the western Pacific region. Data from the POSEIDON Project will also contribute greatly to our knowledge of the earth's interior.

2 Present Status of the POSEIDON Project

Since the publication of the first English language pamphlet on the POSEIDON project in June 1987, we have continued our efforts on a variety of fronts. These efforts, which are summarized in this pamphlet, include the following.

1. Formulating a series of increasingly realistic and detailed plans for the POSEIDON Project, based in part on feedback from ongoing negotiations with agencies of the Japanese government about the availability of funding.

2. Holding preliminary discussions with colleagues from other countries in the western Pacific and Far East regarding the installation and operation of cooperative seismic stations.

3. Installing a network of broadband digital stations in Japan, and organizing a data center which will collect and archive the data. All data will be freely available to researchers inside and outside Japan.

4. Developing prototypes and conducting operational tests of long period ocean bottom seismograph (OBS) systems.

5. Exploring the feasibility of using the TPC-1 telecommunications cable, which is being retired from service, to make ocean bottom seismological observations.

6. Conducting downhole ocean bottom seismological observations as part of the Ocean Drilling Project (ODP).

7. Convening an international conference on the POSEIDON Network in August, 1988, in Tokyo; and an international Winter School on Global Seismology in December, 1989, in Tsukuba.

8. Making quantitative estimates of the improvements in resolution of earth structure that can be expected as a result of the POSEIDON network. We are using these estimates to plan an optimum configuration for the network.

9. Conducting research in global seismology, including work on earth structure, earthquake sources, and related computational and theoretical topics.

For administrative reasons the TPC-1 project and the ODP Borehole seismometer project are not formally considered part of POSEIDON. However, these projects are being carried out in close coordination with POSEIDON.

Preliminary work on POSEIDON has been funded by a series of relatively small grants, but, as POSEIDON grows in size, the establishment of a formal organization is becoming necessary. The Global Seismology Subcommittee[1] of the Japan National Committee for Seismology and Physics of the Earth's Interior of the Science Council of Japan and the Earthquake Research Institute (ERI) of Tokyo University have agreed in principle to establish the POSEIDON Data Center as a part of ERI.

Because of the complexity of the necessary bureaucratic procedures, the POSEIDON Data Center cannot be formally established until April, 1992 at the earliest; we therefore have established an interim organization, the "pre-POSEIDON" Data Center, under the direction of Kunihiko Shimazaki of ERI, and have produced and distributed the first event tape of data from pre-POSEIDON stations. The pre-POSEIDON Data Center (as well as the POSEIDON Data Center when it is established) will coordinate the efforts of the many scientists from Japan and overseas who are participating in POSEIDON.

We are currently negotiating with the Japanese government regarding funding for the POSEIDON project. However, several scientific grants for preliminary work towards establishing the POSEIDON project have already been approved. We are collectively referring to these grants as the "pre-POSEIDON" Project. We have already installed several broadband stations in Japan and will install several more stations overseas, in cooperation with scientific organizations in the host countries. Our plans are to install one station each in the USSR and South Korea in the fiscal year starting April 1, 1990, and to install one station in Indonesia in the fiscal year starting April 1, 1991. Data from the pre-POSEIDON stations will be collected and distributed by the Pre-POSEIDON data center at ERI.

We wish to thank all of the organizations, especially the USGS, GEOSCOPE, IDA/IRIS, and NARS, who have helped us by supplying data and equipment for seismic stations.

3 Overall Plans for POSEIDON

Our current tentative plan for the first five years of the POSEIDON Project is to install stations as shown in Figure 1. This plan is subject to change, as it is dependent on the availability of funding; it also is dependent on the successful conclusion of negotiations

[1]The Global Seismology Subcommittee, which is the representative of Japan to the FDSN (Federation of Broadband Digital Seismograph Networks), serves as a "window" for POSEIDON's agreements for international cooperative research, and also as a forum for communication between the Japanese institutions working on global seismology.

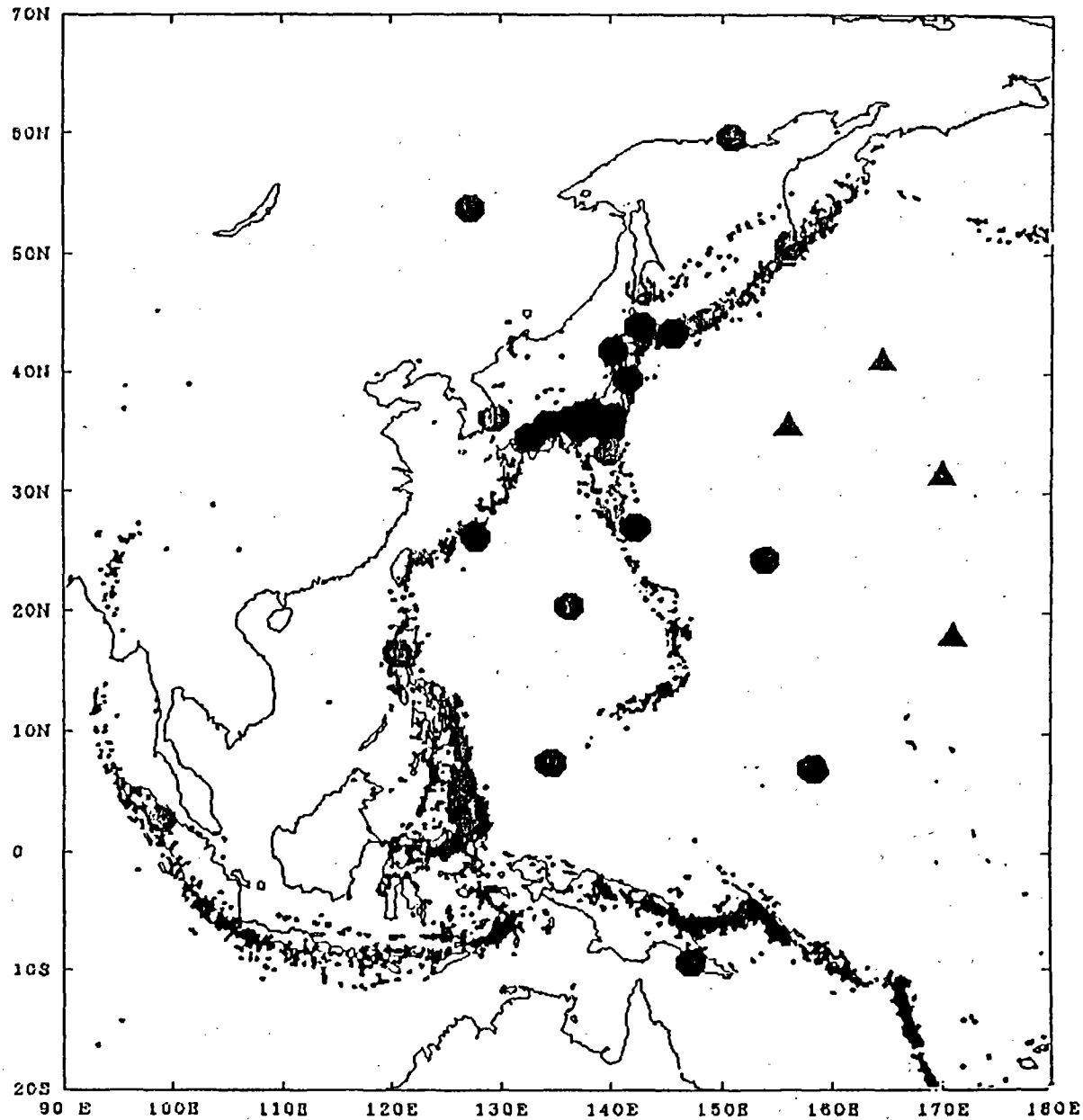

Figure 1: Tentative siting plans for POSEIDON stations. The solid circles are subareal sites. Black circles indicate stations which are already operational, blue circles indicate stations which we plan to install before March 31, 1992, and green circles indicate possible future sites. Green triangles are tentative sites for deployment of the broadband OBS's we are now developing. The smaller colored dots are earthquakes deeper than 50 km. Warmer colors correspond to shallower events and colder colors to deeper events.

with counterpart institutions in the various host countries. In all cases where overseas stations are shown, we have, at a minimum, conducted preliminary discussions with our colleagues and officials of their governments; however, in most cases the conclusion of formal agreements is pending.

Our goal for the first five years of POSEIDON (including the current pre-POSEIDON phase) is to have several OBS stations and on the order of 10 overseas broadband digital stations. We also plan to collect broadband data from cooperating institutions in Japan, and distribute these data through the POSEIDON Data Center. Many of the cooperating stations in Japan are funded by projects other than POSEIDON, e.g., earthquake prediction.

4 POSEIDON Data Center

The POSEIDON Data Center will collect, distribute, and archive data for the POSEIDON project, and coordinate the efforts of cooperating universities and government agencies in Japan and overseas. Personnel from all of the cooperating institutions will develop new instrumentation, carry out maintenance, and manage the mobile-array instruments. The Data Center will publish newsletters, organize meetings and symposia, and generally work to facilitate good communication among the participants.

The following data will be included in the on-line POSEIDON database, which will use optical disks with a jukebox type disk drive.

- Continuous data from broadband seismographs sampled at 1 Hz.
- Event data from broadband seismographs sampled at 40 Hz.
- Strong motion data from oversea stations using triggered recording.
- Data from ocean bottom seismic observations.
- Data from mobile arrays.

The on-line database will also include data from other networks exchanged through FDSN. Due to practical considerations, continuous broadband data with a 40 Hz sampling rate will be stored off-line. Note that the ocean bottom seismic data will include data from the TPC-1 project and borehole seismic data, as well as OBS data. Finally, some non-seismic TPC-1 data (geomagnetic, geoelectric, pressure, ocean temperature, and deep sea current) will also be included in the database.

Data from the POSEIDON network will be exchanged freely and globally in accordance with procedures to be set up by the FDSN. All data will be made available at the earliest opportunity. Users in Japan will access the on-line database through the "Science Information Network" of the National Center for Science Information Systems, Japan. We plan to provide on-line access to users outside Japan through networks such as TISN (Tokyo University International Science Network), which links Tokyo University and Hawaii, or WIDE, which links Keio University and Hawaii. These in turn provide access to most of the world's scientific networks.

We also plan to publish on the order of a dozen CD-ROMs per year when the POSEIDON Project is in full operation. These CD-ROMs will be widely distributed both nationally and internationally. The POSEIDON CD-ROMs will contain data from the above five datasets, but, due to practical considerations, will include only subsets of the 40 Hz broadband data and mobile array data.

5 Subareal Network: Plans and Present State

At present, in cooperation with several other institutions, we are operating more than a dozen broadband digital stations in Japan (as shown in Figure 1), and the National Institute for Polar Research is operating a broadband station at Showa Base in Antarctica.

We plan to be installing stations in Korea, and the USSR in the fiscal year ending March 31, 1991, and in Indonesia in the fiscal year ending March 31, 1992

Future candidate sites are located in the Philippines, USSR, Papua New Guinea, Ponapei (Federated States of Micronesia), Palau, Thailand and Viet Nam. Our plans are not yet definite, but we hope to have them finalized within the next year.

6 Ocean Bottom Seismic Observations

We are currently carrying out preliminary work on three methods of making submarine seismic observations: popup OBS (Ocean Bottom Seismograph) systems; ocean bottom seismometers attached to fully dedicated submarine cables; and borehole seismometers. We anticipate that POSEIDON will use a combination of these three complementary approaches.

6.1 Broadband Ocean Bottom Seismographs

We are currently developing a new generation of digital OBS's on the basis of our experience with previous short-period OBS systems. Our new OBS has a wider dynamic range and better sensitivity at low frequencies. The seismometers are three component geophones suspended by a leveling device. A digital memory with a capacity of over 1 GByte will allow unattended observations on the ocean bottom for about 6 months to one year.

One of the keys to making broadband, wide dynamic range submarine seismic observation is the coupling of the geophones to the bottom. We are testing various devices to ensure the best possible coupling. Our OBS has an acoustic transponder which allows us to release the ballast weight in order to recover the OBS on the sea surface, as well as to determine the exact position of the OBS on the ocean bottom. The acoustic signals can also be used to monitor the number of events recorded by the OBS, the battery voltage, etc.

6.2 TPC-1

In 1990, the Japan-Hawaii submarine telecommunication cable TPC-1 (Trans Pacific Cable-1) will be retired from service and replaced by the TPC-3 fiber optic submarine cable, which has already been placed in service. TPC-1, which was constructed in 1964, is economically obsolescent, but will continue to be usable for a number of years.

We are currently negotiating with the principal owners of TPC-1, AT&T and KDD, to obtain permission to use TPC-1 to make ocean bottom geophysical observations. The reuse of TPC-1 will be a joint US-Japan project; the US counterpart to POSEIDON will be IRIS. Because of the imminent deadline for concluding arrangements for reuse of TPC-1, this project is administratively separate from POSEIDON, and is being managed directly by ERI. However, the TPC-1 data will be archived and distributed by the POSEIDON Data Center.

The first phase of the TPC-1 project will utilize the segment from Ninomiya, Japan to Guam (Figure 2). We plan to deploy two seismic stations and one geophysical station. The former will include conventional velocity type seismometers, very broad band accelerometers and a hydrophone. The design specification of the very broad band accelerometer is: three component, flat spectrum from periods of several hundred seconds to 0.067 s, 120 dB dynamic range, and resolution higher than 100 μgal. The geophysical station will collect geomagnetic, geoelectric, pressure, temperature, and deep sea current speed data, as well as seismic data. The pressure measurements will provide data on tsunami propagation in the deep ocean basins, and may also assist in tsunami warning.

The TPC-1 data will be telemetered to the POSEIDON data center in real-time. Continuous data with a 1 Hz sampling rate and event data with a 40 Hz sampling rate will be included in the on-line database. Continuous data with a 40 Hz sampling rate will be stored off-line.

6.3 ODP Downhole Seismometer

The Second Conference on Scientific Ocean Drilling (COSOD II) in 1987 made the following recommendation.

> "It is critical for ocean-bottom seismic observatories to supplement and become an essential part of the global observing system over the next decade. ... Very broadband seismograph systems emplaced in the drill holes are a necessary complement to the land-based Global Seismographic Network."

We emplaced a broadband digital seismometer in a borehole in the Japan Sea in the fall of 1989. The experiment, which was the first application of digital and feed-back sensor technology to an ocean borehole seismometer, was made at Site 794, Hole D on ODP Leg 128 in the northern part of the Yamato Basin. (Figure 3). The seismometer (Guralp slimline CMG-3: 3-component feedback type accelerometer) is housed in a pressure case together with a 16-bit digitizer (80 Hz sampling rate) and a digital data telemetry unit.

Immediately after installing the borehole seismometer, a controlled source seismic experiment was conducted to determine the detailed crustal structure surrounding the site. An airgun shot record and its power spectrum are shown in Figure 4.

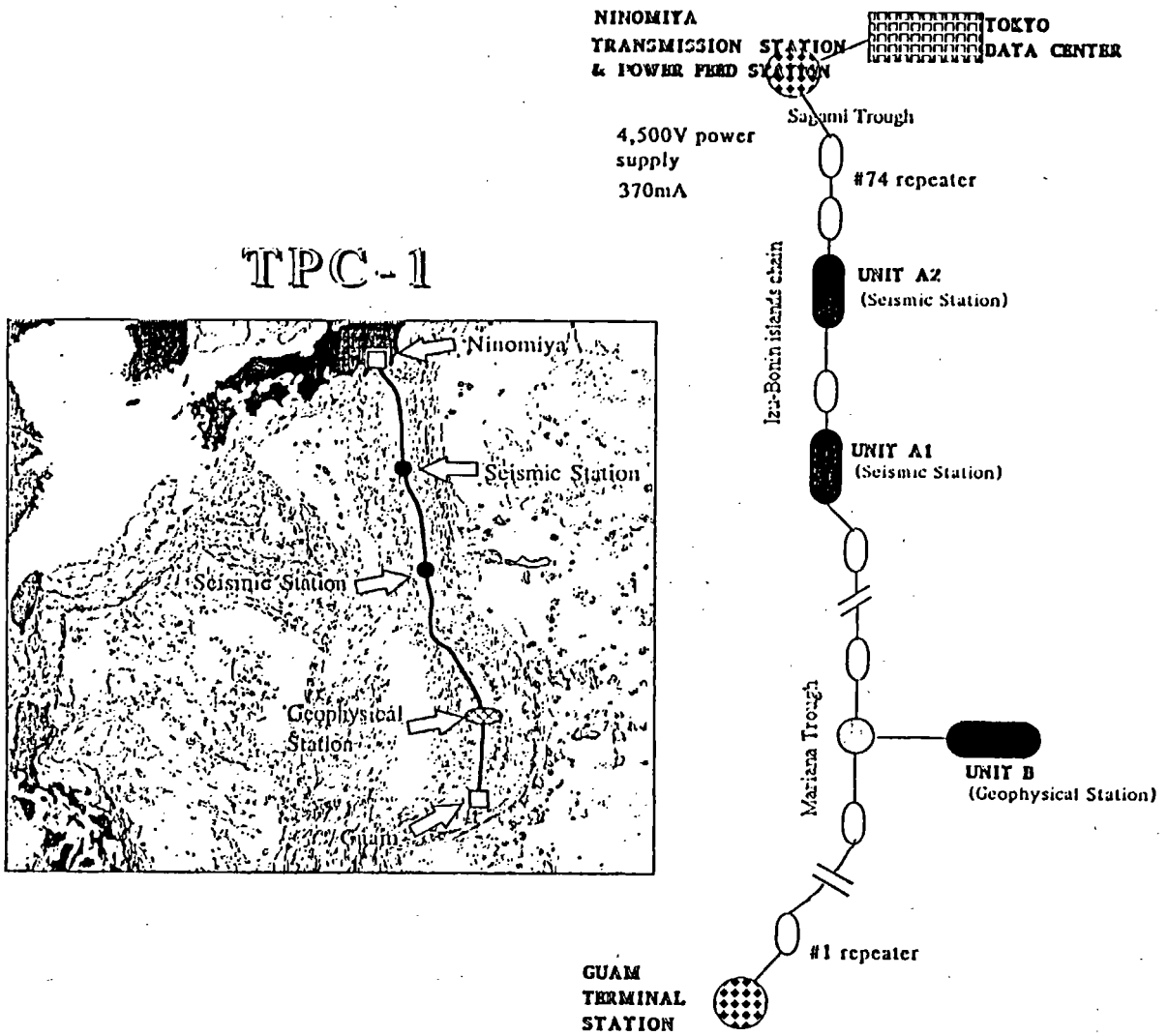

Figure 2: Plan for the TPC-1 segment from Ninomiya, Japan to Guam.

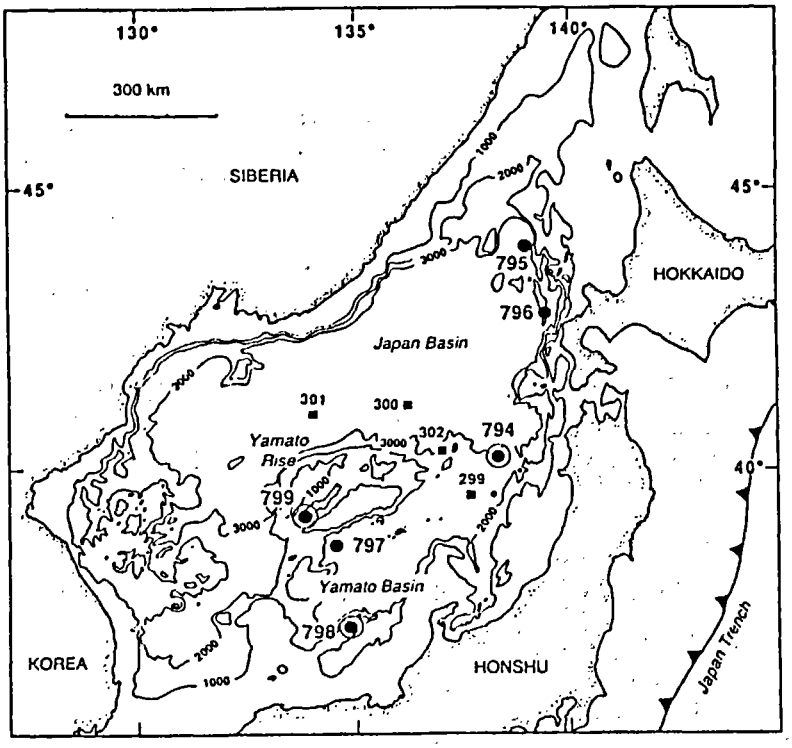

Figure 3: The ODP Borehole seismometer was deployed at Site 794.

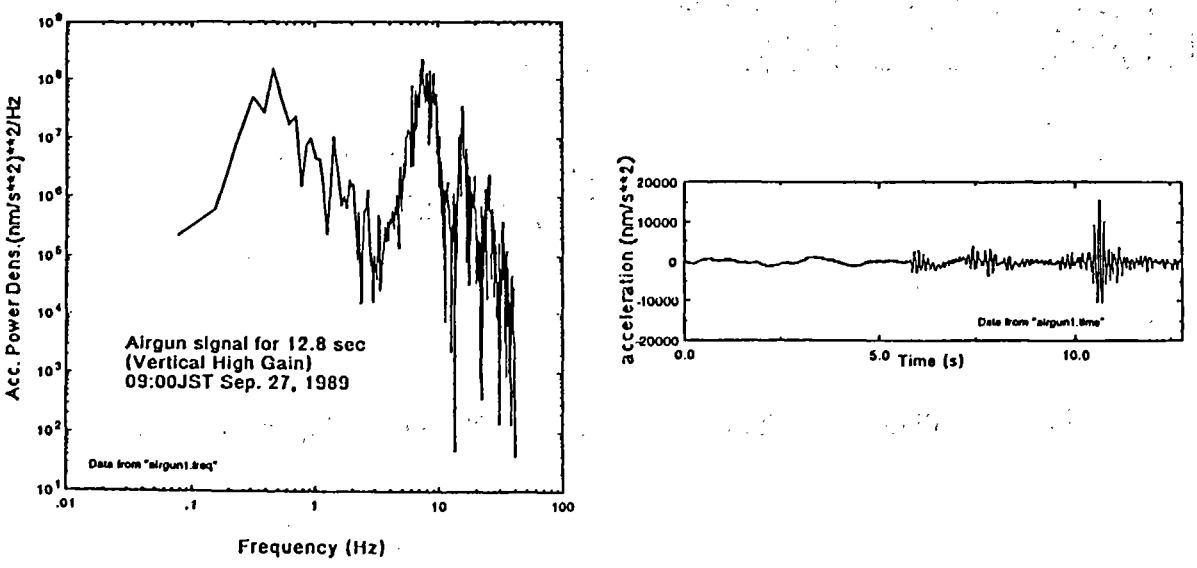

Figure 4: Record from the ODP borehole seismometer and its spectrum.

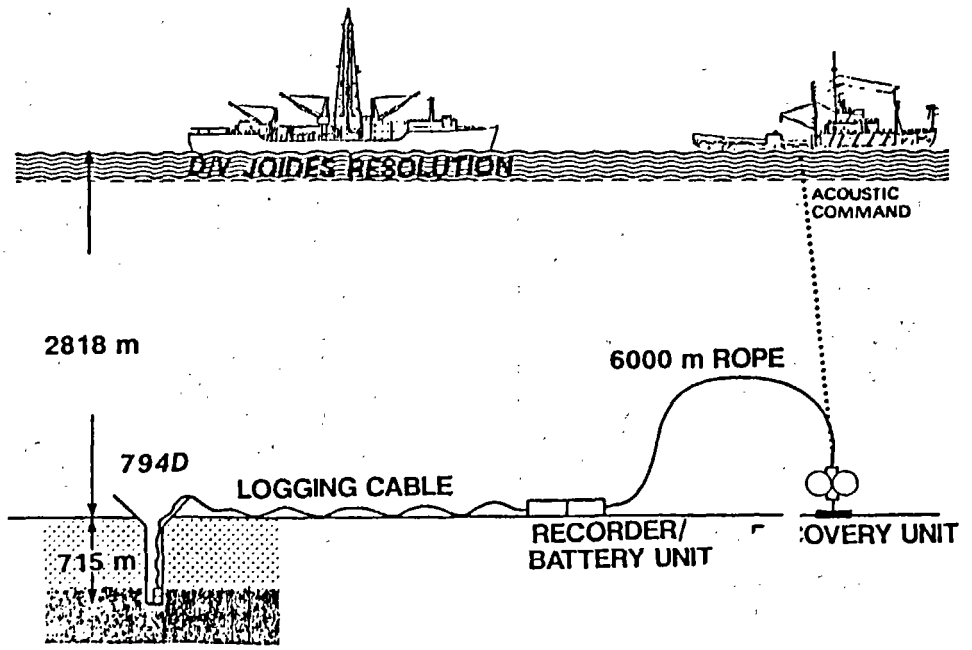

Figure 5: The ODP borehole seismometer s) n.

In the second phase of the experiment, we connected a cable to the seafloor recording unit and deployed it with a recovery system. Figure 5 shows the configuration of our system. Since the recording system has a capacity of less than 24 hr of continuously recorded 80 Hz data, event detection and time windowing are being used.

7 Capabilities of the POSEIDON Network

We have conducted quantitative studies to estimate the improvement in the resolution of three dimensional earth structure and in the determination of earthquake source mechanisms that can be expected as a result of the POSEIDON network.

7.1 Laterally Heterogeneous Mantle Structure

Better knowledge of three-dimensional earth structure in the western Pacific area is important for understanding the geodynamic processes that are taking place in this region. Since the present density of seismic stations in the western Pacific is low (particularly in the oceanic regions), the present spatial resolution is poor.

The POSEIDON network will greatly improve the spatial resolution of laterally heterogeneous earth structure (including anisotropy and anelasticity) in the western Pacific. We assess the improvement in resolution of lateral heterogeneity and azimuthal anisotropy of Rayleigh wave phase velocity that will be obtained as a result of the POSEIDON Network. We also quantitatively consider the improved resolution for the delay time tomography for lateral heterogeneity of P-wave velocity. We compare the resolution expected with

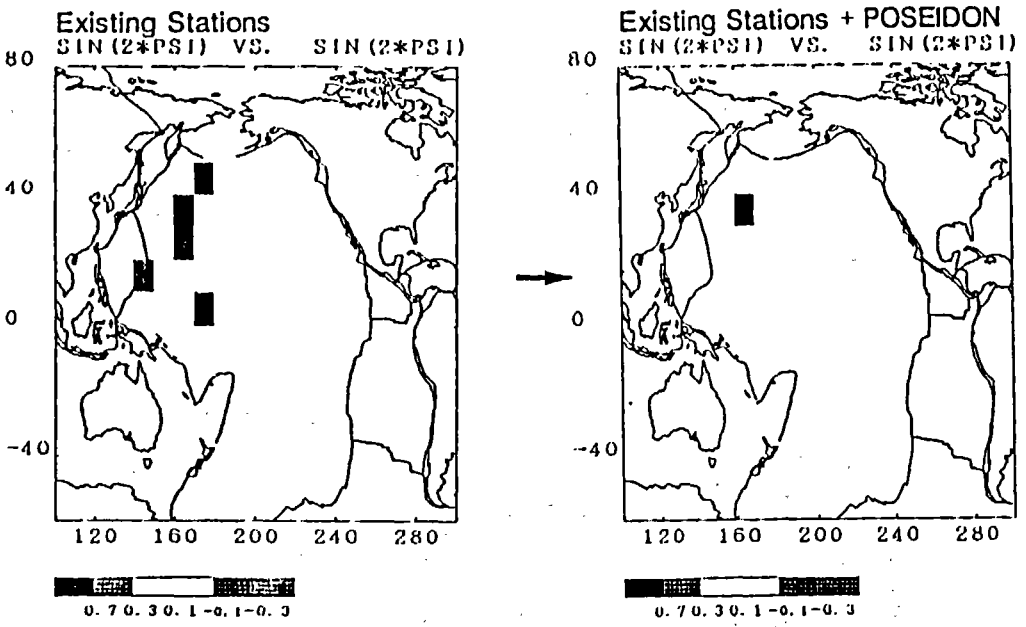

Figure 6: Resolving kernel for anisotropy of Rayleigh wave velocity without POSEIDON Network (left), and including POSEIDON stations (right). The black square is the target 10° by 10° block. The resolution is greatly improved by using the POSEIDON data.

and without the POSEIDON network.

Figure 6 shows the resolution kernels for the azimuthal anisotropy beneath the western Pacific which would be obtained using data from existing GDSN, IDA, GEOSCOPE, and CDSN stations. This figure shows that the resolving kernels are substantially improved when the proposed POSEIDON stations are also included in the dataset. The thirty hypothetical events used in the calculation are located along the subduction zones and ridges in the circum-Pacific area.

To evaluate the improved resolution for body wave tomography, we consider a laterally heterogeneous "checkboard" model (i.e., a model with systematically alternating high and low velocity regions). We calculate theoretical travel times for this model, and then perform a tomographic analysis of the synthetic travel time data. As shown in Figure 7, the resolution of three dimensional structure beneath the western Pacific is greatly improved when the POSEIDON stations are included in the synthetic dataset. The great improvement in resolution is mainly due to the contribution of data from the ocean-bottom seismographs of the POSEIDON network. This demonstrates the importance of having seismic data from the ocean basins in the western Pacific.

7.2 Local & regional earth structure

Figure 8 is a vertical profile showing part of the three-dimensional P-wave velocity model determined using tomographic inversion of ISC data. The cold colors show high velocity regions (whose temperature is colder than the average for that depth) and the warm colors show low velocity regions (which are warmer than average). Because the oceanic plate

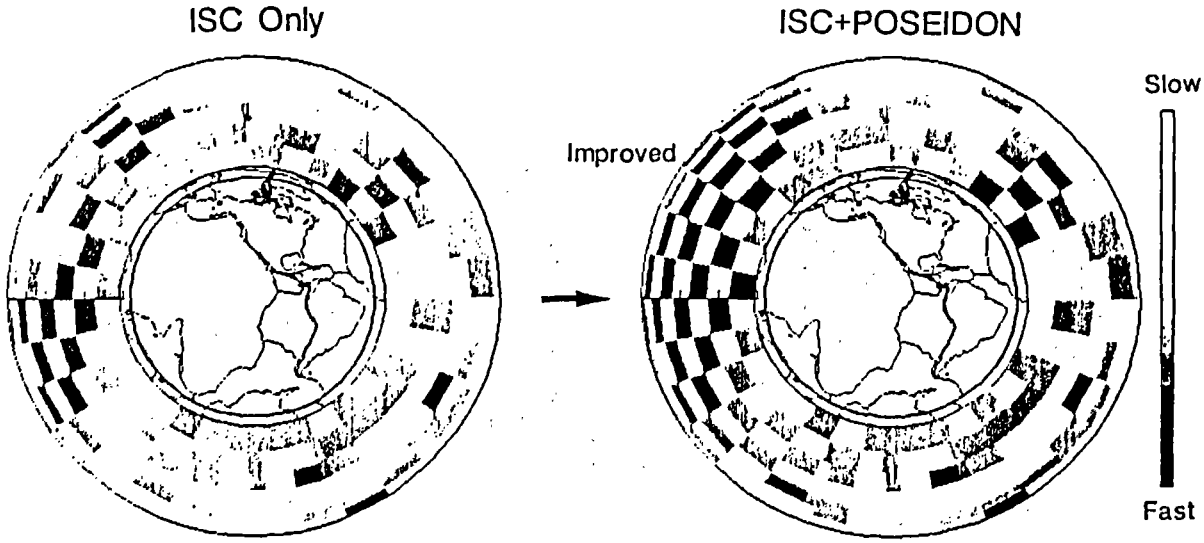

Figure 7: The resolution of the lateral heterogeneity of P-wave wave velocity beneath the western Pacific is greatly improved when POSEIDON data are included in the dataset (right). The improvement is mainly due to data from the ocean-bottom seismographs of the POSEIDON network.

is colder than average, it has an anomolously high velocity; similarly, the surrounding mantle is warm and thus its velocity is slower than the average.

Figure 8 shows high velocity zones corresponding to the Pacific slab (plate) descending from the Japan trench, and low velocity zones corresponding to the overriding mantle. The white zones in Figure 8 show regions for which the velocity cannot be determined, due to the unavailability of data. Figure 8 shows that although we can resolve the structure just beneath the Japanese Islands well, we cannot image the structure beneath the Pacific Ocean, Japan Sea and Asian Continent. By analyzing travel time and waveform data from the POSEIDON network, we will be able to construct a much clearer image of the three dimensional structure beneath Japan and its vicinity.

7.3 Determination of source parameters

We conducted a simulation to determine the accuracy of rapid determination of the seismic moment tensor for nearby events using a single POSEIDON station. We assumed that an initial estimate of the hypocentral coordinates and origin time has already been obtained (e.g., from a local network). We used the broadband station located at Inuyama, Japan in our simulation, and obtained source parameters very similar to those obtained using the global network. This suggests that it should be possible to determine the source parameters of nearby earthquakes with reasonably good accuracy within 10 min after the earthquake. This capability could contribute greatly to early tsunami warning systems and also to disaster relief operations.

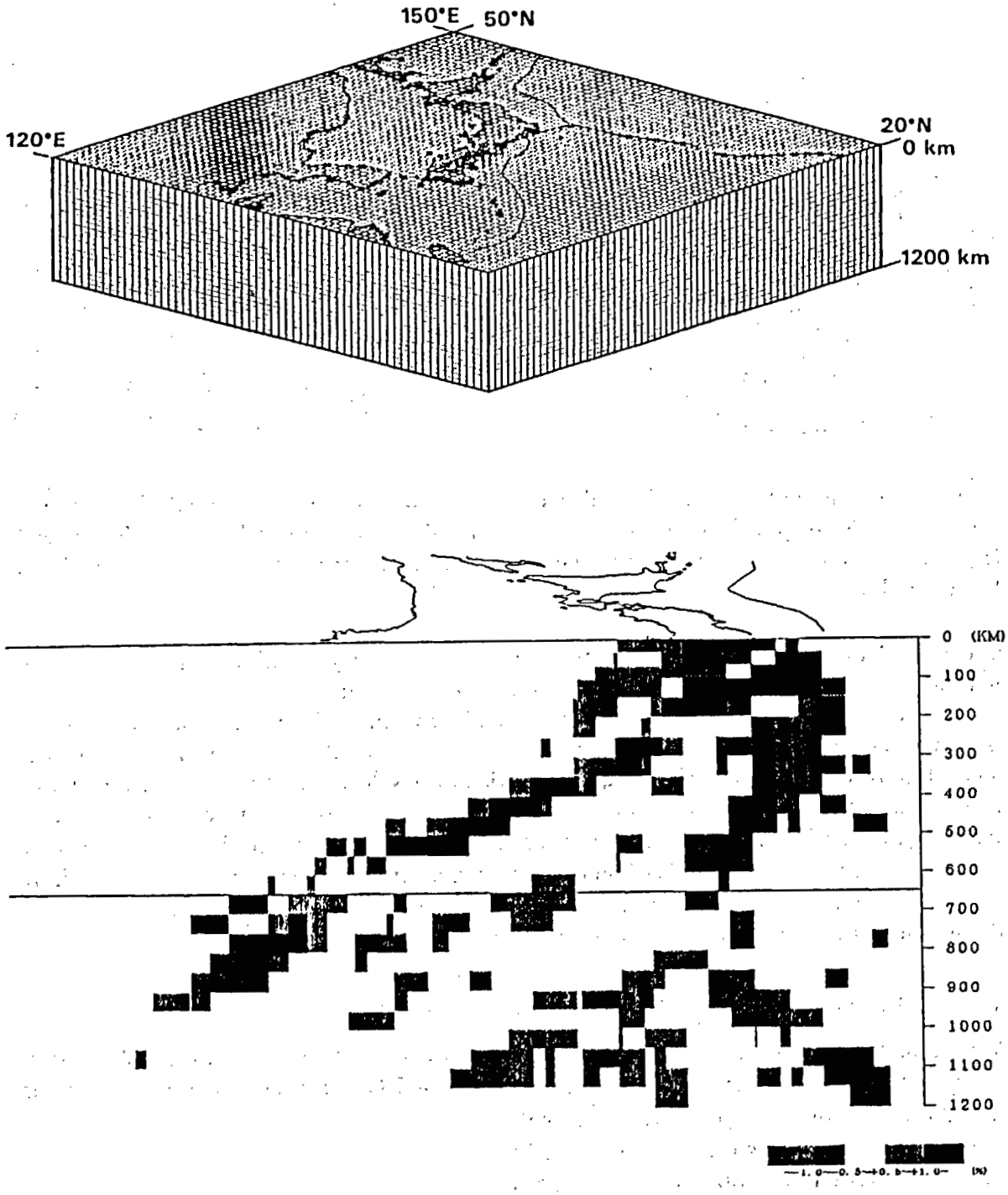

Figure 8: P-velocity beneath the Japan arc, projected onto a vertical cross-section. Cold colors show faster than average velocities, while warm colors show slower than average velocities. White regions are areas for which there are insufficient data.

EARTHQUAKE PREDICTION

George Pararas-Carayannis
International Tsunami Information Center

Abstract

Prediction of large earthquakes can lead to the prediction of future destructive tsunamis. Tsunami prediction at the present time is based primarily on the statistical determination of the recurrence frequency of major earthquakes in well-defined tsunamigenic regions of the Pacific and other areas. A statistical approach is primarily used for long-term tsunami prediction. The approach is not accurate. It is fairly simple to determine the recurrence frequency of small magnitude earthquakes which occur with greater frequency. It is more difficult to determine the recurrence frequencies of the larger destructive tsunamigenic earthquakes particularly by statistical means. Several other methods are presently used for earthquake prediction. These include geophysical, geological and chemical methods, as well as monitoring the behavior of animals. The state-of-the-art in earthquake prediction has come a long way. However, it is still far from being an exact science. What is presently referred to as "prediction" is simply scientific research on understanding the workings of earthquakes. In this paper an overview is provided on the methods employed in earthquake prediction.

INTRODUCTION

In order to reduce the risk of an earthquake and reduce and mitigate its effects, particularly those which may be associated with a generated tsunami, it is necessary to predict where and when a future, large earthquake may occur. Earthquake prediction at the present time is far from an exact science, and forecasts have not been very accurate. Presently, predictions are given in statistical terms. For example, when a prediction is made that "there is a 90 percent chance that an earthquake will occur in the next 50 years," it does not mean that this earthquake cannot happen tomorrow or that it may not be delayed by 50 years. Present predictions are not within a reasonable time frame that can be of usefulness to planners, policy makers, and those in government who deal with public safety.

To understand earthquake prediction, three different time frames have been assigned by scientists: long-, intermediate-, and short-term predictions. Long-term predictions involve a time frame of a decade or more and can only be general and with very limited usefulness for public safety. Intermediate-term prediction would fall into a time span of a few weeks to a few years, and again, it would not be of great practical usefulness. It is the short-term prediction that would be useful for any kind of public safety and evacuation since it gives

specific information on the time and location of an earthquake within days or weeks, not years.

Several statistical, geophysical, geological, and chemical methods are presently used for earthquake prediction. To this list we should add one more method that has been used with much success in China, which is the monitoring of the behavior of animals before quakes.

Presently, what is referred to as "prediction" is not really that. It is simply scientific research on understanding the workings of earthquakes. There is not sufficient historical data on which to base the number of hypotheses that have been proposed for earthquake predictions and, therefore, no way to judge the ultimate success or failure of such predictions. But even if earthquake prediction was more accurate, the social and economic implications of the prediction could be as devastating as the earthquake itself.

Present predictions of earthquakes of destructive magnitude cannot specify the time of occurrence. With one year's advance warning, only the month but not the week or day of the earthquake's occurrence might be known. A 10-year prediction might only indicate the year but not the month. The wider the time-window, the greater the social and economic disruption of the threatened area will be.

Tsunami prediction at the present time is based primarily on a statistical determination of the recurrence frequency of major tsunamigenic earthquakes in well-defined geographical regions of the Pacific and other areas. It is fairly simple to determine the recurrence frequency of smaller magnitude earthquakes for which there is a wealth of recent historical data. However, it is much more difficult to determine the recurrence frequencies of the larger destructive tsunamigenic earthquakes for which no similarly abundant data exists. However, extremely short-term tsunami prediction is possible immediately after the occurrence of a major earthquake. Tsunami Warning Systems are established for such predictions and the issuance of tsunami warnings to the populations of threatened coastal areas. But longer-term tsunami prediction, prior to earthquake occurrence, is limited by the constraints of earthquake prediction.

Methods Employed In Earthquake Prediction

Scientists employ various methods and instrumentation in their attempts to predict earthquakes. These involve statistical probability, physical measurements, geochemical observations, and observations of animal behavior.

1. STATISTICAL METHODS

By collecting adequate historical data, predictions can be made as to the recurrence frequencies of earthquakes of a certain magnitude at a specific location. Obviously, this is a very difficult thing to do, as the historical database often does not go far enough back in time to provide meaningful predictions within reasonable limits of statistical confidence. Although statistical methods may be more accurate for smaller and more frequently occurring earthquakes, they become totally unreliable in the prediction of the larger and less frequent ones. Predictions based on statistical analysis of historical earthquake data can only be given for the long or intermediate time frames. Thus, such methods are of limited reliability and usefulness.

Recurrence Frequency: Recurrence frequency is the relationship between magnitude and repetition of earthquakes. Statistically speaking, recurrence rates of earthquakes of certain magnitude can be determined by plotting magnitudes versus chronology of historical earthquakes. Of course, the more historical data that is available, the more reliable the predictions of the recurrence frequency will be, or the recurrence interval of a certain earthquake in a certain area. This is fairly simple to determine for smaller magnitude earthquakes for which there is a wealth of recent historical data. It is much more difficult to determine for the larger magnitude earthquakes for which no similarly abundant data exists.

Of course, in using a statistical approach, the basic assumption is made that the recurrence frequency of earthquakes is a function of time and that the same set of conditions leading to the occurrence of an earthquake are always at work. The statistical approach usually ignores clustering of earthquakes in time, or changes in geologic and tectonic conditions. However, there is evidence that in the last 25 million years of geologic time, the tectonic stresses of the fault systems have been very similar. Therefore, it can be assumed that the present tectonic movements and release of strain proceed at the same rate. Although over the short term variations in the release of strain are possible, over the longer term a consistency in the behavior of major faults can be expected. Also, we can expect a relative uniformity in the geographic location of earthquakes and their time of recurrence in the Pacific and elsewhere.

Seismic Gap Theory: The focus of statistical earthquake prediction in the last few years has been on the pattern of seismicity of a given region and the search for irregularities or deviations from this pattern that might suggest a forthcoming earthquake. We know the pattern of distribution of most of the world's earthquakes along the boundaries of the earth's major crustal plates. However, along these boundaries there are regions that, in recent years, have not produced earthquakes. These are nearly aseismic regions, or seismic gaps, and these could be the sites for future large earthquakes.

The Seismic Gap Theory provides a method of earthquake prediction based on estimating statistically, earthquake frequency. If a segment of a major seismic belt has not been broken for the last 30 years, such a region can be

considered as a seismic gap and a potential site for a future large event. Of course, identifying regions where large earthquakes are likely to occur is useful, but more specific information is needed as to the time of its occurrence. The 30-year time interval is considered as a minimum because, sometimes, great, shallow earthquakes recur in the same location within several decades. Thus, by studying the statistical recurrence of major earthquakes, we can identify not only the repeat cycle of great earthquakes, but also the areas where these large earthquakes could occur. For example, the Alaska earthquake of 1972, with a magnitude of 7.3, occurred near Sitka. This was in a seismic gap area that had been identified as a likely place for an earthquake. Based on seismic gap studies, the 19 September 1985 earthquake in Mexico also occurred along a seismic gap and was predicted. However, the time of its occurrence had not been pinpointed.

Slip Rates: A different approach has been used in estimating the average recurrence intervals of earthquakes along major faults. Rather than using historical records of earthquakes which are very recent, it is possible to examine the history of slip rates along a fault as preserved in the geologic record and evidenced by offsets in sediments and in the surface configuration of geomorphological features. The advantage of his method is that it utilizes data spanning a much longer period of time, thus getting better estimates of the recurrence frequency of small earthquakes.

Using the variable rates of relative movements between two sides of a fault, as evidenced by fault slip or tectonic creep, the basic average recurrence estimates can be obtained which may be applied in understanding future behavior of the different segments of a fault. The basic assumptions of this approach are that slip on a fault is accomplished by the sudden strain released by the rocks during earthquakes, by gradual slow tectonic aseismic creep, or by a combination of the two processes. It also assumes that in areas of the fault where aseismic creep occurs, strain energy is released gradually. In such areas large catastrophic earthquakes of magnitudes 8 or greater cannot take place. However, along segments of the fault that display little or no creep, very strong earthquakes can occur. Dr. Robert A. Wallace of the U.S. Geological Survey has used effectively such methods for establishing slip rates along the San Andreas fault, where an empirical relationship between probable Richter magnitudes and creep rates has been established.

Using Trees to Date Earthquakes And Crustal Movements: Earthquakes and surface movements along a fault can often be measured or dated using trees as indicators. Trees growing on or near a surface rupture along a fault can provide indirect evidence of historical fault disturbances that may have occurred up to several hundred years ago. Direct evidence may be fracturing, tilting or twisting of trees that grow on the surface break from the actual rupturing during an earthquake or the movement due to aseismic creep.

On either side of the fault, trees may be topped as a result of surface seismic motion. Indirect evidence may include tilting, topping, or burial of trees by earthquake-triggered landslides. Longer-term effects may include changes

in growth rates due to hydrologic and topographical changes. Often, scars on the trunks of trees, indicating an earthquake event, can be dated using tree ring methods. Tilting and fracturing of trees located directly over the fault can often be readily observed and dated by cutting the surfaces of stumps left.

By counting backward in one-year increments from the outermost tree ring, which represents most recent growth, to a scar representing damage by earthquake, it is possible to date past earthquakes and estimate the recurrence of future events. Asymmetries in the cross-sections of tree trunks often indicate a differential rate of growth which could be the result of tilting due to an earthquake or movement along a fault. Growth is generally accelerated on the underside of a tree that has been tilted.

Thus, trees can be used to date disturbances that have occurred up to several hundred years ago. A systematic study of trees over a great distance along a fault can help, and has been used in estimating recurrence of earthquakes, particularly in California where many of the tree species, such as the redwoods, can reach ages of several hundred years.

2. PHYSICAL AND GEOPHYSICAL MEASUREMENTS AND OBSERVATION

At present, statistical methods by themselves, although interesting and informative, are not a reliable way of predicting earthquakes. Therefore, scientists look for precursors and other physical geological changes that take place with consistency before an actual earthquake occurs. Studies of earthquake precursory events require the complete and systematic analysis of large volumes of seismic data by the use of computers and other geophysical techniques, for the complete interpretation of the physical and geochemical changes occurring along a potential earthquake-prone area. Seismographic networks placed along major active faults can measure seismic precursors of earthquakes. Therefore, a study of the seismicity of a region, and an analysis of the smaller events, can lead to conclusions as to the time of occurrence of a major earthquake.

Study Of Precursory Events: The short-term physical and geochemical precursors of earthquakes that can be measured with instruments include:

- Increase in the rate of a seismic creep and the slow movement along the fault;
- Gradual tilting of the land near the fault zone;
- Drop or rise in the water level of a well;
- Increase of hydrogen gas in the soil;
- Release of radon;

- Radioactive gas from wells;
- Decrease in the number of microquakes and foreshocks;
- Lessening of electrical resistance in the rocks;
- Flashes and other lights in the sky;
- Appearance of a ring-like pattern of microquakes surrounding the epicenter of a future quake, called "Mogi's donut;" and
- Many other physical and chemical manifestations.

The trouble with all these instrumentally measurable, short-term precursors is that they may be characteristic of the local geology. For example, "Mogi's donut" precedes major quakes in Japan and China, but it rarely occurs elsewhere. On the other hand, other short-term precursors such as the appearance of radon in the wells, and the increase of hydrogen in the soil hold merit for earthquake prediction.

Other geophysical and geological methods are being used to attempt the forecasting of earthquakes. In many countries besides the United States, the Soviet Union, Japan, and the People's Republic of China, many of the earthquake precursors mentioned above are being monitored. Most of these precursors are thought to result from preliminary stages of failure of the subsurface rocks preceding a major earthquake. Unfortunately, there is not a single geophysical instrument that can measure any direct parameter of the earthquake and give warning in advance.

It is only the secondary precursor parameters, which are bi-products of subsurface tectonic stress, that are being monitored. For example, magnetic field changes, strain, tilt, subsidence, and bulging of the earth's surface, are being studied as precursors. These bits and pieces of miscellaneous information, collected with various instruments, are presently used for earthquake prediction. Instrumental measurement of these precursors provides some evidence of what may be happening along a fault. Dilatancy occurs when the rocks on a fault are stressed and the ground "dilates" or swells. Symmetric tilting of the ground can be expected in a uniform pattern away from the potential earthquake epicenter. Asymmetric tilting of the ground around the earthquake source area can occur also from nonuniform stresses on the rocks, which eventually will result in strike-slip type of faulting when the earthquake strikes.

The theory of dilatancy is complex and has not been generally accepted as being the reason for such observations of precursory events. However, it has been used to predict and explain other precursory phenomena such as variations in magnetic and electrical fields, changes in the flow of groundwater, and anomalous tilts and uplifts of the earth's surface. These are all precursory effects that are presently being investigated and have been associated with dilatancy. Several studies currently are being conducted in measuring earthquake source parameters which can explain the surface tilting which occurs before the actual occurrence of an earthquake. All such studies are based on the concept of the dilatancy of the rocks.

Fault Creep Measurements: Fault creep is a gradual slip produced by the yielding of rocks along the weak boundary of a fault. Creep is defined as an aseismic rupture process which occurs so slowly that no detectable seismic waves are generated. Although creep occurs on normal and thrust faults, it is predominantly observed on strike-slip faults with a steep slip component. Although it is directly observed only at, or near the Earth's surface, it is a process which occurs at depth since creep is the manifestation of aseismic slip movements of large crustal blocks. Thus creep can occur at any fault depth although not necessarily with uniform distribution. In fact, fault creep must be comparatively greater at depths of 12 to 15 kilometers below the surface on strike-slip faults and above the 2- or 3-km depth of certain sections of such faults characterized by the relative absence of even minor earthquakes.

There is a direct relationship between fault creep and earthquakes. Along fault segments where strains are not released by slow fault creep movements, large earthquakes of greater magnitude seem to occur. Conversely, high rates of creep generally inhibit the generation of large - magnitude earthquakes.

For example, the Pacific plate grinds past the North American plate along the San Andreas fault of California, at the rate of about two inches per year. The San Andreas fault system and the other fault systems of California mark this boundary of movement between the two great plates. These fault systems are complex, have kinks and bends, and sections of the faults either move gradually or accumulate strain and rupture suddenly during an earthquake. Furthermore, the strain is confined in the upper 12 miles of the earth's crust. Below that depth the two great plates move elastically and effortlessly. Earthquakes occur in the upper brittle section of the crust near the surface when the strain builds up in the rocks in the locked portions of the faults. Along sections of the San Andreas fault system, displacements of the rocks occur in the form of aseismic creep. In other sections, strain is released in the form of frequent small or moderate earthquakes. Still in other locked sections where great strain accumulates, infrequent but large and extremely destructive earthquakes occur. For a while, the strain resulting from the moving tectonic plates is released through an earthquake, but begins to build again and the process is repeated at some interval of geologic time.

Fault creep is being extensively studied on the San Andreas fault system in California and elsewhere. Instruments known as creepmeters measure the changes in distance between markers set diagonally across a fault. Such aseismic displacements known as creep events, occur frequently on the faults of the San Andreas fault system. Often, some of these events begin suddenly for a few minutes at rates on the order of 0.5 mm/min., and are followed by much longer periods of gradually diminishing creep rate. Thus, movement along a fault may be accommodated without an earthquake, as creep is a very slow rupture process that cannot produce detectable seismic waves. The significance of measuring present creep is the following. In sections of the fault systems where displacements can be accommodated by

this aseismic rupture (creep), the occurrence of even minor earthquakes is comparatively rare. It is the sections of the fault system that are locked, where creep does not occur steadily or periodically where larger destructive earthquakes can occur. But even at the sites of larger earthquakes on such sections, creep events have been observed immediately after a large earthquake has struck. In such instances, such earthquake-creep event associations have been attributed to afterslip effects. Although rare, some creep events have also been recorded prior to the occurrence of a major earthquake.

Instrumentation, which has been developed recently, permits geodetic measurements of surface changes near faults with remarkable precision. For example, instruments such as geodimeters with laser beams can accurately measure distances anywhere from one to 30 kilometers. These instruments are extremely sensitive and have an accuracy of about .2 parts per million, which is equivalent to an average error of less than five millimeters over a distance of 20 kilometers or more in length. Any errors that are introduced in the measurement are not by the instrument itself but from the meteorological conditions surrounding the instrument. For example, atmospheric conditions such as temperature and the refractive index of the light along the path of the laser beam can introduce errors, if not properly compensated.

This capability of precise distance measurements has been applied to earthquake studies and earthquake prediction by using repeated distance measurements to determine any net movements between monuments located on both sides of a major fault. By making measurements over a number of years and by plotting the differences, scientists find the average rate of change. Collection of data with a network of such geodimeters provides information on the fault creep.

For better accuracy, a small array of such geodimeters are placed directly over a fault that has to be measured. Measurable precursor movements occur within periods that range from approximately one month for a magnitude 4.5 earthquake, to several years before a magnitude 6.5 occurs. Although the surface changes are significant in earthquake prediction, scientists have to be careful not to confuse anomalies and instrumental errors with the actual movements related to earthquake activity along a fault.

Strain Measurements: Strain meters are measuring instruments that record the motion of the ground as it relates to a reference point. Usually, these measurements are made across an active fault line, and several of these instruments can be placed to determine net movement along a fault. The instruments record signals related to the failure behavior of the rocks preceding an earthquake. In addition to actual movements, strain meters can measure other effects such as earth tides (the response of the solid earth to the combined forces of the sun and the moon that produce ocean tides) and thermoelastic changes. Thus, the behavior of the fault can be measured continuously as active faults may generate precursory tectonic signals such as creep and strain.

Strain measurements have been used continuously to record creep across major faults before and after earthquakes. Of course, strain signals are more evident in the vicinity of the fault and closer to the epicenter, which is the area of greatest strain and potential failure. Thus, strain meters more effectively record creep events of short duration resulting from local, near surface failures that may be triggered by some kind of movement at a depth below the surface and along the fault. Strain measurements can reveal surface fault creep, tilt, and strain, but have to be recorded at distances of 500 feet from the fault or less, to be accurate. Water level changes in wells are often simultaneously measured, along with other surface strain measurements.

Measuring Changes In Surface Tilt: It is not known with certainty why the earth's surface deforms around active faults, but often does. Tilt meters are instruments that measure vertical displacements or local uplift of the crust near a potential site of an earthquake.

According to scientists of the Geological Survey that monitor tilt meters along an 85-kilometer section of the San Andreas Fault in Central California, systematic tilting of the surface occurs in a fixed direction during periods of low seismicity. Prior to the occurrence of an earthquake, the direction of tilting begins to change dramatically, and after the earthquake, the slow, systematic tilting of the surface again resumes. Thus, tilt changes are precursory events to earthquakes and can help in understanding the cause and prediction of earthquakes.

Anomalous tilting of the earth's surface prior to earthquakes has been reported from other countries including the Soviet Union, Japan, and Italy. Factors that could influence the tilt measurements are meteorological loading effects, thermal and mechanical instabilities, both in the instrument and in the site, and the nonhomogeneous nature of crustal rocks.

Water Level Changes: It has been demonstrated that seismic waves can induce large water level fluctuations in wells. Large amplitude surface seismic waves, such as "Raleigh Waves," force the particles of the rock near the surface to move in an elliptical orbit and thus the aquifer layer also is affected, which in turn results in the water level fluctuation in the well. Thus if appropriate measuring instruments are used, the water level in wells can be used for recording distant earthquakes.

In essence, a well can act as a seismograph by recording the passage of the surface waves through the aquifer and amplifying the amplitude of these waves, much like a seismograph does. Thus, many major earthquakes throughout the world have produced water level changes.

Not only do water level changes occur following an earthquake, but they also precede most earthquakes. Water wells are very sensitive to various earth processes such as earth tides, tilting of the crust, and seismic creeping, particularly if these wells are in the close proximity to an active fault. By drilling

water wells at carefully selected sites and by measuring water level and water quality, the information can be used for earthquake prediction, particularly if it is used in conjunction with a dense network of other instruments such as tilt meters and creep meters. Thus, actual preseismic processes and precursory fluctuations in water levels, can give a clear indication of strain building up along a particular seismic fault.

Hydrogen Monitoring: Geochemical measurements can also be used for earthquake prediction. For example, Dr. Motoaki Sato, a scientist with the Geological Survey, and several of his colleagues, began monitoring hydrogen along various faults in Central California, including the San Andreas Fault, in 1980. In 1982, they found higher concentrations of hydrogen along the fault, and those concentrations jumped from 20 parts per million to over a 1,000 at some stations. Dispersion of hydrogen gas continued sporadically and then increased sharply in April 1982. On 2 May 1983, a major earthquake of 6.5 occurred in Coalinga, an agricultural town north of Parkfield, and this earthquake coincided with peaks in the hydrogen concentration. Similarly, the hydrogen concentration at one station continued to rise immediately receding several of the aftershocks that hit the town, in the subsequent months.

The explanation for such a chemical precursor is not simple. It has nothing to do with the earthquake process itself, but it appears to be a side effect of chemical changes that occur in rocks before quakes. For example, stresses on the rocks could be destroying a distinctive rock called serpentinite which lies along many faults of California, as well as in Japan, and hydrogen is a by-product of the disintegration of serpentinite. As the tectonic plates grind, the rock containing serpentinite at depths of six to 10 miles below the surface, is squeezed releasing gases until, finally, the fault ruptures.

Monitoring Radon Emissions: Radon is a radioactive gas that is constantly emitted from the earth into the atmosphere. The gas has a half-life of 3.8 days. By half-life, we mean the time required for the substance to lose half of its radioactivity through decay. Thus, radon is a very short-lived, radioactive substance. Studies in the concentration of radon, and its isotope thoron, in the vicinity of faults, have been unusually high.

Thus, a number of researchers have monitored the radon content in deep wells, as a potential predictor of earthquake activity. For example, they found a gradual increase in concentrations until the time of the earthquake. After the earthquake occurs, radon emission decreases rapidly, although some variation can be observed related to earthquake aftershocks.

Scientists now routinely monitor the radon content of ground water to determine increases in emission and to correlate the concentrations to earthquake activity. The mechanism for radon generation can be easily explained. Compression along a fault builds up prior to an earthquake and this stress squeezes radon out of the rock and into the atmosphere at an increased rate. Since radon itself has a very short half-life, it is known to move slowly in

ground soils. Therefore, the detected radon concentrations must be from earthquake sources several kilometers underneath the surface.

Observation Of Animal Behavior: Research in China has indicated that recognizing unusual animal behavior in a systematic way can be used, in conjunction with other methods, as a means of predicting large and potentially destructive earthquakes.

The Chinese began to systematically study unusual animal behavior, and the Haicheng earthquake of February 1975 was predicted successfully as early as mid-December 1974. Haiching is in Liaoning Province, northeast China. Snakes came out of hibernation and froze on the surface of the earth. Also, a group of rats appeared. These events were succeeded by a series of earthquakes at the end of December 1974. During the following month, in January 1975, thousands of reports of unusual animal behavior were received from the general area. Local people saw hibernating snakes leaving their holes. In the first three days in February the activity intensified and atypical behavior in larger domestic animals such as cows, horses, dogs, and pigs, was reported. On 4 February 1975, an earthquake of magnitude 7.3 struck Haicheng County, Liaoning Province.

A stock breeder in northern China, feeding his animals before dawn on 28 July 1976, in the area of the Kaokechuang People's Commune, approximately 40 kilometers away from the city of Tangshan, reported that his horses and mules instead of eating were jumping and kicking until they finally broke loose and ran outside. A few seconds later, a dazzling white flash illuminated the sky. Tremendous rumbling noises were heard as a 7.8 magnitude earthquake struck the Tangshan area.

Some reports mention animals such as goats refusing to go into pens, cats and dogs picking up their offspring and carrying them outdoors, pigs squealing strangely, chickens dashing out of coops in the middle of the night, fish swimming about aimlessly, and birds leaving their nests. It has also been reported that zoo animals refuse to go into their shelters at night; snakes, lizards, and other small mammals evacuate their underground nests; insects congregate in huge swarms near the seashores; cattle seek higher ground; domestic animals became agitated; and wild birds leave their usual habitats.

Surveys show that the largest number of cases of atypical animal behavior precede the earthquake, particularly in the 24 hours before it strikes. In other parts of China where major earthquakes have been preceded by fore-shocks, unusual behavior in rats, fish, and snakes has been observed three days prior to the earthquake, continuing to several hours, or even a few minutes before it strikes.

In Japan, similar cases of unusual animal behavior have been noted. For example, it has been reported that deep, cold water species of fish were being caught by commercial fishermen in shallow, warm waters prior to many large earthquakes in the Sea of Japan. However, atypical animal behavior

reported in Japan has primarily concerned fish. This is not surprising considering that 80 percent of all Japanese earthquakes occur in the ocean, and fishing is a major industry in Japan.

Since animals have the capability of acting as predictors of earthquakes, Chinese scientists have carried out surveys of animal behavior variations prior to earthquakes. A team of scientists including biologists, geophysicists, chemists, meteorologists, and biophysicists conducted a survey in the Tangshan area and in 400 communes in 48 counties around it after the 1976 earthquake. The scientists visited a number of places that were hit by other destructive earthquakes and, through interviews and discussions with local people, collected information on over 2,000 cases of unusual animal behavior occurring before an earthquake. The majority of the reports involved domestic animals. Based on this survey, a preliminary report was prepared by the Chinese identifying 58 kinds of domestic and wild animals that had shown unusual behavior before the earthquakes.

The principal focus of research work in China has been on the behavior of pigeons. Biological studies on pigeons determined that 100 tiny units exist between the tibia and fibula on a pigeon's leg. These nerve units are connected to the nerve center, and are very sensitive to vibrations. Scientists determined that prior to an earthquake of magnitude 4.0, which occurred in the area of the study, 50 pigeons that had severed connections between the tibia, fibula, and the nerve centers, remained calm before the earthquake, while those with normal connections became startled and flew away.

Because of the success in monitoring unusual animal behavior for the prediction of certain earthquakes, the Chinese, who have pioneered this work, have looked into ways to construct instruments that would duplicate the sensory organs of animals able to monitor and sense stimuli preceding an earthquake. Researchers found it very difficult to understand the mechanism of response stimuli. Physical or chemical stimuli emanate from the earth prior to an earthquake and animals probably sense them. For example, dogs may be able to hear the microfracturing of rocks a few milliseconds before a quake shock reaches the surface. Electromagnetic changes in the earth prior to an earthquake may be sensed by such animals as sharks and catfish which have low or high frequency receptors and sense such changes actively or passively. Electromagnetic field changes could also affect migrating birds and the navigational ability of fish.

Electromechanic changes occurring prior to the occurrence of a large earthquake may be sensed by certain animals, filtered, and then instinctively interpreted. Animals may have the means and sensitivity to sort out and discriminate the threatening precursory signals of an impending earthquake, thus activating a behavior pattern for survival.

Since China considers such information on animal behavior vital to prediction, it established in 1968 its first experimental station for earthquake prediction making use of biological observations. This experimental station was

established in Xingtai Province. Other similar stations were set up in 1971 in Aksu, Xinjiang Province, where earthquakes were expected to occur. Since 1971, the Chinese have established an operational network in different communes or counties. Whenever unusual events occur and are reported by numerous observers, these are evaluated as a way of predicting earthquakes. So far, by this means, two major earthquakes have been predicted. This is easier for the Chinese since 80 percent of the population live in farming areas in close association with animals. It is a little more difficult for people living in urban areas to observe similar animal behavior. Unfortunately, no similar studies of animal behavior have been undertaken in California.

Experiments with new instruments and electronic solid state sensors are now being used to determine animal response to impending catastrophic occurrences. The benefit from such research would be in duplicating the sensory responses of animals to construct equally responsive instruments that can record or monitor these precursory changes. Thus, observing and studying animal behavior could lead to better earthquake prediction instrumentation.

BIBLIOGRAPHY

Burford, O.R., Nason, R.D. and Harsh, P.W., 1978
"Studies of Fault Creep in Central California"
Earthquake Inf. Bull., Vol. 10, No. 5, Sept.-Oct., p. 174-181.

Chinnery, M.A. and North, R.G., 1975
"The Frequency of Very Large Earthquakes"
Science, Vol. 190, p. 1197-1198.

Dey, A.K., 1983
"Earthquake and Earthquake Prediction"
Disaster Management Quarterly, Vol. 3, No. 1, Jan.-Mar., p. 30-40.

Earthquake Information Bulletin, 1979
"Trees as Indicators of Past Movements on the San Andreas Fault"
Vol. II, No. 4, Jul.-Aug., p. 127-130.

Hunter, N.R., 1976
"Is There a Periodicity in the Occurrence of Earthquakes"
Earthquake Inf. Bull., Sept.-Oct., p. 4-7.

King, Chi-Yu, 1978
"Radon Emanation on the San Andreas Fault"
Nature, Vol. 271, p. 516-519.

Kitazawa, K., 1986
"Earthquake Prediction and Public Response"
Violent Forces of Nature, Chapter 4, Lomond Publications, p. 31-45.

Ling-Huang, S., 1978
"Can Animals Help to Predict Earthquakes?"
Earthquakes Inf. Bull., Vol. 10, No. 6, Nov.-Dec., p. 231-233.

Reasenberg, P., 1978
"Unusual Animal Behavior Before Earthquakes"
Earthquake Inf. Bull., Vol. 10, No. 2, Mar.-Apr., p. 42-50.

Savage, C.J., 1978
"Geodimeter Measurements and the Southern California Uplift"
Earthquake Inf. Bull., Vol. 10, No. 4, Jul.-Aug.

Sieh, K.E., 1978
"Prehistoric Large Earthquakes Produced by Slip on the San Andreas Fault at Pallett Creek, California"
Journal of Geophysical Research, Vol. 83, p. 3907-3939.

Spall, H., 1978
"Water-Level Changes and Earthquake Prediction"
Earthquake Inf. Bull., Vol. 10, No. 2, Mar.-Apr.

Stanford Research Institute, 1977
"Earthquake Prediction, Uncertainty and Policies for the Future: A Technology Assessment of Earthquake Prediction"
Washington: National Science Foundation, 312 p.

Turner, H.R., 1978
"The Challenge of Earthquake Prediction"
Earthquake Inf. Bull., Vol. 10, No. 2, Mar.-Apr.

Wallace, E.R., 1970
"Earthquake Recurrence Interval on the San Andreas Fault"
Geological Society of America Bulletin, Vol. 81, p. 2875-2890.

Wallace, E.R. and LaMarche, C.V., Jr., 1979
"Reference: Trees as Indicators of Past Movements on the San Andreas Fault"
Earthquake Inf. Bull., Vol. II, No. 4, Jul.-Aug.

Waltham, T., 1978
"Catastrophe, The Violent Earth"
New York: Crown Publishers, Inc., 170 p.

Ward, P.L., 1978
"Earthquake Prediction"
Geophysical Predictions, Washington D.C.: National Academy of Sciences, p. 37-46.

M_m: A Variable-Period Mantle Magnitude

EMILE A. OKAL

Department of Geological Sciences, Northwestern University, Evanston, Illinois

JACQUES TALANDIER

Laboratoire de Géophysique, Commissariat à l'Energie Atomique, Papeete, Tahiti, French Polynesia

This paper lays the theoretical groundwork for a variable period mantle magnitude, M_m, based on the measurement of the spectral amplitude $X(\omega)$ of very long period Rayleigh waves. We retain the concept of magnitude by restricting ourselves to single-station measurements, ignoring the focal mechanism and the exact depth of the shallow earthquakes considered. Our measurements are made at a series of periods (in all cases greater than 40 s), and the largest value is retained. This procedure effectively avoids the well-known interference effects leading to saturation of magnitude scales defined at a fixed period. Two corrections are used: a period-dependent distance correction C_D, and a source correction C_S, also period-dependent, compensating for the variation of the excitation of Rayleigh waves with period. Both of these corrections are fully predictable on the basis of standard surface wave excitation and dispersion theory. The result is a formula of the type $M_m = \log_{10} X(\omega) + C_D + C_S + C_0$ in which all coefficients, including the constant C_0 are justifiable on sound theoretical grounds. The analysis of a data set of 256 records from the broadband seismograph at Papeete, Tahiti, the ultra-long period system at Pasadena, and stations of the GEOSCOPE network, shows that the mean error in the estimation of the seismic moment is on the order of 0.1–0.2 units of magnitude, with the standard deviation at each station also on the order of 0.2 units of magnitude. No significant trend with either distance, period, or station can be identified. The method can also be transposed to the time domain, under some simple assumptions which are justifiable theoretically for typical teleseismic distances across the Pacific Basin. Both versions of the method lend themselves well to automation. Thus, by providing a real-time estimate of the seismic moment of distant earthquakes, M_m has considerable potential for tsunami warning purposes. Its concept can easily be extended to Love waves and also to intermediate and deep earthquakes.

1. Introduction and Background

Magnitudes and Seismic Moments

Ever since it was introduced in the pioneering work of *Richter* [1935], the concept of earthquake magnitude has been used extensively to obtain a rapid evaluation of the size of a seismic event, through the measurement of the amplitude of seismic waves, taken in real time and at a single seismic station. C. F. Richter's original formula, developed empirically for California earthquakes, was later extended to distant earthquakes recorded at Pasadena by *Gutenberg and Richter* [1936], and in the early 1960s, standardized magnitude scales were defined for surface waves at 20 s and body waves at or around 1 s [*Vaněk et al.*, 1962]. For about 30 years, magnitudes of one scale or another were the only available measurements of the size of earthquakes. In all cases, magnitudes were directly related to the logarithm (base 10) of the recorded amplitude of ground motion.

The situation evolved significantly in the 1960s when various combinations of systems of forces were investigated as physical descriptions of earthquake sources. *Aki* [1966] showed that the physical characterization of most earthquake sources was a double couple quantified by its seismic moment M_0 having dimensions of energy. Because of the linearity of all the physical laws involved, the excitation of all seismic waves by a point source double-couple is proportional to M_0. As such, in the absence of any additional effects, the relationship between M_0 and any magnitude M would be expected to take the form

$$M = \log_{10} M_0 + \text{const} \qquad (1)$$

the theoretical value of the slope being exactly 1.

However, a well-known problem of any of the classical magnitude scales is their saturation, as the true size of the seismic source, M_0, keeps growing. This has been explained in detail by *Aki* [1967, 1972] and later *Geller* [1976], as due to the destructive interference resulting from the spatiotemporal extent of the seismic source. In simple terms, as an earthquake grows in size, it reaches a point when the actual duration of the source process becomes comparable to, if not longer than, the period ($T = 20$ s for M_s) at which the magnitude is measured, leading to variation in the initial phase of the wave during the rupture process, and eventually to destructive interference.

In *Geller*'s [1976] model, interference effects bringing nonlinearity between $\log_{10} M_0$ and M_s start at about $M_0 = 4 \times 10^{25}$ dyn-cm. Between this value and $M_0 = 5 \times 10^{27}$ dyn-cm, a slope of 2/3 between M_s and

Paper number 88JB04010.
0148-1227/89/88JB-04010$05.00

$\log_{10} M_0$ is predicted. Beyond $M_0 = 1.5 \times 10^{28}$ dyn-cm, full saturation is predicted. Thus earthquakes with measured M_s values of 8.0–8.3 can have seismic moments differing by a factor of 1000. Obviously, this makes the use of M_s in interpreting the "size" of gigantic earthquakes worthless, if not outright dangerous, for example when assessing their tsunamigenic potential.

Purpose of This Study

Because it relies on a real-time measurement of the seismic signals recorded at a single station, the magnitude concept remains a simple and powerful tool of observational seismology. The purpose of the present paper is thus to explore the possibility of developing a magnitude scale, M_m, allowing the retrieval of the seismic moment within an acceptable range of precision, while keeping the basic philosophy of the magnitude concept, i.e., the use of a single station, and the rapidity of the measurement.

The rationale behind this philosophy derives from the importance of measuring M_0 in the context of tsunami warning. While it has been known for a long time that the static value of the seismic moment is a key factor in tsunami genesis, we have recently shown that the influence on tsunami excitation of focal mechanism, and to a large extent of depth in the 0–75 km range, is actually minimal [*Okal*, 1988]. Thus it may be futile to use the precious time separating the arrivals of surface and tsunami waves for the purpose of refining depth estimates or of obtaining an exact focal geometry. This is especially true when the epicentral distance is short, as can be the case between the Aleutian Islands and Alaska or between the Tonga arc and Tahiti. In particular, it must be borne in mind that most reliable moment tensor inversions still require the acquisition of seismic data at a large number of stations; for such short distances there may not be sufficient time to wait for the arrival of even the first passage of Rayleigh waves at more distant seismic stations. Therefore, even in the days of supposedly instant worldwide satellite telecommunications, the possibility of determining a seismic moment from the records of a single seismic observatory remains very valuable. One of our goals will be to make sure that the concept of M_m remains valid at relatively short distances (see section 5).

An additional goal in this study will be to provide an analytic expression for the magnitude scale derived from theoretical grounds, so that all constants in the eventual formula for M_m can be fully predicted from theoretical models of earthquake sources and seismic propagation. We will relate the mantle magnitude M_m to the seismic moment through:

$$M_m = \log_{10} M_0 - 20 \qquad (2)$$

where M_0 is measured in dyn-cm. The choice of the constant 20 in (2) is of course arbitrary; however, it has the advantage of keeping the values of M_m within a practical, usual, range; for example, an earthquake of moment 10^{28} dyn-cm has an M_m of 8.0 . We will derive and test ways of measuring an estimate of M_m in real time from the records of a single seismic observatory.

In order to avoid the saturation phenomena described above, it is clear that we need to move to very long periods. We will make the measurement wherever in the frequency domain the signal has sufficient energy. Thus emerges the concept of a variable-period magnitude. In practice, we will always seek to measure M_m on the flat portion of the source spectrum, i.e., at a frequency less than the corner frequency ω_{CF} of the source.

What makes this approach possible is the development, in recent years, of a new generation of broadband seismometers [*Wieland and Streckeisen*, 1982] with large dynamic range, which allow the reliable recording of the seismic signal without the all too frequent problems of nonlinearity and saturation (clipping) which used to plague the recording of the first passage of surface waves from truly large events on older instruments. We refer to *Monfret and Romanowicz* [1986] for a discussion of the theoretical advantages of using first passages; in addition, in the context of tsunami warning, it is crucial to obtain a measurement as rapidly as possible.

However, we want to emphasize that a number of stations did operate reliable low-gain ultra-long-period or broadband instruments, as far back as the 1960s. Notable among such systems is the Pasadena ultra-long-period vertical ("number 33") seismometer [*Gilman*, 1960; *Brune and King*, 1967] and the LDG broadband operated at Papeete, Tahiti since 1972. Records from these instruments will, together with the recent GEOSCOPE digital data, provide the experimental backbone of the present study. A typical example, shown on Figure 1, emphasizes the prominence of long-period energy in the 200–s range; it is safe to say that had such records been available at the time, the founding fathers of magnitude scales would probably have attempted to quantify the earthquake source from information at the lower end of the frequency spectrum, rather than around 20 s. The development of M_m can then be regarded as a modernization of the concept of magnitude in view of recent developments in instrumentation.

Finally, in this study we restrict ourselves to shallow earthquakes ($h < 75$ km). Our experience shows that it is generally possible from a single seismic observatory to ascertain immediately the general character (shallow, intermediate, deep) of a teleseismic event. In section 6 we propose to extend the concept of M_m to intermediate and deep earthquakes; these events, however, do not carry substantial tsunami risk, and thus some of the motivation for the fast retrieval of their seismic moment disappears.

2. PREVIOUS WORK ALONG SIMILAR LINES

Brune and King [1967]

A similar attempt at quantifying earthquakes from the very long period characteristics of their seismic source can be traced back to *Brune and King* [1967], who investigated the spectral amplitude of 100-s Rayleigh waves. However, these authors were working at a fixed period, and any such magnitude M_{100} would still be expected to saturate for sufficiently large earthquakes. Indeed, nonlinear effects should yield a 2/3 slope between M_{100} and

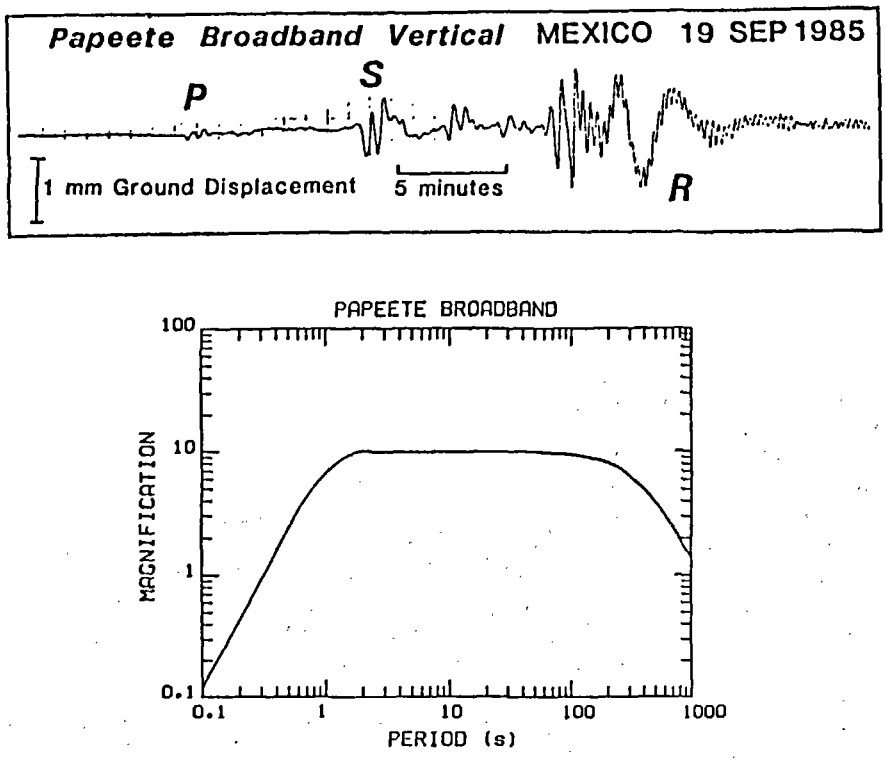

Fig. 1. (Top) Example of broadband record at PPT. Note the prominent mantle Rayleigh waves. (Bottom) Frequency response of the broadband system at PPT.

$\log_{10} M_0$ beyond 10^{28} dyn-cm, precisely in the range of great earthquakes with significant tsunamigenic potential. This limitation is partly responsible for the "S curve" behavior of M_{100} versus M_s, as reported for example on *Brune and King*'s [1967] Figure 3.

In turn, *Brune and Engen* [1969] proposed a mantle wave magnitude, based empirically on this very figure; however, they did not provide a simple formula for the exact expression of their magnitude scale but rather gave two plots, one in the time domain for Rayleigh waves and one in the frequency domain for Love waves, relating amplitudes at 100 s to seismic moment and to the proposed 100-s magnitude. In addition, it is noteworthy that they characterized the 1964 Alaskan earthquake as larger than the 1960 Chilean event, whereas most ultra-long-period studies [*Kanamori*, 1970; *Kanamori and Cipar*, 1974; *Geller*, 1977; *Cifuentes and Silver*, 1989] indicate that it was at least 3 times smaller in moment. This is a direct illustration of the failure of any magnitude computed at a fixed period for sufficiently large seismic sources, as noted also by *Purcaru and Berckhemer* [1982].

Kanamori's [1977] *Moment Magnitude* M_w

In order to alleviate some of the difficulties inherent in saturation, *Kanamori* [1977] proposed the concept of a moment magnitude (which he also called "energy magnitude"):

$$M_w = \frac{2}{3} (\log_{10} M_0 - 16.1) \qquad (3)$$

In this approach, M_w is actually computed from M_0, once the latter has been obtained through moment tensor inversion or similar techniques. Specifically, Kanamori was seeking to extend M_s beyond its point of total saturation and thus to provide continuity with large, but not gigantic, earthquakes (typically in the range 10^{27} dyn-cm, where interference effects are significant, but full saturation is not yet attained). Thus, he introduced an a priori slope of 2/3 in the definition of M_w. In doing so, he also extended *Gutenberg*'s [1956] relation between the total seismic energy released and magnitude, $\log_{10} E = 1.5\,M + 11.8$, which, in the framework of modern source theory, is now understood to hold only in the same range of magnitudes. Therefore one can predict that while M_w will behave like M_s for these large, "interesting" earthquakes, a significant discrepancy will occur for smaller events, for which M_s should be smaller than M_w.

Along similar lines, *Purcaru and Berckhemer* [1978] introduced their energy magnitude, M_E, which differs from M_w in that an allowance is made for a variable stress drop $\Delta\sigma$.

Ekström and Dziewonski's [1988] $\overline{M_s}$ *: An Improved* M_w

The observation of an M_s:M_w discrepancy for small events, and the resulting systematic bias in the estimate of seismic moment release if (3) is used backward to compute M_0 from M_s, prompted *Ekström and Dziewonski* [1988] to propose a magnitude $\overline{M_s}$ combining M_w behavior for large earthquakes while remaining comparable to M_s for smaller ones and with a gradual transition in between. Whereas $\overline{M_s}$ is clearly superior to M_w, this

approach does not differ substantially from *Kanamori*'s [1977], in that it consists fundamentally of recasting a measurement of M_0 (obtained from a full moment tensor inversion) into the more popular range of magnitude values; or conversely of using 20-s M_s measurements predating digital seismology to obtain an estimate of moment release.

Williams' [1979] AR Method

An interesting attempt at recovering M_0 in real time can be found in *Williams* [1979]. It consists of measuring the so-called *AR* parameter, which amounts to integrating the square of the displacement during the first passage of Love and Rayleigh waves. Basically, Williams follows our philosophy of using the records of a single long-period station. However, because she limits herself to WWSSN records dominated mostly by 20- to 50-s energy, she must use two different formulae (with slopes close to 1.0 and 1.5) to reproduce the initiation of saturation around $M_0 = 7 \times 10^{27}$ dyn-cm. By the same token, her method would fail when total saturation is reached: it is noteworthy that the largest moment in her data set is only 1.5×10^{28} dyn-cm.

Finally, a preliminary version of the present study was published by *Okal and Talandier* [1987] and *Talandier et al.* [1987]. In the present paper we give the full theoretical treatment justifying the expressions of M_m and present an extensive data set of more than 250 measurements worldwide, fully upholding the validity of the endeavor and its reliability.

3. THEORY

Since we seek a very long period measurement of the seismic moment of an earthquake, we will base the development of M_m on the theory of the excitation and propagation of Rayleigh waves. We adopt the formalism and notation of *Kanamori and Stewart* [1976]. The spectral amplitude at angular frequency ω of a Rayleigh wave recorded at a distance Δ from an earthquake can be written as

$$X(\omega) = a\sqrt{(\pi/2)}\left[e^{-\omega a \Delta/2UQ} / \sqrt{\sin\Delta}\right] \times \left[\frac{1}{U}\left| s_R K_0 l^{-1/2} - p_R K_2 l^{3/2} - i q_R K_1 l^{1/2} \right| M_0\right] \quad (4)$$

In this equation we have separated terms due to propagation (on the first line) and to excitation (on the second line). The effect of propagation consists of the geometrical spreading $1/\sqrt{\sin\Delta}$ and of the anelastic attenuation along the path $a\Delta$. The excitation terms include the seismic moment M_0 and the combination of the excitation coefficients K_i (depending on depth and frequency), and of the trigonometric terms p_R, q_R, s_R describing the geometry of the faulting in relation to the azimuth of the station. We refer to *Kanamori and Cipar* [1974] and *Kanamori and Stewart* [1976] for the exact expressions of these coefficients; finally, a is the Earth's radius, l the angular order of the equivalent normal mode, and U the group velocity of the wave.

Conversely, the seismic moment M_0 (or the mantle magnitude M_m) of the event can be retrieved from the spectral amplitude through

$$\log_{10} M_0 = M_m + 20 = \log_{10} X(\omega) + C_D + C_S + C \quad (5)$$

where C_D is a distance correction related to the first bracket in (4), C_S is a source correction related to the second bracket, and $C = \log_{10}(\sqrt{(2/\pi)}/a)$ is a constant. $C = -3.90$ if a is in kilometers.

Distance Correction

The distance correction is simply

$$C_D = \frac{1}{2}\log_{10}\sin\Delta + (\log_{10} e)\frac{\omega a \Delta}{2UQ} \quad (6)$$

These terms are obviously independent of focal mechanism and depth. In order to reflect the possible influence of lateral heterogeneity on U and Q, we use a model of the Earth regionalized into seven tectonic regions, using a $10° \times 10°$ grid (Figure 2). This regionalization generally follows the previous work of *Okal* [1977], *Jordan* [1981], and, for the oceanic areas, *Mitchell and Yu* [1980]. The seven regions considered are four oceanic age bands (0–20 Ma; 20–50 Ma; 50–100 Ma; older than 100 Ma); two continental regions, shields and mountains (which we can define as active in the past 500 m.y.); and finally a "trench and subduction zone" area.

In view of the recent results in seismic tomography [e.g., *Woodhouse and Dziewonski*, 1984] showing some decoupling of the pattern of deep heterogeneity from that of the obvious tectonic features at the surface, the accuracy of this regionalization at very long periods can be doubted. However, as expected from (6) and discussed later in section 5, when the period becomes very large, the attenuation correction decreases to the point where the effect of regionalization becomes minimal and the issue insignificant.

Regionalized values of U and Q were obtained based on the work of *Canas and Mitchell* [1978], *Mitchell and Yu* [1980], *Nakanishi* [1981], and *Hwang and Mitchell* [1987]. Table 1 lists all the values of U and Q used in the computation of C_D. Once an epicenter has been obtained, the path under study is split into segments belonging to the various regions, and their contributions to the second term in C_D are simply added.

Source Correction

This correction

$$C_S = -\log_{10}\left|\left(s_R\frac{K_0}{\sqrt{l}} - p_R K_2 l^{3/2} - i\, q_R K_1 l^{1/2}\right) / U\right| \quad (7)$$

is expected to be a priori dependent on focal mechanism and depth, through the coefficients K_i. In keeping with the magnitude concept, and the discussion in the introductory section, we assume that these parameters are unknown and proceed to compute C_S for an average excitation, representative of an average focal mechanism and station orientation and of an average depth in the range 10–75 km.

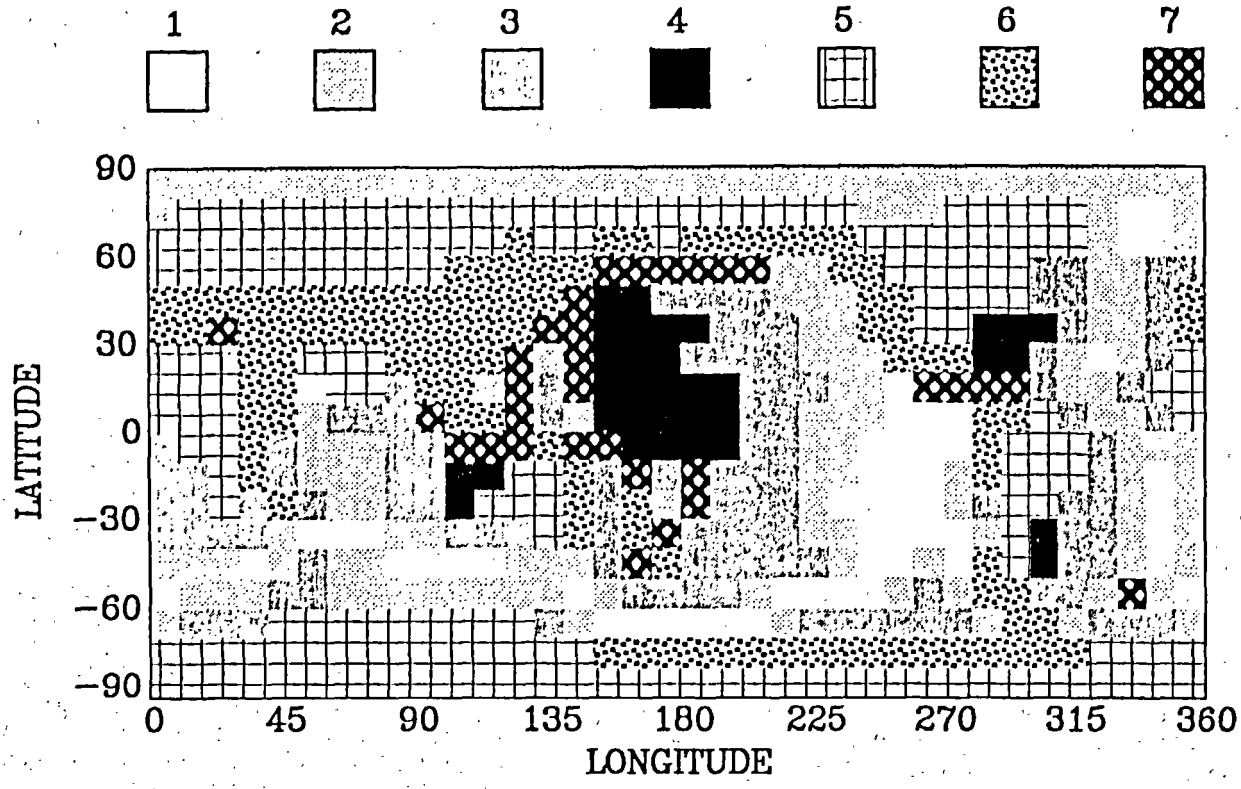

Fig. 2. Tectonic regionalization used in the computation of the distance correction C_D. The various shading patterns refer to oceans (1, less than 20 Ma; 2, 20–50 Ma; 3, 50–100 Ma; 4, older than 100 Ma); continents (5, shields; 6, tectonic regions); and trenches (7). See Table 1 for corresponding values of U and Q.

Whether or not one can neglect the influence of focal mechanism and depth and still obtain a reliable estimate of the seismic moment M_0 will eventually make or break the concept of M_m, the variable-period mantle magnitude, as a viable measurement of the "size" of the earthquake. As discussed more in detail in section 5, we believe that our results are extremely encouraging in this respect.

For our purpose, we define the excitation of a Rayleigh

TABLE 1. Regionalized Dispersion and Attenuation Models Used in Computing Distance Correction

	Region 1 0–20 Ma		Region 2 20–50 Ma		Region 3 50–100 Ma		Region 4 > 100 Ma		Region 5 Shields		Region 6 Mountains		Region 7 Trenches	
T, s	U, km/s	Q	U, km/s	Q	U, km/s	Q	U, km/s	Q	U, km/s	Q	U, km/s	Q	U, km/s	Q
35	3.845	158	4.005	168	4.046	200	4.013	251	3.455	236	2.950	98	2.880	96
38	3.836	152	3.995	162	4.061	191	4.040	234	3.536	220	3.070	95	2.900	90
42	3.819	147	3.976	155	4.063	181	4.064	217	3.634	204	3.170	92	2.920	85
46	3.799	143	3.953	150	4.055	173	4.074	204	3.722	192	3.250	90	2.940	82
51	3.772	139	3.927	145	4.043	166	4.073	191	3.818	181	3.300	92	2.960	79
56	3.746	136	3.899	140	4.023	159	4.062	183	3.858	177	3.380	94	2.980	78
63	3.714	133	3.863	136	3.992	153	4.037	175	3.899	181	3.520	96	3.000	79
70	3.690	131	3.831	134	3.958	149	4.007	169	3.920	179	3.560	98	3.040	80
78	3.670	129	3.799	132	3.919	145	3.972	166	3.936	192	3.620	100	3.070	81
87	3.657	129	3.770	131	3.879	143	3.934	165	3.954	212	3.690	103	3.100	82
90	3.649	130	3.743	132	3.836	142	3.893	166	3.952	251	3.710	106	3.130	84
111	3.642	133	3.718	134	3.794	144	3.850	170	3.928	260	3.700	109	3.170	87
127	3.632	138	3.694	140	3.753	148	3.806	177	3.896	295	3.680	112	3.218	92
145	3.617	146	3.671	149	3.715	155	3.761	188	3.854	333	3.700	116	3.419	99
167	3.590	159	3.643	161	3.673	168	3.710	203	3.797	280	3.780	120	3.515	108
193	3.554	177	3.611	180	3.631	187	3.657	222	3.743	250	3.580	125	3.623	119
223	3.524	201	3.586	204	3.601	209	3.617	245	3.666	283	3.550	130	3.526	131
259	3.541	231	3.606	234	3.620	239	3.628	272	3.645	312	3.470	155	3.475	149
300	3.669	262	3.727	266	3.742	271	3.745	297	3.706	345	3.610	200	3.699	170

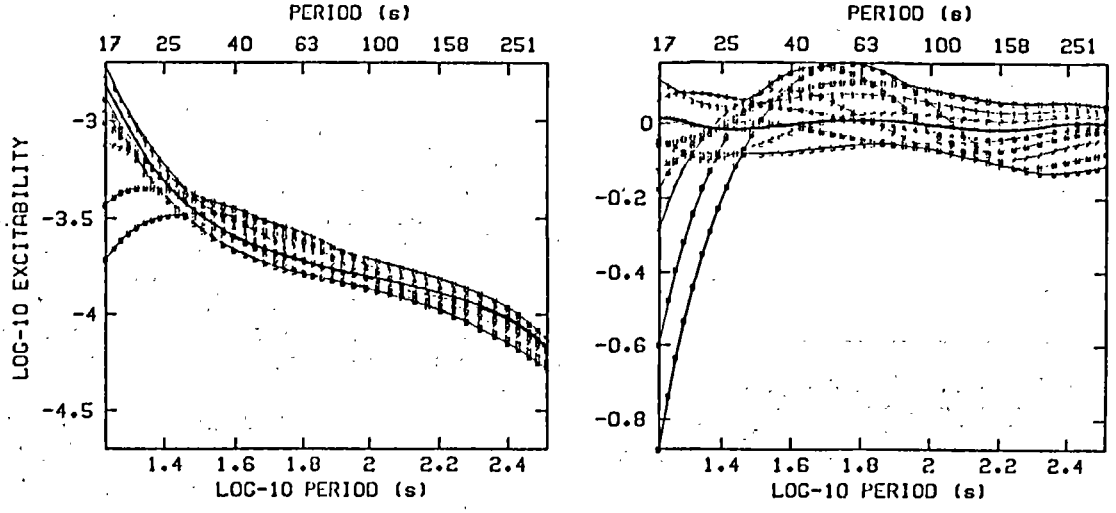

Fig. 3. (Left) Logarithmic average excitability as defined by (9) plotted as a function of period and depth. The various symbols (from 0 to 9) refer to 10 sampling depths between 10 and 75 km. The thicker trace corresponds to $h = 20$ km, which is retained for the computation of C_S. (Right) Same as left, after the correction C_S given by (10) has been applied. Note that beyond $T = 35$ s, the maximum error remains at most ±0.15 orders of magnitude.

wave of angular frequency ω by an earthquake at depth h and in a particular geometry as

$$E(\phi_f, \delta, \lambda; \phi_s; h; \omega) = \left| (s_R K_0 l^{-1/2} - p_R K_2 l^{3/2} - i\, q_R K_1 l^{1/2}) / U \right| \quad (8)$$

and the "logarithmic average excitability" of the wave for a given depth and frequency as

$$L_{av} = \log_{10} E_{av}(h, \omega) = \log_{10} \left[\frac{1}{N} \sum E(\phi_f, \delta, \lambda; \phi_s; h; \omega) \right] \quad (9)$$

i.e., the logarithm of the average of E, taken over a large number N of combinations of the fault dip δ, slip λ, strike ϕ_f, and station azimuth ϕ_s. In practice, we used the PREM model [*Dziewonski and Anderson*, 1981] to compute the coefficients K_i at 10 depths ranging from 10 to 75 km and 44 periods from 16 to 300 s. We then averaged over $N = 6480$ geometries. We want to point out that this definition is somewhat different from the value of E_{av} proposed by *Okal and Talandier* [1987]. In that preliminary work we had averaged the logarithms, thus placing extreme emphasis on nearly nodal geometries (when these exist) and hence biasing C_S toward higher values. Here we average the excitations themselves before taking the logarithm in (9).

At any depth the use of an average excitation instead of the exact value of E results in a substantial systematic error only in the case of an event with a "pure" focal mechanism (either purely horizontal or purely vertical slip on a perfectly vertical fault plane) and a station at the node of the radiation pattern, for which the expected excitation is identically zero. For other mechanisms, and in particular for the thrust and normal faults typical of the great majority of the truly gigantic events bearing substantial tsunami risk, it is usually possible to find a period at which the sharpness of the nodes of the radiation pattern is considerably reduced; under these conditions the systematic error on $\log_{10} E$ usually remains less than ± 0.2 units of magnitude.

Results are shown in Figure 3, with the coefficients K_i expressed in units of 10^{-27} dyn^{-1} and U in km/s. It is clear that at periods greater than 40 s, the dependence of L_{av} on h is minimal and that the logarithmic average excitability at 20 km is an adequate depth average, except for shorter periods. We thus restrict ourselves from now on to periods $T \geq 40$ s and further smooth L_{av}(20 km) by a cubic spline. This leads to the following expression for C_S:

$$C_S = 1.6163\, \theta^3 - 0.83322\, \theta^2 + 0.42861\, \theta + 3.7411 \quad (10)$$

where $\theta = \log_{10} T - 1.8209$. Figure 3 (right) shows that the deviation of L_{av} due to depth-averaging is at most ±0.15 orders of magnitude between the depths of 10 and 75 km. The range of variation of C_S itself is from 3.590 at $T = 40$ s to 4.120 at $T = 300$ s. In the above formulæ, we use practical seismological units, i.e., T is in seconds, a in kilometers, U in km/s, K_i in 10^{-27} dyn^{-1}. By combining the previous equations, we obtain

$$M_m = \log_{10} X(\omega) + C_D + C_S + C_0 \quad (11)$$

with C_D computed according to (6), C_S given by (10), $C_0 = -0.90$, and $X(\omega)$ measured in μm-s, following the practice, common in magnitude studies, of measuring ground displacements in microns.

From Theory to Application: How to Avoid Source Finiteness Effects

The above theory was developed for a point source, both in the time and space domains. Before we can apply our results to real data, we must devise a strategy

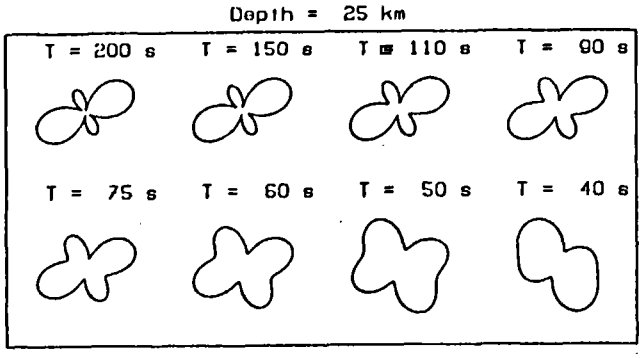

Fig. 4. Variation of the azimuthal radiation pattern of the spectral amplitude $X(\omega)$ as a function of period, in the geometry $\phi = 13°$; $\delta = 71°$; $\lambda = 36°$. Note the disappearance of secondary nodes at higher frequencies [after *Okal and Talandier*, 1987].

for choosing the frequency at which the measurement will be made and in particular ensuring that this frequency is indeed on the flat portion of the spectrum, below the corner frequency. The simplest idea in this respect is to use many frequencies, say all periods between 40 and 300 s, and retain the largest computed value of M_m. The rationale behind this procedure is that the interference due to finiteness of the source is always destructive and thus biases M_m toward lower values. We will see that in general, this algorithm does indeed retain a measurement taken at a very long period.

Another possibility would be to always measure M_m at some fixed, but very long period (e.g., 300 s). The problem with this approach is twofold: first, there may not always be an adequate signal-to-noise ratio especially for smaller events in the 10^{26} dyn-cm range, and we may actually be measuring noise; second, and more importantly, a variable period helps guard against the possibility of a station sitting in a node of Rayleigh radiation at a particular period. Obviously, in the case of a "pure" mechanism, the azimuths of the nodes are frequency independent; however, as shown on Figure 4, the shape of radiation patterns can strongly depend on frequency for mechanisms involving nonvertical faults and/or oblique slip. Then a change of reference period can literally move the station out of a node. Thus we prefer to compute M_m at many frequencies and keep the largest value.

If, on the other hand, our measurements were taken in a portion of the spectrum beyond the first corner frequency due to finite length of rupture, ω_{CF}, one would have to add to (4) an additional factor [sinc $(\omega\tau_s/2)$], where τ_s is the duration of rupture. Conversely, beyond ω_{CF}, one would expect an additional correction to (11)

$$C_{CF} = \log_{10} (\pi\tau_s / T) \qquad (12)$$

since the sine function in "sinc" approaches 1 beyond ω_{CF}.

If τ_s scales with $M_0^{1/3}$, one predicts a relationship of the form $M_0 \propto [\omega X(\omega)]^{3/2}$. Conversely, M_m computed from (11) would actually vary as (2/3) $\log_{10} M_0$. If τ_s can be taken as constant, one predicts $M_0 \propto [\omega X(\omega)]$, and M_m computed from (11) should be off by a term $[C_1 - \log_{10} T]$. This constant behavior of τ_s would be suggested to some extent by the parameters of moderate to large earthquakes obtained from the Harvard centroid moment tensor inversions [*Dziewonski et al.*, 1983*a,b,c*, 1984*a,b*, 1985*a,b,c,d*, 1986*a,b,c*, 1987*a,b,c,d,e,f,g*, 1988 *a,b,c,d,e*]. We refer to *Okal and Talandier* [1987] for a full discussion of these effects and for the exact formulæ expected under these conditions.

An important series of tests, which we will conduct in the section 5, is to verify that the best fitting slope between published values of $\log_{10} M_0$ and M_m computed from (11) is indeed close to 1. This will be the ultimate test to ascertain that we remain beyond the corner frequency of the event and are not affected by the saturation effects.

Should we find a slope of 3/2 (or simply significantly greater than 1) between $\log_{10} M_0$ and M_m, we would conclude that we have failed to avoid saturation. Similarly, should we find a strong variation in the quality of our fit with period, we could still be contaminated by finiteness with the earthquake data set following a model with constant τ_s.

4. APPLICATION TO DATA

Our data for this study consist of three sets: (1) records obtained at the broadband station operated at Papeete, Tahiti (PPT), since 1972; (2) records obtained on the ultra-long-period vertical instrument at Pasadena, California (PAS); and (3) records from the GEOSCOPE network.

Papeete Records

As shown on Figure 1, the response of this system is flat in displacement from 1 s to 150 s and decreases by a factor $\sqrt{2}$ at 300 s. We concentrate here on a data set of 45 earthquakes, listed in Table 2, and having published moments between 7.6×10^{25} and 1.8×10^{28} dyn-cm. Their locations and focal mechanisms are shown on Figure 5.

For each event, we Fourier-transformed a 4096-point time series (with digital sampling rate 0.2 s) and at each Fourier period $T \geq 50$ s obtained the spectral amplitude $X(\omega)$ after removal of the instrument response; we then applied the corrections (6) and (10) and computed a value of M_m using (11). We list in Table 2 only the largest value, and the period at which it is obtained, but keep all measurements as a permanent data set.

Pasadena Records

This system (commonly called ULP33) has been described by *Gilman* [1960] and its response is given by *Okal and Geller* [1979]. This is not a broadband system but rather a classical electromagnetic seismograph system with a filtered galvanometer, resulting in an overall maximum response peaked at 145 s. We selected all available records of events with published moments greater than 10^{26} dyn-cm from 1970 to 1986. Unfortunately, the instrument was not operating between April 1983 and the

TABLE 2. Papeete Data Set

Event	Station	Passage	Δ	M_m^{pub}	M_m	T	r	M_c	r_c
1973 06 17	PPT	1	84.68	7.85	8.20	273.0	0.35	7.85	0.00
1974 10 03	PPT	1	69.18	8.26	8.13	164.0	-0.13	8.17	-0.09
1977 04 21	PPT	1	48.74	7.08	7.08	63.0	0.00	7.24	0.16
1977 06 22	PPT	1	25.24	8.15	8.23	117.0	0.08	8.02	-0.13
1978 03 23	PPT	1	83.95	7.43	7.30	273.0	-0.13	7.25	-0.18
1978 03 24	PPT	1	83.32	7.36	7.29	205.0	-0.07	7.09	-0.27
1978 06 12	PPT	1	84.80	7.53	7.51	273.0	-0.02	7.43	-0.10
1978 11 29	PPT	1	62.01	7.72	7.27	205.0	-0.45	7.59	-0.13
1979 02 16	PPT	1	73.03	6.79	6.68	82.0	-0.11	6.47	-0.32
1979 02 28	PPT	1	78.34	7.27	7.15	273.0	-0.12	7.02	-0.25
1979 03 14	PPT	1	59.17	7.24	7.35	205.0	0.11	7.30	0.06
1979 10 12	PPT	1	46.82	7.00	7.00	164.0	0.00	6.96	-0.04
1980 07 08	PPT	1	42.78	7.29	7.52	205.0	0.23	7.26	-0.03
1980 07 17	PPT	1	43.19	7.90	7.95	205.0	0.05	7.67	-0.23
1981 07 06	PPT	1	36.59	7.41	7.22	82.0	-0.19	7.47	0.06
1981 07 15	PPT	1	40.79	6.76	7.01	205.0	0.25	6.72	-0.04
1981 09 01	PPT	1	22.72	7.29	7.28	273.0	-0.01	7.40	0.11
1981 10 25	PPT	1	58.68	6.85	7.12	273.0	0.27	6.95	0.10
1982 06 07 A	PPT	1	61.04	6.46	6.52	205.0	0.06	6.70	0.24
1982 06 07 B	PPT	1	60.84	6.43	6.71	273.0	0.28	6.73	0.30
1982 08 05	PPT	1	43.16	6.51	6.96	273.0	0.45	6.63	0.12
1982 12 19	PPT	1	25.39	7.30	7.47	273.0	0.17	7.36	0.06
1983 05 26	PPT	1	87.84	7.66	7.99	164.0	0.33	7.57	-0.09
1983 10 04	PPT	1	72.74	7.53	7.55	205.0	0.02	7.37	-0.16
1984 02 07	PPT	1	48.97	7.40	7.55	59.0	0.15	7.50	0.10
1984 03 24	PPT	1	83.67	6.80	6.93	273.0	0.13	6.72	-0.08
1985 03 03	PPT	1	70.32	8.01	7.89	164.0	-0.12	7.69	-0.32
1985 04 09	PPT	1	70.53	6.70	6.87	55.0	0.17	6.59	-0.11
1985 09 19	PPT	1	58.40	8.04	7.94	205.0	-0.10	7.81	-0.23
1985 09 21	PPT	1	58.87	7.40	7.44	205.0	0.04	7.30	-0.10
1985 11 28 A	PPT	1	42.58	6.48	7.01	273.0	0.53	6.60	0.12
1985 11 28 B	PPT	1	42.64	6.56	6.75	82.0	0.19	6.80	0.24
1985 12 21	PPT	1	42.33	6.76	6.98	205.0	0.22	6.71	-0.05
1986 04 30	PPT	1	58.18	6.49	6.64	205.0	0.15	6.51	0.02
1986 05 07	PPT	1	72.38	8.02	8.13	205.0	0.11	7.85	-0.17
1986 10 20	PPT	1	27.08	7.95	7.83	63.0	-0.12	7.69	-0.26
1987 02 08	PPT	1	62.16	7.05	7.30	117.0	0.25	7.04	-0.01
1987 03 05	PPT	1	73.50	7.39	7.51	51.0	0.12	7.26	-0.13
1987 03 06	PPT	1	75.33	6.80	6.87	137.0	0.07	6.57	-0.23
1987 06 27	PPT	1	72.44	5.92	6.10	59.0	0.18	6.16	0.24
1987 07 06	PPT	1	41.06	5.98	6.45	117.0	0.47	6.03	0.05
1987 08 08	PPT	1	74.88	6.90	7.12	68.0	0.22	6.72	-0.18
1987 09 03	PPT	1	55.90	7.15	6.88	205.0	-0.27	7.35	0.20
1987 09 28 A	PPT	1	40.17	6.28	6.40	137.0	0.12	6.16	-0.12
1987 09 28 B	PPT	1	40.15	5.88	5.98	164.0	0.10	5.72	-0.16

fall of 1986, which prevents a direct comparison with PPT and GEOSCOPE records, especially for the large earthquakes of 1985 and 1986. We also had to eliminate a number of records featuring gross nonlinearity in the response of the instrument; (e.g., October 11, 1975; March 14, 1979). Records were hand-digitized at a sampling rate of 1 s, and the analysis proceeded as for the PPT records. However, in view of the faster falloff of the response curve at long periods, we take our measurements only in the range 50–250 s. We include in the PAS data set records of multiple passages of Rayleigh waves for some of the largest events involved. For such records we restrict our measurements to $T \geq 75$ s for R_2 and $T \geq 100$ s for R_3 and R_4. The full data set comprises 42 records from 31 earthquakes, whose locations and mechanisms are shown on Figure 6. Results are listed in Table 3.

GEOSCOPE records

We refer to *Romanowicz et al.* [1984] for a description of the GEOSCOPE network, including its frequency response. In this study we targeted all available GEOSCOPE records from shallow earthquakes of moment $M_0 \geq 10^{26}$ dyn-cm; however, we eliminated records with poor signal-to-noise ratios, records early in the history of the network for which high magnification led to digital clipping and/or nonlinearity, and records from the station MBO (M'Bour, Senegal) for which the magnification level is in doubt. Table 4 lists all records in the GEOSCOPE study. Data processing was analogous to that for PPT. However, in view of the time sampling of the VLP channel ($\delta t = 10$ s), we take measurements only at periods $T \geq 64$ s. As in the case of PAS, we include a number of second passages of Rayleigh waves, for which

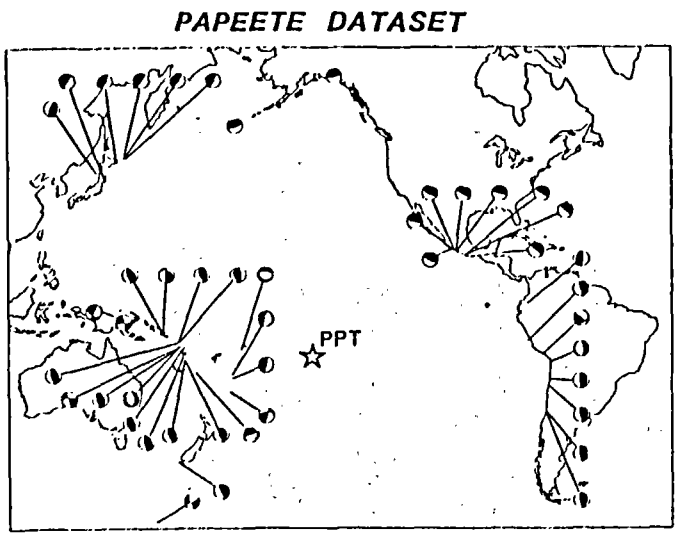

Fig. 5. Map of the epicenters and focal mechanisms for the Papeete data set.

we restrict measurements to $T \geq 75$ s. We also include in the data set all multiple passages, up to and including R_4, in the case of the Aleutian earthquake of May 7, 1986, our purpose being to test any systematic bias of the measured M_m as a function of distance; we do not include similar records for the preceding large events (e.g., the Chilean and Mexican 1985 earthquakes), since at the time the network was not yet fully developed. As explained below, measurements for R_5 deteriorate substantially, suggesting that the signal-to-noise ratio is by then too low for a significant measurement. We list the corresponding values at the end of the data table but do not use R_5 values in our statistical evaluations. The full data set comprises 169 records (178 with R_5) from 41 earthquakes, whose location and mechanisms are shown on Figure 7.

In studying the performance of the magnitude scale M_m, we consider separately the three data sets described above and also regroup them as a single data set comprising all 256 measurements. Thus we will commonly refer to four data sets.

Published Moments and Focal Mechanisms

We take most of our published moments from the Harvard moment tensor inversion solutions [*Dziewonski et al.*, 1983*a,b,c*, 1984*a,b*, 1985*a,b,c,d*, 1986*a,b,c*, 1987*a,b, c,d,e,f,g*, 1988*a,b,c,d,e*]. A variety of sources are used for events predating 1977. We occasionally use our own solutions for earthquakes which we have studied in detail. Table 5 lists all pertinent epicentral data. In Tables 2, 3, and 4, the published moments are reported through M_m^{pub}, obtained by applying (2) to the published value of the moment, as listed in Table 5.

Finally, we note that the largest event analyzed is the 1977 Indonesian earthquake ($M_0 = 3.6 \times 10^{28}$ dyn-cm). Obviously, the systematic study of the performance of the method for truly gigantic events (in the 10^{29} to 10^{30} dyn-cm range) would be a fundamental test of the method. However, such events have not occurred since 1965. Our purpose in the present paper is to test the concept on a set of data with homogeneous recording characteristics. The extension of M_m measurements to conventional (i.e., WWSSN) or historical seismograms is currently under way and will be the subject of a separate paper.

5. DISCUSSION OF RESULTS

In order to assess the success of the method, we conduct in this section a critical study of the fit between measured values of the mantle magnitude and published values of the seismic moment, as resulting from moment tensor inversion or other low-frequency seismological techniques. Figure 8 presents all of our data, either split into individual data sets or treated as a whole.

Slope of $\log_{10} M_0$ Versus M_m

First, and for each of the four data sets involved, we regressed the published values of $\log_{10} M_0$ against the corresponding values of M_m computed from (11). The best fitting slopes are 0.95 for the PAS data set, 1.06 for the PPT records, and 1.03 for the GEOSCOPE data set. If all 256 records are regressed together, the best slope is 1.04 . These values do not depart significantly from the slope of 1 expected theoretically; this result and the generally large values of the periods at which the maximum value of M_m is obtained serve as an a posteriori verification of the fact that we indeed stay on the flat portion of the spectrum.

We also attempted to regress $\log_{10} M_0$ versus $[M_m - \log_{10} T]$, where T is the period at which the measurement is made; for all four data sets, this resulted in a deterioration of the quality of the fit, as measured by the root-mean-square residual of the regression, ranging from 25% to 53%. We conclude that our method of measuring M_m does indeed produce a magnitude scale growing linearly with $\log_{10} M_0$ and successfully avoiding the range of saturation effects.

Accuracy of M_m

There remains to discuss the accuracy of the seismic moment values inferred from a single measurement of

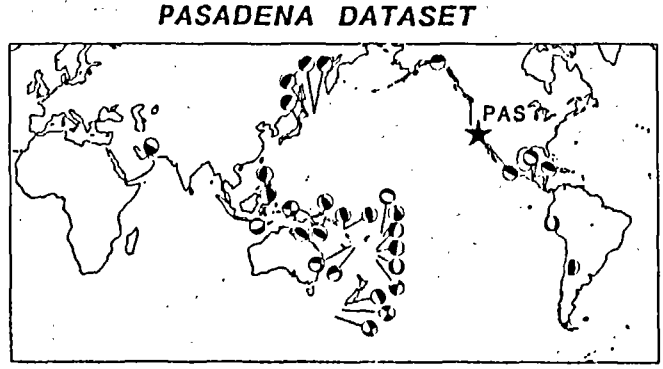

Fig. 6. Map of the epicenters and focal mechanisms for the Pasadena data set.

TABLE 3. Pasadena Data Set

Event	Station	Passage	Δ	M_m^{pub}	M_m	T	r	M_c	r_c
1970 05 31	PAS	1	57.11	8.00	7.76	107.8	-0.24	7.88	-0.12
1970 05 31	PAS	2	302.89	8.00	8.19	85.3	0.19	8.36	0.36
1973 06 17	PAS	1	71.49	7.83	7.47	85.3	-0.36	7.70	-0.13
1975 07 20 A	PAS	1	91.02	7.53	7.55	128.0	0.02	7.12	-0.41
1975 07 20 B	PAS	1	91.22	7.08	7.11	128.0	0.03	6.84	-0.24
1976 08 16	PAS	1	108.86	8.28	8.32	81.9	0.04	8.22	-0.06
1976 08 16	PAS	2	251.14	8.28	8.18	204.8	-0.10	7.96	-0.32
1976 08 16	PAS	3	468.86	8.28	8.36	227.6	0.08	8.13	-0.15
1977 03 18	PAS	1	103.27	6.95	7.02	128.0	0.07	7.16	0.21
1977 04 02	PAS	1	72.12	7.01	7.23	60.2	0.22	7.71	0.70
1977 06 22	PAS	1	79.01	8.15	8.02	107.8	-0.13	8.06	-0.09
1977 06 22	PAS	2	280.99	8.15	7.96	146.3	-0.19	8.13	-0.02
1977 08 19	PAS	1	123.68	8.56	8.14	136.5	-0.42	8.51	-0.05
1977 08 19	PAS	2	236.32	8.56	8.32	240.9	-0.24	8.53	-0.03
1977 08 19	PAS	3	483.68	8.56	8.03	170.7	-0.53	8.34	-0.22
1977 08 19	PAS	4	596.32	8.56	8.08	186.2	-0.48	8.37	-0.19
1977 10 10	PAS	1	80.78	7.01	7.32	128.0	0.31	7.22	0.21
1977 11 23	PAS	1	80.51	7.27	7.61	227.6	0.34	7.35	0.08
1978 03 23	PAS	1	68.92	7.43	7.18	64.0	-0.25	7.56	0.13
1978 03 24	PAS	1	68.94	7.36	7.24	64.0	-0.12	7.55	0.19
1978 06 12	PAS	1	76.43	7.53	7.44	93.1	-0.09	7.75	0.22
1979 02 28	PAS	1	30.53	7.27	7.48	113.8	0.21	7.51	0.24
1979 05 01	PAS	1	87.94	7.16	7.42	107.8	0.26	7.27	0.11
1979 09 12	PAS	1	103.98	7.37	7.95	157.5	0.58	7.59	0.22
1979 09 12	PAS	2	256.02	7.37	7.78	89.0	0.41	7.40	0.03
1979 10 12	PAS	1	105.67	7.00	6.68	170.7	-0.32	6.70	-0.30
1980 07 08	PAS	1	85.22	7.29	7.42	204.8	0.13	7.13	-0.16
1980 07 17	PAS	1	85.67	7.68	7.93	136.5	0.25	7.69	0.01
1980 07 17	PAS	2	274.33	7.68	7.66	128.0	-0.02	7.44	-0.24
1981 05 25	PAS	1	107.57	7.44	7.70	128.0	0.26	7.59	0.15
1981 05 25	PAS	2	252.43	7.44	7.69	85.3	0.25	7.65	0.21
1981 07 06	PAS	1	87.17	7.41	7.30	102.4	-0.11	7.43	0.02
1981 07 28	PAS	1	115.90	6.95	6.99	55.3	0.04	7.07	0.12
1981 09 01	PAS	1	71.57	7.29	7.92	107.8	0.63	7.61	0.32
1981 09 01	PAS	2	288.43	7.29	7.80	107.8	0.51	7.50	0.21
1981 10 25	PAS	1	21.55	6.85	7.11	204.8	0.26	7.21	0.36
1982 06 19	PAS	1	33.39	7.02	7.11	51.2	0.09	7.33	0.31
1982 07 07	PAS	1	110.95	6.83	6.70	73.1	-0.13	7.08	0.25
1982 12 19	PAS	1	79.86	7.30	7.14	53.9	-0.16	7.32	0.02
1983 03 18	PAS	1	91.28	7.67	7.80	78.8	0.13	7.94	0.27
1983 04 03	PAS	1	40.97	7.26	6.82	227.6	-0.44	6.99	-0.27
1986 10 20	PAS	1	82.99	7.95	7.94	227.6	-0.01	8.01	0.06

M_m. For this purpose, we study the population of residuals

$$r = M_m \text{ (measured)} - \log_{10} M_0 \text{ (published)} + 20 \quad (13)$$

for each of our measurements. Table 6 lists the mean value $\bar{r}$ and standard deviation σ of the residuals for all four data sets. We also list the value for the data set of 20 records measured at PPT in our preliminary study [*Talandier et al.*, 1987]. The significant decrease in the mean value of the residual $\bar{r}$, between the two studies (from 0.18 to 0.02), is due to the use of an improved source correction C_s (see section 3).

We obtained mean residuals $\bar{r}$ in general smaller than 0.2 units. The mean residuals are extremely small at PAS and PPT, somewhat larger at the GEOSCOPE stations. Similarly, the standard deviation σ of the residuals is always less than 0.3 . This means that the measurement of M_m according to (11), once corrected by subtracting $\bar{r}$ at the appropriate station, results in an uncertainty on the value of the seismic moment of a multiplicative or divisive factor f which stays below 2 (we write $f = */10^{\sigma}$). These results must be assessed in the context of the performance of the classical magnitude scales, for which few single stations can boast of having a systematic magnitude bias, and a standard deviation of their magnitude estimates of ~ 0.2 magnitude units. In addition, it is not uncommon for several independent investigators to obtain estimates of M_0 differing by a factor of */ 1.5 to 2.0 .

Investigation of Possible Systematic Biases

In this section we investigate systematically the possible correlation of the residuals r with various parameters, such as distance, period, etc. The existence of any such bias would invalidate one of more assumptions in our theoretical models.

Distance. Figure 9 plots the residuals r as a function

TABLE 4. GEOSCOPE Data Set

Event	Station	Passage	Δ	M_m^{pub}	M_m	T	r	M_c	r_c
1982 06 19	SSB	2	276.61	7.02	7.39	284.4	0.37	7.18	0.16
1982 07 07	SSB	1	162.98	6.83	7.10	160.0	0.27	7.13	0.30
1982 12 19	PCR	1	112.60	7.30	7.36	98.5	0.06	7.55	0.25
1983 01 17	PAF	1	97.81	6.36	6.31	91.4	-0.05	6.98	0.62
1983 01 17	PCR	1	67.84	6.36	6.04	98.5	-0.32	6.52	0.16
1983 01 24	PAF	1	65.51	6.23	6.45	64.0	0.22	6.51	0.28
1983 01 24	PCR	1	50.56	6.23	6.34	256.0	0.11	6.16	-0.07
1983 04 03	PAF	1	133.72	7.26	7.30	256.0	0.04	7.22	-0.04
1983 04 03	PCR	1	138.35	7.26	7.07	232.7	-0.19	7.29	0.03
1983 04 03	SSB	1	82.18	7.26	7.97	256.0	0.71	7.64	0.38
1983 04 04	PAF	1	58.99	6.53	6.79	71.1	0.26	6.70	0.17
1983 04 04	PCR	1	46.92	6.53	6.60	85.3	0.07	6.50	-0.03
1983 04 04	SSB	1	86.16	6.53	6.88	256.0	0.35	6.68	0.15
1983 05 26	PAF	1	108.11	7.66	7.94	256.0	0.28	7.89	0.23
1983 05 26	PCR	2	261.18	7.66	8.09	284.4	0.43	7.78	0.12
1983 05 26	SSB	2	274.63	7.66	7.97	284.4	0.31	7.68	0.02
1983 10 04	PAF	1	96.61	7.53	7.29	256.0	-0.24	7.50	-0.03
1983 10 22	PAF	1	51.10	6.66	7.23	256.0	0.57	6.72	0.06
1983 11 30	PAF	1	42.42	7.61	8.13	213.3	0.52	7.65	0.04
1983 11 30	TAM	1	71.49	7.61	7.82	213.3	0.21	7.86	0.25
1984 01 08	PCR	1	64.06	6.08	6.44	67.4	0.36	6.35	0.27
1984 01 08	TAM	1	112.52	6.08	6.41	256.0	0.33	6.18	0.10
1984 02 07	PCR	1	100.02	7.40	7.79	256.0	0.39	7.46	0.06
1984 02 07	SSB	1	139.10	7.40	7.43	64.0	0.03	7.51	0.11
1984 02 07	PCR	2	259.98	7.40	7.76	284.4	0.36	7.43	0.03
1984 03 24	PCR	1	106.41	6.81	6.83	256.0	0.02	6.89	0.08
1984 03 24	SSB	1	85.14	6.81	7.08	256.0	0.27	6.94	0.13
1984 03 24	TAM	1	105.02	6.81	7.12	256.0	0.31	6.94	0.13
1984 05 17	PCR	1	15.34	6.40	6.18	256.0	-0.22	6.47	0.07
1984 05 17	TAM	1	74.47	6.40	6.80	106.7	0.40	6.43	0.03
1984 05 17	WFM	1	140.03	6.40	6.68	256.0	0.28	6.51	0.11
1984 08 06	TAM	1	104.77	6.46	6.68	65.6	0.22	6.58	0.12
1984 09 18	PCR	1	98.34	6.32	6.55	67.4	0.23	6.43	0.11
1984 09 18	WFM	1	96.82	6.32	6.62	256.0	0.30	6.38	0.06
1984 11 01	PCR	1	96.94	6.60	6.81	128.0	0.21	6.69	0.09
1984 11 01	TAM	1	44.90	6.60	7.04	116.4	0.44	6.70	0.10
1984 11 01	WFM	1	46.54	6.60	7.03	256.0	0.43	6.68	0.08
1984 11 17	PCR	1	46.61	6.76	6.71	256.0	-0.05	6.72	-0.04
1984 11 17	WFM	1	136.77	6.76	6.48	65.6	-0.28	6.62	-0.14
1984 11 23	PCR	1	107.65	6.28	6.58	67.4	0.30	6.50	0.22
1984 11 23	SSB	1	147.10	6.28	6.62	213.3	0.34	6.31	0.03
1984 12 30	PAF	1	72.76	6.26	6.63	116.4	0.37	6.45	0.19
1984 12 30	PCR	1	100.40	6.26	6.57	256.0	0.31	6.43	0.17
1984 12 30	WFM	1	125.88	6.26	6.43	256.0	0.17	6.36	0.10
1985 01 21	PCR	1	73.75	6.15	6.79	67.4	0.64	6.52	0.37
1985 01 21	SSB	1	113.99	6.15	6.72	116.4	0.57	6.46	0.31
1985 01 21	WFM	1	133.64	6.15	6.59	75.3	0.44	7.18	1.03
1985 03 02	PAF	1	63.27	6.04	6.50	80.0	0.46	6.76	0.72
1985 03 02	SSB	1	108.91	6.04	6.71	67.4	0.67	6.97	0.93
1985 03 03	PAF	1	91.08	8.01	7.95	256.0	-0.06	8.08	0.07
1985 03 03	PCR	1	106.25	8.01	8.21	256.0	0.20	8.07	0.06
1985 03 03	SSB	1	104.42	8.01	8.05	256.0	0.04	7.94	-0.07
1985 03 03	TAM	1	92.49	8.01	8.24	256.0	0.23	8.00	-0.01
1985 03 03	WFM	1	75.61	8.01	7.71	256.0	-0.30	8.01	0.00
1985 03 03	PAF	2	268.92	8.01	8.05	213.3	0.04	8.25	0.24
1985 03 03	PCR	2	253.75	8.01	8.18	256.0	0.17	8.04	0.03
1985 03 03	SSB	2	255.58	8.01	8.00	256.0	-0.01	7.90	-0.11
1985 03 03	WFM	2	284.39	8.01	7.78	256.0	-0.23	8.08	0.07
1985 04 09	TAM	1	92.60	6.70	6.91	256.0	0.21	6.73	0.03
1985 04 13	TAM	1	117.67	6.45	6.95	232.7	0.50	6.60	0.15
1985 04 13	WFM	1	131.92	6.45	6.39	85.3	-0.06	6.77	0.32
1985 05 10	PCR	1	93.10	6.84	7.20	128.0	0.36	7.08	0.24
1985 05 10	WFM	1	125.39	6.84	7.21	98.5	0.37	7.11	0.27
1985 07 03	PCR	1	95.12	6.92	7.48	182.9	0.56	7.09	0.17
1985 07 03	AGD	2	249.54	6.92	7.25	94.8	0.33	7.10	0.18
1985 08 23	AGD	1	40.01	6.52	6.60	128.0	0.08	6.85	0.33
1985 08 23	CAY	1	114.56	6.52	6.72	64.0	0.20	6.93	0.41
1985 08 23	PCR	1	63.20	6.52	6.91	182.9	0.39	6.69	0.17
1985 08 23	TAM	1	60.54	6.52	6.73	64.0	0.21	6.87	0.35
1985 09 19	CAY	1	50.79	8.04	7.89	64.0	-0.15	8.64	0.60

TABLE 4. (continued)

Event	Station	Passage	Δ	M_m^{pub}	M_m	T	r	M_c	r_c
1985 09 19	PCR	1	159.22	8.04	7.88	71.1	-0.16	8.64	0.60
1985 09 19	SSB	1	88.64	8.04	8.24	182.9	0.20	8.06	0.02
1985 09 19	CAY	2	309.21	8.04	7.77	256.0	-0.27	8.04	0.00
1985 09 19	SSB	2	271.36	8.04	8.27	256.0	0.23	8.05	0.01
1985 09 21	AGD	1	134.34	7.40	7.68	128.0	0.28	7.55	0.15
1985 09 21	CAY	1	49.89	7.40	7.38	64.0	-0.02	7.70	0.30
1985 09 21	PCR	1	158.31	7.40	7.41	71.1	0.01	7.81	0.41
1985 09 21	SSB	1	88.32	7.40	7.66	182.9	0.26	7.47	0.07
1985 09 21	AGD	2	225.66	7.40	7.65	256.0	0.25	7.47	0.07
1985 09 21	PCR	2	201.69	7.40	7.23	256.0	-0.17	7.47	0.07
1985 09 26	CAY	1	122.37	6.38	6.63	64.0	0.25	6.76	0.38
1985 09 26	PCR	1	104.14	6.38	6.68	116.4	0.30	6.67	0.29
1985 11 17	PCR	1	79.57	6.69	6.99	64.0	0.30	6.75	0.06
1985 11 17	TAM	1	126.66	6.69	7.21	75.3	0.52	6.96	0.27
1985 12 21	AGD	1	125.14	6.76	7.24	256.0	0.48	6.88	0.12
1985 12 21	CAY	1	140.70	6.76	7.24	256.0	0.48	6.90	0.14
1985 12 21	NOC	1	8.11	6.76	6.74	213.3	-0.02	6.93	0.17
1985 12 21	PCR	1	103.66	6.76	7.22	256.0	0.46	6.84	0.08
1985 12 21	WFM	1	120.68	6.76	7.12	256.0	0.36	6.80	0.04
1985 12 23	CAY	1	77.29	6.18	6.76	64.0	0.58	6.36	0.18
1985 12 23	NOC	1	100.40	6.18	6.76	256.0	0.58	6.27	0.09
1985 12 23	SSB	1	65.13	6.18	6.91	75.3	0.73	6.62	0.44
1985 12 23	TAM	1	86.25	6.18	6.88	71.1	0.70	6.53	0.35
1985 12 23	WFM	1	34.94	6.18	6.80	71.1	0.62	6.38	0.20
1986 03 24	AGD	1	96.26	6.05	6.18	64.0	0.13	6.34	0.29
1986 03 24	DRV	1	64.13	6.05	6.10	67.4	0.05	6.45	0.40
1986 03 24	NOC	1	33.18	6.05	6.37	85.3	0.32	6.18	0.13
1986 03 24	SSB	1	121.43	6.05	6.46	64.0	0.41	6.24	0.19
1986 04 20	DRV	1	64.22	6.20	6.30	213.3	0.10	6.33	0.13
1986 04 20	KIP	1	65.65	6.20	6.22	182.9	0.02	6.21	0.01
1986 04 20	NOC	1	32.77	6.20	6.32	64.0	0.12	6.38	0.18
1986 04 20	WFM	1	129.78	6.20	6.49	213.3	0.29	6.29	0.09
1986 04 30	AGD	1	134.95	6.49	6.81	98.5	0.32	6.69	0.20
1986 04 30	CAY	1	51.21	6.49	6.34	182.9	-0.15	6.66	0.17
1986 04 30	DRV	1	117.40	6.49	6.81	256.0	0.32	6.56	0.07
1986 04 30	KIP	1	51.60	6.49	6.34	256.0	-0.15	6.62	0.13
1986 04 30	NOC	1	97.48	6.49	6.65	213.3	0.16	6.63	0.14
1986 04 30	SSB	1	88.73	6.49	6.81	256.0	0.32	6.59	0.10
1986 04 30	TAM	1	98.99	6.49	6.69	256.0	0.20	6.59	0.10
1986 04 30	WFM	1	34.14	6.49	6.82	256.0	0.33	6.59	0.10
1986 05 07	AGD	1	109.23	8.02	8.38	256.0	0.36	8.09	0.07
1986 05 07	CAY	1	105.52	8.02	7.73	284.4	-0.29	7.93	-0.09
1986 05 07	CRZ	1	149.40	8.02	7.87	256.0	-0.15	8.07	0.05
1986 05 07	DRV	1	122.77	8.02	8.16	256.0	0.14	8.01	-0.01
1986 05 07	KIP	1	32.70	8.02	8.27	213.3	0.25	7.98	-0.04
1986 05 07	NOC	1	75.28	8.02	8.14	256.0	0.12	7.97	-0.05
1986 05 07	PAF	1	139.78	8.02	7.86	160.0	-0.16	8.25	0.23
1986 05 07	SSB	1	83.50	8.02	8.35	256.0	0.33	8.08	0.06
1986 05 07	TAM	1	105.96	8.02	8.33	256.0	0.31	8.05	0.03
1986 05 07	WFM	1	63.59	8.02	7.79	256.0	-0.23	7.97	-0.05
1986 05 07	AGD	2	250.77	8.02	8.34	256.0	0.32	8.05	0.03
1986 05 07	CAY	2	254.48	8.02	7.81	284.4	-0.21	8.01	-0.01
1986 05 07	CRZ	2	210.60	8.02	7.82	256.0	-0.20	8.02	0.00
1986 05 07	DRV	2	237.23	8.02	8.17	256.0	0.15	8.02	0.00
1986 05 07	KIP	2	327.30	8.02	8.41	256.0	0.39	8.10	0.08
1986 05 07	NOC	2	284.72	8.02	8.16	256.0	0.14	8.00	-0.02
1986 05 07	PAF	2	220.22	8.02	7.83	284.4	-0.19	8.05	0.03
1986 05 07	SSB	2	276.50	8.02	8.36	256.0	0.34	8.09	0.07
1986 05 07	TAM	2	254.04	8.02	8.30	284.4	0.28	8.01	-0.01
1986 05 07	WFM	2	296.41	8.02	7.77	196.9	-0.25	8.01	-0.01
1986 05 07	AGD	3	469.23	8.02	8.33	284.4	0.31	8.04	0.02
1986 05 07	CAY	3	465.52	8.02	7.76	284.4	-0.26	7.96	-0.06
1986 05 07	CRZ	3	509.40	8.02	8.00	182.9	-0.02	8.29	0.27
1986 05 07	DRV	3	482.77	8.02	8.26	284.4	0.24	8.10	0.08
1986 05 07	KIP	3	392.70	8.02	8.22	256.0	0.20	7.91	-0.11
1986 05 07	NOC	3	435.28	8.02	8.20	284.4	0.18	8.03	0.01
1986 05 07	PAF	3	499.78	8.02	7.84	160.0	-0.18	8.23	0.21
1986 05 07	SSB	3	443.50	8.02	8.35	213.3	0.33	8.09	0.07
1986 05 07	TAM	3	465.96	8.02	8.32	284.4	0.30	8.03	0.01
1986 05 07	WFM	3	423.59	8.02	7.84	256.0	-0.18	8.03	0.01

TABLE 4. (continued)

Event	Station	Passage	Δ	M_m^{pub}	M_m	T	r	M_c	r_c
1986 05 07	AGD	4	610.77	8.02	8.40	232.7	0.38	8.12	0.10
1986 05 07	CAY	4	614.48	8.02	7.85	256.0	-0.17	8.08	0.06
1986 05 07	CRZ	4	570.60	8.02	7.84	111.3	-0.18	8.28	0.26
1986 05 07	DRV	4	597.23	8.02	8.21	284.4	0.19	8.05	0.03
1986 05 07	KIP	4	687.30	8.02	8.45	284.4	0.43	8.13	0.11
1986 05 07	NOC	4	644.72	8.02	8.20	284.4	0.18	8.02	0.00
1986 05 07	PAF	4	580.22	8.02	7.94	111.3	-0.08	8.47	0.45
1986 05 07	SSB	4	636.50	8.02	8.23	284.4	0.21	7.96	-0.06
1986 05 07	WFM	4	656.41	8.02	7.73	196.9	-0.29	7.98	-0.04
1986 07 09	DRV	1	69.21	6.20	6.24	256.0	0.04	6.20	0.00
1986 07 09	KIP	1	75.69	6.20	6.50	256.0	0.30	6.25	0.05
1986 07 09	RER	1	72.92	6.20	6.50	256.0	0.30	6.26	0.06
1986 07 09	SCZ	1	106.31	6.20	6.29	256.0	0.09	6.21	0.01
1986 07 09	SSB	1	110.48	6.20	6.70	256.0	0.50	6.36	0.16
1986 07 09	TAM	1	117.55	6.20	6.73	256.0	0.53	6.31	0.11
1986 08 14	DRV	1	69.07	7.36	7.14	64.0	-0.22	7.21	-0.15
1986 08 14	KIP	1	75.69	7.36	7.40	256.0	0.04	7.50	0.14
1986 08 14	NOC	1	45.46	7.36	7.41	182.9	0.05	7.39	0.03
1986 08 14	PPT	1	84.63	7.36	7.54	128.0	0.18	7.47	0.11
1986 08 14	RER	1	72.91	7.36	7.38	256.0	0.02	7.51	0.15
1986 08 14	SCZ	1	106.36	7.36	7.20	256.0	-0.16	7.61	0.25
1986 08 14	SSB	1	110.62	7.36	7.36	150.6	0.00	7.46	0.10
1986 08 14	TAM	1	117.66	7.36	7.49	256.0	0.13	7.42	0.06
1986 08 14	KIP	2	284.31	7.36	7.48	256.0	0.12	7.60	0.24
1986 08 14	NOC	2	314.54	7.36	7.40	256.0	0.04	7.36	0.00
1986 08 14	PPT	2	275.37	7.36	7.51	213.3	0.15	7.44	0.08
1986 08 14	RER	2	287.09	7.36	7.35	284.4	-0.01	7.48	0.12
1986 08 14	SSB	2	249.38	7.36	7.25	284.4	-0.11	7.34	-0.02
1986 08 14	TAM	2	242.34	7.36	7.52	75.3	0.16	7.41	0.05
			Additional (R_5) Passages for 1986 Aleutian Event						
1986 05 07	AGD	5	829.23	8.02	8.36	111.3	0.34	8.14	0.12
1986 05 07	CAY	5	825.52	8.02	7.99	111.3	-0.03	8.46	0.44
1986 05 07	CRZ	5	869.40	8.02	8.15	196.9	0.13	8.42	0.40
1986 05 07	DRV	5	842.77	8.02	8.18	284.4	0.16	8.02	0.00
1986 05 07	KIP	5	752.70	8.02	8.01	284.4	-0.01	7.70	-0.32
1986 05 07	NOC	5	795.28	8.02	8.05	256.0	0.03	7.88	-0.14
1986 05 07	PAF	5	859.78	8.02	8.01	182.9	-0.01	8.36	0.34
1986 05 07	SSB	5	803.50	8.02	8.37	196.9	0.35	8.12	0.10
1986 05 07	WFM	5	783.59	8.02	8.16	100.4	0.14	8.56	0.54

of the distance Δ at which the measurement is taken. Any significant trend would indicate that our distance correction C_D is inadequate, probably reflecting inappropriate Q models. It is clear from this figure that no such trend exists; a regression of r against $\log_{10}\Delta$ produced a slope of -0.057 for the whole data set, and the steepest slope found was -0.129 for the PAS data set. We further explored the possibility of any systematic bias of M_m with distance through two experiments: first, the data presented in Figure 10*a* show no systematic difference in the residual population between M_m values for first and multiple passages. Then we studied in detail M_m values measured on 10 stations of the GEOSCOPE network following the Aleutian earthquake of May 7, 1986. We use 48 records, including multiple passages up to R_5. The top frames of Figure 10*b* show no systematic trend with distance of the residuals r up to and including R_4. In the case of fifth passages, the signal-to-noise ratio has deteriorated to the point that we may be measuring noise. This explains the trends toward larger and more scattered residuals. In the bottom frames, we compare each residual $r(n)$ for an nth passage to the residual $r(1)$ of R_1 at the same station, thereby eliminating any focal mechanism effect. Again the stability of this new residual with distance is excellent up to and including R_4, but starts to deteriorate for R_5. This justifies a posteriori the elimina-

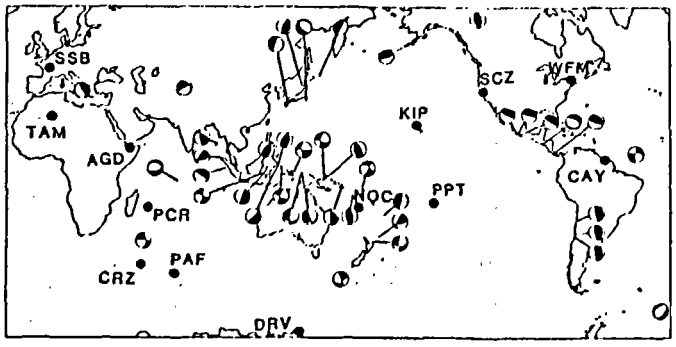

Fig. 7. Map of the epicenters and focal mechanisms for the GEOSCOPE data set. The stations are shown as dots; the post-1986 location of the Réunion Island station (RER), only 18 km away from PCR, is not shown.

TABLE 5. Source Parameters of Events Used in This Study

Date	Epicenter °N	Epicenter °E	Depth, km	Published Moment, 10^{27} dyn-cm	Focal Mechanism ϕ, deg	Focal Mechanism δ, deg	Focal Mechanism λ, deg	Reference
1970 05 31	-9.2	-78.8	33.	10.00	160	37	250	a
1973 06 17	43.0	145.8	33.	6.70	230	27	111	b
1974 10 03	-12.3	-77.7	15.	18.00	160	80	85	c,d
1975 07 20 A	-6.6	155.1	16.	3.40	306	36	90	e
1975 07 20 B	-7.1	155.1	33.	1.20	303	40	90	e
1976 08 16	6.3	124.0	33.	19.00	327	22	68	f
1977 03 18	16.8	122.3	35.	0.89	207	27	108	g
1977 04 02	-16.7	-172.1	50.	1.03	317	41	45	g
1977 04 21	-10.0	160.7	40.	1.20	326	35	79	g
1977 06 22	-22.9	-175.9	61.	14.00	197	79	271	g
1977 08 19	-11.1	118.5	23.	36.00	260	24	287	g
1977 10 10	-25.9	-175.4	23.	1.02	18	38	293	g
1977 11 23	-31.0	-67.8	21.	1.86	183	44	90	g
1978 03 23	44.1	149.0	28.	2.70	224	11	91	h
1978 03 24	144.2	148.9	31.	2.30	223	18	93	h
1978 06 12	38.2	142.0	38.	3.40	184	14	59	h
1978 11 29	16.0	-96.6	16.	5.27	127	84	94	h
1979 02 16	-16.4	-72.7	34.	0.62	59	16	25	i
1979 02 28	60.6	-14..6	19.	1.90	271	13	96	i
1979 03 14	17.8	-101.3	27.	1.72	306	15	110	i
1979 05 01	-21.2	169.8	73.	1.45	18	41	190	i
1979 09 12	-1.7	136.0	16.	2.40	100	71	5	i
1979 10 12	-46.7	165.7	20.	1.00	19	15	136	i
1980 07 08	-12.4	166.4	44.	2.00	157	42	78	j
1980 07 17	-12.6	165.9	34.	4.85	351	31	102	j
1981 05 25	-48.8	164.4	33.	2.75	302	83	355	k
1981 07 06	-22.3	171.7	58.	2.60	345	30	181	k
1981 07 15	-17.3	167.6	30.	0.58	338	27	83	k
1981 07 28	30.0	57.8	15.	0.90	150	13	119	k
1981 09 01	-15.0	-173.1	20.	1.95	115	37	287	k
1981 10 25	18.0	-102.1	32.	0.70	287	20	82	k
1982 06 07 A	16.6	-98.2	11.	0.29	268	10	48	l
1982 06 07 B	16.6	-98.3	19.	0.27	286	12	76	l
1982 06 19	13.3	-89.3	52.	1.05	102	25	254	l
1982 07 07	-51.2	160.5	10.	0.68	65	62	182	l
1982 08 05	-12.7	165.9	24.	0.32	337	32	83	l
1982 12 19	-24.1	-175.9	30.	1.98	198	15	90	l
1983 01 17	38.1	20.2	10.	0.23	34	14	153	m
1983 01 24	12.9	93.6	73.	0.17	291	50	39	m
1983 03 18	-4.9	153.6	70.	4.63	170	49	120	m
1983 04 03	8.7	-83.1	28.	1.82	310	25	110	n
1983 04 04	5.7	94.8	72.	0.34	207	51	51	n
1983 05 26	40.4	139.1	13.	4.60	16	27	86	n
1983 10 04	-26.6	-70.8	39.	3.40	9	20	110	o
1983 10 22	-60.6	-25.4	10.	0.46	231	35	278	o
1983 11 30	-6.9	72.1	10.	4.10	293	35	308	o
1984 01 08	-2.8	118.8	15.	0.12	13	16	85	p
1984 02 07	-9.9	160.5	22.	2.50	296	37	30	p
1984 03 24	44.2	148.3	31.	0.64	229	17	109	p
1984 05 17	-36.5	53.5	10.	0.25	1	64	177	q
1984 08 06	32.4	131.8	29.	0.29	337	7	224	r
1984 09 19	34.0	141.4	35.	0.21	264	26	220	r
1984 11 01	8.1	-38.8	10.	0.40	274	73	183	s
1984 11 17	0.2	98.0	25.	0.58	334	10	116	s
1984 11 23	-14.3	171.3	27.	0.19	300	66	353	s
1984 12 30	-36.7	177.5	19.	0.18	86	56	348	s
1985 01 21	-1.0	128.5	21.	0.14	203	76	188	t
1985 03 02	-2.0	119.7	44.	0.11	283	84	357	t
1985 03 03	-33.2	-72.0	41.	10.30	11	26	110	t
1985 04 09	-34.2	-71.5	47.	0.50	0	21	99	u
1985 04 13	1.7	126.6	40.	0.28	12	34	69	u
1985 05 10	-5.6	151.1	25.	0.69	193	67	194	u
1985 07 03	-4.5	152.8	31.	0.83	169	37	106	v
1985 08 23	39.4	75.3	15.	0.33	315	29	159	v
1985 09 19	18.2	-102.6	21.	11.00	301	18	105	v
1985 09 21	17.8	-101.7	21.	2.50	296	17	85	v
1985 09 26	-34.6	-178.7	61.	0.24	196	54	39	v
1985 11 17	-1.6	135.0	13.	0.49	179	64	174	w

TABLE 5. (continued)

Date	Epicenter °N	Epicenter °E	Depth, km	Published Moment, 10^{27} dyn-cm	Focal Mechanism ϕ, deg	Focal Mechanism δ, deg	Focal Mechanism λ, deg	Reference
1985 11 28 A	-14.0	166.2	24.	0.30	161	36	251	w
1985 11 28 B	-14.0	166.2	44.	0.36	262	68	13	w
1985 12 21	-14.0	166.5	46.	0.57	165	44	85	w
1985 12 23	62.2	-124.3	15.	0.15	354	45	98	w
1986 03 24	-2.5	138.7	15.	0.11	94	39	356	x
1986 04 20	-2.4	139.3	21.	0.16	88	29	20	y
1986 04 30	18.4	-102.9	21.	0.31	290	18	87	y
1986 05 07	51.4	-174.8	23.	10.40	246	22	85	y
1986 07 09	2.0	126.6	35.	0.16	9	39	71	z
1986 08 14	1.8	126.6	20.	2.30	224	81	104	z
1986 10 20	-28.1	-176.4	50.	9.00	270	56	158	aa,ab,ac
1987 02 08	-5.9	147.8	15.	1.11	82	83	4	ad
1987 03 05	-24.5	-70.2	42.	2.48	12	23	106	ad
1987 03 06	0.15	-77.8	15.	0.64	113	24	183	ad
1987 06 27	-2.2	138.2	27.	0.08	118	53	5	ae
1987 07 06	-14.1	167.8	15.	0.10	159	42	84	af
1987 08 08	-19.0	-70.0	79.	0.79	176	20	273	af
1987 09 03	-58.90	158.30	15.	1.40	155	69	188	af
1987 09 28 A	-18.45	168.11	23.	0.19	346	25	98	af
1987 09 28 B	-18.36	168.14	22.	0.08	349	26	105	af

References: a, *Abe* [1972]; b, *Shimazaki* [1974]; c, *Dewey and Spence* [1979]; d, *Kanamori* [1977]; e, *Lay and Kanamori* [1980]; f, *Stewart and Cohn*[1979]; g, *Dziewonski et al.* [1987a]; h, *Dziewonski et al.* [1987b]; i, *Dziewonski et al.* [1987c]; j, *Dziewonski et al.* [1988a]; k, *Dziewonski et al.* [1988b]; l, *Dziewonski et al.* [1983a]; m, *Dziewonski et al.* [1983b]; n, *Dziewonski et al.* [1983c]; o, *Dziewonski et al.* [1984a]; p, *Dziewonski et al.* [1984b]; q, *Dziewonski et al.* [1985a]; r, *Dziewonski et al.* [1985b]; s, *Dziewonski et al.* [1985c]; t, *Dziewonski et al.* [1985d]; u, *Dziewonski et al.* [1986a]; v, *Dziewonski et al.* [1986b]; w, *Dziewonski et al.* [1986c]; x, *Dziewonski et al.* [1987d]; y, *Dziewonski et al.* [1987e]; z, *Dziewonski et al.* [1987f]; aa, *Dziewonski et al.* [1987g]; ab, *Lundgren and Okal* [1988]; ac, B. Romanowicz and T. Monfret (personal communication, 1987); ad, *Dziewonski et al.* [1988c]; ae, *Dziewonski et al.* [1988d]; af, *Dziewonski et al.* [1988e].

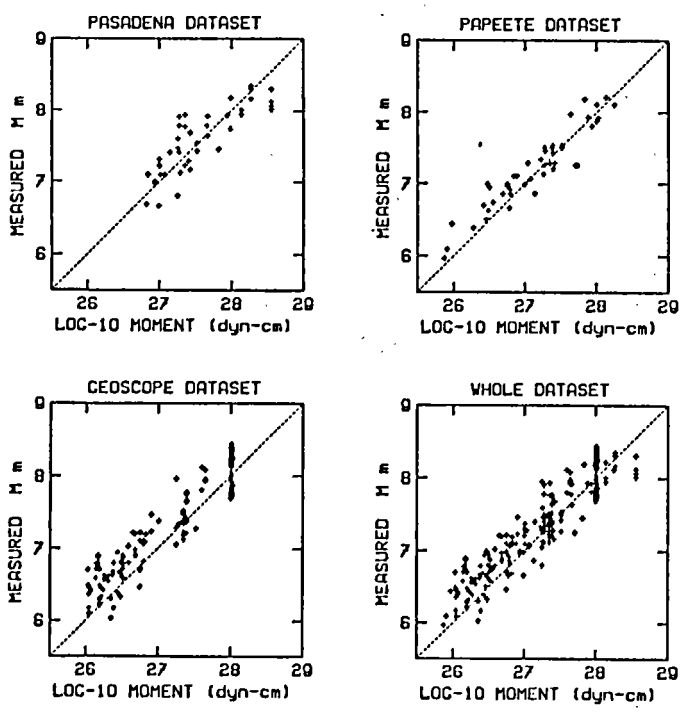

Fig. 8. Full populations of M_m values plotted as a function of published moment M_0, either as individual data sets (top; lower left), or as a whole data set (lower right). In all cases, the dashed line is the expected relation $M_m = \log_{10} M_0 - 20$.

tion of the R_5 values from the data sets described in the previous sections. On the basis of these various experiments, we conclude that the corrections C_D are adequate.

In another test we isolated the 10 records with the shortest epicentral distances. The latter vary between 8.11° and 32.77°, with seismic moments ranging from 1.6×10^{26} to 1.4×10^{28} dyn-cm. As Table 6 and Figure 11 show, there is no anomalous trend for these measurements taken at short distances. This means that the accuracy of the M_m scale is still appropriate at distances as short as 8° (Vanuatu event of December 21, 1985 recorded at Noumća). This result is crucial for tsunami warning. At such short distances, less than an hour separates the passage of the surface wave from the arrival of the tsunami, and there may not be time to wait for surface wave reports from other Pacific stations.

Periods. Figure 12 similarly shows the residuals r as a function of the period T at which the measurement is taken. Since the previous test has suggested that the period-dependent C_D is not systematically biased, any significant trend would indicate that our corrections C_S are inadequate or that we suffer from source finiteness effects. Again, it is clear from Figure 12 that no such trend exists; a regression of r against $\log_{10} T$ produced a slope of -0.021 (or less than 0.01 magnitude unit per octave) for the whole data set, and the maximum value was -0.149 at PAS. Our conclusion is, again, that no significant bias is evidenced by this analysis.

TABLE 6. Averages and Standard Deviations of the Residuals r.

Data Set	Station Code	Number of Records	$\bar{r}$	σ	$\bar{r}_c$	σ_c
Whole data set		256	0.14	0.25	0.09	0.19
Pasadena	PAS	42	0.02	0.28	0.05	0.23
Papeete	PPT	45	0.09	0.19	-0.05	0.16
GEOSCOPE		169	0.18	0.24	0.13	0.17
Special Sub-Data Sets						
PPT subset [*Talandier et al.*, 1987]	PPT	20	0.02	0.18	-0.10	0.13
10 shortest distances		10	0.07	0.15	0.08	0.17
Individual GEOSCOPE *Stations*						
Pointe des Cafres, Réunion†	PCR,RER	31	0.18	0.24	0.14	0.14
Saint-Sauveur de Badole, France	SSB	25	0.31	0.21	0.14	0.21
Tamanrasset, Algeria	TAM	19	0.33	0.15	0.12	0.11
Westford, Massachusetts	WFM	18	0.10	0.31	0.12	0.24
Port-aux-Français, Kerguelen Islands	PAF	16	0.11	0.26	0.22	0.21
Cayenne, French Guyana	CAY	12	0.00	0.29	0.17	0.20
Arga, Djibouti	AGD	11	0.29	0.11	0.14	0.10
Nouméa, New Caledonia	NOC	11	0.17	0.15	0.06	0.08
Dumont d'Urville, Antarctica	DRV	9	0.11	0.14	0.06	0.14
Kipapa, Hawaii	KIP	9	0.18	0.18	0.07	0.10
Crozet Island††	CRZ	4	-0.14	0.07	0.14	0.12
Santa Cruz, California††	SCZ	2	-0.04	0.13	0.13	0.12
Papeete, Tahiti††	PPT	2	0.16	0.02	0.10	0.02
Time Domain Measurements						
Papeete	PPT	45	-0.07	0.22	-0.16	0.17

†We treat as a single dataset records from the Réunion Island station before and after it was moved (about 18 km) to Rivière de l'Est (RER) in 1986.

††Due to the small number of events, the values obtained at these stations may not be statistically significant.

We found little systematic correlation between the period yielding the largest M_m and M_m itself. In general, the biggest earthquakes in our data set have M_m measured at periods over 100 s. A notable exception is the Kermadec earthquake (October 20, 1986). Significantly, this is an event for which available estimates of M_0 vary widely. The Harvard CMT solution for this event ($M_0 = 4.52 \times 10^{27}$ dyn-cm) is significantly less than

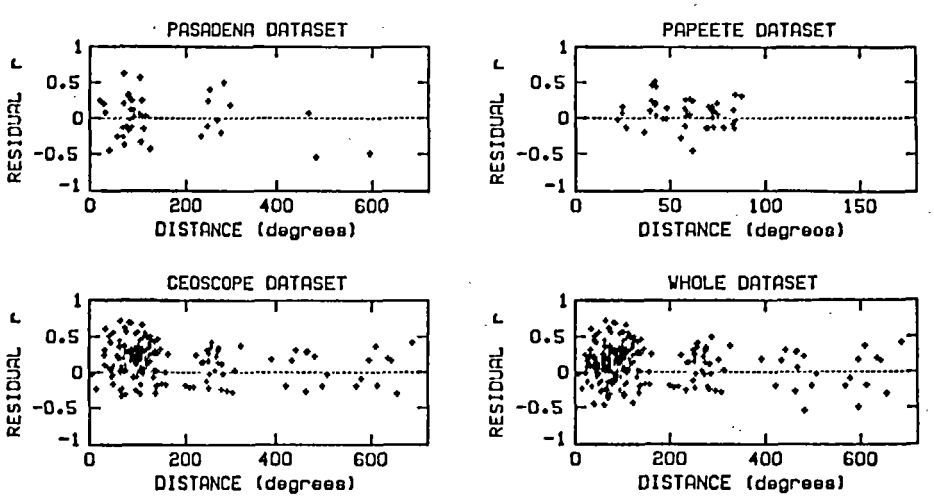

Fig. 9. Residual population $r = M_m - \log_{10} M_0 + 20$ plotted as a function of distance Δ. The horizontal scale is different at PPT, where we have no multiple passages. Any systematic trend on these diagrams would invalidate the correction C_D and probably the Q models.

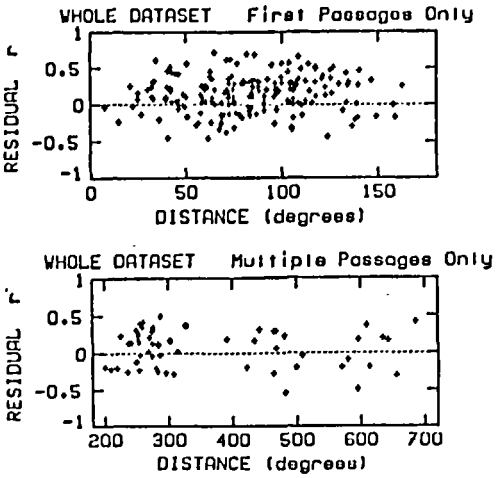

Fig. 10*a*. Comparison of residual populations plotted as a function of distance for first and multiple passages, respectively. Any systematic difference between trends on these diagrams would indicate an inappropriate C_D.

reported by other investigators: *Lundgren and Okal* [1989] have proposed $(8.5–10) \times 10^{27}$ on the basis of body wave deconvolution and B. Romanowicz and T. Monfret (personal communication, 1987) have obtained 9×10^{27} from the GEOSCOPE data set. We obtain values of M_m of 7.83 at PPT and 7.94 at PAS, in much better agreement with the higher values. It is noteworthy that the PPT measurement is obtained at a period of only 63 s, a clear anomaly for an earthquake this size. Similarly, while M_m at PAS is obtained at a longer period (227 s), the value measured at 51 s is very large (7.85). *Lundgren and Okal* [1988] have shown that this event is characterized by a body wave source spectrum anomalously rich in high frequencies. This earthquake is an example of how the use of M_m can retrieve valuable information on the source characteristics of the earthquake in the form of the period T at which the final measurement is made.

Influence of focal mechanism and depth. The most far-reaching approximation that we made in deriving the expression of M_m is the replacement of the true excitation E by its average taken over many focal geometries and depths. In this section we investigate systematically the influence of the source characteristics on our measurements. In keeping with the concept of magnitude, we do not envision incorporating a correction for focal geometry into the computation of M_m; the purpose of this section is simply to assess whether the residuals r are due significantly to the effects of radiation pattern and depth.

Focal mechanism and depth information is listed in Table 5 for all earthquakes used in this study. For each record we use (8) to compute the true excitation E in the exact focal and receiver geometry. We then define the "focal mechanism contribution" as

$$C_{FM} = -\log_{10} E - C_S \tag{14}$$

and a corrected value of M_m as

$$M_c = M_m + C_{FM} \tag{15}$$

M_c is the value of M_m which we would have computed at the same period had we known the focal mechanism exactly, instead of using the average excitation (10). Values of M_c and of the residual $r_c = M_c - \log_{10} M_0 + 20$, are listed as the last two columns of Tables 2–4. We then conducted some statistical analyses on r_c similar to those in section 4. Results are shown in the last two columns of Table 6.

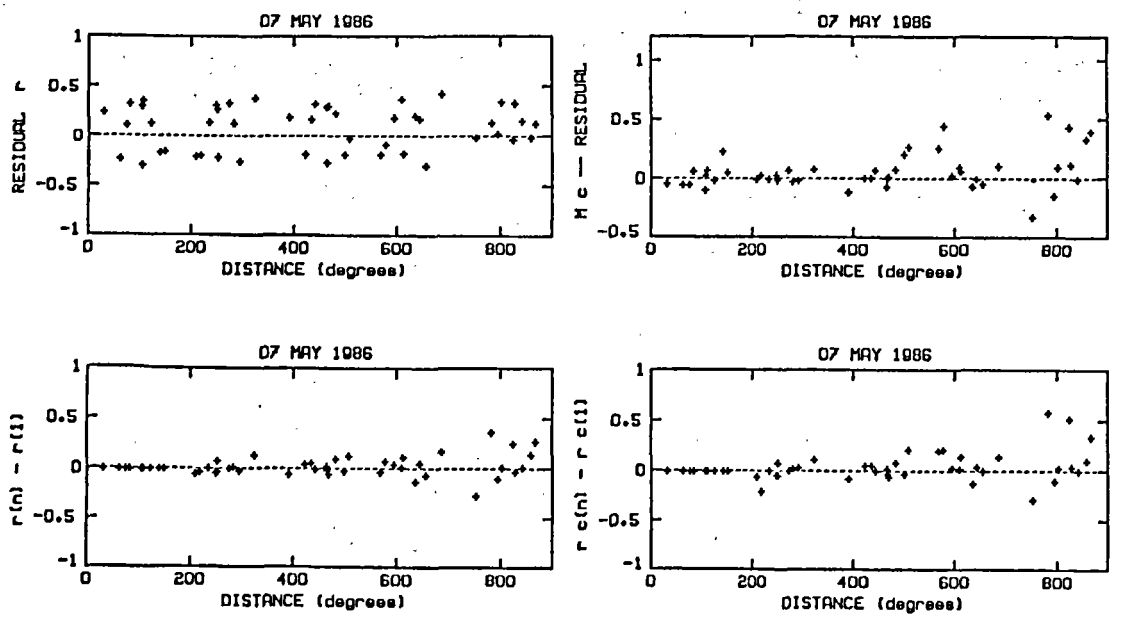

Fig. 10*b*. Residual population for 48 GEOSCOPE records of the 1986 Aleutian event, up to and including R_5. (Top Left) Same as Figure 9. (Bottom Left) The residual $r(n)$ for each passage R_n has been subtracted from the fundamental $r(1)$ at the same station. (Right) Same as left, for the corrected values r_c (see text and Figure 13 for details).

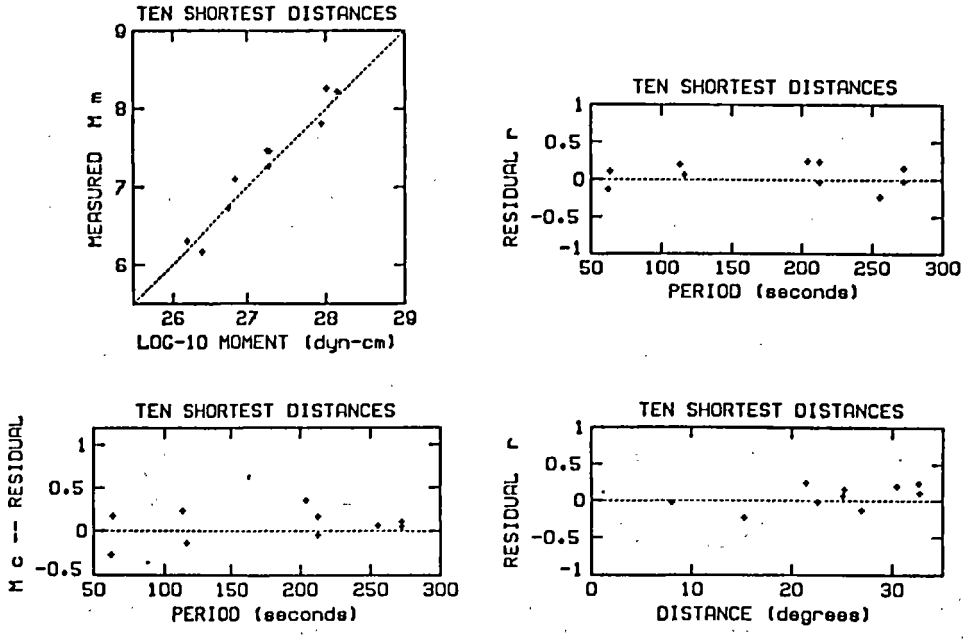

Fig. 11. Same as Figures 8, 9, 12, and 13 for the 10 shortest paths. Note the absence of any systematic trend which could invalidate the use of M_m at regional distances.

The average absolute value of C_{FM} is 0.21 or 0.22 for all four data sets. Not surprisingly, the mean residuals $\bar{r}_c$ and standard deviations σ_c computed for the M_c data sets are generally improved with respect to their M_m counterparts. The only exception is $\bar{r}_c$ at PAS, but the difference (0.03 units of magnitude) is not significant. The variance reduction introduced by the use of C_{FM} is rather limited, on the order of only 30–40%. In some individual cases the inclusion of C_{FM} results in a significant deterioration of the estimate of M_0. Examples are the Samoa event (April 2, 1977) at PAS and the Mexican earthquake (September 19, 1985) at Cayenne. These are cases when the station is located close to a node of excitation of the published mechanism, and yet significant energy is found in the seismogram. There may be two reasons for this situation: either inaccuracy in the published focal mechanism (and/or depth) or multipathing due to lateral heterogeneity, resulting in a distorted value of the take-off azimuth ϕ_s in (8). The latter is suggested by the observation that the large r_c residuals occur preferentially at shorter periods, as shown on Figure 13. In such geometries it actually makes sense to use the concept of magnitude which is found to be more robust than a measurement taking into account a supposedly exact value of

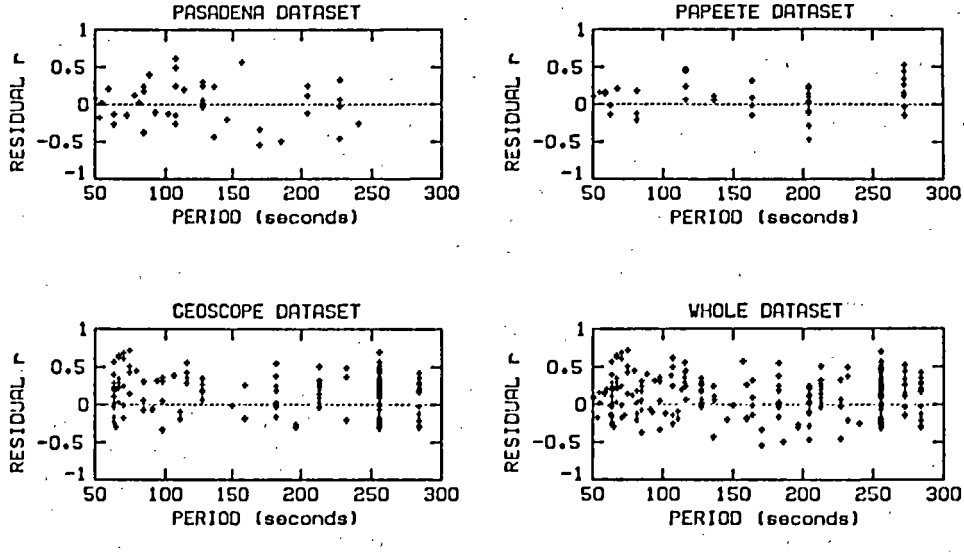

Fig. 12. Residual population $r = M_m - \log_{10} M_0 + 20$ plotted as a function of the period T at which the measurement is taken. Any systematic trend on these diagrams would invalidate C_s or the assumption that we stay on the flat portion of the spectrum.

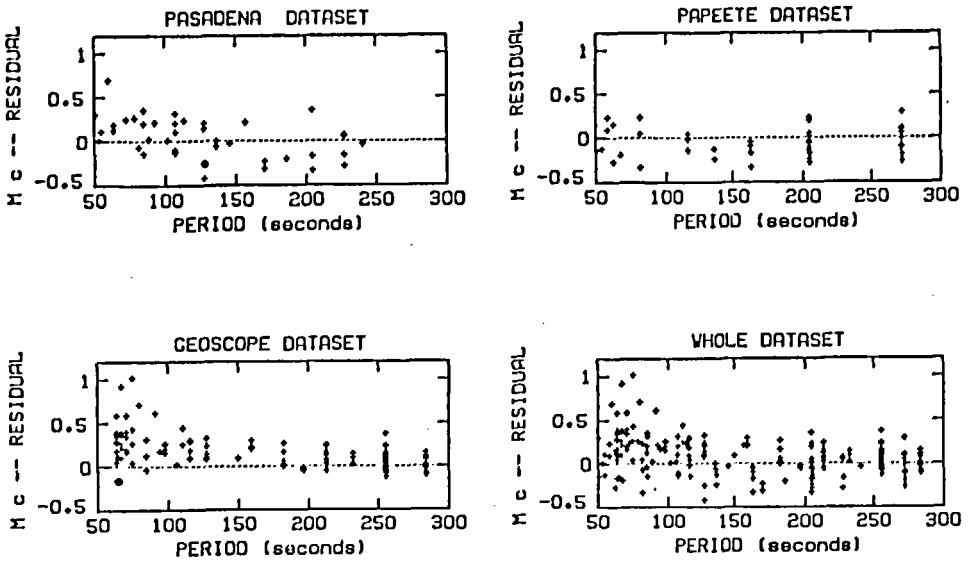

Fig. 13. Same as Figure 12 for the corrected residuals $r_c = r + C_{FM}$. Note that the largest residuals occur at the short-period end of the spectrum, suggesting that multipathing may be responsible.

the excitation, which can be strongly affected by phenomena such as multipathing or incorrect values of the source parameters.

Finally, Table 3 shows that the somewhat deficient values of M_m for the largest earthquake in the data set (the 1977 Indonesian event) are an artifact of the use of a single station (PAS) at an unfavorable azimuth, rather than the expression of saturation.

Station corrections? We also investigated any possible systematic trends in r at individual stations. We are motivated in this respect by the common practice of using "station corrections" for magnitude scales measured at higher frequencies, although we would expect them to disappear at longer periods. Table 6 shows the values of $\bar{r}$ and σ at individual stations. Most values of $\bar{r}$ fall within the 0.1—0.2 range, with the exception of the GEOSCOPE stations AGD (Djibouti), TAM (Tamanrasset, Algeria), and SSB (Saint-Sauveur, France), which have values of $\bar{r}$ in the 0.29–0.33 range. The general proximity of these three stations could suggest some kind of lateral heterogeneity effect. However, this pattern disappears when the M_c values are used, indicating that the higher residuals at these three stations are an artifact of preferential focal geometry. We do not have a simple explanation for the fact that the GEOSCOPE data set has $\bar{r}_c$ slightly larger than PAS (by 0.08 units) and PPT (by 0.13 units). Also, the results are probably not significant at SCZ (Santa Cruz, California) and PPT (GEOSCOPE station, Papeete) for each of which we have only two records and at CRZ (Crozet Island), for which all four records pertain to the Aleutian event of May 7, 1986.

We currently do not have a satisfactory explanation of the global residual $\bar{r} = 0.14$. We have shown in the previous sections that r has no systematic correlation with distance, period, or station. In general, by using an average excitation instead of the exact focal mechanism, we introduce a slight bias amounting to 0.05 units of magnitude. The remaining $\bar{r}_c = 0.09$ must be considered an unexplained bias inherent in the methodology. The small amplitude of this number constitutes in itself one of the successes of the theory. Only the future application of this method to much larger data sets could conceivably help answer this question.

Path. Finally, we want to discuss the possible influence on the computed value of M_m of the tectonic nature of the particular path involved. The calculation of C_D in (6) uses regionalized values of the group velocity U and attenuation factor Q^{-1}: this practice is motivated by the difficulty of defining a single value of these parameters (especially attenuation) at each frequency. However, the question then arises of the stability of M_m measurements with respect to a change in tectonic model or, in practical terms, how erroneous will be our estimate of the seismic moment M_0 if we happen to use the wrong tectonic model for U and Q.

We examined this question in several ways. First, we considered pure paths, assumed to sample only provinces of homogeneous tectonic character. For periods ranging from 50 to 300 s and for distances varying between 5 and 115°, we computed all seven values of C_D and retained their range of variation. This quantity, directly expressed in units of magnitude, is contoured on Figure 14. As expected, the range of variation of C_D is important only for short periods and large distances. It remains below 0.1 unit of magnitude over most of the distance-period field. In addition, these calculations are clearly made under a worst case scenario: for example, the maximum range of variation of nearly 1.0 unit of magnitude would correspond to the case of a 50-s wave traveling 115° in a pure shield structure and mistakenly interpreted as traveling the same distance over a "trench and back arc" region. Either path is geographically impossible at the surface of the Earth; in the real world the lateral heterogeneity of the planet acts to reduce considerably the range of variations of C_D over realistic paths.

In turn, this observation led us to assess the validity of

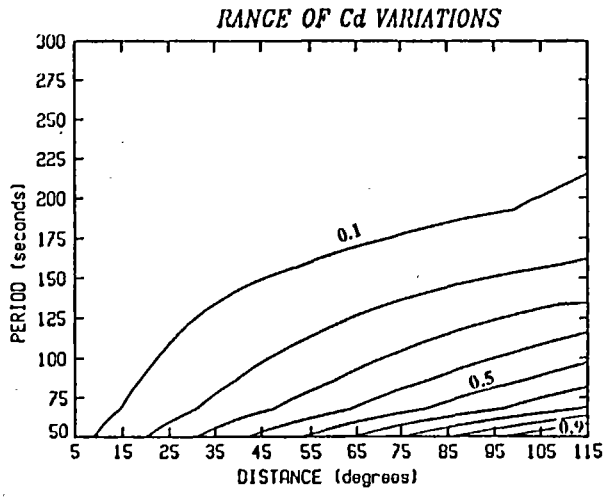

Fig. 14. Range of variation of C_D with tectonic province, as a function of distance and period. Contoured (in units of magnitude) is the difference between the maximum and minimum values of C_D obtained by applying (6) to seven pure paths sampling exclusively the seven tectonic regions described in Table 1.

using an average model of U and Q in the computation of C_D. Specifically, at each period we define

$$U_{aver} = \frac{1}{7} \sum_{k=1}^{7} U_k \tag{16}$$

and

$$Q_{aver}^{-1} = \frac{1}{7} \sum_{k=1}^{7} Q_k^{-1} \tag{17}$$

where the index k is related to tectonic region (note that as a further simplifying assumption, these averages are not weighted in proportion to the true extent of each region at the surface of the Earth). We then used the PPT data set to compare the resulting corrections C_D^{aver} to the actual corrections obtained through regionalization and used in the compilation of Table 2. The average error thus introduced was found to be less than 0.01 unit of magnitude, and its root mean square is 0.03 units of magnitude. The largest value, obtained for the 1986 Kermadec earthquake, is 0.06 units. A similar experiment on first passages R_1 at PAS yields an average of 0.01 unit of magnitude, a root mean square error of 0.03 units, and a maximum value of 0.06 unit for the 1977 Samoa event. In view of the general precision of our method, we believe that these errors are negligible.

The argument could then be made that regionalization may be superfluous and that the use of C_D^{aver} is satisfactory. For spectral measurements taken in the frequency domain, and thus requiring computer processing, regionalization is straightforward and can be achieved at very little programming cost. As we discuss below, our method can be extended to the time domain and applied in the absence of computer support. Our results show that in this latter case, the use of an average tectonic model should not lead to significant errors. With such an application in mind, and for reference, we compile in Table 7 values of C_D^{aver} at a number of representative distances and periods. We also include the distance-independent source correction C_S; their combination allows immediate use of (11) or (19) (for the latter, see the time-domain discussion below).

6. Extension to Time-Domain Measurements

All of the previous theory and measurements were taken in the frequency domain. However, the notion of magnitude was developed primarily in the time domain, and it may be interesting to extend the concept of M_m to time domain measurements.

It is tempting, on a seismogram such as shown on Figure 1, to measure the amplitudes of the prominent oscillations of the Rayleigh wavetrain in its inversely dispersed period range (typically between 50 and 250 s) and to use them to characterize the earthquake's size. In this section we present a simple, phenomenological, justification of this concept. A more rigorous investigation of the relationship of time domain magnitudes and seismic moment, based on phase-stationary asymptotics to the Fourier integral, is given in a companion paper [*Okal*, this issue].

At short distances the inversely dispersed portion of the Rayleigh wave often can be modeled as a single full oscillation of a sinusoid of period T_0 (see Figure 15). The Fourier amplitude of such a signal at the corresponding angular frequency $\omega_0 = 2\pi/T_0$ is related to the zero-to-peak amplitude a_0 of the apparent sinusoid through

$$X(\omega_0) = \frac{1}{2} a_0 T_0 \tag{18}$$

Away from ω_0, the spectral amplitude falls off as the function sinc [½ $(\omega - \omega_0)$ T_0].

As the distance becomes larger, the waveform becomes more dispersed, and several oscillations with clearly increasing periods are identifiable (Figure 1). We make the simplifying assumption that each oscillation is sufficiently different in frequency from the previous one, so that when computing the spectral amplitude at its

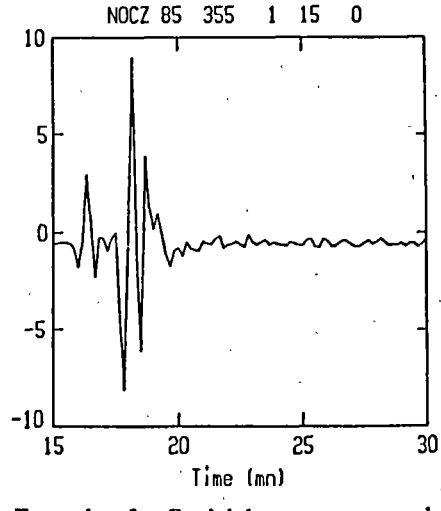

Fig. 15. Example of a Rayleigh wave at very short distances (Vanuatu event of December 21, 1985 at Nouméa), clearly showing one prominent oscillation at a period $T \sim 45$ s.

TABLE 7. Source Correction C_S According to (10), and Distance Correction C_D^{aver} for an Average Earth Model, as a Function of Period and Distance

Distance, deg	Corrections (Magnitude Units) at Various Periods T										
	T = 50 s	T = 75 s	T = 100 s	T = 125 s	T = 150 s	T = 175 s	T = 200 s	T = 225 s	T = 250 s	T = 275 s	T = 300 s
	Correction C_S (Independent of Distance)										
	3.674	3.746	3.781	3.805	3.826	3.847	3.870	3.895	3.922	3.951	3.982
	Correction C_D^{aver}										
5	-0.498	-0.506	-0.511	-0.515	-0.518	-0.520	-0.521	-0.522	-0.523	-0.524	-0.525
10	-0.317	-0.332	-0.343	-0.350	-0.355	-0.360	-0.363	-0.365	-0.367	-0.369	-0.370
15	-0.198	-0.221	-0.237	-0.249	-0.256	-0.263	-0.268	-0.271	-0.274	-0.277	-0.279
20	-0.106	-0.137	-0.158	-0.173	-0.184	-0.192	-0.199	-0.203	-0.207	-0.211	-0.213
25	-0.028	-0.067	-0.093	-0.112	-0.125	-0.136	-0.144	-0.150	-0.155	-0.159	-0.163
30	0.040	-0.006	-0.038	-0.061	-0.077	-0.090	-0.099	-0.106	-0.112	-0.117	-0.121
35	0.101	0.048	0.011	-0.016	-0.034	-0.050	-0.061	-0.069	-0.076	-0.082	-0.087
40	0.158	0.096	0.054	0.024	0.003	-0.015	-0.027	-0.037	-0.045	-0.051	-0.057
45	0.210	0.141	0.094	0.059	0.036	0.016	0.002	-0.009	-0.018	-0.025	-0.031
50	0.259	0.182	0.130	0.092	0.066	0.044	0.028	0.016	0.006	-0.002	-0.009
55	0.306	0.221	0.163	0.121	0.092	0.069	0.051	0.038	0.027	0.018	0.010
60	0.349	0.257	0.194	0.148	0.117	0.091	0.072	0.057	0.046	0.036	0.027
65	0.391	0.291	0.223	0.173	0.139	0.111	0.090	0.075	0.062	0.051	0.042
70	0.431	0.323	0.250	0.196	0.159	0.129	0.106	0.090	0.076	0.065	0.055
75	0.468	0.353	0.274	0.217	0.178	0.145	0.121	0.103	0.089	0.076	0.066
80	0.504	0.381	0.297	0.236	0.194	0.159	0.134	0.115	0.099	0.086	0.075
85	0.538	0.408	0.319	0.254	0.209	0.172	0.145	0.125	0.108	0.094	0.082
90	0.571	0.433	0.338	0.269	0.222	0.183	0.154	0.133	0.116	0.101	0.088
95	0.602	0.456	0.356	0.283	0.234	0.192	0.162	0.139	0.121	0.106	0.092
100	0.631	0.477	0.372	0.296	0.243	0.200	0.168	0.144	0.125	0.109	0.094
105	0.659	0.497	0.387	0.307	0.252	0.206	0.172	0.147	0.127	0.110	0.095
110	0.684	0.515	0.400	0.316	0.258	0.210	0.175	0.149	0.128	0.110	0.094
115	0.708	0.531	0.411	0.323	0.262	0.212	0.176	0.148	0.126	0.107	0.091

exact frequency, we can neglect the side lobes of the other sinc functions. *Okal and Talandier* [1987] tested this assumption on a very crude model of the Rayleigh waveform and found that it should not introduce an error of more than ±0.15 orders of magnitude. Under these conditions we can substitute (18) into (11) and obtain the time domain mantle magnitude

$$M_m^{TD} = \log_{10} [a\ T] + C_S + C_D - 1.20 \qquad (19)$$

where a is the zero-to-peak amplitude in microns, T the period in seconds of a prominent oscillation of the long-period inversely dispersed Rayleigh wave, and C_D and C_S are given by (6) and (10).

Comparison With Data

In order to test the concept of a time-domain mantle magnitude, we computed M_m^{TD} values from (19) for 42 records at Papeete. As in the case of spectral measurements, we take measurements at all prominent periods, and retain the largest value of M_m^{TD}. In order to stay in the well-dispersed part of the spectrum, and as suggested from *Okal* [this issue], we restrict ourselves to the period range 60–200 s. Results are given in Table 8 and Figure 16. The average residual $\bar{r}^{TD}$ for the entire data set of 42 events is -0.07, and the standard deviation $\sigma^{TD} = 0.22$. As in the case of spectral amplitudes, we computed the influence of the exact focal mechanism and depth of the event on the residual; again, we find a slight improvement of σ^{TD} but in this case a deterioration of the mean residual. These values are compiled as part of Table 6. The populations of residuals obtained in the time and frequency domains are comparable in mean values and standard deviations. However, direct comparison between individual values for the same event is not significant, since the two measurements can be taken at different periods.

Other Extensions of M_m: a Perspective

It would be simple in principle to extend the concept of M_m in at least two other directions.

An extension to Love waves could provide an additional safeguard against the problem of a nodal station, since it is well known that for "pure" mechanisms Rayleigh nodes are Love maxima, and vice-versa. M_m can then be defined as the greater of $M_m^{Rayleigh}$ and M_m^{Love}. The computation of the source correction C_S is straightforward. The distance correction requires the compilation of new models of Q and U. Because Love waves are not efficiently dispersed, prominent frequencies are difficult to identify in their wave shapes, and thus we do not expect that a time domain M_m^{Love} could be defined.

It is also possible to extend the M_m concept to deeper earthquakes. While the motivation of accurate tsunami warning no longer exists, it is still useful to develop a simple one-station mantle magnitude for such events. The

TABLE 8. Time Domain Measurements at Papeete

Event	Station	Passage	Δ	M_m^{pub}	M_m^{TD}	T	r^{TD}	M_c^{TD}	r_c^{TD}
1973 06 17	PPT	1	84.68	7.85	7.77	148	-0.08	7.51	-0.34
1974 10 03	PPT	1	69.18	8.26	7.99	149	-0.27	7.94	-0.32
1977 04 02	PPT	1	21.54	7.03	6.97	69	-0.06	6.92	-0.11
1977 06 22	PPT	1	25.24	8.15	8.01	88	-0.14	7.70	-0.45
1978 03 24	PPT	1	83.32	7.36	7.06	158	-0.30	7.03	-0.33
1978 06 12	PPT	1	84.80	7.53	7.03	171	-0.50	6.99	-0.54
1979 02 16	PPT	1	73.03	6.79	6.42	141	-0.37	6.69	-0.10
1979 02 28	PPT	1	78.34	7.27	7.01	140	-0.26	6.91	-0.36
1979 03 14	PPT	1	59.17	7.24	7.10	158	-0.14	7.07	-0.17
1979 10 12	PPT	1	46.82	7.00	6.73	99	-0.27	6.66	-0.34
1980 07 08	PPT	1	42.78	7.29	7.26	118	-0.03	7.22	-0.07
1980 07 17	PPT	1	43.19	7.90	7.85	165	-0.05	7.62	-0.28
1981 07 06	PPT	1	36.59	7.41	6.84	91	-0.57	7.11	-0.30
1981 07 15	PPT	1	40.79	6.76	6.88	125	0.12	6.66	-0.10
1981 10 25	PPT	1	58.68	6.85	6.84	131	-0.01	6.77	-0.08
1982 06 07 A	PPT	1	61.04	6.46	6.46	97	0.00	6.57	0.11
1982 06 07 B	PPT	1	60.84	6.43	6.33	139	-0.10	6.38	-0.05
1982 08 05	PPT	1	43.16	6.51	6.74	130	0.23	6.49	-0.02
1982 12 19	PPT	1	25.39	7.30	7.28	116	-0.02	7.24	-0.06
1983 05 26	PPT	1	87.84	7.66	7.82	161	0.16	7.40	-0.26
1983 10 04	PPT	1	72.74	7.53	7.37	155	-0.16	7.23	-0.30
1984 02 07	PPT	1	48.97	7.40	7.43	115	0.03	7.51	0.11
1984 03 24	PPT	1	83.67	6.80	6.65	120	-0.15	6.52	-0.28
1985 03 03	PPT	1	70.32	8.01	7.75	96	-0.26	7.62	-0.39
1985 04 09	PPT	1	70.53	6.70	6.72	120	0.02	6.60	-0.10
1985 09 19	PPT	1	58.40	8.04	7.76	151	-0.28	7.66	-0.38
1985 09 21	PPT	1	58.87	7.40	7.38	161	-0.02	7.25	-0.15
1985 11 28 A	PPT	1	42.58	6.48	6.92	132	0.44	6.59	0.11
1985 11 28 B	PPT	1	42.64	6.56	6.69	132	0.13	6.78	0.22
1985 12 21	PPT	1	42.33	6.76	6.82	122	0.06	6.77	0.01
1986 04 30	PPT	1	58.18	6.49	6.51	131	0.02	6.41	-0.08
1986 05 07	PPT	1	72.38	8.02	7.99	168	-0.03	7.71	-0.31
1986 10 20	PPT	1	27.08	7.95	7.65	63	-0.30	7.51	-0.44
1987 02 08	PPT	1	62.16	7.05	7.18	104	0.13	6.92	-0.13
1987 03 05	PPT	1	73.50	7.39	7.42	121	0.03	7.30	-0.09
1987 03 06	PPT	1	75.33	6.80	6.86	129	0.06	6.84	0.04
1987 06 27	PPT	1	72.44	5.92	5.72	61	-0.20	5.79	-0.13
1987 07 06	PPT	1	41.06	5.98	6.49	104	0.51	6.07	0.09
1987 08 08	PPT	1	74.88	6.90	7.05	111	0.15	6.78	-0.12
1987 09 03	PPT	1	55.90	7.15	6.69	91	-0.46	7.17	0.02
1987 09 28 A	PPT	1	40.17	6.28	6.33	113	0.05	6.10	-0.18
1987 09 28 B	PPT	1	40.15	5.88	5.94	116	0.06	5.70	-0.18

distance corrections for Rayleigh waves are of course unchanged. In order to define suitable source corrections, it is necessary to restrict the depth range to intervals where the excitation E does not vary too much. Preliminary work shows that this is possible at very long periods in the two depth intervals 80–200 km and 400–670 km, where the most intense intermediate and deep seismicity takes place.

7. CONCLUSIONS

We have shown that spectral amplitude measurements of mantle Rayleigh waves can be converted to a magnitude scale, M_m, which is directly related to the seismic moment M_0 of the earthquake. The philosophy of a magnitude measurement, which uses the records of a single station and ignores the focal geometry and the exact depth of the source, can be used successfully to obtain a real-time estimate of the seismic moment. A study of more than 250 records shows that average residuals at typical stations are on the order of 0.1–0.2 magnitude units, and standard deviations are on the order of 0.2. These numbers compare very favorably with the typical performance of classical magnitude scales, or even with the scatter in moment values published by individual investigators.

Furthermore, by letting the period at which the measurement is made vary and by keeping the largest resulting magnitude, we effectively guard against interference and saturation effects, which have plagued the standard magnitude scales, such as M_s, for 50 years. Only for a station sitting in an exact node of radiation in the case of a "pure" focal mechanism would our method be systematically inaccurate. Our experience shows that in such a geometry, multipathing effects can to some extent reduce the expected error; furthermore, the extension of the concept to Love waves should help guard against this problem.

In addition, we want to emphasize that (11) is, to our knowledge, the first magnitude scale in which all

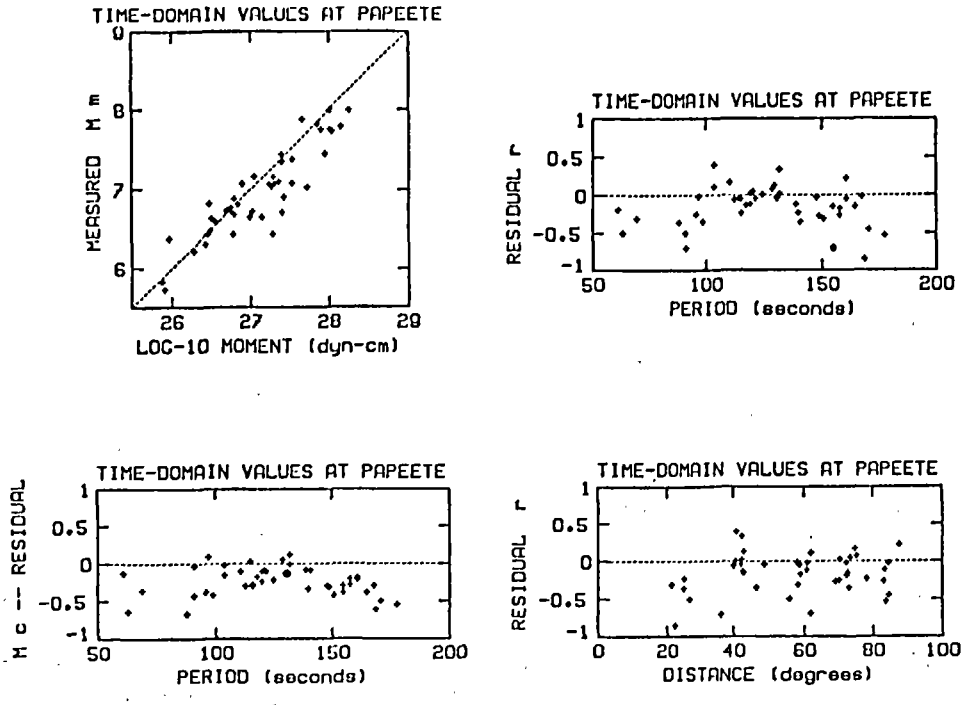

Fig. 16. Time-domain values of M_m^{TD} and population of residuals r^{TD} and r_c^{TD} plotted as a function of M_0, period, and distance for 42 earthquakes at Papeete.

coefficients and constants are fully justified on the basis of theoretical arguments. Therefore the present study is the first attempt to set the concept of magnitude on a firm theoretical basis.

By providing in real time, upon arrival of the Rayleigh wave train, an estimate of the seismic moment of the earthquake source, M_m has obviously a considerable potential for accurate tsunami warning. Since the method does not break down at very short distances, it is particularly valuable for the rapid evaluation of tsunami danger at regional distances, especially in sparsely populated areas where direct reports from the source region may not be available. Obvious examples are the Alaska-Aleutian arc and the whole Southwest Pacific region.

The calculations involved in the computations of M_m are extremely simple. They can easily be implemented on a personal computer and, as shown on Figure 17, lend themselves well to full automation [*Talandier et al.*, 1987; *Talandier and Okal*, 1989]. Even in the absence of such commonly available hardware the method has great potential: for any given seismic observatory, the regionalized distance corrections can be tabulated in advance for all epicentral areas bearing substantial tsunami risk. As an alternative, the average distance corrections C_D^{aver} listed in Table 7 can be used with negligible loss of accuracy. The time domain variant of the method can then be implemented with no more than a ruler, a pencil, and a hand-calculator.

Finally, we wish to conclude by illustrating the effectiveness of the method in tsunami warning: the seismic record shown on Figure 17 was used to evaluate tsunami potential immediately following the Aleutian earthquake of May 7, 1986. As a result of the estimate $M_m = 8.0$, no tsunami warning was issued for Polynesia. In contrast, a false alarm based largely on reported M_s values was issued for Oahu and along the Pacific Northwest coast of the U.S. mainland.

While the assessment of the relative dangers of failure to warn and false alarms is largely a philosophical and social task outside the responsibility of Earth scientists, it is clear that the scientific community has a duty to the public to provide swiftly the most accurate information possible on the parent earthquake and its tsunamigenic characteristics. We strongly believe that the use of the magnitude scale M_m is an important step in that direction.

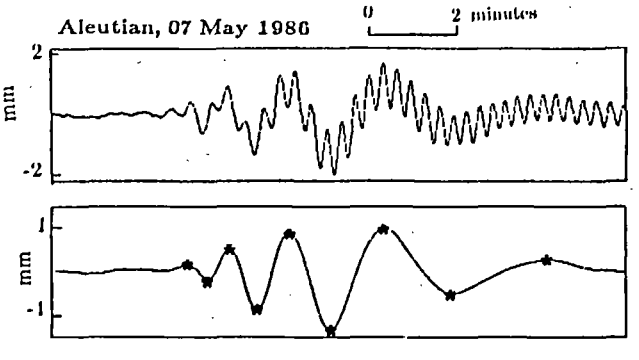

Fig. 17. Example of the use of M_m^{TD} in the automatic retrieval of the seismic moment of an earthquake. (Top) Broadband seismic record of the Aleutian earthquake (May 7, 1986) at Papeete. (Bottom) After filtering out the periods shorter than 40 s, the minima and maxima of the wave are automatically detected (asterisks), and the computation of the magnitude proceeds according to (19).

Acknowledgments. We are grateful to our Caltech colleagues for the use of the Pasadena archives. The PAS records were hand-digitized at Northwestern by Christina Lee. The maps on Figures 5–7 were produced using software developed by Paul Stoddard. We are grateful to Barbara Romanowicz for access to the GEOSCOPE data and for discussions of her results prior to publication. We thank John Woodhouse and Göran Ekström for updated tapes of the Harvard CMT data set. The paper benefited from careful reviews by Katsuyuki Abe and George Purcaru. Finally, we wish to pay tribute to the memory of Otto Nuttli, whose last discussion with one of us (E.A.O.) was about the potential of this new magnitude scale. This research has been supported by Commissariat à l'Energie Atomique (France), and the National Science Foundation, under grant EAR-87-20549.

REFERENCES

Abe, K., Mechanisms and tectonic implications of the 1966 and 1970 Peru earthquakes, *Phys. Earth Planet. Inter., 5,* 367-379, 1972.

Aki, K., Generation and propagation of *G* waves from the Niigata earthquake of June 16, 1964, part 2, Estimation of earthquake moment, released energy, and stress-strain drop from the *G* wave spectrum, *Bull. Earthquake Res. Inst. Univ. Tokyo, 44,* 73-88, 1966.

Aki, K., Scaling law of earthquake spectrum, *J. Geophys. Res., 72,* 1217-1231, 1967.

Aki, K., Scaling law of earthquake source-time function, *Geophys. J. R. Astr. Soc., 31,* 3-25, 1972.

Brune, J.N., and G.R. Engen, Excitation of mantle Love waves and definition of mantle wave magnitude, *Bull. Seismol. Soc. Am., 59,* 923-933, 1969.

Brune, J.N., and C.-Y. King, Excitation of mantle Rayleigh waves of period 100 s as a function of magnitude, *Bull. Seismol. Soc. Am., 57,* 1355-1365, 1967.

Canas, J., and B.J. Mitchell, Lateral variation of surface-wave anelastic attenuation across the Pacific, *Bull. Seismol. Soc. Am., 68,* 1637-1650, 1978.

Cifuentes, I.L., and P.G. Silver, Low-frequency characteristics of the great 1960 Chilean earthquake, *J. Geophys. Res., 94,* 643-663, 1989.

Dewey, J.W., and W. Spence, Seismic gaps and source zones of recent large earthquakes in coastal Peru, *Pure Appl. Geophys., 117,* 1148-1171, 1979.

Dziewonski, A.M., and D.L. Anderson, Preliminary reference Earth model, *Phys. Earth Planet. Inter., 25,* 297-356, 1981.

Dziewonski, A.M., A. Friedman, D. Giardini, and J.H. Woodhouse, Global seismicity of 1982: Centroid moment tensor solutions for 308 earthquakes, *Phys. Earth Planet. Inter., 33,* 76-90, 1983*a*.

Dziewonski, A.M., A. Friedman, and J.H. Woodhouse, Centroid moment-tensor solutions for January–March 1983, *Phys. Earth Planet. Inter., 33,* 71-75, 1983*b*.

Dziewonski, A.M., J.E. Franzen, and J.H. Woodhouse, Centroid moment-tensor solutions for April–June 1983, *Phys. Earth Planet. Inter., 33,* 243-249, 1983*c*.

Dziewonski, A.M., J.E. Franzen, and J.H. Woodhouse, Centroid moment-tensor solutions for October–December 1983, *Phys. Earth Planet. Inter., 34,* 129-136, 1984*a*.

Dziewonski, A.M., J.E. Franzen, and J.H. Woodhouse, Centroid moment-tensor solutions for January–March 1984, *Phys. Earth Planet. Inter., 34,* 209-219, 1984*b*.

Dziewonski, A.M., J.E. Franzen, and J.H. Woodhouse, Centroid moment-tensor solutions for April–June 1984, *Phys. Earth Planet. Inter., 37,* 87-96, 1985*a*.

Dziewonski, A.M., J.E. Franzen, and J.H. Woodhouse, Centroid moment-tensor solutions for July–September 1984, *Phys. Earth Planet. Inter., 38,* 203-213, 1985*b*.

Dziewonski, A.M., J.E. Franzen, and J.H. Woodhouse, Centroid moment-tensor solutions for October–December 1984, *Phys. Earth Planet. Inter., 39,* 147-156, 1985*c*.

Dziewonski, A.M., J.E. Franzen, and J.H. Woodhouse, Centroid moment-tensor solutions for January–March 1985, *Phys. Earth Planet. Inter., 40,* 249-258, 1985*d*.

Dziewonski, A.M., J.E. Franzen, and J.H. Woodhouse, Centroid moment-tensor solutions for April–June 1985, *Phys. Earth Planet. Inter., 41,* 215-224, 1986*a*.

Dziewonski, A.M., J.E. Franzen, and J.H. Woodhouse, Centroid moment-tensor solutions for July–September 1985, *Phys. Earth Planet. Inter., 42,* 205-214, 1986*b*.

Dziewonski, A.M., J.E. Franzen, and J.H. Woodhouse, Centroid moment-tensor solutions for October–December 1985, *Phys. Earth Planet. Inter., 43,* 185-195, 1986*c*.

Dziewonski, A.M., G. Ekström, J.E. Franzen, and J.H. Woodhouse, Global seismicity of 1977; Centroid moment tensor solutions for 471 earthquakes, *Phys. Earth Planet. Inter., 45,* 11-36, 1987*a*.

Dziewonski, A.M., G. Ekström, J.E. Franzen, and J.H. Woodhouse, Global seismicity of 1978; Centroid moment tensor solutions for 512 earthquakes, *Phys. Earth Planet. Inter., 46,* 316-342, 1987*b*.

Dziewonski, A.M., G. Ekström, J.E. Franzen, and J.H. Woodhouse, Global seismicity of 1979; Centroid moment tensor solutions for 524 earthquakes, *Phys. Earth Planet. Inter., 48,* 18-46, 1987*c*.

Dziewonski, A.M., J.E. Franzen, and J.H. Woodhouse, Centroid moment-tensor solutions for January–March 1986, *Phys. Earth Planet. Inter., 45,* 1-10, 1987*d*.

Dziewonski, A.M., G. Ekström, J.E. Franzen, and J.H. Woodhouse, Centroid moment-tensor solutions for April–June 1986, *Phys. Earth Planet. Inter., 45,* 229-239, 1987*e*.

Dziewonski, A.M., G. Ekström, J.E. Franzen, and J.H. Woodhouse, Centroid moment-tensor solutions for July–September 1986, *Phys. Earth Planet. Inter., 46,* 305-315, 1987*f*.

Dziewonski, A.M., G. Ekström, J.H. Woodhouse, and G. Zwart, Centroid moment-tensor solutions for October–December 1986, *Phys. Earth Planet. Inter., 48,* 5-17, 1987*g*.

Dziewonski, A.M., G. Ekström, J.E. Franzen, and J.H. Woodhouse, Global seismicity of 1980; Centroid moment tensor solutions for 515 earthquakes, *Phys. Earth Planet. Inter., 50,* 127-154, 1988*a*.

Dziewonski, A.M., G. Ekström, J.E. Franzen, and J.H. Woodhouse, Global seismicity of 1981; Centroid moment tensor solutions for 542 earthquakes, *Phys. Earth Planet. Inter., 50,* 155-182, 1988*b*.

Dziewonski, A.M., G. Ekström, J.H. Woodhouse, and G. Zwart, Centroid moment-tensor solutions for January–March 1987, *Phys. Earth Planet. Inter., 50,* 116-126, 1988*c*.

Dziewonski, A.M., G. Ekström, J.H. Woodhouse, and G. Zwart, Centroid moment-tensor solutions for April–June 1987, *Phys. Earth Planet. Inter., 50,* 215-225, 1988*d*.

Dziewonski, A.M., G. Ekström, J.H. Woodhouse, and G. Zwart, Centroid moment-tensor solutions for July–September 1987, *Phys. Earth Planet. Inter., 53,* 1-11, 1988*e*.

Ekström, G., and A.M. Dziewonski, Evidence of bias in estimations of earthquake size, *Nature, 332,* 319-323, 1988.

Geller, R.J., Scaling relations for earthquake source parameters and magnitudes, *Bull. Seismol. Soc. Am., 66,* 1501-1523, 1976.

Geller, R.J., Part I. Earthquake source models, magnitudes and scaling relations. Part II. Amplitudes of rotationally split normal modes for the 1960 Chilean and 1964 Alaskan earthquakes, Ph.D. dissertation, 211 pp., Calif. Inst. of Technol., Pasadena, 1977.

Gilman, R., Report on some experimental long-period systems, *Bull. Seismol. Soc. Am., 50,* 553-559, 1960.

Gutenberg, B., The energy of earthquakes, *Quat. J. Geol. Soc. London, 112,* 1-14, 1956.

Gutenberg, B., and C.F. Richter, On seismic waves (third paper), *Gerlands Beitr. Geophys., 47,* 73-131, 1936.

Hwang, H.-J., and B.J. Mitchell, Shear velocities, Q_β, and the frequency dependence of Q_β in stable and tectonically active regions from surface wave observations, *Geophys. J. R. Astr. Soc., 90,* 575-613, 1987.

Jordan, T.H., Global tectonic regionalization for seismological data analysis, *Bull. Seismol. Soc. Am., 71,* 1131-1141, 1981.

Kanamori, H., The Alaska earthquake of 1964: Radiation of long-period surface waves and source mechanism, *J. Geophys. Res., 75,* 5029-5040, 1970.

Kanamori, H., The energy release in great earthquakes, *J. Geophys. Res.*, *82*, 2981-2987, 1977.

Kanamori, H., and J.J. Cipar, Focal process of the great Chilean earthquake, May 22, 1960, *Phys. Earth Planet. Inter.*, *9*, 128-136, 1974.

Kanamori, H., and G.S. Stewart, Mode of strain release along the Gibbs Fracture Zone, Mid-Atlantic Ridge, *Phys. Earth Planet. Inter.*, *11*, 312-332, 1976.

Lay, T., and H. Kanamori, Earthquake doublets in the Solomon Islands, *Phys. Earth Planet. Inter.*, *21*, 283-304, 1980.

Lundgren, P.R., and E.A. Okal, Source processes of 'anomalous' subduction zone earthquakes in the Southwest Pacific (abstract), *Seismol. Res. Lett.*, *59*, 37, 1988.

Mitchell, B.J., and G.-K. Yu, Surface-wave dispersion, regionalized velocity models, and anisotropy of the Pacific crust and upper mantle, *Geophys. J. R. Astr. Soc.*, *63*, 497-514, 1980.

Monfret, T., and B.A. Romanowicz, Importance of on-scale observations of first-arriving wave trains for source studies: example of the Chilean event of March 3, 1985 observed on GEOSCOPE and IDA networks, *Geophys. Res. Lett.*, *13*, 1015-1018, 1986.

Nakanishi, I., Shear velocity and shear attenuation models inverted from the world-wide and pure-path average data of mantle Rayleigh waves ($_0S_{25}$ to $_0S_{80}$) and fundamental normal modes ($_0S_2$ to $_0S_{24}$), *Geophys. J. R. Astr. Soc.*, *66*, 83-130, 1981.

Okal, E.A., The effect of intrinsic oceanic upper-mantle heterogeneity on the regionalization of long-period Rayleigh wave phase velocities, *Geophys. J. R. Astr. Soc.*, *49*, 357-370, 1977.

Okal, E.A., Seismic parameters controlling far-field tsunami amplitudes: A review, *Nat. Hazards J.*, *1*, 67-96, 1988.

Okal, E.A., A theoretical discussion of time domain magnitudes: The Prague formula for M_s and the mantle magnitude M_m, *J. Geophys. Res.*, this issue, 1989.

Okal, E.A., and R.J. Geller, On the observability of isotropic seismic sources: The July 31, 1970 Colombian earthquake, *Phys. Earth Planet. Inter.*, *18*, 176-196, 1979.

Okal, E.A., and J. Talandier, M_m: Theory of a variable-period mantle magnitude, *Geophys. Res. Lett.*, *14*, 836-839, 1987.

Purcaru, G., and H. Berckhemer, A magnitude scale for very large earthquakes, *Tectonophysics*, *49*, 189-198, 1978.

Purcaru, G., and H. Berckhemer, Quantitative relations of seismic source parameters and a classification of earthquakes, *Tectonophysics*, *84*, 57-128, 1982.

Romanowicz, B., M. Cara, J.-F. Fels, and D. Rouland, GEOSCOPE: A French initiative in long-period three-component global seismic networks, *Eos, Trans. AGU*, *65*, 753-754, 1984.

Richter, C.F., An instrumental earthquake magnitude scale, *Bull. Seismol. Soc. Am.*, *25*, 1-32, 1935.

Shimazaki, K., Nemuro-Oki earthquake of June 17, 1973: A lithospheric rebound at the upper half of the interface, *Phys. Earth Planet. Inter.*, *9*, 314-327, 1974.

Stewart, G.S., and S.N. Cohn, The 1976 August 16, Mindanao, Philippine earthquake (M_s = 7.8) — Evidence for a subduction zone South of Mindanao, *Geophys. J. R. Astr. Soc.*, *57*, 51-65, 1979.

Talandier, J., and E.A. Okal, An algorithm for automated tsunami warning in French Polynesia, based on mantle magnitudes, *Bull. Seismol. Soc. Amer.*, *79*, in press, 1989.

Talandier, J., D. Reymond, and E.A. Okal, M_m: Use of a variable-period mantle magnitude for the rapid one-station estimation of teleseismic moments, *Geophys. Res. Lett.*, *14*, 840-843, 1987.

Vaněk, J., A. Zátopek, V. Kárník, N.V. Kondorskaya, Yu. V. Riznichenko, E.F. Savarenskii, S.L. Solov'ev, and N.V. Shebalin, Standardization of magnitude scales, *Izv. Akad. Nauk SSSR, Ser. Geofiz.*, *2*, 153-158, 1962.

Wieland, E., and G. Streckeisen, The leaf-spring seismometer: design and performance, *Bull. Seismol. Soc. Am.*, *72*, 2349-2367, 1982.

Williams, B.R., M_0 calculations from a generalized *AR* parameter method for WWSSN instruments, *Bull. Seismol. Soc. Am.*, *69*, 329-351, 1979.

Woodhouse, J.H., and A.M. Dziewonski, Mapping the upper mantle: Three-dimensional modeling of Earth structure by inversion of seismic waveforms, *J. Geophys. Res.*, *89*, 5953-5986, 1984.

E.A. Okal, Department of Geological Sciences, Northwestern University, Evanston, Illinois 60208.

J. Talandier, Laboratoire de Géophysique, Commissariat à l'Energie Atomique, Boîte Postale 640, Papeete, Tahiti, French Polynesia.

(Received June 1, 1988;
revised October 20, 1988;
accepted November 2, 1988.)

ON THE FEASIBILITY OF NEW TSUNAMI WARNING SYSTEM BY MEASURING THE LOW FREQUENCY T PHASE

SIN-ITI IWASAKI(HIRATSUKA BRANCH OF OCEANOGRAPHIC STUDIES, NATIONAL RESEARCH CENTER FOR DISASTER PREVENTION, 9-2 NIJIGAHAMA HIRATSUKA KANAGAWA 254 JAPAN)

1. Introduction.

It is widely known that , before a tsunami attacked a coast, big sounds like thunders were heard in coastal areas and/or vessels in the ocean felt sea shocks. Sea shocks are violent shocks with long durations felt by ocean vessels at the moment of submarine earthquakes. The cause of sea shocks is thought to be the T phase. Tsunami-producing earthquakes, large and shallow focus seismic events occurring at sea , can generate the T phase , that is, seismic waves generated by their conversion at an ocean bottom, propagate over large distance at the speed of the sound wave in the sea water along the SOFAR channel. Many studies have been done about the use of the T phase for tsunami warnings. For example, Tolstoy and Ewing(1950) pointed out a remarkable correlation between the occurrence of the T phase and the occurrence of tsunamis.

In this paper , considering the compressibility of the sea water, it is shown that another mechanism also can generate the low frequency T phase. It is also shown that the low frequency T phase carry the informations of the magnitude and the duration of the displacement of the ocean bottom and are useful for tsunami warnings , in particular, for near shore tsunami warnings.

2. Historical records.

Many instances can be cited from the historical records of sea shocks. For example, at the moment of the Ansei Tokai Earthquake(1854.12.23), Russian frigate Diana which was anchored at Shimoda harbor south east side of Izu peninsula was heavily damaged by the tsunami(see FIG.1 and FIG.2) . At that time, Admiral Putyatin and an officer of the frigate left the records of the sea shock and the tsunami. Followings are a part of their records.

"at 10 o'clock in the morning I felt a quake in the cabin. It was felt more heavily in the officers room. ••••• After a half an hour of this quake , as soon as the water surface near the town of Shimoda became rough , the flow of the river rose and raging waves and splashes were generated everywhere of the shoals."

" at 9:45 , the frigate felt the violent vibrations for one minutes. The sea surface was entirely calm so I thought nothing happened any more and the work on the board was carried on. At 10 o'clock big rolling waves rushed upon the frigate."

Two important points exist in these documents. First, the frigate felt the sea shock continued 1 minutes. Second, the tsunami attacked the frigate 15 or 30 minutes after the sea shock.

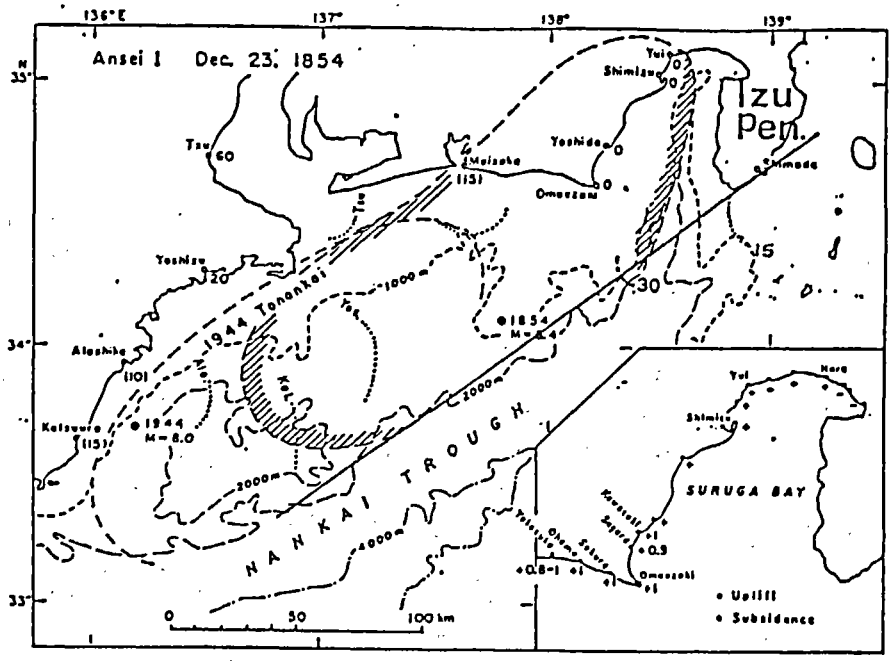

FIG. 1 THE ESTIMATED SOURCE AREA OF THE ANSEI TSUNAMI. (FROM HATORI, 1976) A SOLID LINE AND DASHED LINES WITH NUMBERS 15 AND 30 ARE APPENDED BY THE AUTHOR. DISPLACEMENTS ARE ASSUMED TO PROPAGATE ALONG THE SOLID LINE. DASHED LINES REPRESENT LIMITATIONS OF THE TSUNAMI PROPAGATION FROM SHIMODA IN 15 AND 30 MINUTES.

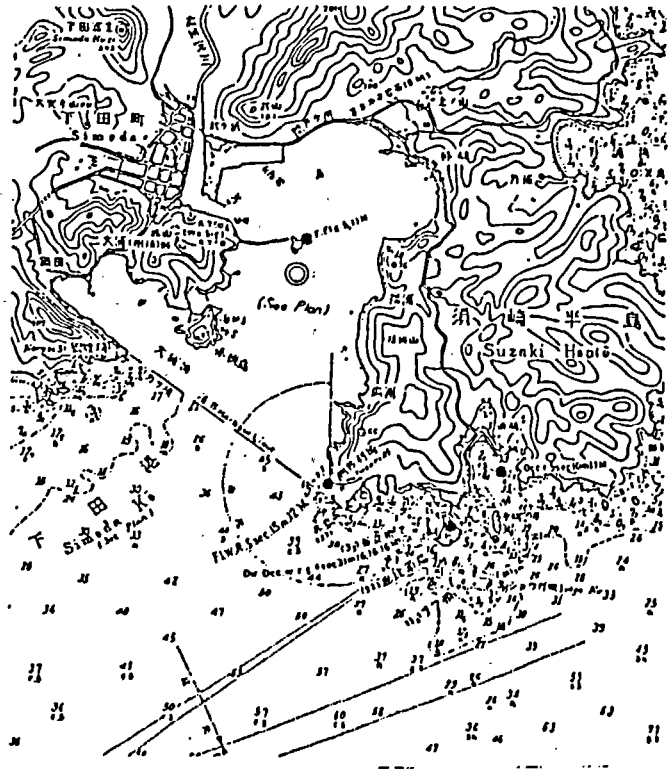

FIG. 2 THE PRESENT VIEW OF SHIMODA HARBOR. DOUBLE CIRCLE REPRESENTS THE POSITION WHERE THE FRIGATE DIANA WAS THOUGHT TO BE ANCHORED. (DEPTH IN METERS)

3. Wave generation due to the bottom deformation in the compressible water.

When a large area of the ocean bottom displaced upward with any velocities, the sea water above the displaced area are compressed and waves of condensation and rarefaction are generated and propagate toward the free surface. Sells(1965) investigated this type of wave generation theoretically using the 2-dimensional model with a rigid bottom moved upward a distance ζ_0 abruptly. FIG. 3 shows a system of Cartesian coordinates(x, z) adopted by Sells(1965) with the origin at the midpoint of the whole block on the ocean floor, the x axis in a horizontal direction, and the z axis vertically upward. The total width of the whole block is 2a, the ocean will be taken as having constant depth h.

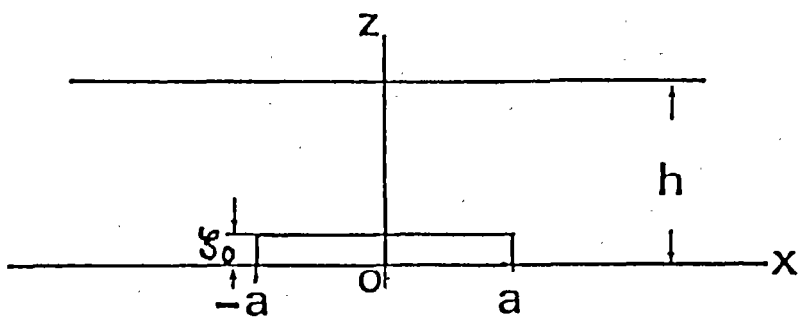

FIG. 3 THE CO-ORDINATE SYSTEM.

The basic equation for the displacement potential Φ , in a gravitating compressible fluid with constant sound velocity c throughout its depth, is given by

$$\frac{1}{c^2}\frac{\partial^2 \Phi}{\partial t^2} = \Delta \Phi - 2\gamma \frac{\partial \Phi}{\partial z} \qquad \text{----------(1)}$$

where $\gamma = g / 2c^2$

The boundary condition at the free surface is

$$g\frac{\partial \Phi}{\partial z} + \frac{\partial^2 \Phi}{\partial t^2} = 0 \quad \text{at } Z = h \qquad \text{----------(2)}$$

And, for the boundary condition at the bottom, Sells(1965) only considered the abrupt movement of the block, however, I also considered an upward movement of the block with a constant velocity v_0. The boundary condition for the abrupt upward movement of the block is given by

$$\frac{\partial \Phi}{\partial z} = \zeta_0 H(t) \quad |x| \leqq a$$

$$= 0 \quad \text{otherwise} \qquad \text{----------(3)}$$

$H(t)$: Heaviside's step function

For the movement of the block with a constant velocity v_0 for a time interval $0 < t < \tau$, the boundary condition is given by

$$\frac{\partial \Phi}{\partial z} = v_0 G(t, \tau) \quad |x| \leqq a$$

$$= 0 \quad \text{otherwise} \qquad \text{----------(4)}$$

where

$$G(t, \tau) = 0 \quad t \leqq 0$$

$$= t \quad 0 \leqq t \leqq \tau$$

$$= \tau \quad \tau \leqq t$$

According to Sells(1965), free surface displacement η_1 due to the pure acoustic effect for the abrupt movement of the block mathematically separates into two parts, disturbances from the edges and from the nearest block. η_1 can be written as

$$\eta_1 = \eta_{as} + \eta_{bs} \qquad \text{----------(5)}$$

$$\eta_{as} = \eta_s(a+x, t) + \eta_s(a-x, t) \quad |x| \leqq a$$

$$= \eta_s(x+a, t) - \eta_s(x-a, x) \quad |x| \geqq a$$

$$\text{----------(6)}$$

where

$$\eta_s(X, t) = -\frac{2\zeta_o}{\pi}\exp(\gamma h)\sum_{n=0}^{\infty}(-1)^n H\left(t-\frac{R_n}{c}\right) \cdot \tan^{-1}\left(\frac{h_n(c^2t^2 - R^2_n)^{1/2}}{Xct}\right)$$

$$R^2_n = h^2_n + X^2 \qquad \text{----------(7)}$$

$$h_n = (2n+1)h$$

and

$$\eta_{bs}(X, t) = 2\zeta_o \exp(\gamma h)\sum_{n=0}^{\infty}(-1)^n H\left(t-\frac{h_n}{c}\right) \quad |x| \leqq a$$

$$= 0 \qquad |x| \geqq a \qquad \text{----------(8)}$$

where 'n' represents the number of reflection at the bottom(see FIG. 4).

After a small algebra, free surface displacement η_2 due to the pure acoustic effect for the upward movement of the block with a constant velocity v_o also can be written as

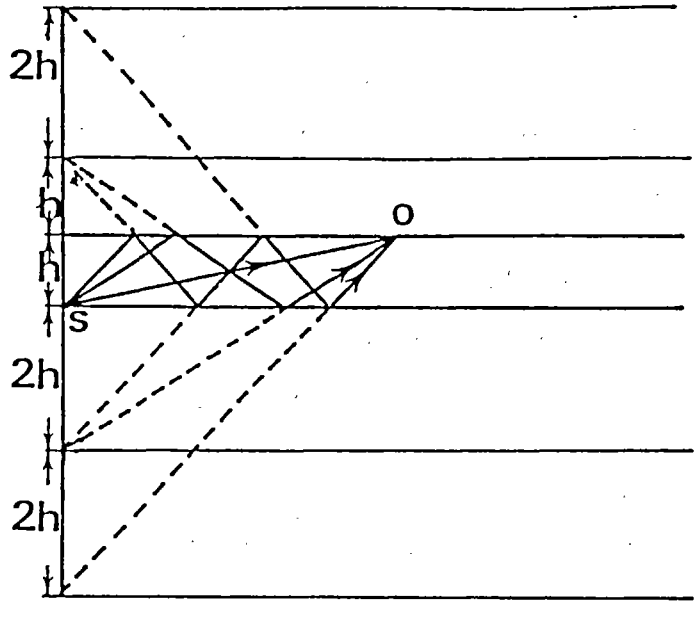

FIG. 4 THE IMAGE OF DIRECT AND REFLECTED ARRIVALS OF THE SOUND WAVE.
S:SOURCE, O:OBSERVING POINT. (FROM SELLS, 1965)

$$\eta_2 = \eta_{ar} + \eta_{br} \qquad \text{----------(9)}$$

$$\eta_{ar}(x, t) = \eta_r(a+x, t) + \eta_r(a-x, t) - \eta_r(a+x, t-\tau) - \eta_r(a-x, t-\tau) \qquad |x| \leqq a$$

$$\eta_{ar}(x, t) = \eta_r(x+a, t) - \eta_r(x-a, t) - \eta_r(x+a, t-\tau) + \eta_r(x-a, t-\tau) \qquad |x| \geqq a$$

$$\text{---------(10)}$$

where

$$\eta_r(X, t) = -\frac{2v_o}{\pi} \exp(\gamma h) \sum_{n=0}^{\infty} (-1)^n H\left(t - \frac{R_n}{c}\right) \cdot \left\{ t \cdot \tan^{-1}\left(\frac{h_n (c^2 t^2 - R^2_n)^{1/2}}{X c t}\right) - \frac{h_n}{c} \tan^{-1}\frac{(c^2 t^2 - R^2_n)^{1/2}}{X} \right\}$$

$$\text{----------(11)}$$

and

$$\eta_{br}(X, t) = 2v_o \exp(\gamma h) \sum_{n=0}^{\infty} (-1)^n \left\{ \left(t - \frac{h_n}{c}\right) \cdot H\left(t - \frac{h_n}{c}\right) - \left(t - \tau - \frac{h_n}{c}\right) \cdot H\left(t - \tau - \frac{h_n}{c}\right) \right\} \qquad |x| \leqq a$$

$$= 0 \qquad |x| \geqq a$$

$$\text{---------(12)}$$

FIG. 5a and FIG. 5b. show Sells' (1965) results for the free surface displacement η_{bs} over the displaced block and η_{as} not over the block as a function of nondimensional time T. Both of the profiles of disturbances, in particular that for over the block, rises and falls steeply due

to a number of reflection of the waves at free surface and the rigid bottom. But, in reality, the subsequent shocks would not be severe, because the reflections at the sea bottom are subject to attenuation. So, his model would not explain the long durations of sea shocks.

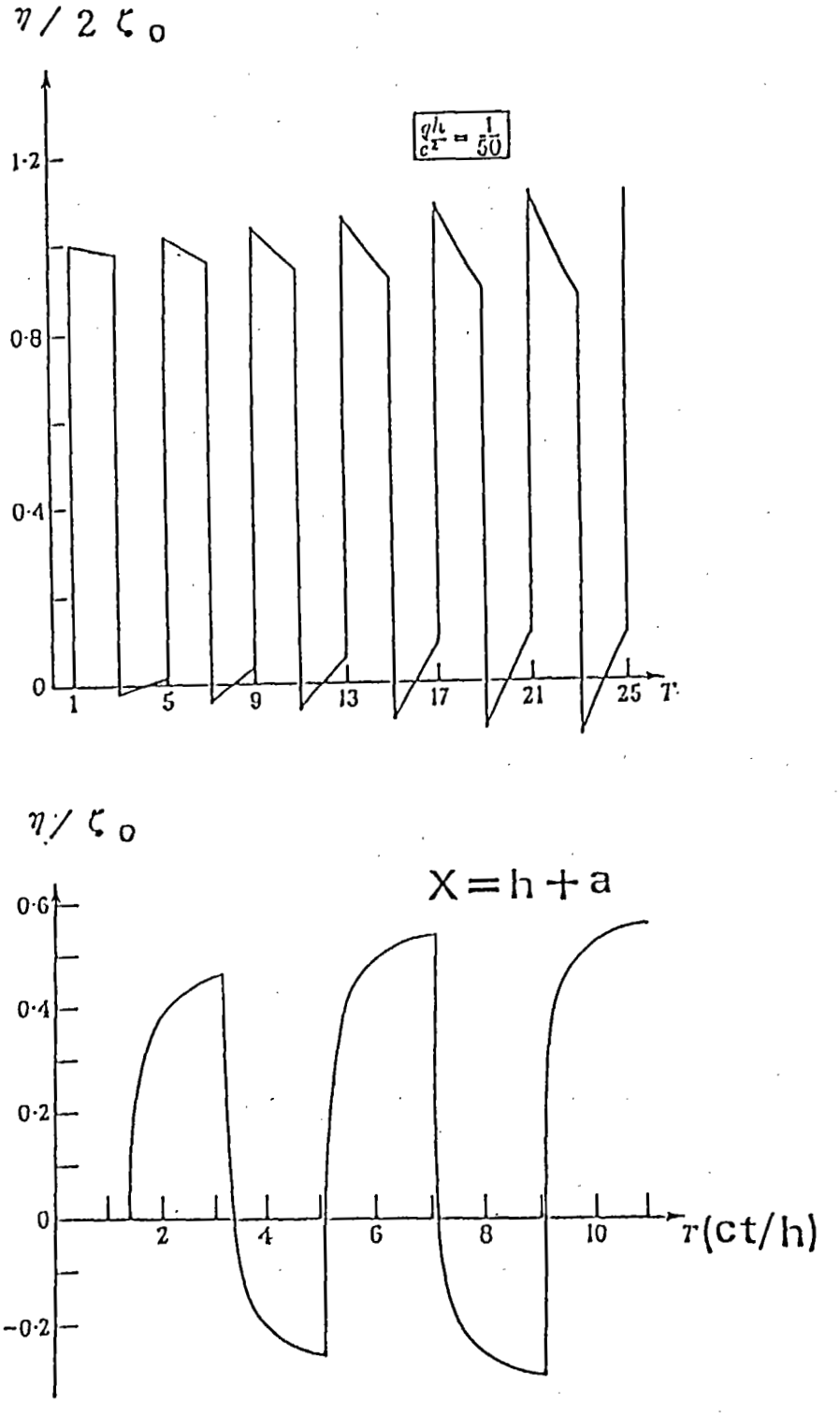

FIG. 5a, b JUMP ARRIVALS OVER THE BLOCK(UPPER) AND ARRIVALS FROM EDGES AT A POINT NOT OVER THE BLOCK(LOWER).
(FROM SELLS, 1965)

4. Propagating displacement model.

To explain the long durations of the sea shock, I adopted a propagating displacement model. FIG. 6 is a schematic view of propagating displacements of the sea-bed. At time $t=0$ the small block of the bottom with a length da jerked upward a distance ζ_0 abruptly(case 1) or jerked upward with a constant velocity v_0 for a time interval $0 < t < \tau$ (case 2) and successively outward small block jerked as the same manner with an interval dt. Displacements propagate toward the both edges of the whole block. So that, the boundary conditions at the bottom are given by

case 1:

$$\frac{\partial \Phi}{\partial z} = \zeta_0 \sum_{n=0}^{N} H(t-n\cdot dt)\cdot\{H(x-n\cdot da) - H(x-(n+1)\,da) + H(x+(n+1)\,da) - H(x+n\cdot da)\} \quad \text{----------(13)}$$

where $N = a/da$

case 2.

$$\frac{\partial \Phi}{\partial z} = v_0 \sum_{n=0}^{N} G(t-n\cdot dt, \tau)\cdot\{H(x-n\cdot da) - H(x-(n+1)\,da) + H(x+(n+1)\,da) - H(x+n\cdot da)\} \quad \text{--------(14)}$$

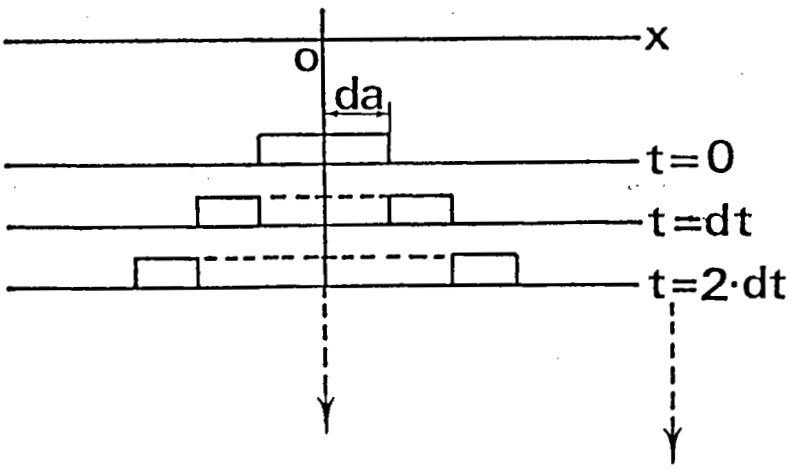

FIG. 6 A SCHEMATIC VIEW OF PROPAGATING DISPLACEMENTS. A SMALL BLOCK WITH A LENGTH da JERKED UPWARD SUCCESSIVELY WITH AN INTERVAL dt.

Free surface displacement η for the propagating displacement model can be calculated by the superposition of equations (5) and (9).

To simulate the sea shock felt by the frigate at the moment of the Ansei Tokai earthquake, I take up to the second arrival of (5) and (9). Free surface displacements were calculated at the point O_{15} and O_{30} (see FIG. 7). O_{15} and O_{30} are the points where the tsunami reached from the nearest edge in 15 and 30 minutes, respectively. Following parameters were adopted under the assumptions that rapture started at the center of the whole block and propagated bilaterally along the solid line shown in FIG. 1

a=80km : a half length of the whole block.
da=4km : the length of a small block.
dt=1sec : the interval of successive movements of small blocks.
τ=10sec. : the rise time of a small block for the case2
h=1500m : the water depth.
c=1500m/s : the speed of the sound wave in the ocean.
X15=10km : the distance from the nearest edge to O_{15}.
X30=50km : the distance from the nearest edge to O_{30}.

Profiles of the free surface at O_{15} and O_{30} for the case 1 and the case 2 are shown in FIG. 8a and 8b. For the case 1, profiles steeply rise and comparatively high frequency vibrations continue about 1 minutes. These would explain the sea shock felt at the moment of the Ansei Tokai earthquake. But, for the case 2, profiles gradually rise and no high frequency vibrations exist. Actually, the sea shock was the intermediate disturbance between that for the case 1 and case 2.

All of the profiles show the existence of low frequency disturbances(the low frequency T phase). The maximum magnitudes are almost the same for both of the case 1 and the case 2 but decrease as the increase of the distance.

The first arrivals begin at 25.7sec and 52.3sec after the start of the displacements at O_{15} and O_{30}, respectively. Each of these is a sum of the time required for the displacement to propagate from the center of the whole block to the edge(19sec.) and the time required for the sound wave to propagate from the nearest edge of the block to the observing points(6.7 and 33.3 sec.).

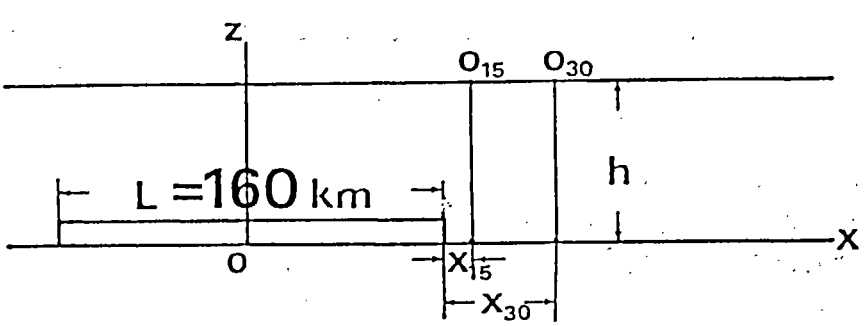

FIG. 7 DIMENSIONS OF SOURCE AREA AND LOCATIONS OF THE OBSERVING POINTS.

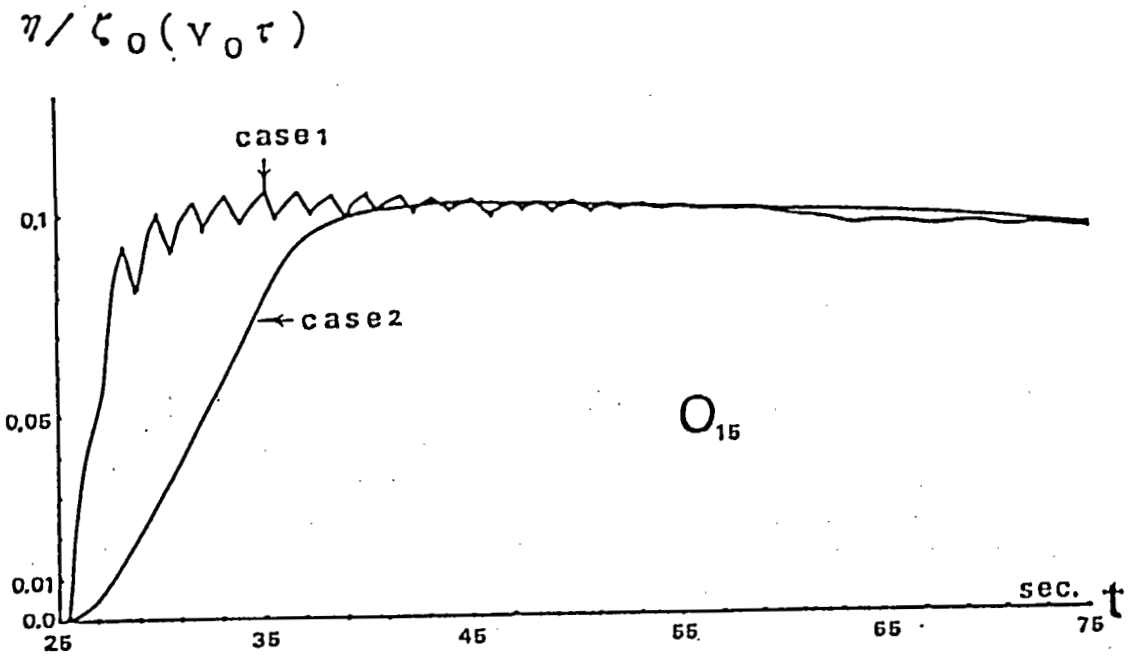

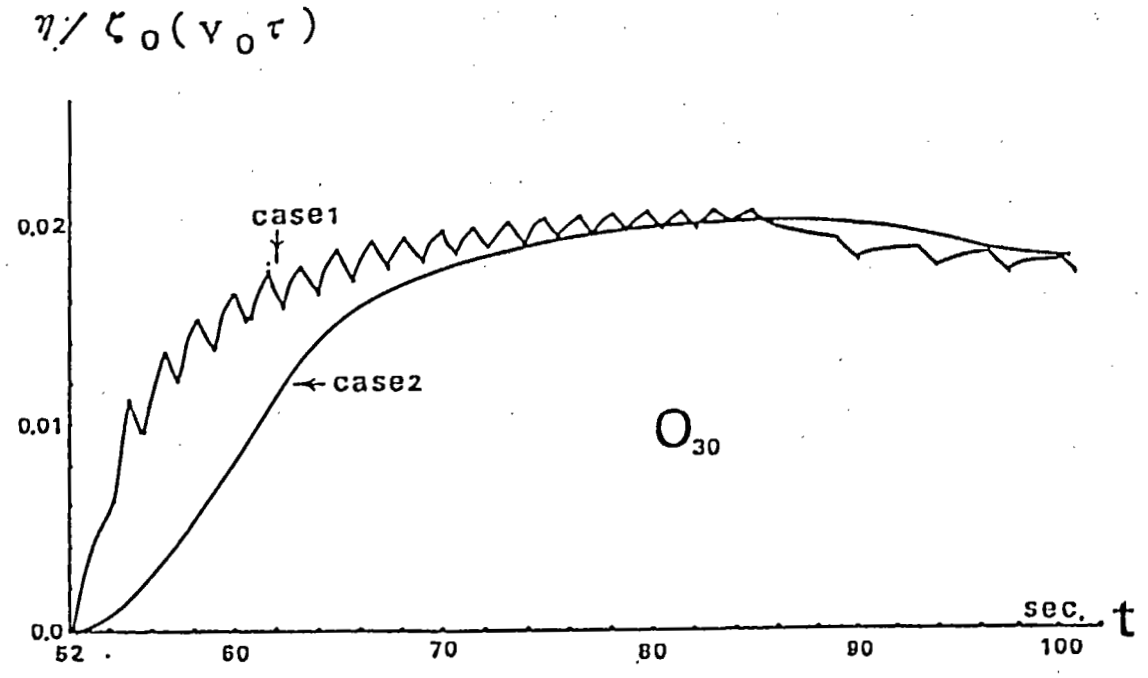

FIG. 8a, b CALCULATED WAVE FORMS AT O_{15}(UPPER) and O_{30}(LOWER).
CASE1:ABRUPT MOVEMENT OF THE BOTTOM
CASE2:MOVEMENT OF THE BLOCK WITH A UNIFORM VELOCITY
THE TIME MEASURED FROM THE BEGINNING OF THE DISPLACEMENT

5. The feasibility of measuring the low frequency T phase for tsunami warnings.

The low frequency T phase could be detected by a hydrophone and must be useful for tsunami warnings as a precursor, in particular, for emergency evacuations at the moment of the near shore tsunamis . Simply speaking, at the moment of an earthquake, whether tsunami was generated or not could be judged immediately by whether the low frequency T phase exists or not. Here, I present a system composed of a hydrophone and a seismograph to know the arrival time and wave height of tsunami. For the destination mentioned above, we must know tsunami wave form at the initial stage and its location. Using the time difference between the signals detected by a hydrophone and a seismograph, the location of the source region could be fixed. And, initial wave form could be predicted using the maximum magnitude of the low frequency T phase and the distance from the source region to an observing point.

To predict the maximum height of a tsunami at an observing point quantitatively, we must make numerical simulations in advance. Since, locations and dimensions of source regions of earthquakes which bring disastrous tsunamis to a point are limited and well known, we can get amplification factors of tsunami waves during the propagation from the source regions to an observing point .

6. Remarks

Super computers enable us to make rapid, exact and minute real time tsunami simulations for tsunami warnings. But, at now, it takes 7 minutes to simulate. Some near shore tsunamis will attack one coast in 5 minutes or so, in particular, in Japan. So, we must predict the tsunami height and the arrival time at the point where the tsunami will attack. If we can predict the tsunami informations locally, we need very short time for the distributions of our tsunami warnings and/or evacuation orders. A system mentioned in this paper is useful for these destinations.

7. Acknowledgment

I would like to express my sincere thanks to Dr. D. N. Romashko(Institute of electric current, Moscow, USSR) for his critical reading of the manuscript.

References

1. T. Hatori "Documents of tsunami and crustal deformation in Tokai district associated with the Ansei earthquake of Dec. 23, 1854", Bull. of Earthq. Inst., 51, 13-28(1976)

2. C. C. L. Sells, "The effect of a sudden change of shape of the bottom of a slightly compressible ocean", Phil. Trans. Roy. Soc. A, 258, 495-528(1965)

3. I. Tolstoy and M. Ewing, "The T phase of shallow-focus earthquakes", Bull. Seism. Soc. Am., 40, 25-51(1950)

APPLICATION OF NEW NUMERICAL METHODS FOR NEAR-REAL TIME TSUNAMI HEIGHT PREDICTION

V.K. Gusiakov, An.G. Marchuk, V.V. Titov

Computing Center, Siberian Division of the USSR Academy of Science, Novosibirsk, USSR

1.INTRODUCTION.

Numerical methods have been long and successfully used for mathematical modeling of tsunami generation, propagation and run-up. The ability of numerical models to reproduce the basic features of this complicated natural phenomenon has been more than once demonstrated by the computer simulation of many historical tsunamis. However, up to now its application to the operative tsunami prognosis was somewhat limited. It could be explained by two main reasons: first , the lack of time for issuing warnings in case of regional events and, second, the lack of available computer facilities in the existing tsunami warning centers. At present, both of these reasons can be eliminated by the development of new effective numerical algorithms and, even to more extent, by the fast increase of mini- and micro- computer facilities of the regional tsunami warning centers.

2.TSUNAMI MODELING SYSTEM.

The interactive tsunami modeling system (ITMS) for the numerical simulation of tsunami generation and propagation in the ocean with real bathymetry has been elaborated at Novosibirsk Computing Center. It was developed to be a simulation subsystem within regional tsunami warning center's software, so the following factors have been taken into account:

1) all numerical models in the system are to be united by an easy-to-use graphical interface;

2) the system should work in two modes - pre-event mode, and real-time mode;

3) the output of computations in the real-time mode should appear on the screen during computations, not waiting for the end of modeling;

4) the results of simulation should be suitable for the operative analysis and decision making.

Functioning of ITMS in the pre-event mode includes pre-event tsunami modeling, which provides estimates of wave heights along the coast for various positions of the tsunami source, computation of inverse isochrone charts for the regional network of tide-gage stations, choosing the optimal parameters for the real-time computations (such as, appropriate numerical

grid for the chosen regions,typical parameters of the tsunami source, etc.). Functioning in the real-time mode includes only the computation of tsunami propagation and plotting of the computed distribution of tsunami heights and travel time charts.

The basic functions of the system are as follows:

1) automatic construction of the computational grid for the specific areas from the regional bathymetric data base;

2) computation of the initial displacement in the tsunami source;

3) computation and plotting of tsunami travel time charts;

4) computation and plotting of wave forms at any point of the computation grid, and distribution of the maximum tsunami heights along the coast.

The ITMS is functioning as menu-driven system. All menus of ITMS are designed as operational panels with buttons and input windows on the right side of the screen.The central part of the screen is an output window for visualizing computation results, which are usually imposed on the map of the modeling region. Every function of ITMS is accessible from the main panel (Fig.1). Let us briefly describe each item, using as an example the simulation of hypothetic tsunami near the North of Japan.

3.CHOOSING OF MODELING REGION

The ITMS uses the bathymetric data of the whole area of responsibility for the regional tsunami warning center. But this area can be too large to compute tsunami propagation over it in short time, using existing computer facilities. Besides, most of the regional tsunamis with near-shore sources cause the damage only within the limited part of the shore nearest to the source area. Taking these facts into account, the 'MODEL REGION' unit (initiated by 'AREA' button of main menu) has been installed in ITMS to automate the process of selecting the region for tsunami calculations (Fig.2). The frame on the map of the whole area indicates the region to be chosen. Using arrow buttons or mouse, user manipulates with the frame and selects the desired modeling region. Then the map of selected region appears in the output window.

4.CONSTRUCTION OF COMPUTATIONAL GRID.

The next step is the construction of the finite-difference grid for the region chosen. To carry on this task the 'NUMERICAL GRID' menu is used (Fig.3). The user is requested to input the parameters of the grid into the panel window. The 'CREATION OF GRID' button initiates a special algorithm that constructs the finite-difference grid, which approximates the bathymetry of the modeling region. To provide the necessary accuracy of simulation

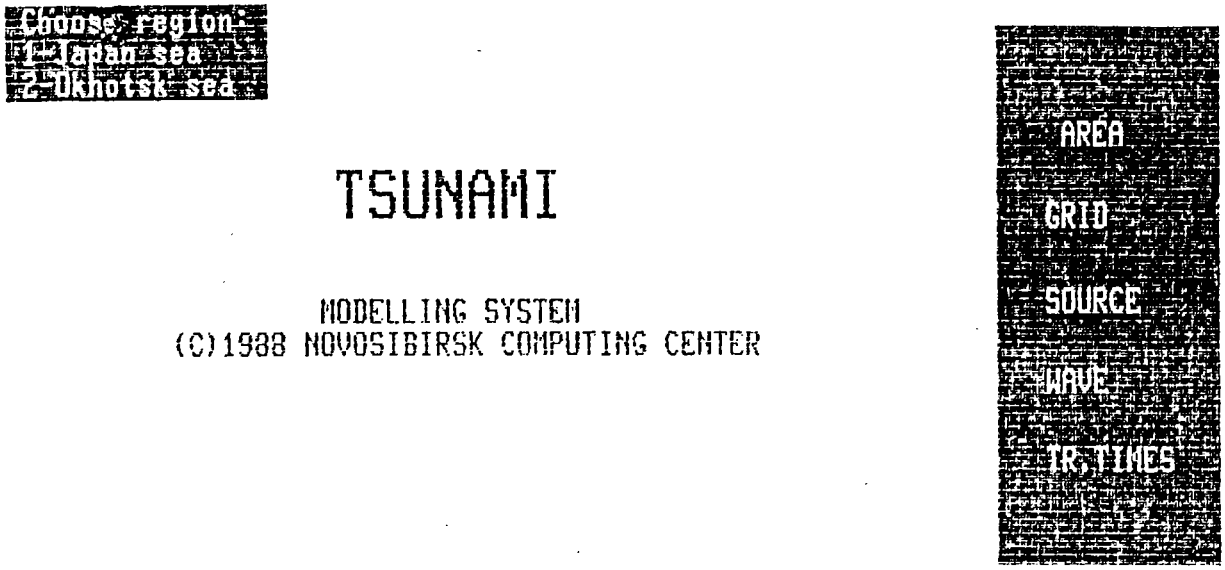

Figure 1. The main menu of ITMS with an operational panel on the right.

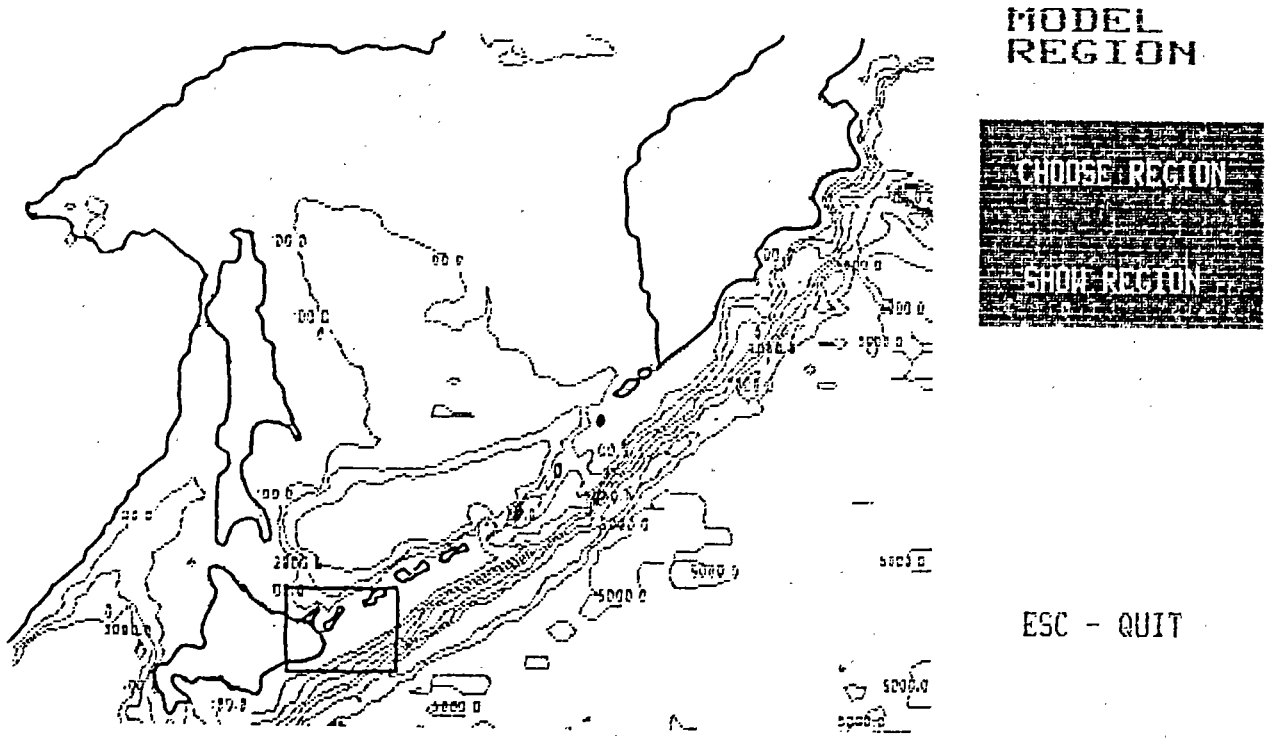

Figure 2. Menu for selection of region for tsunami simulation. The rectangular area on the map shows the region chosen for numerical experient.

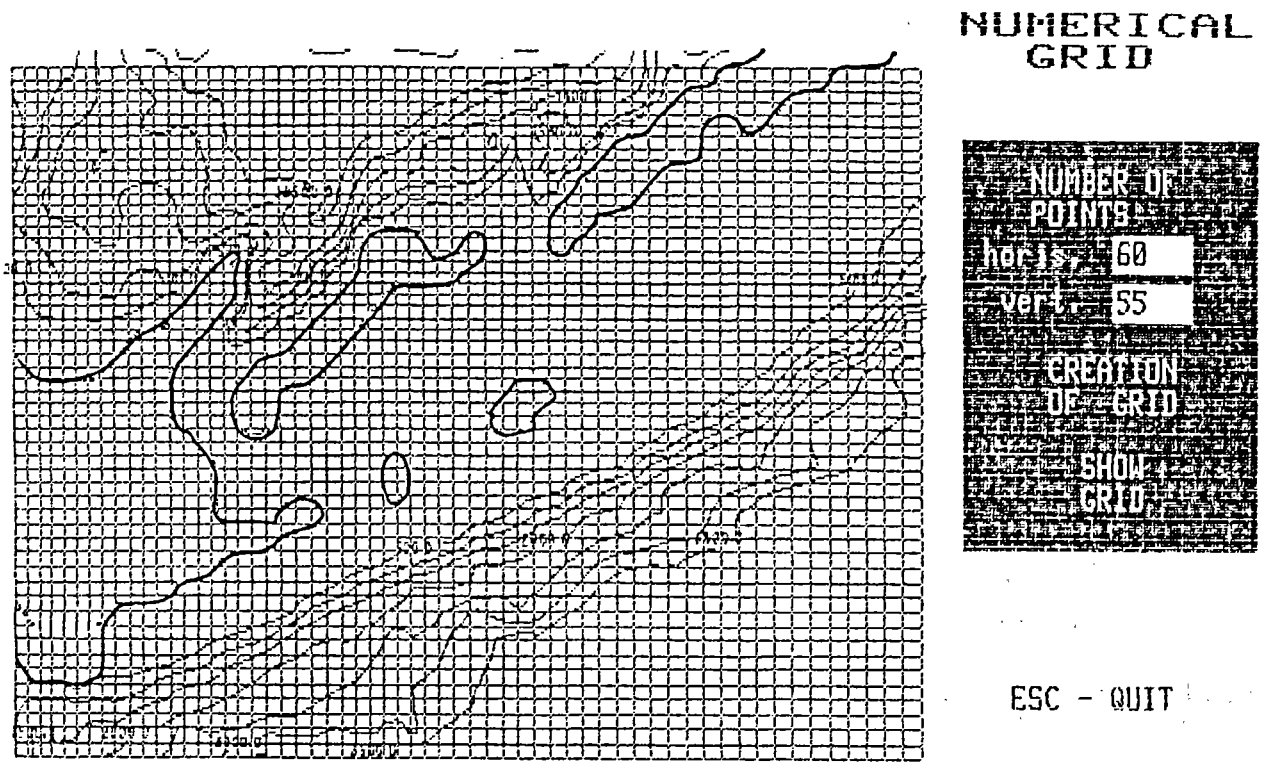

Figure 3. Construction of numerical grid with the help of ITMS.

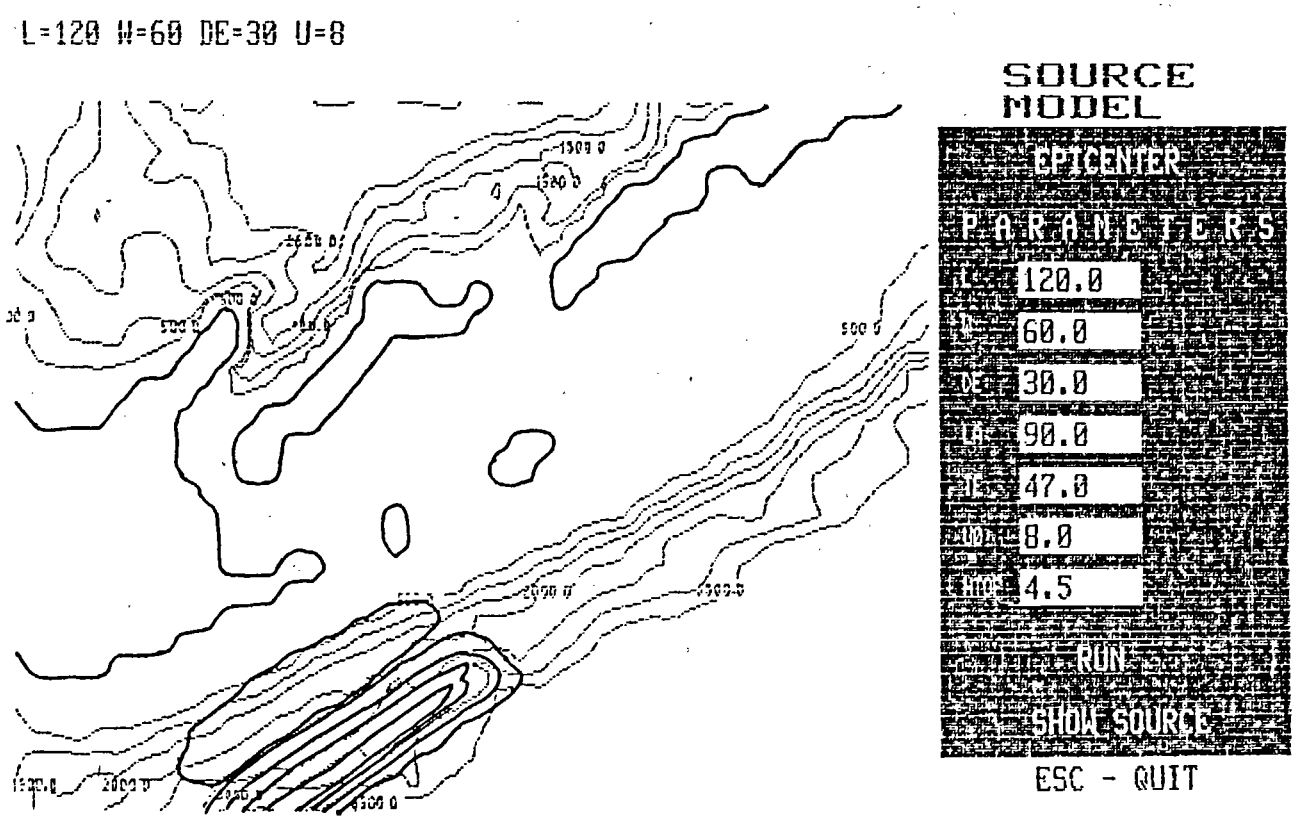

Figure 4. Menu for computation of the initial bottom displacement. The computed tsunami source is shown on the map.

of tsunami propagation in near-shore field a finite-difference grid with a variable space step length is used. The algorithm automatically constructs a variable grid for the given region.

An optimal grid results from the interplay of two main factors:

- accuracy of computation (the more grid points the better the accuracy)
- speed of computation (the less grid points the faster the computation).

So, a few numerical experiments might be required to choose the optimal grid, and the task of constructing a numerical grid is supposed to be done in the pre-event mode.

5.MODEL OF TSUNAMI SOURCE.

Using 'SOURCE MODEL' menu we calculate the vertical static displacement on the surface of elastic homogeneous halfspace with the inner distributed source of dislocation type. This source is a simple fault plain of a rectangular shape described by six parameters: the length L, the width W, the depth of upper rim of the fault HTOP, the deep angle of the fault plane DE, the strike angle of the fault dislocation measured from the horizontal axis LA and the average dislocation over the fault UO (Fig.4). The details of the solution of this static elastic problem can be found in Gusiakov (1978).

The computed vertical displacement is introduced in the discontinuity equation of the shallow water model, which is used for the description of tsunami propagation in the ocean with variable depth.

6.COMPUTING THE TRAVEL TIMES CHARTS.

One of the problems ITMS has to solve in the real-time mode is calculation of tsunami travel times from computed tsunami source to any given point of the region for experiment. After activating the 'TR. TIMES' button on main menu the quick algorithm for travel times computation begins to work. The initial wave front (initial isochrone) is the boundary of the bottom displacement computed by subprogram 'SOURCE'. Algorithm is based on calculating of travel times between neighbouring grid points and it uses 16-point "star". It means that we compare and minimize travel times from the center of the "star" to 16 nearest grid points. In this method we assume that the depth is linearly changes along the straight path between two neighbouring grid points. So, tsunami travel time from point 1 to point 2 can be approximately expressed as:

$$T = 2L/(c1 + c2)$$

where L is the distance between these points, c1 and c2 are tsunami propagation velocity at grid points 1 and 2 (in deep ocean tsunami waves velocity is equal to the square root of gravity acceleration multiplied by ocean depth). Few minutes later travel times from the numerical tsunami source to every marine and coastline grid points will be computed and after activating 'PLOTTING' button of the special menu the tsunami isochrones can be plotted on the map of the region (time interval between isochrones can be chosen by user). It is possible to output tsunami arrival times to the most important grid points (towns,villages, coastal objects etc.). Fig.5 shows isochrones with the density 1 min from tsunami source near the east of Hokkaido. If user wants to estimate tsunami arrival times as quick as possible he can start isochrone program (algorithm) before seismic source computations. It means that in this case instead of the boundary of calculated initial bottom displacement the isochrone program will use initial wave front as model ellipsoid. It is necessary to input only epicenter location, long axis orientation and lengths of both axes. These parameters can be taken from seismic source data (length of the seismic fault correlates with the earthquake magnitude (Poplavsky et.al.1988)). Using this method it is possible to estimate travel times just after obtaining main source parameters from seismic data. If the earthquake source locates in deep ocean, travel-time difference between computed initial tsunami source and model ellipsoidal source will not be so big (about a few minutes). The isochrone computation unit can be used for more precise definition of historical tsunami sources location using tidal records.

7.COMPUTATION OF TSUNAMI WAVE PROPAGATION.

The last and most important stage is the numerical simulation of tsunami propagation using a nonlinear shallow water model. These equations neglect the wave dispersion effects which can be admitted in simulating the regional tsunamis.A shallow water model permits us to compute the partial velocities and water level at any point of numerical grid. Bottom displacement computed by 'SOURCE' unit is the initial condition for the simulation of tsunami propagation. The details of the model can be found in Titov (1989).

The 'MODEL OF TSUNAMI PROPAGATION' menu is used at this stage (Fig.6) to add the set of parameters for computation (time step, total number of time steps, coastline depth) and to indicate 'control points' on the map. The computed wave forms or the distribution of current water levels at these points will be output on the screen during the computation of tsunami propagation.

The complete set of parameters (grid, source, control points, etc.) should be prepared during the pre-event mode; in real-time mode the user could only correct some parameters, such

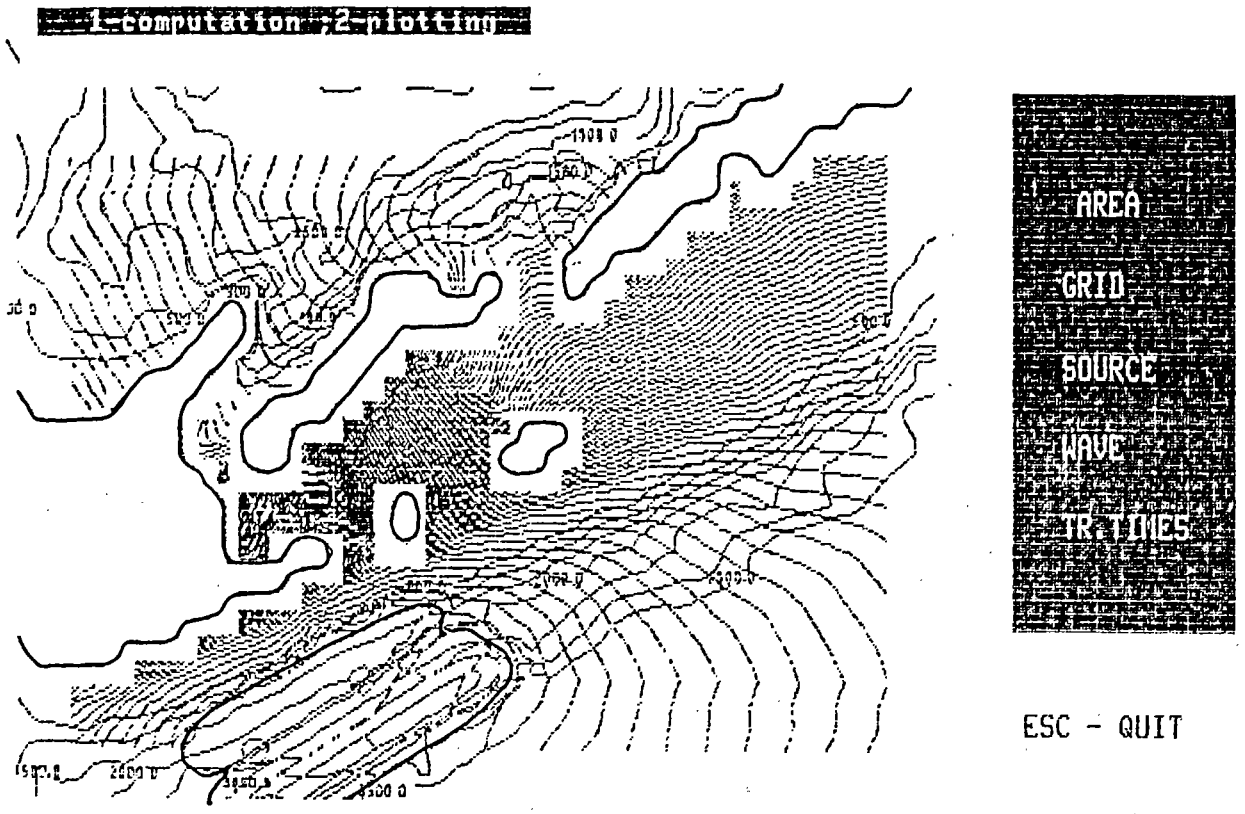

Figure 5. Travel times chart of tsunami generated by computed bottom displacement.

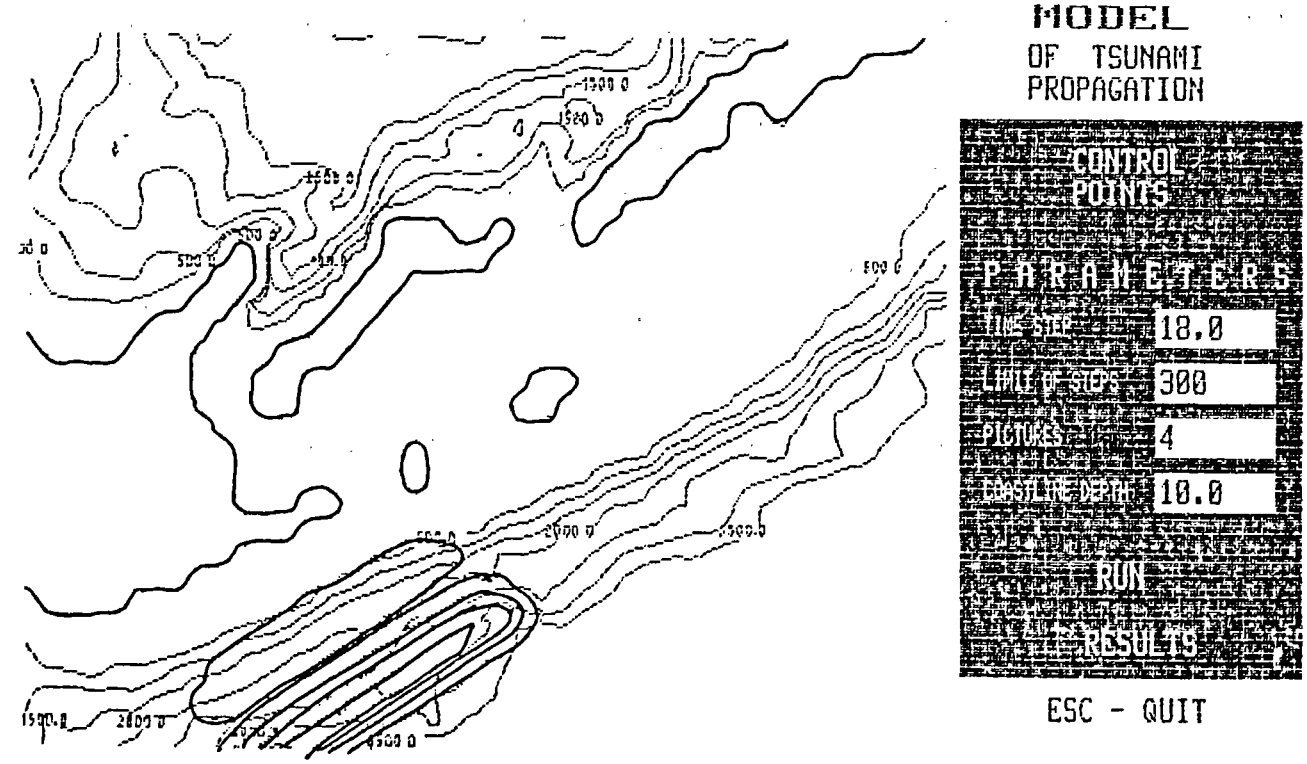

Figure 6. Menu for computation of tsunami propagation.

as, coordinates of the epicentre, orientation and magnitude of the tsunami source and perhaps some others.

'RUN' button initiates the simulation task. During the computation the user can see its results on the right of the screen. It shows the distribution of current and maximum tsunami wave heights at control points (Fig.7). The user can select any particular point and look at the computed wave form. If in the vicinity of a point there is a tide gauge and its recordings are transmitted to the center, the observed record can be imposed on the computed wave form and reliability of the initial data can be verified. If necessary, the computation may be repeated with a new set of source data.

REFERENCES

Gusiakov, V.K., 1978, Static displacements on the surface of an elastic halfspace, Uslovno Korrektnye zadachi matematicheskoj fiziki v interpritacii geofizicheskikh nabludenij, Novosibirsk: VC SOAN SSSR, pp. 23-51, (in russian).

Poplavsky, A.A., Kulikov, Ye.A., Poplavskaya, L.N., 1988, Methods and algorithms of automized tsunami prognosis, Moscow, Nauka, 128 p., (in russian).

Titov, V.V., 1989, Numerical modeling of tsunami propagation by using variable grid, Presented at the International Tsunami Symposium, Novosibirsk, USSR, (to appear).

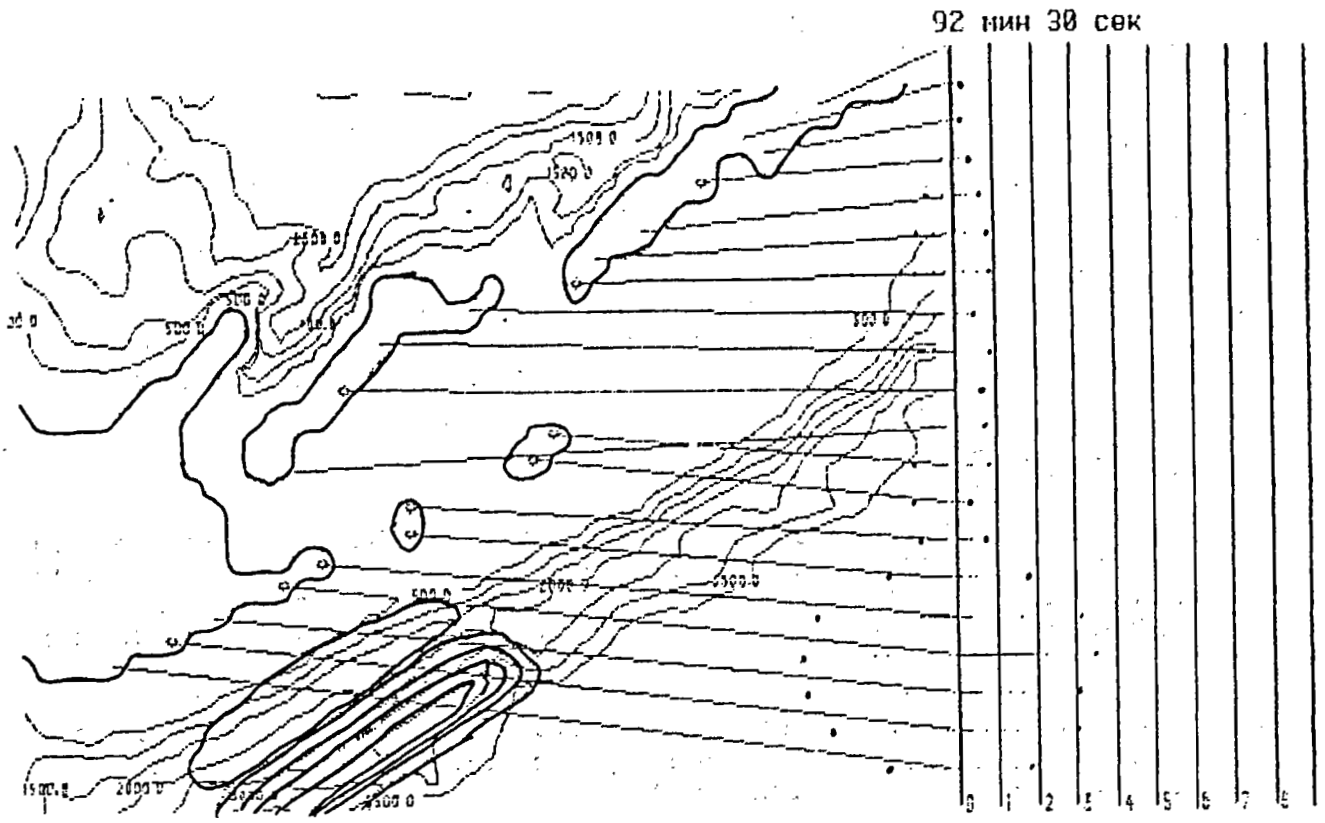

Figure 7. Vew of screen of ITMS during computation of tsunami propagation. Distribution of current and maximum tsunami wave heights at control points is shown on the right of the screen.

THE GOALS AND EFFICIENCY OF THE AUTOMATED TSUNAMI WARNING SYSTEM PROJECT IN THE FAR EAST OF THE USSR

I. Kuzminykh, M.Malyshev, A.Metalnikov

1. Goals of the United Automated Tsunami Warning Service (UATWS)

The Far East coast of the USSR is subjected to the effects of tsunamis generated closely in the Kuril-Kamchatka trench and the sea of Japan, and distantly in the Pacific. The Tsunami Warning Services were organized in Sakhalinsk and Kamchatsk regions in 1956. In 1983 service was set up in the Primorsky Krai area. The Warning Services use 6 seismic and 53 tide stations. The principal method of tsunami prediction is seismic based on the registration of earthquake waves preceeding the tsunami wave, by determining earthquake magnitude epicenter and tsunami generation probability based on these parameters. Sea level observations are of secondary importance but are used in the forecasting of waves far from the source.

Currently a number of papers have been published containing evaluations of the quality of the Tsunami Warning Services' operation [1,2,3,4]. Paper [1] analysing the Services' operations for 1958-1980 period gives the following data: During this period 70 earthquakes with magnitude $M \geq 7.0$ took place in the region. Tsunami Warning was issued for 30 of them (43%). Ten of the events generated tsunami waves with height of 0.5m, while 20 warnings are considered false. In 20% of the cases no tsunami wave occurred. Paper [2] offers as a quality criterion evaluation for the services particularly, "False alarm percent" $d=m_1/M_1$, "Tsunami missing percent" $B=m_2/M_2$ and forecast reliability $K=1-\frac{S+B}{2}$ ($0 \leq K \leq 1-\frac{\alpha+b}{2}$), where m_1 is number of false alarm cases of M_1 non-tsunamigenic earthquakes, m_2 - number of tsunami cases missed of M_2 tsunamigenic earthquake cases, $S=\frac{m_1}{M_1+(M_2-m_2)}$ - the ratio of the false alarm number to the total number of false alarms.

These results indicate that the Tsunami Warning Service efficiency is not high and for 20 years it is characterized by indicators S=0.73; K=0.53; b=0.20; α=0.44. (The indicators practically coincide with estimates given in paper [1]). Therefore the tsunami warning reliability needs to be improved substantially.

The time of evaluating tsunami generation and of warning coastal organizations and population could be reduced since probable sources of submarine earthquakes are situated some distance from populated areas. It takes about 15 minutes for tsunami

waves to reach such areas. Presently areas of significant tsunami risk depend on seismic Stations to solve the problems of tsunami warning and prediction. Not only it is necessary to improve the average statistical reliability of prediction but also it is important to exclude probability of errors of personnel.

These are the main deficiencies of conventional warning services that must be eliminated, and to apply up-to-date informational technology as the basis for UATWS creation. Table 1 gives the main objectives of the UATWS creation and ways of achieving them. As it is evident from the table that tsunami warning quality improvement may be obtained through the development of a system which is totally automated in data collection and processing. Reducing the time required for tsunami prediction is obtained through automated informational technology and the development of networks of data collection and transmission of tsunami warnings.

2. Structure and Functions of UATWS

It is planned to create within the framework of the UATWS the following subsystems:

a) An observational subsystem incorporating:

- 11 automated seismic stations (ASS), supplied with facilities for receiving three component seismic signals for analog-to-digital conversion, initial data processing and for composition of reports transmitting via communication channels; these messages include digitized seismogram, earthquake parameters, and facility control test data;
- 22 stations for tsunami coastal remote measurements (TCRM) incorporating gauges and devices for initial processing of signals and telemetry. Data telemetry includes data sets of measured data, data on long wave characteristics, and data on equipment test control;
- 4 sets of data via cable to hydrophysical stations (CHS) giving measurements of ocean level variation on the edge of the shelf, and transmission of signals to the shore measuring complexes (TCRM) via cable (at distances up to 100 kilometers);
- 4 sets of data from buoy hydrophysical stations (BHS) similar to CHS, but transmitting data to shore stations via radio-channel;

b) Data processing subsystem including collection and processing centres for seismic and hydrophysical data equipped with computer facilities:

- The Main (Basic) centre (CS) in Juzbno-Sakhalinsk;
- Standby (Alternative) centres (SC in Vladivostok and Petropavlovsk-Kamchatsky;
- Intermediate centres (IC) in Severo-Kurilsk, Kurilsk, Malokurilsk, Ust-Kamchatsk, on the Bering Island.

The multi-level structure of the data collection and processing system is required

Table 1

The UATWS goals, and ways to achieve them

1. Improvement of the prediction quality (verification, reliability)

1.1 Improvement of the tsunami prediction; seismic method reliability (verification)

a) Objective data acquisition through automation of seismic wave measurement and earthquake parameter calculation

b) Introduction of additional criteria for earthquake tsunamigenity (primarily, depth of the quake source)

c) Simultaneous processing of data obtained from several distributed points of seismic measurements, or from a group of seismic stations

d) Optimization of threshold magnitude values as tsunamigenity criteria

e) Optimization of the seismic measurement network siting

1.2 Improvement of efficiency in the use of sea level data

a) Creation of a network of automated or distant (remote) measurement sites for sea level variation near the coast-line and on the shelf's edge

b) Creation of international system for real-time data exchange on tide-control observations in the Pacific

1.3 Prediction of tsunami generation on the basis of sea level measurements

a) Creation of mathematical methods and computer software for modelling (simulation) of tsunami wave propagation and transformation near shore; presentation of tsunami generation forecast to the users

Table 1 (Continued)

The UATWS goals, and ways to achieve them

2. Reduction of response time for prediction and for presentation to users

   a) Automation of all measurements, data processing, message preparation and warnings

   b) Computer-assisted interrogational systems for processing and displaying data in deciding about tsunami risk

mainly to improve the system's reliability. Unlike the system with common centre and telemeter network use as the one suggested in paper [5], and systems functioning in Alaska and Hawaii [4] such a solution makes the system much more expensive, but justifiable.

It would be helpful to have independent measurements of data and processing in the most important tsunami-risk, populated areas. Quick warning is also provided in the zone of responsibility of the respective centre.

c) Communication subsystem for data collection from ASS, TCRM, CHS, BHS in the centres of the system, and for data exchange. It is considered reasonable for UATWS to use standard communication channels including satellite, and equipment for digital data transmission with speeds of 50 or 200 bits/per second - from TCRM, 200 or 1200 bits/per second - from ASS, 1200-2400 bits/per second for exchange between centres.

d) Communication subsystem for warning transmissions. This subsystem incorporates both standard communication channels and special automatic warning system for transmitting coded signals to the populated area and ships in the sea via communication channels and broadcasting stations. The UATWS exchanges data with foreign tsunami warning centres via GST (WMO) channels (via Khabarovsk, Tokyo, Honolulu). The distribution of system elements is shown in Figure 1. In this figure, the structure of responsibilities is outlined.

Intermediate centres are placed together with ASS and points of location of TCRW complexes. Accordingly the following functions are performed on this level:

- continuous analog registration and real-time digital processing of seismic signals;
- detection of major earthquakes and digital registration and transmission of seismic wave data for processing in SC and BC;
- identification of the earthquake epicenter and magnitude;
- assessment of the tsunami risk of the earthquakes in the vicinity, and issuance of tsunami warnings to responsible agencies for dissemination to the public;
- real-time and continuous analog registration and digital processing of signals from tide gauges from coastal and distant ocean (CHS, BHS) stations;
- digital processing of iterated mean average analog-to-digital signals and detection of anomalous water levels through the application of a series of local criteria ;
- transmission of anomalous sea level variations for processing in BC and SC;
- assessment of the tsunami risk and issuance of tsunami warnings to the responsible authorities;
- inclusion of automated alarm systems informing population and organizations of the tsunami threat.

Functions and tasks performed by SC and BC are similar, since they duplicate each other's duties in part or fully if the necessity arises. On condition of satisfactory operation these centres differ mainly in the responsibility zones.

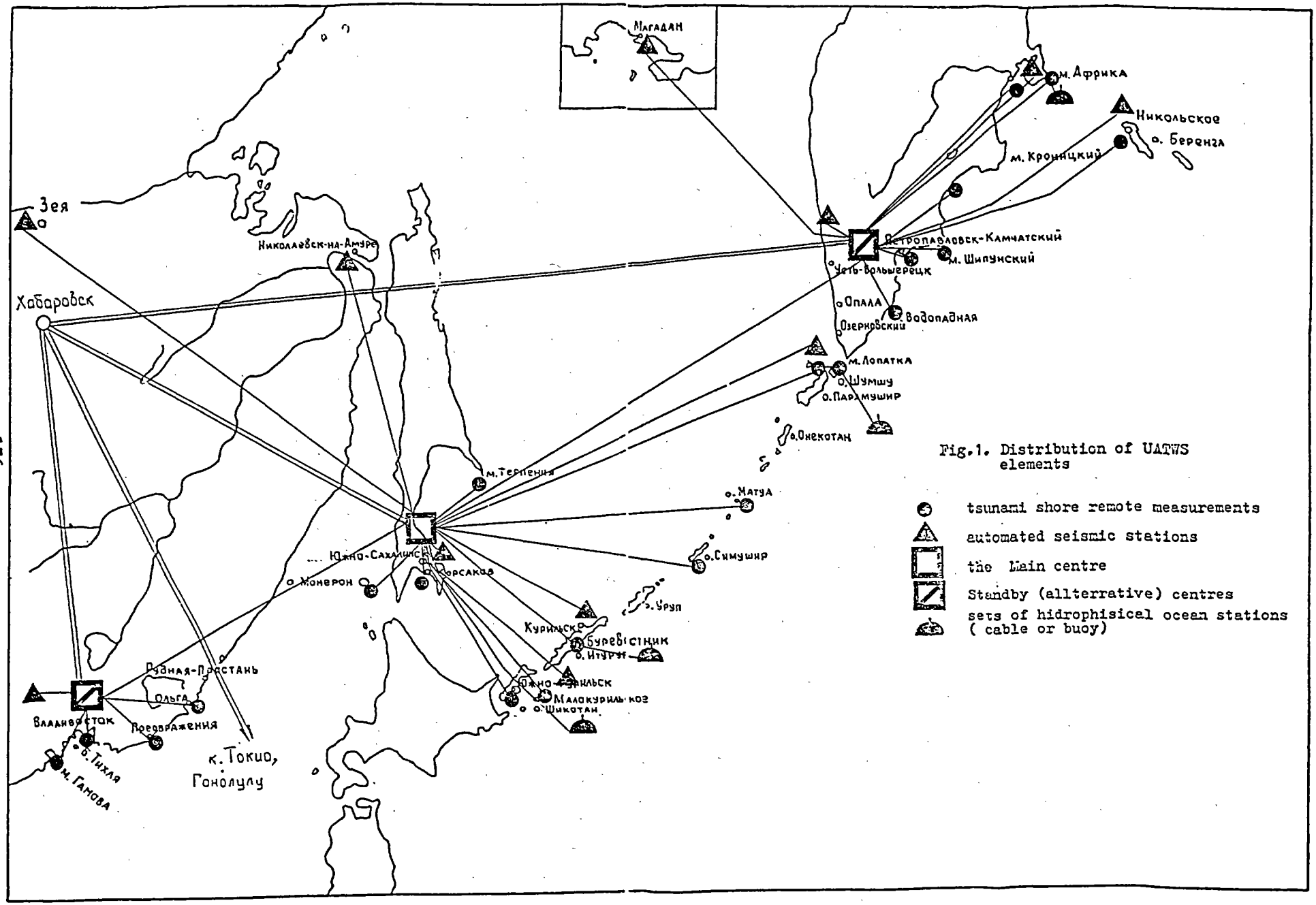

Fig.1. Distribution of UATWS elements

- tsunami shore remote measurements
- automated seismic stations
- the Main centre
- Standby (allterrative) centres
- sets of hidrophisicel ocean stations (cable or buoy)

On the level of SC and BC the following functions are performed:

- receiving sections of digitized records of seismographic and mareographic data from IC, ASS and TCRM, or their on-line processing results obtained at the UATWS lower level, or by visual means;
- quick-scan computer processing of seismogram records to identify earthquake parameters from the signals of individual ASS and three or more ASS; source depth estimates and successive parameter verification as new parameters are acquired;
- assessment of the earthquake tsunamigenity and its verification in the course of acquiring new parameters;
- quick-scan computer processing of mareographic data, and assessment of tsunami risk at point of measurement;
- estimation of tsunami propagation time from source to the coastal sites and refinement of this estimation with data obtained from ocean gauges;
- tsunami risk assessment for coastal areas based on ocean gauge measurements;
- composition of text messages on earthquake parameters, tsunami threat and automatic transmission of this information to the given addresses in the system;
- computer data archiving of tsunamigenic earthquakes and tsunamis.

To solve the above problems original software was developed, based on mathematical methods and algorithms, theoretical grounds of which had been published by several authors [2,6,7].

3. The UATWS Technical Facilities

ASS UATWS complexes are developed on the basis of equipment for a long-period "Volna" seismic station especially developed by the Integrated Constructors' Bureau of the Institute of the Earth's Physics of the USSR Academy of Sciences. The "Volna" station registers seismic oscillations with magnitude up to 600 μm in frequency range (band) 0.0065 - 7 Hz in three coordinates. Its electrical output signal is 0 - 10 V and has the means for selecting the amplification coefficient.

Conversion and processing of seismic signals is carried out by the "TBCO-1" complex and computer "CM 50/60," which are designed on the basis of processors of the "CM 1634" type and supplemented with blocks of signal analog filtration and of arithmetic device extension. The latter are added with a view to providing faster operation. Also it has a video-terminal device and data transmission equipment of "KH-03" or "YTIC 50/200" type. The complex permits carrying out rather sophisticated seismogram processing and to calculating the earthquake parameters within 5-6 minutes.

A TCRM "Mega" set is developed by the Central Constructors' Bureau for Hydrometeorological Instrument-Engineering especially for UATWS. The complex consists of the central block (CB) and submarine measurement container (MC). Coastal blocks of CHS and BHS data receiving and decoding may be also connected to it. CB is

designed on the basis of the micro-computer ("Diplomat" processor on microcircuits of K588 series) and it permits the performance of a great number of measurement operations, data conversion, and processing for the purpose of detecting dangerous changes in sea level [8].

MC incorporates hydrostatic pressure gauges, water temperature gauges, and gauges for the water specific electric conductivity.

Atmospheric pressure measurement is provided for the purpose of making corrections during sea level calculation.

CHS and BHS are implemented as experimental models. They are designed for checking principles of receiving information on the sea level variations on the shelf's edge and also for determining the optimum value for such complex structures.

Data collection and processing centres are provided with reliable computer facilities and with equipment for data telemetry using satellite communication channels. The experimental BC complex is designed on the basis of two "CM2M" computers and each has two processors. Automated operators' positions are provided for the centre personnel on the basis of "PMOT-2" complexes. The latter are supplied with alphanumeric and colour graphical displays. Further development of the system is calculated both on the computer "CM 1210," "PC 1001" and on personal professional IBM computers of PS/2, PC/AT types.

4. The UATWS Efficiency

In the process of the UATWS design technical, economical, and social aspects of the system's efficiency were investigated.

Unfortunately, in the course of the UATWS design, optimistic evaluations of the UATWS high potential efficiency were not confirmed in some published papers [5].This results from the fact that many methods suggested for improving the UATWS efficiency (e.g. source mechanism, etc.) were not included in designing appropriate methodology and software.

For example, in paper [2] it is proposed to improve the quality of seismic prediction only by 7-13 percent through optimization of magnitude criterion threshold value and also by taking into account the depth of the source. However, the design acknowledged the UATWS positive social and economic effect [9].

The UATWS is a monitoring system, which evaluates the measured environmental parameters and makes decisions of whether there is or there is not tsunami threat. To assess the technical efficiency of such a monitoring systems decision correctness characteristics are used, for example conditional probabilities of missing a dangerous event (errors of the first kind) P_{np} and of false alarm (errors of the second kind) P_{AT} [4]. When designing the system, it is very important to choose optimal threshold values

of tsunami detection criteria that could meet the requirements of the given social and economic strategy. From the social point of view the most important thing is to save human lives. This is achieved mainly through the reduction of P_{np}. Economic effect may be achieved through the reduction of both P_{np} and P_{AT}, and it may be estimated on the basis of available false alarm.and wave missing statistics. There is no other unified scale for risk estimation, i.e. joint assessment of economic damage and social factors. So optimization of threshold values for decision making about the threat actually depends on the selection of values valid under particular social and economic circumstances [2.9].

In accordance with the results of statistical processing of tsunami and earthquake characteristics taken from the associated catalogues, the Central Constructors' Bureau for Hydrometeorological Instrument-Engineering developed frequency curve functions for tsunamigenic, $f_1^{(n)}(M)$, and non-tsunamigenic, $f_i^{(n)}(M)$, earthquakes depending upon their magnitude M and the number of seismic measurement stations n. After intergrating the probability dependencies P_{AT} and P_{np} on the threshold M_o, the following relationships were obtained:

$$P_{AT}^{(n)}(M_o) = \int_{M_o}^{\infty} f_1^{(n)}(M)\,dM \;;$$

$$P_{np}^{(n)}(M_o) = \int_{-\infty}^{M_o} f_o^{(n)}(M)\,dM$$

These dependencies are displayed in Figure 2. (They are similar to the probability distribution functions for tsunami generation $F(P_j(M))$, given in different papers). In the same figure the complex indicator is plotted:

$$K^{(1)}(M) = 1 - \frac{1}{2}\left[P_{AT}(M_o) + P_{np}(M_o)\right]$$

As one can see from the figure, the best value of this indicator is $K^{(1)}=0.88$ if $M_o^{(1)}=7.25$. However, for practical purposes a rational value $M_o^{(3)}=6.8$ is recommended which using data from three seismic stations n=3, $P_{np}^{(3)}(M_0)=0.01$, $P_{AT}^{(3)}(M_0)=0.55$, $K^{(3)}(M_0)=0.72$.

This data is obtained for the Kuril-Kamchatka area if the mean statistial value of the source depth is h=60km. Similar statistic analysis may be provided for $P_{np}^{(n)}(h_o)$, $P_{AT}^{(n)}(h_o)$. For practical needs, paper [2] recommends the assumption of h_o=80km (for the Kuril trench), which permits the computation for $M_o^{(3)}$=7.5.

The use of M_0 and h_0 criteria gives $P_{np}^{(3)}(M_0,h_0) < 0.01$, $P_{AT}^{(3)}(M_0,h_0)=0.1$, and the reliability increases up to $K^{(3)}=0.95$.

However, such a possibility occurs only in the system of several stations. Emergency decision with near sources should be made at each operating station. Here it is necessary to have the threshold value $M_o^{(1)}$ =6.5 for $P_{np}^{(1)}(M_0)=0.01$ and then we have $P_{AT}^{(1)}$ (6.5)=0.8, $K^{(1)}$=0.6. From our viewpoint such estimates characterize the threshold potentialities of the seismic method for tsunami generation prediction implemented in the UATWS.

Statistical characteristics P_{AT} and P_{np} are also applied to the estimation of the potentialities of the hydrophysical tsunami detection method. In this case the UATWS

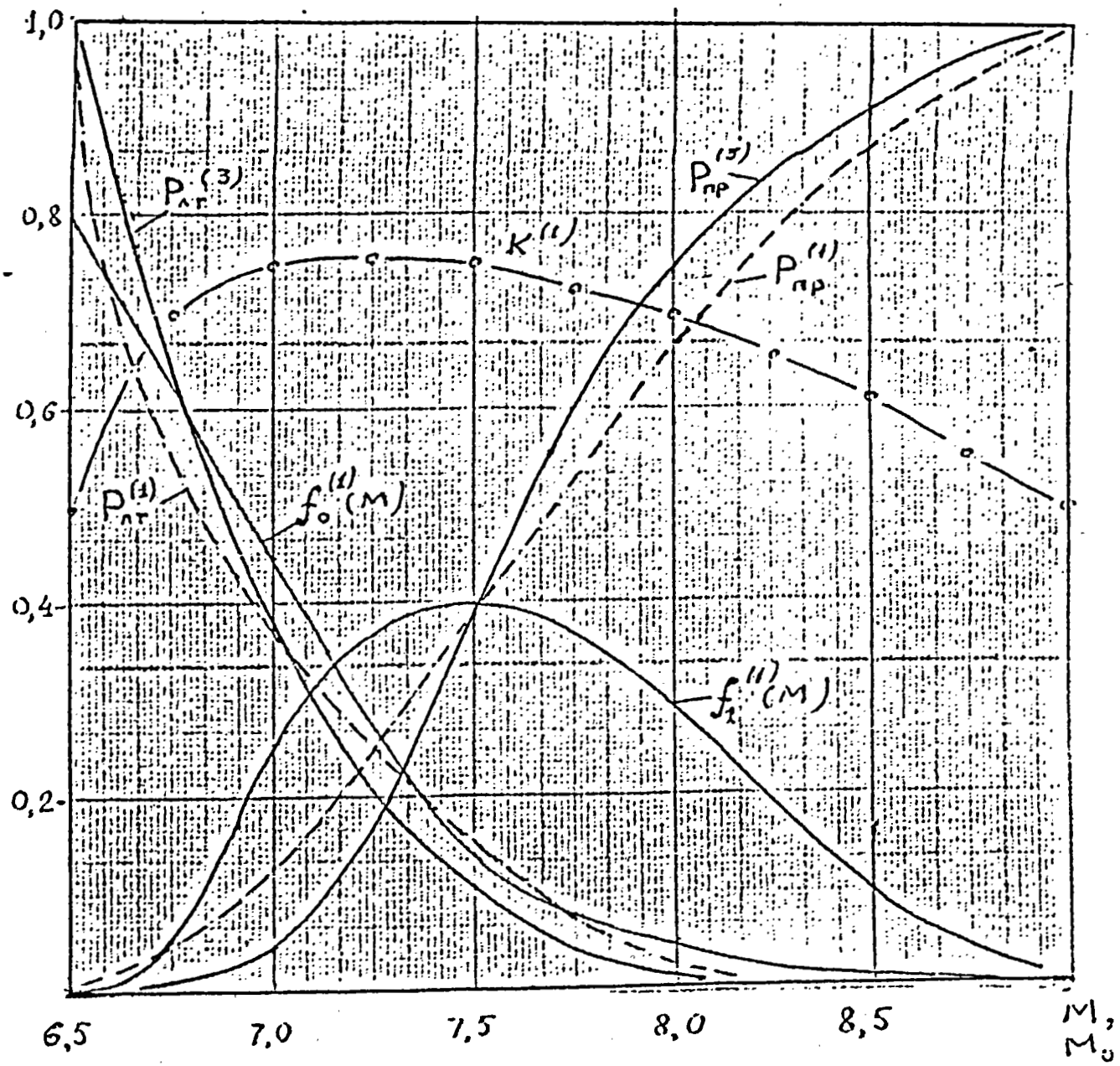

Fig.2. Statistic characteristics of seismic method

solves the task of dangerous wave detection as if it was a non-stationary long-wave process on the background of all other wave processes (tides, wind-generated waves etc.) and occasional noise. Methods of analog and digital filtration used in the system permit the cancellation of short-wave oscillations and the determination of long-wave components. Because of this the task is limited to the occasional signal detection against the background of noise, which includes errors of the measurement system and filtration, and of ocean noise, which results in flat (Gaussian) noise. Then P_{AT} and P_{np} are computed in accordance to the recurrent relation:

$$F^{(-)}(P_{np}) + F^{(-)}(P_{AT}) = -\sqrt{\frac{E_c}{N}} \cong \frac{q_c^2}{\sigma^2}$$

where $F^{(-)}$ is a function inverse to the Laplace function

$$F(y) = \frac{1}{\sqrt{2\pi}} \int_{-\infty}^{y} e^{-z^2/2} \cdot dz \quad ;$$

$E_c = \int_0^t s^2(t)dt$ - total signal energy;

N - flat noise spectral density;

Q_c - signal threshold level amplitude;

σ^2 - noise dispersion.

The tsunami wave may be considered dangerous if it has amplitude in the open ocean a=10...20 cm [2] and noise power according to our assessment of about σ^2=6.8 cm. Then assuming P_{np}=0.01 and depending on the time of wave detection and wave period T, one can evaluate P_{AT}. For instance, if t/T=0.06 P_{AT}=0.40, and if t/T=0.25 $P_{AT} \tilde{=} 10^{-8}$. Detection delay t=0.25T may be permitted if the hydrophysical station is situated at 1000km or more from the coast. But for detection of waves generated in the source region on the shelf's edge if is necessary that t=0.05T. In that case a great number of false alarms is inevitable because of the system excessive sensitivity a_c<5sm.

So, in spite of the system ayutomatization, the conventional tsunami prediction and observation methods do not result in radical improvement of the system's reliability.

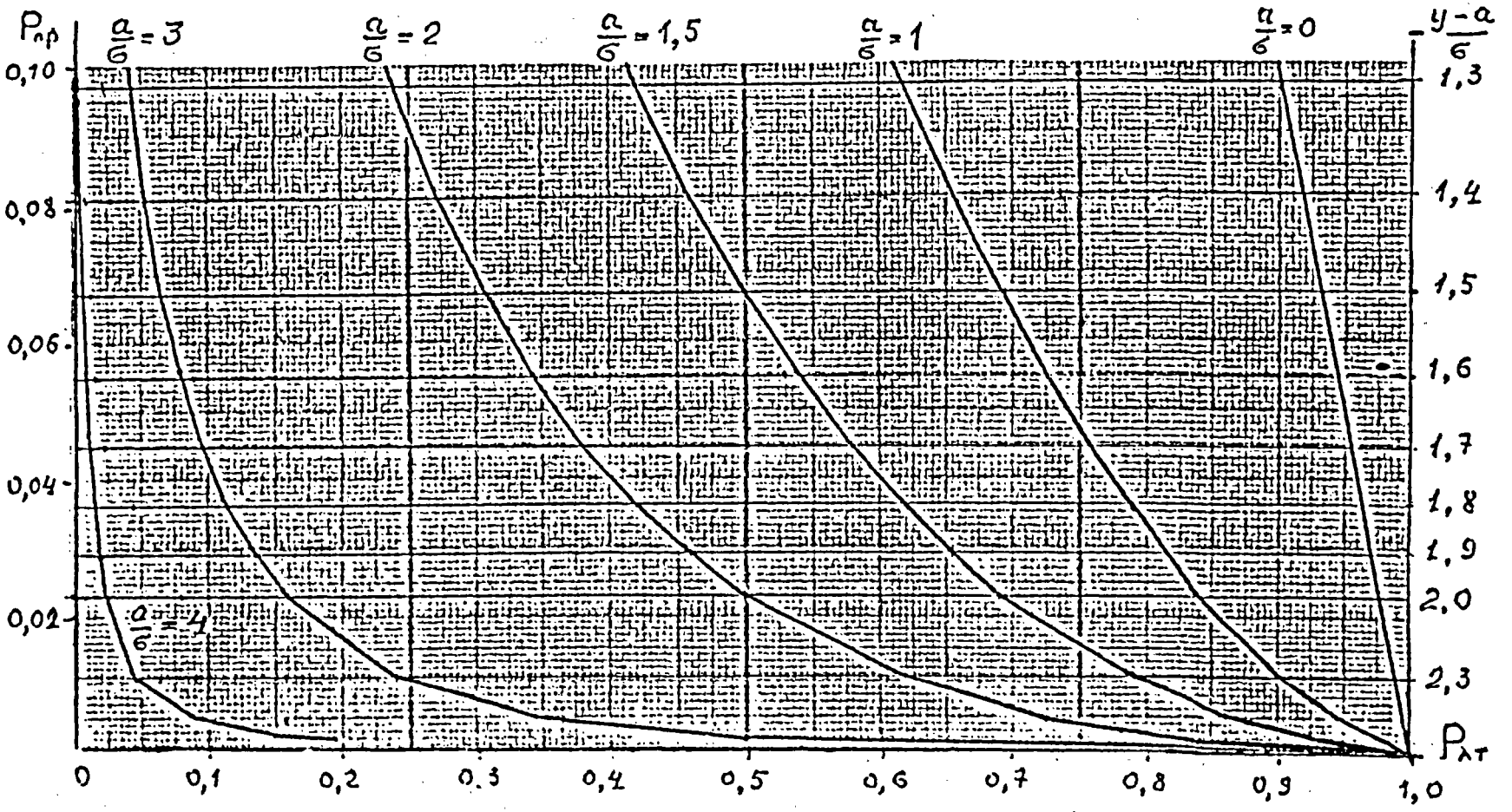

Fig.3. Figure of relation $F^{(-)}(P_{np}) + F^{(-)}(P_{\lambda T}) = \frac{a^2}{\sigma^2}$

Bibliography:

I. Воробьев Е.А., Го Ч.Н. и др. Об уточнении магнитудно-географического критерия оперативного прогноза цунами на Дальнем Востоке // Состояние исследований и разработок по созданию единой автоматизированной системы "Цунами":Тезисы докладов совещания г.Обнинск, 1985/отв.ред И.П.Кузьминых. ЦКБ ГМП.-Обнинск,1985.-С.38-40.

2. Поплавский А.А., Куликов Е.А., Поплавский Л.Н. Методы и алгоритмы автоматизированного прогноза цунами.-М.: Наука, 1988г.-С.80-101.

3. Гусяков В.К., Венценосцева Е.Ю., Глускина Т.Е. Развитие и современное состояние систем предупреждения о цунами на Тихом океане /ЦКБ ГМП.-Обнинск,1988.-40 С.

4. Евмененко В.В. К оценке качества функционирования ЕАСЦ// Теоретические основы, методы и аппаратурные средства прогноза цунами: Тезисы докладов совещания, г.Обнинск, 1988 /Отв.ред. С.Л.Соловьев, ИОАН СССР; ЦКБ ГМП.-Обнинск, 1988.- С.76-77.

5. Алексеев А.С., Гусяков В.К. Сейсмическая система прогноза цунами. Принцип построения: Препринт 428./Новосибирск, ВЦ СО АН. СССР.-1983.-36С.

6. Никифоров И.В., Тихонов И.Н. Пакет алгоритмов для первичной обработки трехкомпонентной сейсмограммы: Препримт / СахКНИИ ДВ НЦ АН СССР.-Южно-Сахалинск,1984.-60С.

7. Мар Г.Н., Шендерович И.М. Метод обнаружения длиннопериодных колебаний уровня моря типа волн цунами // Метеорология и гидрология.- 1987. - №7.- С107-109

8. Рыбин Г.С. Комплекс прибрежных дистанционных измерений цунами "МЕГА" // Вопросы создания и внедрения перспективных технических средств и систем. Сборник № 2 /ЦКБ ГМП.- М,: Гидрометеоиздат, 1988. - С.28-32.

9. Кузьминых И.П., Бренерман Ю.Б., Крылова Т.Л., Семенченко Е.В. Об оценке эффективности единой автоматизированной системы наблюдений и предупреждений о цунами // Труды ДВНИГМИ.- Л.: Гидрометеоиздат, 1988. - вып.132. - С.134-140.

INTEGRATED WARNING SYSTEM FOR TSUNAMI AND STORM SURGES IN CHINA

Yang Huating
China Institute for Marine Development Strategy
Beijing, China

Abstract

Tsunami and storm surges result in unusual oscillation of sea level, flooding the coastal zones and constitute the major marine disasters in China. Damage by storm surges occurs frrequently. According to statistics there are 14 storm surge events exceeding 1 every year on the average. Six of them are typhoon surges and the other eight are extra-tropical surges. In general, in China, there is one severe disaster of storm surge every two years. Monitoring, forecasting and warning for storm surges, including the drop of water level, are the major part of the operational oceanographic services in China. Such warning system has been set up and is operated by the State Oceanic Administration since 1974.

The results of the historical study of tsunami in the last few years pointed out that the anomaly of sea level generated by tele-tsunamis originating in the Pacific Ocean Basin is less than 30 cm on the mainland coast, but local tsunami in the China Seas can be very dangerous. For example, more than 50,000 people were killed by a tsunami in Taiwan and in Taiwan Strait in 1781. It resulted in more deaths than any other tsunami in recorded history. However, the frequency of tsunami disaster is very low for the coast of China, averaging only one every 100 years. It is impossible to set up an independent tsunami warning system in China. It is more practical to set up an integrated warning system on tsunami and on storm surges consisting of:

- A sea level observing network with real time sea level data acquisition capability
- A monitoring system of weather causing the storm surges and of seismic stations monitoring tsunamigenic earthquakes
- A tidal prediction scheme for operational use
- A forecasting scheme for storm surges and tsunami analysis
- The means for warning dissemination

1. Introduction

China is a large continental country on the west Pacific Ocean. Its heavily populated coastline is over 18000 km long and the economy along this zone is developing much more rapidly and intensely than the other parts of the country.

Marine and coastal natural hazards such as storm surges, severe waves, serious sea ice and tsunami have caused extensive damage and loss of life in the nation's history. Storm surges and tsunami are responsible for many flooding disasters in the coastal regions. Damaging storm surges are frequent, but tsunami disasters are infrequent for the coastal areas of China, although in 1781 a tsunami in the Taiwan Province killed 50,000 people. Because of the infrequency of the tsunami hazard, it is impossible to form an independent tsunami warning system in China, but it is practical to set up a combined warning system for tsunami and for storm surges.

2. Study of Historical Tsunamis in China

In recent years the history of tsunami disasters on the coast of China was studied by many authors (see References). From 1831 B.C. to A.D. 1980, 4117 earthquakes with magnitude greater than 4 3/4 have been reliably documented in China. Altogether there were 51 earthquakes greater than 6 1/2 that occurred offshore along the coast of China according to Zhou and Adams. Figure 1 shows some of their locations and dates of occurrence. Of these, only 26 events are certain or probable tsunamigenic and produced tsunamis. Table 1 lists these tsunamis and damages sustained. The probability rating for the validity of a tsunami and tsunami magnitude, m on the Imamura-Iida scale are shown in Tables 2 and 3. Of these 26, at least 8 or 9 events are damaging with considerable loss of human life and property. For example, as mentioned previously, the tsunami of May 22, 1781 (Qian Long 46 of the Qing Dynasty) in the Taiwan Province and Taiwan Strait was very destructive and resulted in more deaths than any other tsunami in recorded history. Because of this, the total loss of human life and property of local tsunamis along the coast of China has not been less than in other parts of the Pacific Ocean. But, the frequency of local tsunami diasters has been rather low for the coast areas of China.

The China Seas are surrounded by extensive continental shelves. Therefore, the tsunamis originating in distant regions of the Pacific Ocean Basin cannot easily reach mainland China with high energy except for the east coast of Taiwan Island. For example, the water level anomaly on the coast of China caused by the earthquake and tsunami from the Sea of Japan in 1983 was only 20 cm. The water level anomaly from the Chile tsunami of 1960 and of the Alaska tsunami of 1964 were also less than 20-30 cm.

3. Disasters of Storm Surges in China

China is a country which has frequent disasters. Extratropical and typhooon surges take place every year. According to statistics there are 14 storm surge events exceeding 1 meter which occur on the average, every year. Eight of them are extratropical and the other six are typhoon surges. Of these, one or two a year result in property damage and loss of life.

The east and south coastal areas of China are generally low-lying and the most vulnerable to flooding. During 1949-1986, there were many severe floods of storm surges. One of the most severe extratropical storm surges in China occurred on 23 April 1969 at Laizhou Bay in Bohai Sea. The highest recorded surge was 3.55 m and the sea water piled up so high on land that inundation extended inland for about 20 kilometers. Another most severe typhoon surge occurred on 22 July 1980 in the east coast of Leizhou Peninsula, Guangzhou Province. The highest surge of 5.94 m was measured at the Nandu Hydrographic Station. The sea water flooded the fields and burst dykes and dams for hundreds of kilometers. Millions mu 15 mu=1 hectare) of fields were inundated.

4. Present Monitoring and Warning System on Storm Surges

a. Observation of Sea Level. China has a long continental and island coastal line. There are more than 200 tidal gauge stations observing sea level with Automatical Tide-Recorder. These stations are under the management of the Ministry of Water Resources (151 stations), State Oceanic Administration (26 stations), Ministry of Communication (17 stations) and the Navy (11 stations) respectively. Of these, only 52 tidal gauge stations (Figure 2) report the tide in real-time by telegram or radio-telegram to the forecasting centers. The other gauge stations are reported to local forecasting agencies in real-time during the storm surges or in non-real-time only.

b. Tidal Prediction. The data of tide about one hundred stations have been collected and archived by the National Marine Environmental Forecasting Center (NMEFC). Using the harmonic analysis method, the long series of tide level data are analysed to produce harmonic constituents which in turn are used to predict astronomical tides by electronic computer. The data of storm surges for about 60 stations have been computed carefully by subtracting predicted astronomical tides data from observed ones following the same procedure. These data play an important role in research work and forecast operations of storm surges.

c. Present Warning System on Storm Surges. The forecasts of storm surges have been issued by the "Common Prediction Scheme" in NMEFC and Regional Marine Forecasting Centers in Qingdao, Shanghai and Guangzhou. In general, the effectiveness of the forecast is about 12 to 36 hours prior to the time of high water. Mean errors in practice are 20 to 30 cm.

As soon as a storm surge warning is issued by the forecaster, it will be disseminated by telephone, telegram, teleprinter to the Central Flood Control Headquarters and its Provincial Agencies, and to various government departments concerned about marine operations and to special users, and then, through radio, television and the press to the general public (Figure 3).

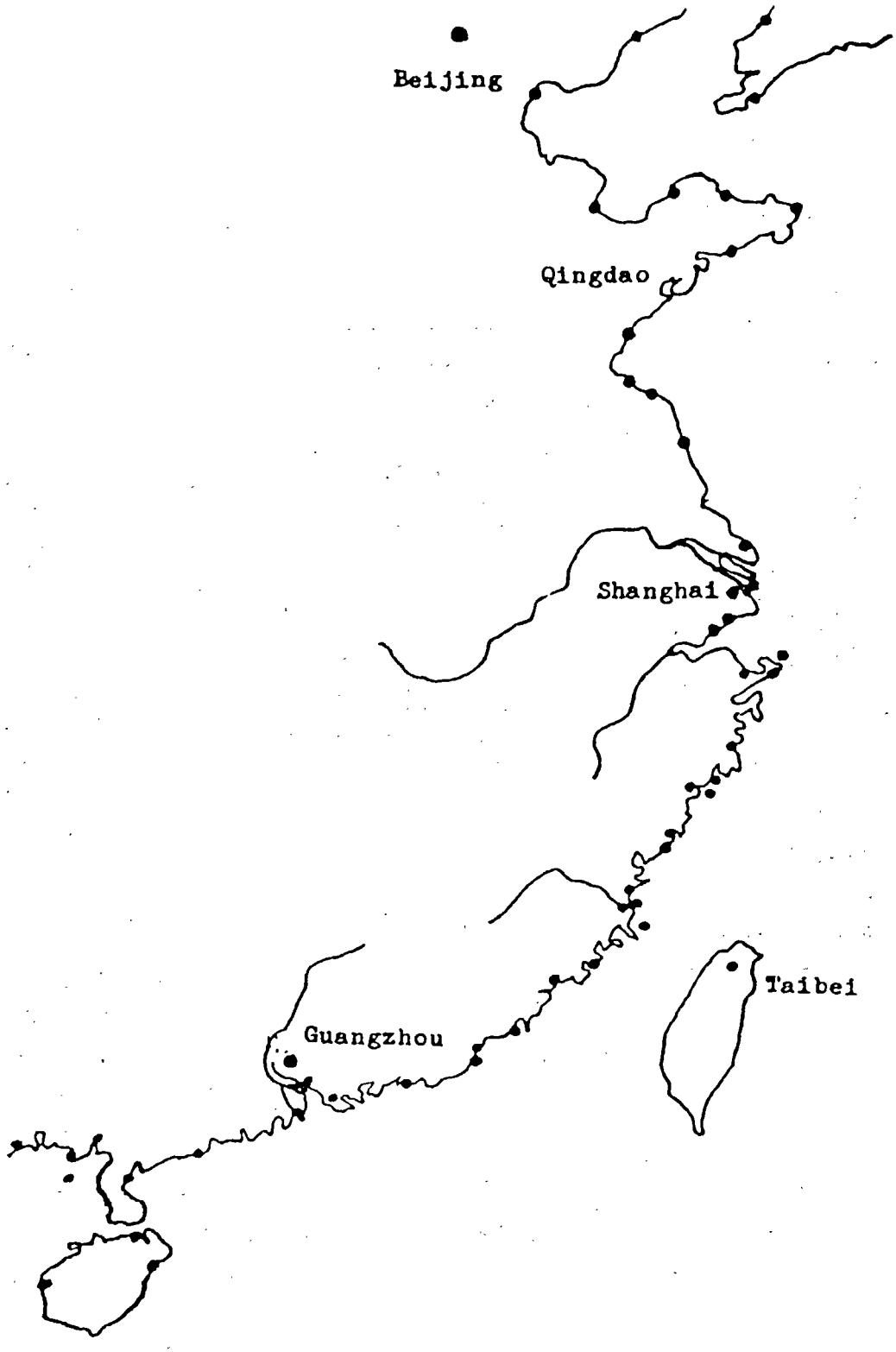

Figure 2: Map of location of 52 tidal gauge stations

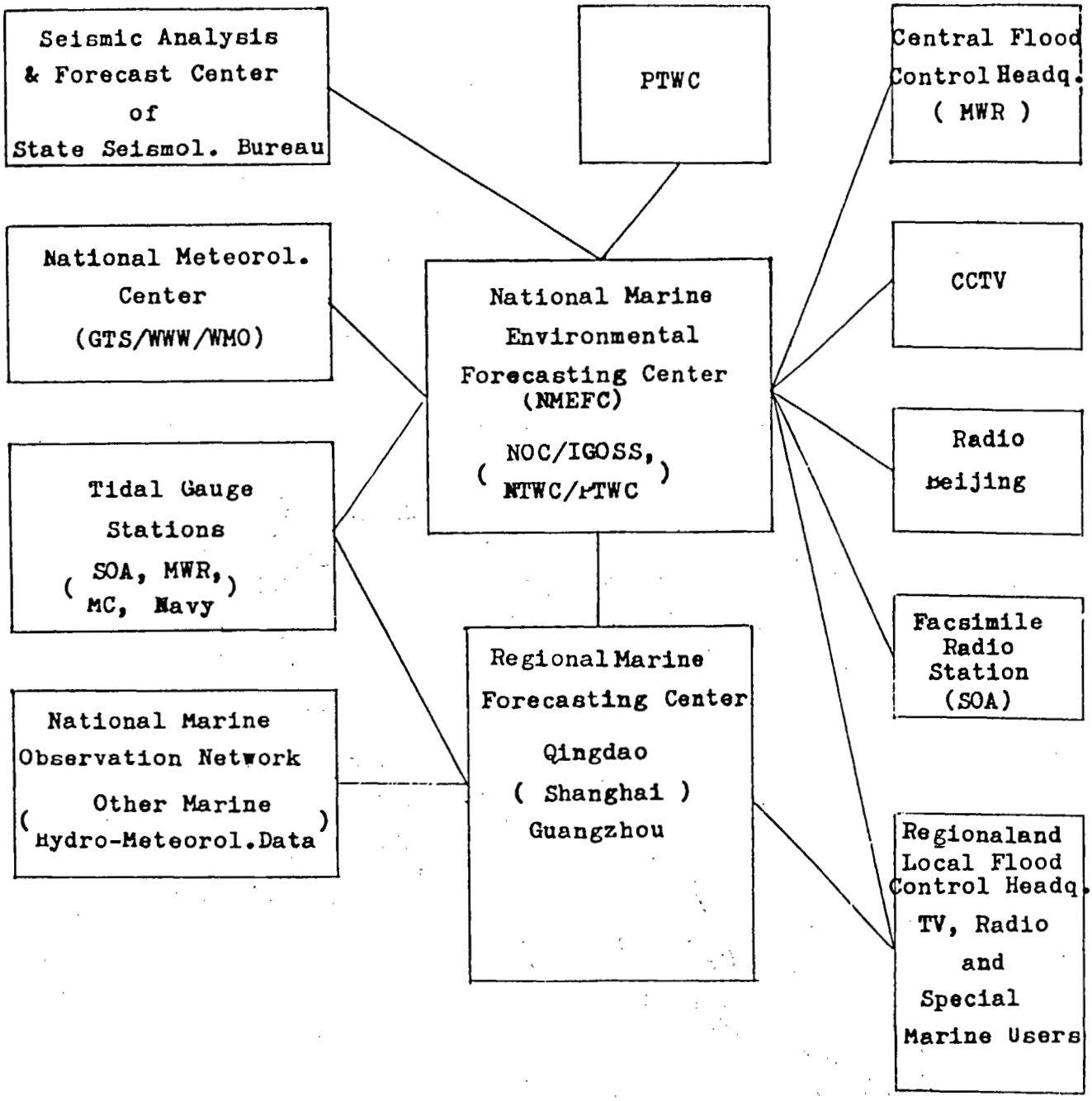

Figure 3: Scheme of the Integrated System for Tsunami and Storm Surges in China

5. Strategical Aspects and Summary

Based on the above analysis, we find many similarities between tsunami and storm surges both in theoretical research and in operational aspects as follows:

a. Tsunami and storm surges fall into the classification of long gravity waves and interact with another type of gravity waves, namely tides (T.S. Murty).

b. Both tsunami and storm surge warning operations need a well equipped sea-level observing network. The tidal gauge data must be collected and transmitted in real-time to forecasting centers.

c. The forecast and warning must be disseminated by the same ways to emergency agencies, marine users, and general public.

The differences between tsunami and storm surges are the following:

a. Tsunamis are generated by under earthquakes, under water volcanic explosions or submarine landslides. So the warning operation needs close cooperation with agencies dealing in seismic observation and analysis.

b. Storm surges occur in offshore water bodies due to the tangential wind stress and pressure gradients associated with travelling strong weather systems, such as tropical and extratropical cyclones. We look upon the good forecasts of storm surges as the result of close cooperation with marine meteorological analysis and prognostic operations.

Having both the similarities and the differences between tsunami and storm surges, considering that the frequency of the tsunami disaster is far lower than that of storm surges for China and that the present monitoring and warning (forecasting) system on storm surges is very effective, reliable and successful, we can conclude that the recommendation to set up an integrated warning system for tsunami and storm surges by developing the present forecasting operation in China is probably feasible. Figure 3 shows the scheme of operations of such a system.

6. References

Lu Renji, 1984: Historical Data of Tide Disasters in China (in Chinese), Ocean Press, Beijing, China.

Iida Kumizi, 1984: Catalog of Tsunami in Japan and Its Neighboring Countries, AIT, Japan

Murty T.S., 1987: Dynamic Similarities and Differences Between Tsunami and Storm Surges, Programme and Abstracts of ISSS, Beijing, China.

NGDC & WDC-A, 1984: Tsunami in the Pacific Basin 1900-1983, Boulder, Colorado, USA.

Soloviev S.L. & Ch. N. Go, 1974: Catalogue of Tsunamis on the Western Shore of the Pacific Ocean, "Nauka," Moscow, USSR.

Yang Huating, 1987: Tsunami and Pacific Tsunami Warning System, Supplementary issue "Storm Surges and Tsunami" of "Marine Forecasts," Beijing, China.

Ye Lin, 1987: The Present System of Forecasting and Monitoring on Storm Surges in China, Programme and Abstracts of ISSS, Beijing, China.

Zhou Qinghai & William M. Adams, 1985: Tsunamigenic Earthquakes in China, 1831 B.C.-1980, ITS, Victoria, B.C., Canada.

1987: Tsunami Risk Analysis for China, Proceedings of ITS, Vancouver, B.C., Canada.

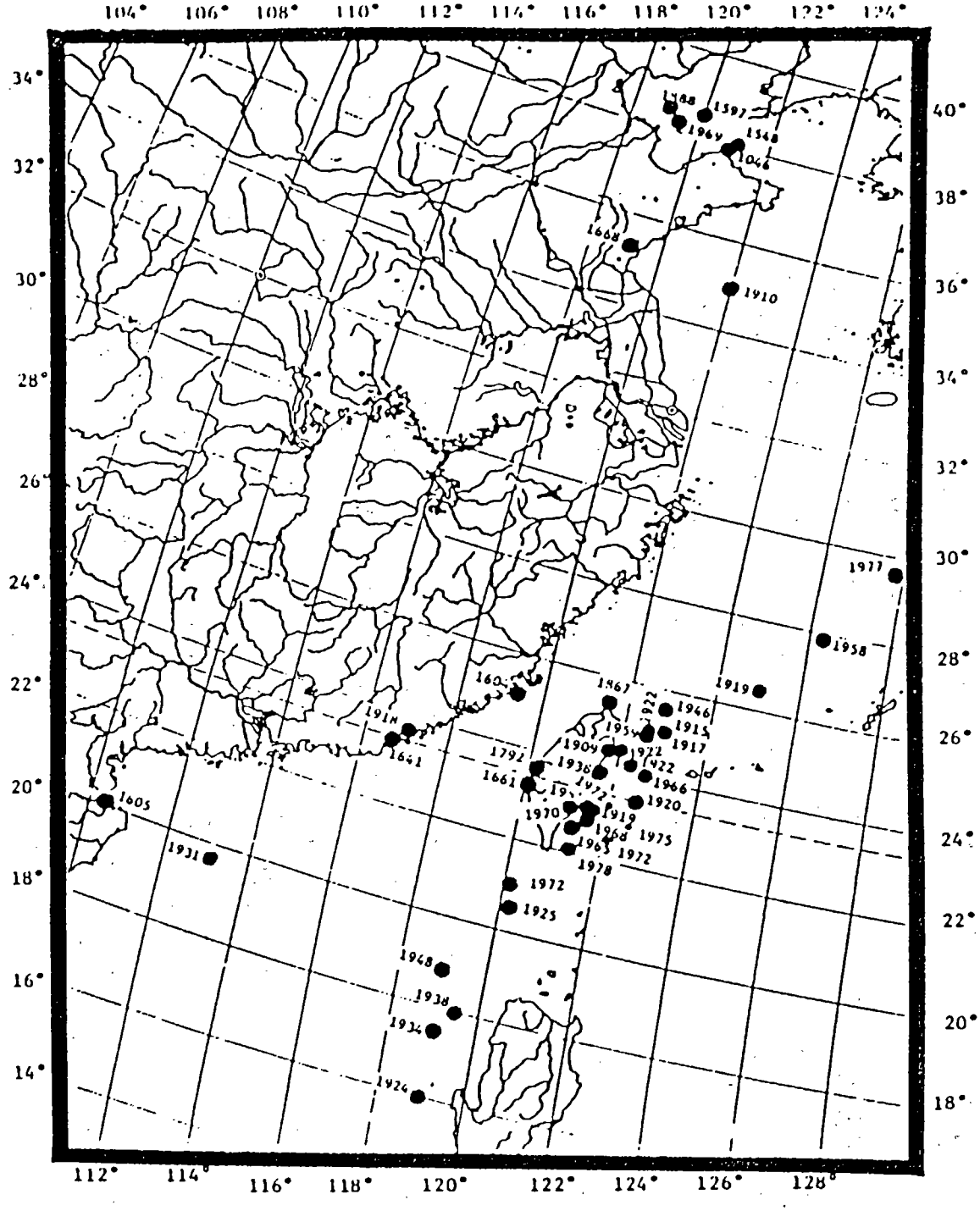

Figure 1: Location map of earthquakes

Table I. Tsunamis Occurred in China

No.	Event: Date(Local) C. C. y. m. d. t.	Earthquake: Epicenter °E °N M	Tsunami: m Rating	Damage Sustained	Authors
I	47B.C. 9.-(2?)	Laizhou Bay, Guangrao,Wi County, Shangdong Pr. -	0-I -	'Record on July*:.... Mid-year,quake,surges in North-sea County, People killed!.'Quake in Qi**,Surges in North-sea County'.	L. ZA[I,2]
2	I71.2.I4 -	Offshore of Huangxiang Coun. Shangdong Pr.	- -	'Quake,surges of sea water'. Tsunami in Laizhou Bay'.	L.
3	I73.6.27.- 7.27. -	Laizhou Bay, Shangdong Pr.	0 3	'June*,quake in North-sea,surges in East Laizhou and North-sea Counties'.	L.,I. SG. ZA[I,2]
4	I046.4.27 -	I20.7 37.8 5 Ponglai coast Shangdong Pr.	0 -		ZA[I,2]
5	I324.9.23(?)-	Wenzhou, Zhejiang Pr. -	I -	'Night of Aug.27*, storm, quake, surge'.	L. ZA[I,2]
6	I327.7.- -	Wenzhou -	- -	'Hurricane, quake, surge'.	L.
7	I344.8.I7(?)-	Wenzhou, Zhejiang Pr. -	I -	'Tsunami forwards inland for 20-30 li***'. 'Quake'.	L. ZA[I,2]
8	I509.6.I7- 7.I6. -	Baoshan County,- Shanghai	0 3	'June*,ZhengDe 4,Ming Dynasty,quake,floods, of sea water, Yangtze river tsunami month'.	L. I. WDC-A, SG.
9	I604.I2.29 -	II9.5 25.0 8 Offshore Quanzhou Fujiang Pr.	0-I -		ZA[I,2]
I0	I605.7.I3. -	II0.5 I9.9 7.5 Qongshan,Wenchang of Guangdon Pr.	0 -		ZA[I,2]
II	I640.9.I6- I0.I4. -	II7 23 - Jeyang,Chenghai and Chaoyang Cun. Guangdon Pr.	0 4	'ChongZhen I3,Ming dynasty,many quakes,surges of sea and lake water'.	L. I. WDC-A, SG.
I2	I642.9.I6- II.26. -	II6.5 23.5 5.75 Chenghai and Chaoyang Counties Guangdon Pr.	0 -		ZA[I,2]
I3	I66I.I.8/9.-- 2.I5	I20.I 23.0 6.0 SW of Taiwan Pr.	I 4	Great Taiwan-Anpin Tsunami.	I. WDC-A, ZA[I,2]

To be continued

Continued Table I.

No.	Event Date(Local) y. m. d. t.	Earthquake Epicenter °E °N	M	Tsunami m	Rating	Damage Sustained	Authors
I4	1668.7.25. -	II8.6 35.3 Luixian County, Shangdon Pr.	8.5	0-I	-		I. ZA[I,2]
I5	I670.8.I9-9.7. -	I22.5 33.0 Shanghai	6.75	I	4	Earthquake and tsunami in some counties of Shanghai. Many people drowned along the coast	L. I. WDC-A,SG
I6	I754.4.- -	I2I.4 25.3 Danshui,Taiwan Pr.	<6	I	3	April earthquake and some houses damaged by tsunami.	I. WDC-A
I7	I78I.5.22. -	Taiwan Island and Taiwan Strait	-	I	3	'April or May,Qianlong 46,Qing dynasty,Sea rose with great violence and swells,flood of several metres remained its height I or 8 hrs. Tsunami swept away villages and many people drowned. Then sea water has receded rapidly .More than 50000 residents died'.	
I8	I792.8.9. -	I20.5 23.6 Jiayi County, Taiwan Pr.	6.75	I	-		ZA[I,2]
I9	I867.12.I2.-	I2I.7 25.5 Keelung City, Taiwan Pr.	6.0	2	4	After quake, water run out of harbor. Number of ships and houses washed away, several hundred people drowned.	I. SG. ZA[I,2]
20	I917.I.25. -	II9.5 24.5 Xiamen and Tung'an, Fujian Pr.	6.5	I	4	Jan.'3,I9I7,earthquake and sea water retreated,then backed again. Many fishing boats wrecked.	L. I. SG
21	I917.5.6. 2I:I9	I2I.6 23.2 Keeluog City, Taiwan Pr.	5.8	-I	4	Keeluong I00 cm. Most prominent period 26 min.	I. SG.
22	I9I8.2.I3. I4:07	II7.0 24.0	7.3	1	4	Shantou, moderate tsunami.	1. ZA[I,2]
23	I92I.9.- -	Tainan City, Taiwan Pr.		0-I	-		ZA[I,2]
24	I92I.8.4. -	Dangdong City, Liaoning Pr.		0	-		ZA[I,2]
25	1966.3.13. -	I22.6 24.I NE of Hualien City, Taiwan Pr.	7.5	-I	4	Moderate tsunami killed 7 people.	I.
26	I978.7.23.	I2I.5 22.3 Taiwan Province	7.4	0-I	2	Hualienkang minor tsunami.	WDC-A,I.

To be continued

Continued Table I.

Note: * —Lunar Calendar

** —In the history of China Qi was a country which located in recent Shangdon Province.

*** — I li=0.5 km

Authors: L.— Lu Renji

I.— Iida Kumizi

SG.— Soloviev S. L. and Ch. N. Go

WDC-A— NGDC and WDC-A

ZA.— Zhou Qinghai and William M. Adams,1985 & 1987

Table 2. Probability rating used for the validity of a tsunami

rating 4: definite tsunami (probability approximately I.0)

rating 3: probable tsunami (probability approximately 0.75)

rating 2: questionable tsunami (probability approximately 0.50)

rating I: very doubtful tsunami (probability approximately 0.25)

rating 0: no tsunami (probability approximately 0.00)

Table 3. Tsunami magnitude,m on the Imamura-Iida scale

m	Tsunami height	Tsunami energy	Damage sustained
-I	≲50 cm	0.06×10^{22} erg	negligible damage
0	I m	0.25x	slight damage
I	2 m	Ix	damage to houses and boats
2	4—6 m	4x	los of human life and houses
3	I0 m	I6x	heavy damage along coast for about 400 km
4	≳30 m	64x	heavy damage along coast for more than 500 km

AN AUTOMATED CATALOGUE OF TSUNAMIS SUMMARY

A.Bobkov, C.Go, N.Zhigulina, K.Simonov
Institute of Marine Geology and Geophysics, Fast East Branch,
USSR Academy of Sciences, Yuzhno-Sakhalinsk, USSR

The purpose of a tsunami data catalogue, using magnetic carriers, is to ensure the users with all the available information on real events in a most natural form. And in this case access is provided to the original data as well as to their computer pre-processed form. The information part of the Automated Catalogue of Tsunamis consists of two files: a catalogue of tsunamigenic earthquakes (over 800 events), and a catalogue of observed tsunami heights (over 5000 records). The main sources for the Catalogue were "The Catalogue of Tsunamis in the Pacific Ocean" (Soloviev, Go, Kim, 1986) and "Directories of Pacific Coastal Sites Subjected to Tsunami Actions" (Soloviev, Go, 1978), compiled in the USSR. We also used materials compiled by scientists in Japan (Abe, Iida, Hatori, Kajiura, Watanabe), in USA (Pararas-Carayannis), and Canada (Wigen).

These catalogues contain data on tsunamis for the period of A.D. 173 to 1982. Materials for the period from 1983 up to present time are prepared for publication as a catalogue. At present, these catalogues contain data on tsunamis for the Pacific Ocean only. Work is carried out for the compilation of complete data for other tsunamigenic regions of the World Oceans (Caribbean and Mediterranean Seas, Atlantic and Indian Oceans).

The catalogue of tsunamigenic earthquakes contains the following data: dates and origin times of the earthquakes, hypocenter coordinates, magnitudes, numbers of the Pacific tsunamigenic zones, and estimates of tsunami intensities. Also, it may contain supplementary information on earthquake foci and tsunami sources.

The catalogue of observed tsunami heights contains the following information: zone number, locality (point) name, location of measurement, date and hour of the observation, and information on the wave height. Remarks contain other wave information, such as run-up, etc. Data on tsunami heights are presented in the catalogue in the form of two numbers: the minimum and maximum estimates of wave height, but there are possible cases when each of them may be absent.

Zone numbers, dates of events, and the map of the Pacific Ocean are common elements for both files.

All data are stored on the computer. This enables to work with the Catalogue in an interactive mode by means of a common dialogue system: recording of new lines, making corrections, supplementing lines with new information.

The dialogue system enables a user to fulfill many display operations with the data. By means of selection, sorting and combination commands, a user may create practically and subsets from the main data base. The system enables the simultaneous storage of four files. All the functions operate in an interactive mode. If an operator omits or misindicates a parameter, the system enters into a dialogue with him in order to clarify the meaning of the command.

In order to make selections, the numerical parameters are given as a range of values, and textual parameters as cliches. An additional command is needed for the selection of records that do not contain the parameter value. The selection function may operate with all the parameters simultaneously, but it may also work with all the parameters simultaneously or with one or any number of parameters at a time. Any functions can be applied not only to the initial data base, but also to a subset recorded earlier.

By means of special commands, for instance, one can select from the main base all data on earthquakes having magnitudes exceeding 7.3, that occurred from 6 to 8 a.m., or create a file of tsunami heights of 3 to 4.5 m from the event of 8 October 1883. The system selection potentialities are restricted only by the fact that all the parameters are considered independently one from the another, i.e. only the "rectangular" selections are created. If a possibility to work with at least paired parameters was introduced into the system, it would result in considerable complication and lower effectiveness of the system.

In order to perform the sorting of data, one indicates the names of parameters to be sorted and the sorting order (down or up) for each numerical parameter. One also indicates what has to be done with the records where the parameter value is absent. The system may put such records in the beginning or at the end of a file, and it can also omit them in creating a file. Textual parameters are always sorted in the order of the Russian alphabet. Sorting for several parameters is performed according to the common algorithm: data are first sorted according to the first of the parameters indicated by the user, records with coinciding values are sorted by the second parameter and so on.

Data, selected and sorted out, can be printed out, recorded in a file for further processing by independent programs or erased after being read by a user on the display. The main data base is protected from recording and erasing by the program.

A subsidiary dialogue system has been developed for further data processing. It consists of a small set of commands enabling it to make selections from the Catalogues, combine, classify and print out data in a specified form or plot them as graphs. The system also includes the possibility to use a set of applied programs to analyse specified data in order to solve specific problems of prompt and long-term predictions of tsunamis, and the tsunami zoning of a coastal zone.

This Catalogue can be used in solving applied problems of the tsunami problem especially in the tsunami forecast and tsunami risk evaluation and in the tsunami zoning

of a coastal region, including local tsunami risk prediction for a specific point of the coast.

References

Soloviev, S.L., Go, C.N., 1974. The Catalogue of Tsunamis for the West Coast of the Pacific Ocean. Nauka, M., 309 pp.

Soloviev, S.L., Go, C.N., 1975. The Catalogue of Tsunamis for the East Coast of the Pacific Ocean. Nauka, M., 203 pp.

Soloviev, S.L., Go, C.N., 1978. Directories of the Pacific Coastal Sites, Subjected to the Tsunami Actions. Part I, II. Yuzhno-Sakhalinsk, 55 pp.

Soloviev, S.L., Go, C.N., Kim, Kh.S., 1986. The Catalogue of Tsunamis of 1969-1982 in the Pacific Ocean. M., 163 pp.

Zone 15. Ecuador, Colombia, Panama

Point	Region	Data	Height (m)
Aquada	Panama	1884.11.05	
Amarales	Colombia	1906.01.31	
Bahia de Caraques	Ecuador	1906.01.31	0.90
Bahia Solano	Colombia	1964.03.27	0.20
Barbacoas	Colombia	1906.01.31	
Boca Grande	Colombia	1906.01.31	
Boquerones	Colombia	1906.01.31	
Buenaventura	Colombia	1877.10.11	
Buenaventura	Bay(Colombia)	1942.05.22	
Varela	Colombia	1906.01.31	
Galapagos	Is.(Ecuador)	1960.05.22	0.45
		1964.03.27	0.50
		1966.10.17	0.30
		1966.12.28	0.20
		1969.08.12	0.10
Gorgona	I.(Colombia)	1942.05.22	
		1979.12.12	
Guapi	Colombia	1906.01.31	
Guayaquil	Ecuador	1882.09.07	
		1906.01.31	
		1958.01.19	
Gulecama	Colombia	1906.01.31	
Domingo Ortiz	Colombia	1906.01.31	
Caballos	Colombia	1906.01.31	
Kabo-Manglares	Colombia	1906.01.31	
Cansara	Colombia	1906.01.31	
Quiroga	Colombia	1906.01.31	
Colon(Aspin Wall)	Panama	1883.08.27	0.35

DATA BASE FOR BRITISH COLUMBIA TSUNAMI WARNING SYSTEM

T.S. Murty and W.J. Rapatz
Institute of Ocean Sciences
Department of Fisheries and Oceans
P.O. Box 6000
Sidney, British Columbia V8L 4B2
Canada

ABSTRACT Maximum expected tsunami amplitudes, currents, and travel times to 185 locations on the coast of British Columbia from four different earthquake epicentres are tabulated. This information is used by the regional tidal superintendent in arriving at the advice that is provided to the Provincial Emergency Program in the case of a real tsunami event.

1. INTRODUCTION

Maximum tsunami water levels and currents along the British Columbia outer coast have been computed (Dunbar *et al.* 1989, 1990) for waves originating from Alaska, Chile, the Aleutian Islands (Shumagin Gap), and Kamchatka (Fig. 1). Three computer models have been developed to generate and propagate a tsunami from each of these source regions in the Pacific Ocean to the continental shelf off Canada's west coast, and into twenty separate inlet systems (Table 1, Figs. 2 and 3). The model predictions have been verified against water level measurements made at tide gauges after the March 28, 1964 Alaska earthquake. Simulated seabed motions giving rise to the Alaskan and Chilean tsunamis have been based on surveys of vertical displacements made after the great earthquakes of 1964 (Alaska) and 1960 (Chile). Hypothetical bottom motions have been used for the Shumagin Gap and Kamchatka simulations. These simulations represent the largest tsunamigenic events to be expected from these areas.

Maximum wave and current amplitudes and travel times have been tabulated for each simulated tsunami at 185 key locations (Table 2, Fig. 4) along the British Columbia coast (Tables 3 and 4). On the north coast of British Columbia, the Alaska tsunami generated the largest amplitudes. In all other regions of the west coast, the largest amplitudes were generated by the Shumagin Gap simulation (Table 5). Wave amplitudes in excess of 9 m were predicted at several locations along the coast and current speeds of 3 to 4 m/s were produced (Table 6). The most vulnerable regions are the outer coast of Vancouver Island, the west coast of Graham Island, and the central coast of the mainland. Some areas, such as the north central coast, are sheltered enough to limit expected maximum water levels to less than 3 m.

2. RESULTS

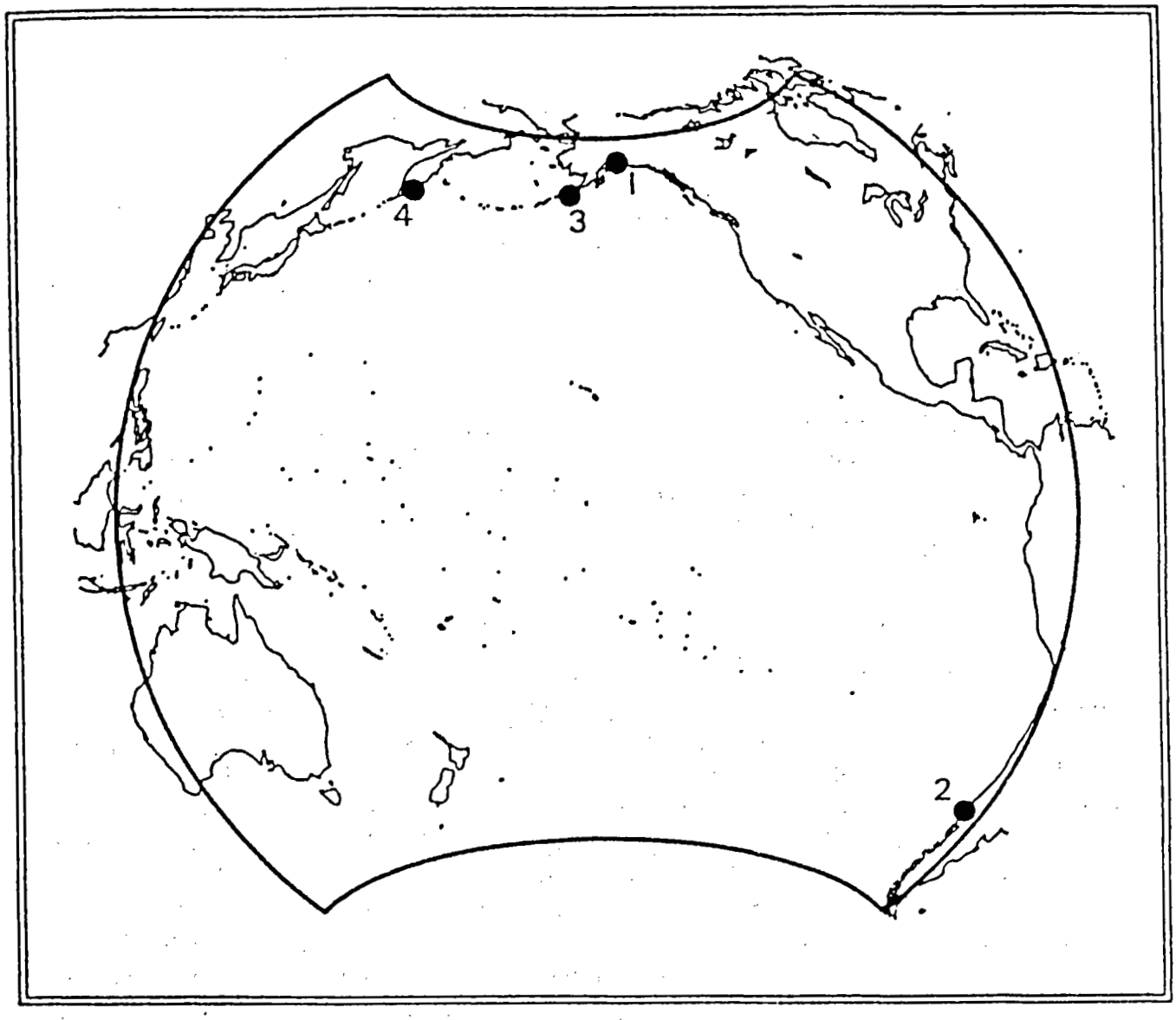

Fig. 1 Epicentres of earthquakes used in tsunami simulations. The bold line is the boundary of the deep ocean model (DOM). (1: Alaska, 2: Chile, 3: Shumagin Gap, 4: Kamchatka)

Table 1 British Columbia inlet systems included in tsunami simulations.

System	Areas Included	System	Areas Included
A	Portland Canal	J	Smith Inlet
	Observatory Inlet-Hastings Arm		
	Alice Arm	K	Mereworth Sound
	Khutzeymateen Inlet		Belize Inlet
	Work Channel		Nugent Sound
			Seymour Inlet
B	Prince Rupert Inlet		
		L	Holberg–Rupert Inlet
C	Rennell Sound		Quatsino Sound–Neroutsos Inlet
			Forward Inlet
D	Tasu Sound		
		M	Klaskino Inlet
E	Douglas Channel		
	Kildala Arm	N	Quoukinsh Inlet
	Gardner Canal		
	Sheep Passage–Mussel Inlet	O	Nuchalitz Inlet
F	Spiller Channel	P	Port Eliza
	Roscoe Inlet		Espinosa Inlet
	Cousins Inlet		Tahsis Inlet
	Cascade Inlet		Cook Channel–Tlupana Inlet
	Dean Channel		Zuciarte Channel–Muchalat Inlet
	Kwatna Inlet		
	South Bentinck Arm	Q	Sydney Inlet
			Shelter Inlet
G	Laredo Inlet		Herbert Inlet
H	Surf Inlet	R	Pipestem Inlet
I	Rivers Inlet	S	Effingham Inlet
	Moses Inlet		
		T	Alberni Inlet

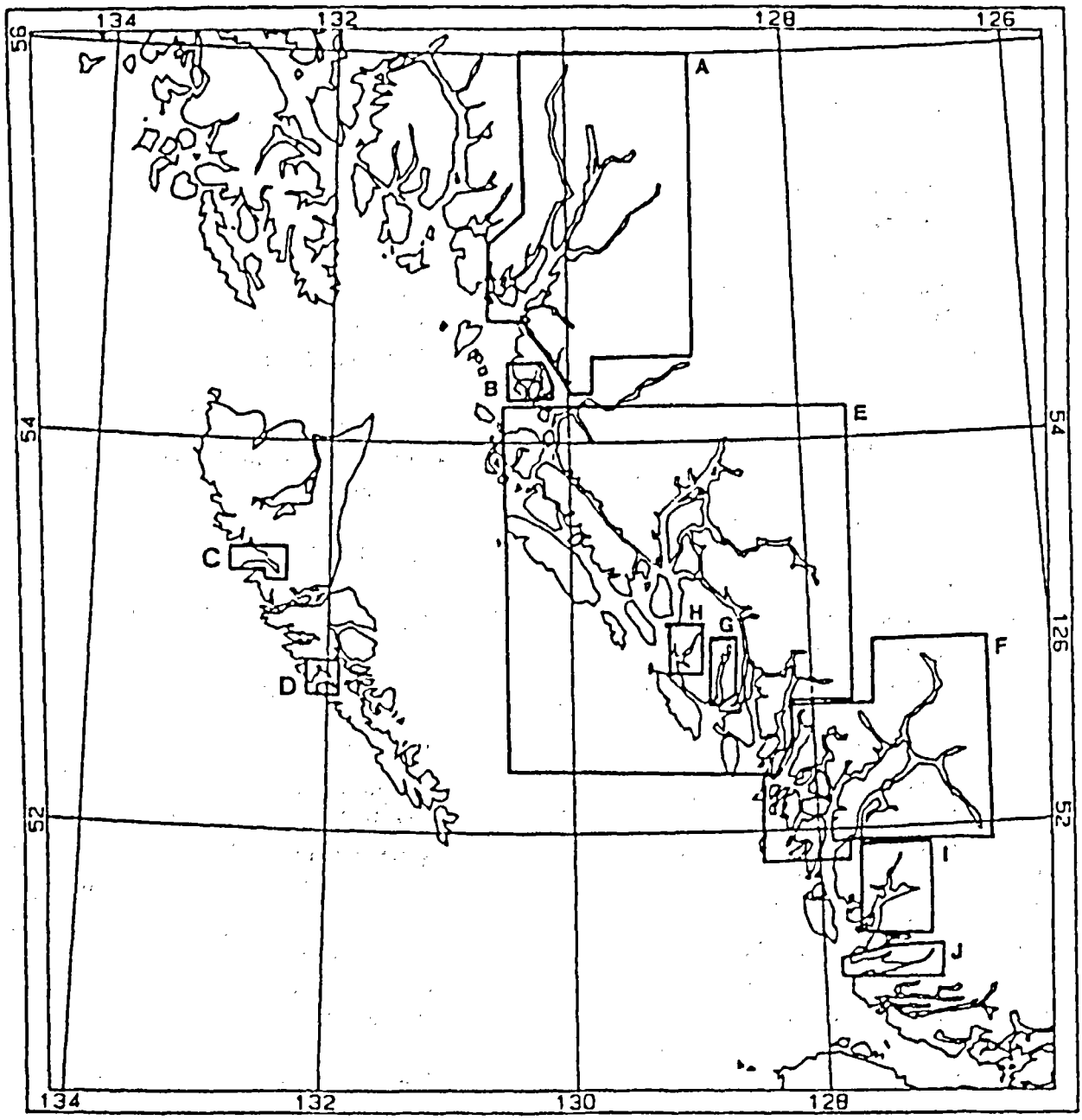

Fig. 2 Inlet systems for the north coast of British Columbia.

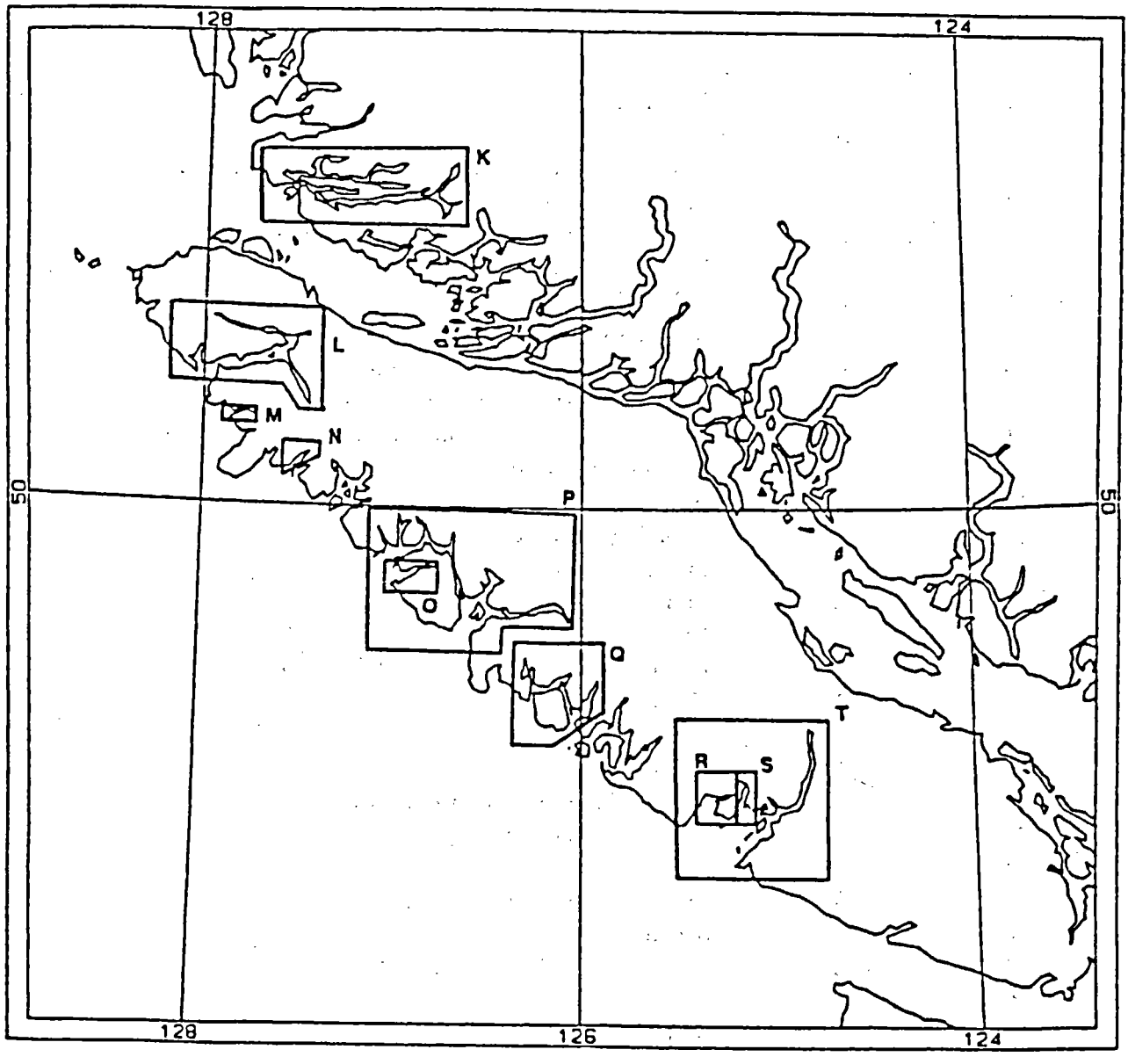

Fig. 3 Inlet systems for the south coast of British Columbia.

Table 2 Selected locations from the fjord model.

Number	Fjord System	Description
1	A	Indian Reserve
2	A	Indian Reserve
3	A	Indian Reserve at Grave Bay-Ensheshese River
4	A	Indian Reserve near Reservation Point
5	A	Indian Reserve at head of Quottoon Inlet
6	A	Indian Reserve/Pile
7	A	Indian Reserves
8	A	Indian Reserve
9	A	Indian Reserve at Union Inlet
10	A	Indian Reserve at Steamer Passage
11	A	Indian Reserve at Kumeon Bay
12	A	Booming Grounds
13	A	Booming Grounds
14	A	Booming Grounds
15	A	Indian Reserve
16	A	Indian Reserve
17	A	Gwent Cove
18	A	Arrandale/Indian Reserve at Bay Point
19	A	Kincolith
20	A	Indian Reserve
21	A	Indian Reserve
22	A	Indian Reserve at Salmon Cove
23	A	Indian Reserve at Stagoo Creek
24	A	Indian Reserve
25	A	Indian Reserve at Perry Bay
26	A	Kitsault
27	A	Alice Arm/Indian Reserve
28	A	Anyox
29	A	Indian Reserve
30	A	Indian Reserve at head of Hastings Arm
31	A	Indian Reserve at Whiskey Bay
32	A	Indian Reserve
33	A	Indian Reserve at George River
34	A	Hyder, Alaska
35	A	Stewart
36	A	Port Simpson
37	A	Indian Reserve near Reservation Point
38	A	Indian Reserve at Spakels Point
39	A	Indian Reserve
40	B	Indian Reserve at Venn Passage

Table 2 Continued

Number	Fjord System	Description
41	B	Oldfield
42	B	Port Edward
43	B	Seal Cove
44	B	Prince Rupert/Salt Lake Prov. Park/Damsite
45	B	Seal Cove
46	C	Last point in Rennell Sound
47	D	Floats
48	D	Magneson Point–Westrob Mines/Causeway /Ramp/Mooring/etc.
49	D	Mooring Chain at Hunger Harbour
50	E	Port Blackney
51	E	Klemtu
52	E	Butedale
53	E	Hartley Bay/Indian Reserve/Public Wharves
54	E	Kitkiata Inlet/Indian Reserve/Log Dump
55	E	Kemano Bay/Steamer Landing
56	E	Kitlope Anchorage
57	E	Kildala Arm
58	E	Kitimat
59	E	Port Essington
60	E	Kitkatla
61	E	Oona River
62	F	North Pulpwoods Ltd./Logging Camp/etc. on South Bentinck Arm
63	F	Bella Coola
64	F	Kimsquit (abandoned)
65	F	Ocean Falls
66	F	Indian Reserve at Clatse Creek
67	F	Indian Reserve
68	F	Shearwater
69	F	Indian Reserves
70	F	Indian Reserve
71	F	Indian Reserve at Kyarti
72	F	Bella Bella/New Bella Bella
73	F	Cabin/Ruins near head of Spiller Inlet
74	F	Namu
75	G	Head of Laredo Inlet
76	H	Head of Surf Inlet leading to Belmont Surf Inlet Mine
77	I	Duncanby Landing

Table 2 Continued

Number	Fjord System	Description
78	I	Wadhams/P.O./ Union Oil Co.
79	I	Dawson Landing/Oil Tanks
80	I	Brunswick Cannery at Sandell Bay
81	I	Shell Oil Tanks at Scandinavia Bay
82	I	Rivers Inlet Cannery at the head of Rivers Inlet
83	I	Head of Hardy Inlet
84	I	Head of Moses Inlet
85	I	Good Hope
86	J	Imperial Oil Co. store at Boswell
87	J	Nalos Landing
88	J	Last point in Branch 7–Ahclakerho Channel
89	J	Wyclese Indian Reserve
90	K	Village Cove
91	K	Village Cove
92	K	Chief Nollis Bay
93	K	Holmes Point
94	K	Eclipse Narrows
95	K	Holmes Point
96	K	Eclipse Narrows
97	L	Indian Reserve
98	L	Indian Reserve
99	L	"A" Frame/Log Dump/Wharf at Mahatta River
100	L	Customs Office
101	L	Jeune Landing/Wharf/Piles/"A" Frame
102	L	Rumble Beach/Yacht Club/Booming Ground
103	L	Port Alice
104	L	Indian Reserve/Booming Ground
105	L	Indian Reserve
106	L	Indian Reserve
107	L	Indian Reserve
108	L	Island Copper Mines at Rupert Inlet
109	L	Coal Harbour
110	L	Barge/Ramp/Float
111	L	Indian Reserve
112	L	Holberg/"A" Frame
113	L	Indian Reserve
114	L	Winter Harbour
115	L	Indian Reserve/Booming Ground
116	L	Government Wharf/Float/etc. at Bergh Inlet
117	M	Klaskino Anchorage

Table 2 Continued

Number	Fjord System	Description
118	M	Head of Klaskino Inlet
119	N	Indian Reserve at head of Ououkinsh Inlet
120	N	Indian Reserve at Byers Cove
121	O	Port Langford
122	O	Indian Reserve at narrows between here and next point
123	O	Indian Reserve at narrows between here and last point
124	O	Indian Reserve at head of Nuchatlitz Inlet
125	O	Indian Reserve
126	P	Nootka/Piles
127	P	Indian Reserve/Log Dump at Mooyah Bay
128	P	Log Dump
129	P	Gold River/Tahsis Pulp Mill
130	P	Indian Reserve/Log Dump at Matchlee Bay
131	P	Indian Reserve
132	P	Indian Reserve
133	P	Indian Reserve
134	P	Indian Reserves
135	P	Indian Reserve/Log Dump
136	P	Plumper Harbour/Log Dump
137	P	Indian Reserve
138	P	Indian Reserve/Booming Ground
139	P	Float/Pier/Booming Ground at Blowhole Bay
140	P	Boat House/Building/"A" Frame/Booming Ground
141	P	Tahsis/Barge/Mooring/Indian Reserve/Float /Public Wharves/Booming Ground
142	P	Indian Reserve/Float
143	P	Indian Reserve at head of Port Eliza
144	P	Indian Reserve/Road/Float at Little Espinosa Inlet
145	P	Indian Reserve
146	P	Booming Ground/Float
147	P	Indian Reserve at Graveyard Bay
148	P	Ehatisaht (abandoned)/Indian Reserve
149	P	Indian Reserve
150	P	Float
151	P	Zeballos/Public Wharves/Indian Reserve/Float /Seaplane Float
152	P	Yuquot/Public Wharves
153	P	Indian Reserve at Catala Island
154	P	Indian Reserve

Table 2 Concluded

Number	Fjord System	Description
155	P	Hecate (abandoned)/Esperanza/Ways Float /Imperial Oil/Public Wharves
156	Q	Indian Reserve
157	Q	Indian Reserve at head of Sydney Inlet
158	Q	Stewardson Inlet
159	Q	Indian Reserve at head of Shelter Inlet
160	Q	Indian Reserve at head of Herbert Inlet at Moyeha Bay/Moyeha River
161	Q	Indian Reserve
162	Q	Indian Reserve at Megin River
163	Q	Ahousat/Public Wharves/Chevron
164	R	Indian Reserve at Toquart River
165	R	Head of Pipestem Inlet
166	S	Indian Reserve at Coeur d'Alene Inlet
167	S	Booms at head of Effingham Inlet
168	S	Indian Reserve
169	T	Indian Reserve
170	T	Indian Reserve
171	T	Indian Reserve
172	T	Indian Reserves at Rainy Bay and Ecole in Rainy Bay
173	T	Fishpen/Public Wharves at San Mateo Bay
174	T	Green Cove/Piles/Booms
175	T	Kildonan/Piles/Booms
176	T	Booms/Indian Reserve at Snug Basin
177	T	Indian Reserve at Nahmint River
178	T	Public Wharves
179	T	Sproat Narrows/Piles/Fishpen/Booms
180	T	Fishpens at Underwood Cove
181	T	China Creek Provincial Park
182	T	Floats/Indian Reserve at Stamp Narrows
183	T	Fog Signal/Indian Reserve at Iso River/Polly Point
184	T	Port Alberni
185	T	Indian Reserve

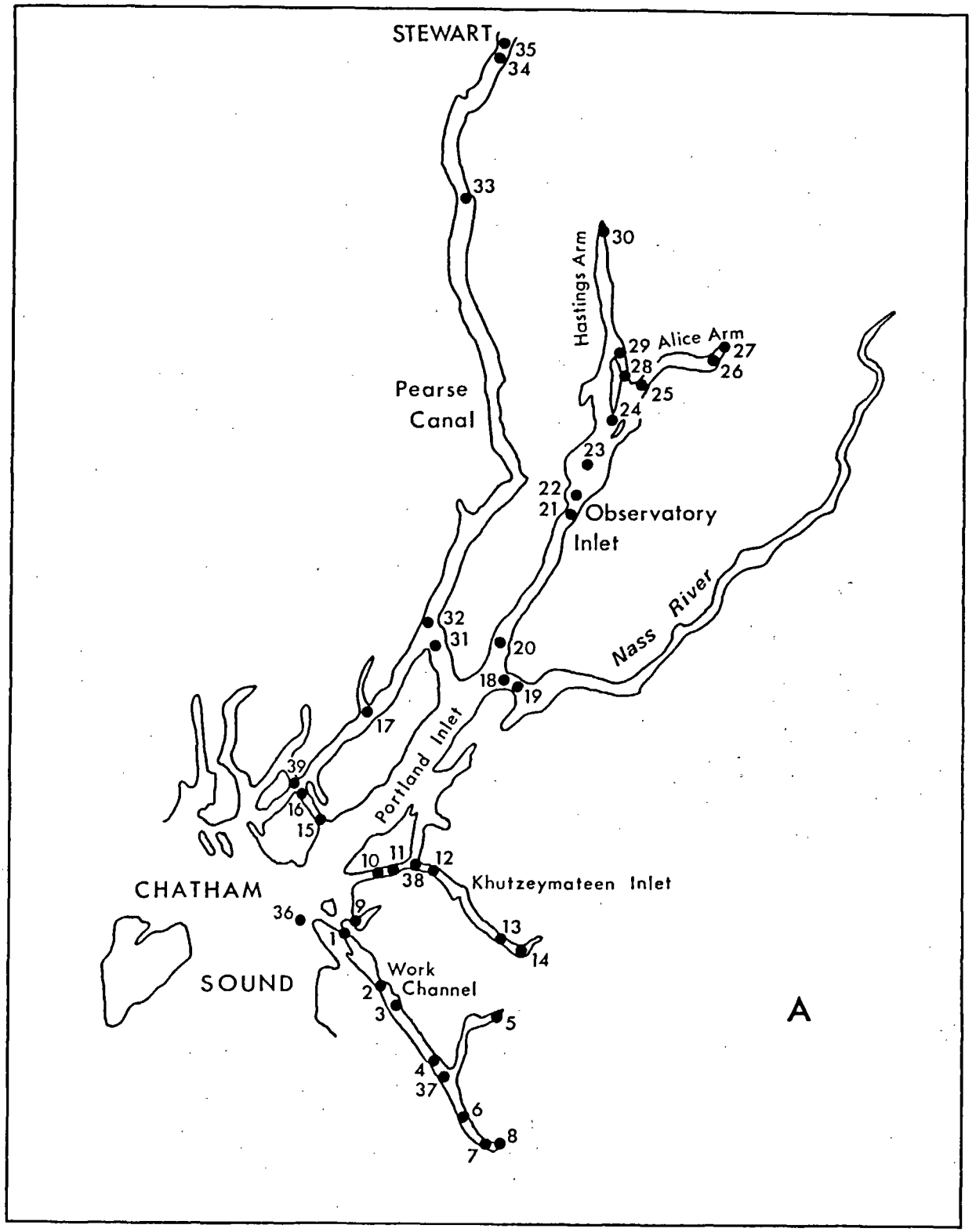

Fig. 4 Map showing water level and current locations listed in Table 2.

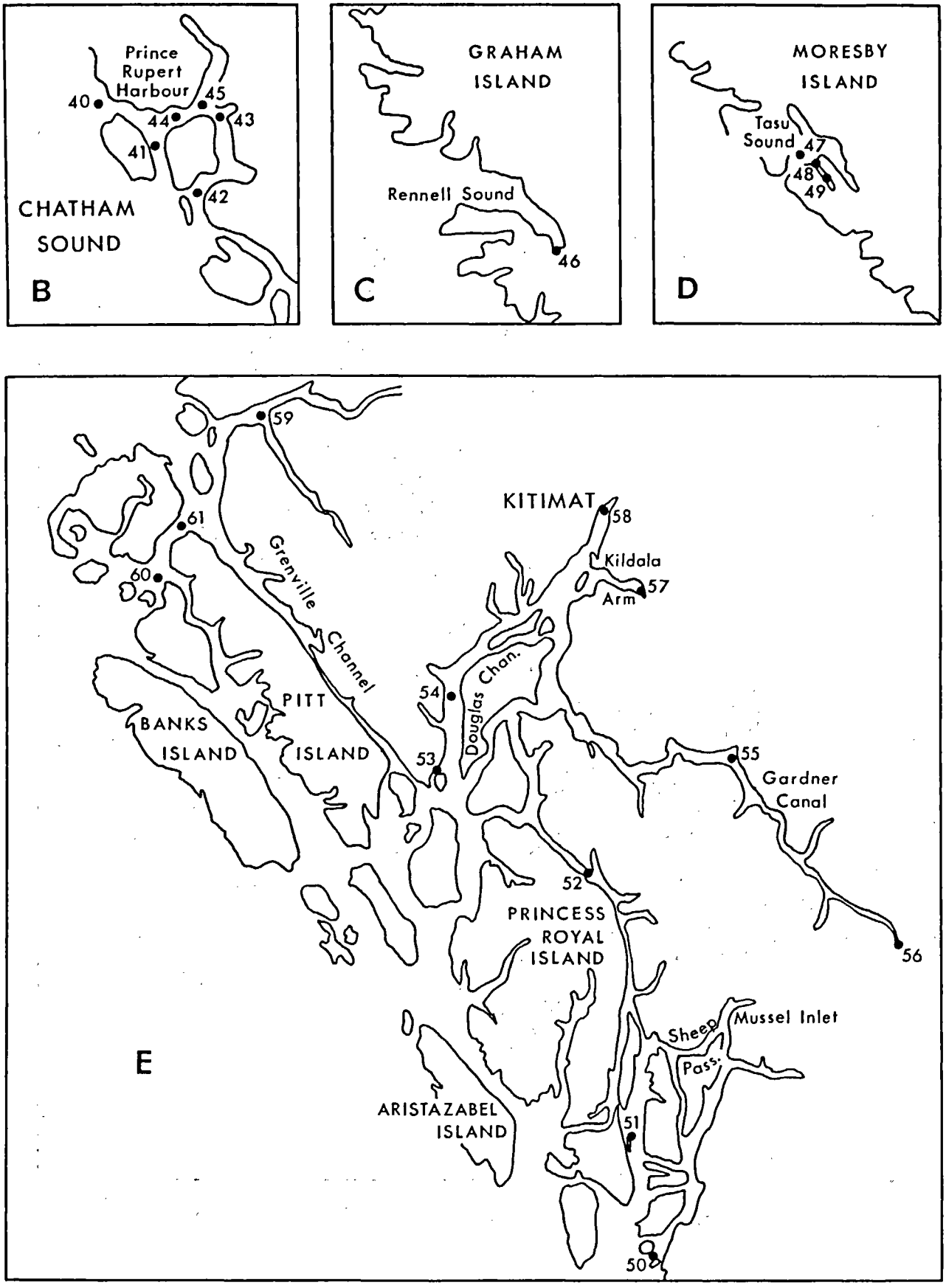

Fig. 4 Continued

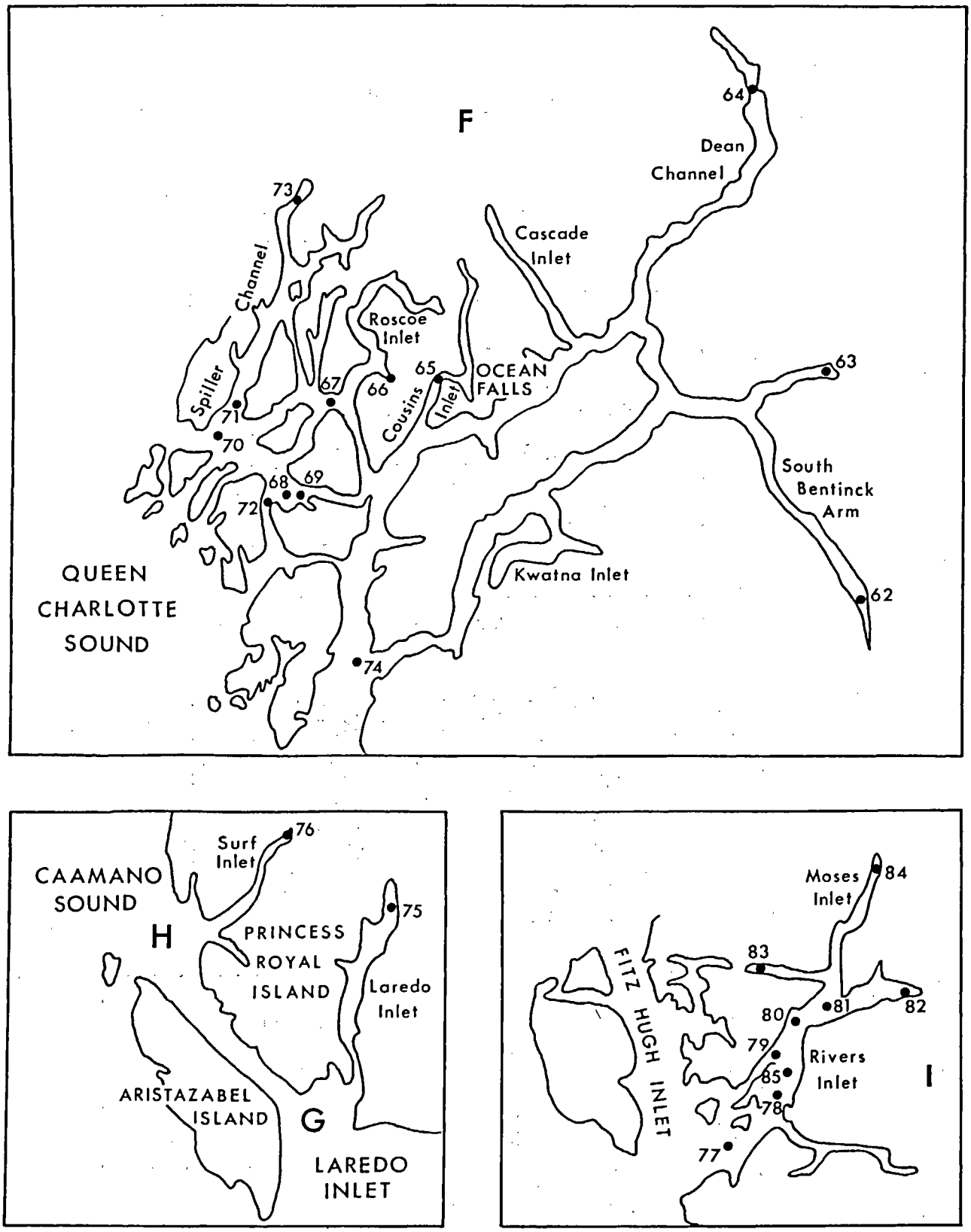

Fig. 4 Continued

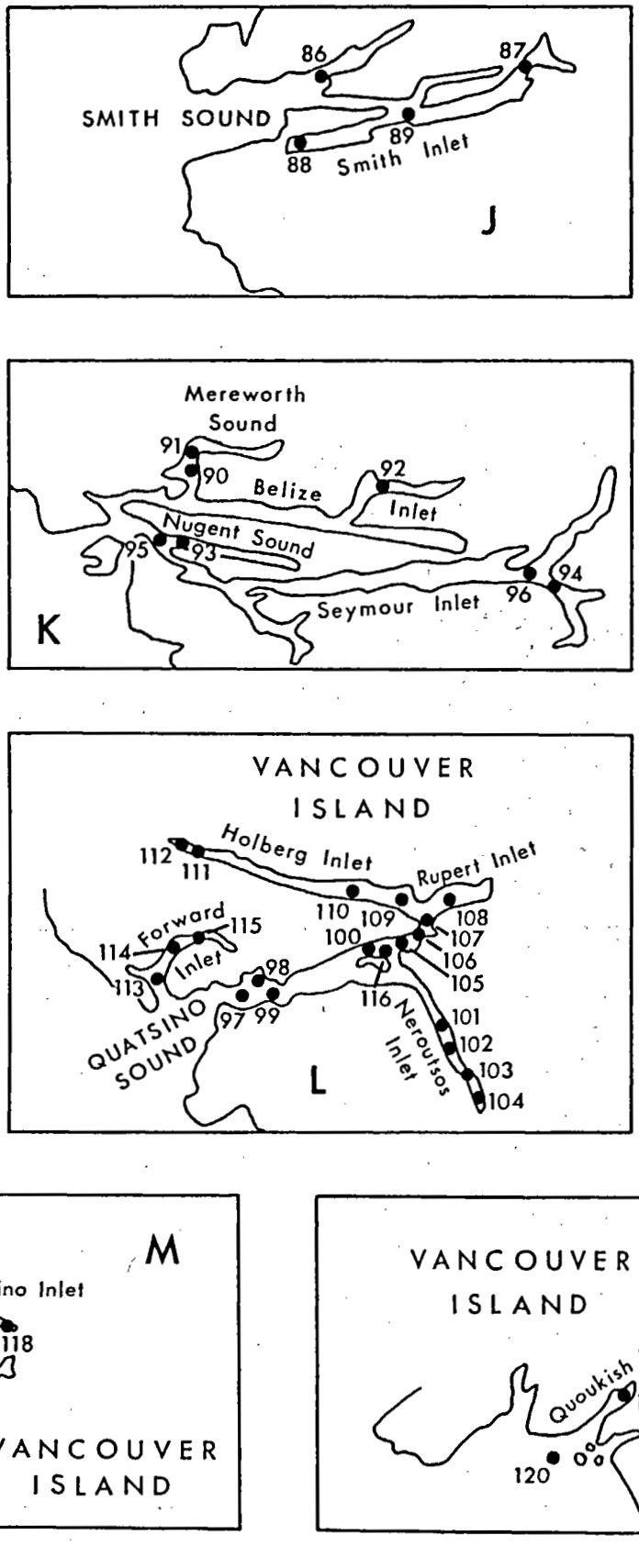

Fig. 4 Continued

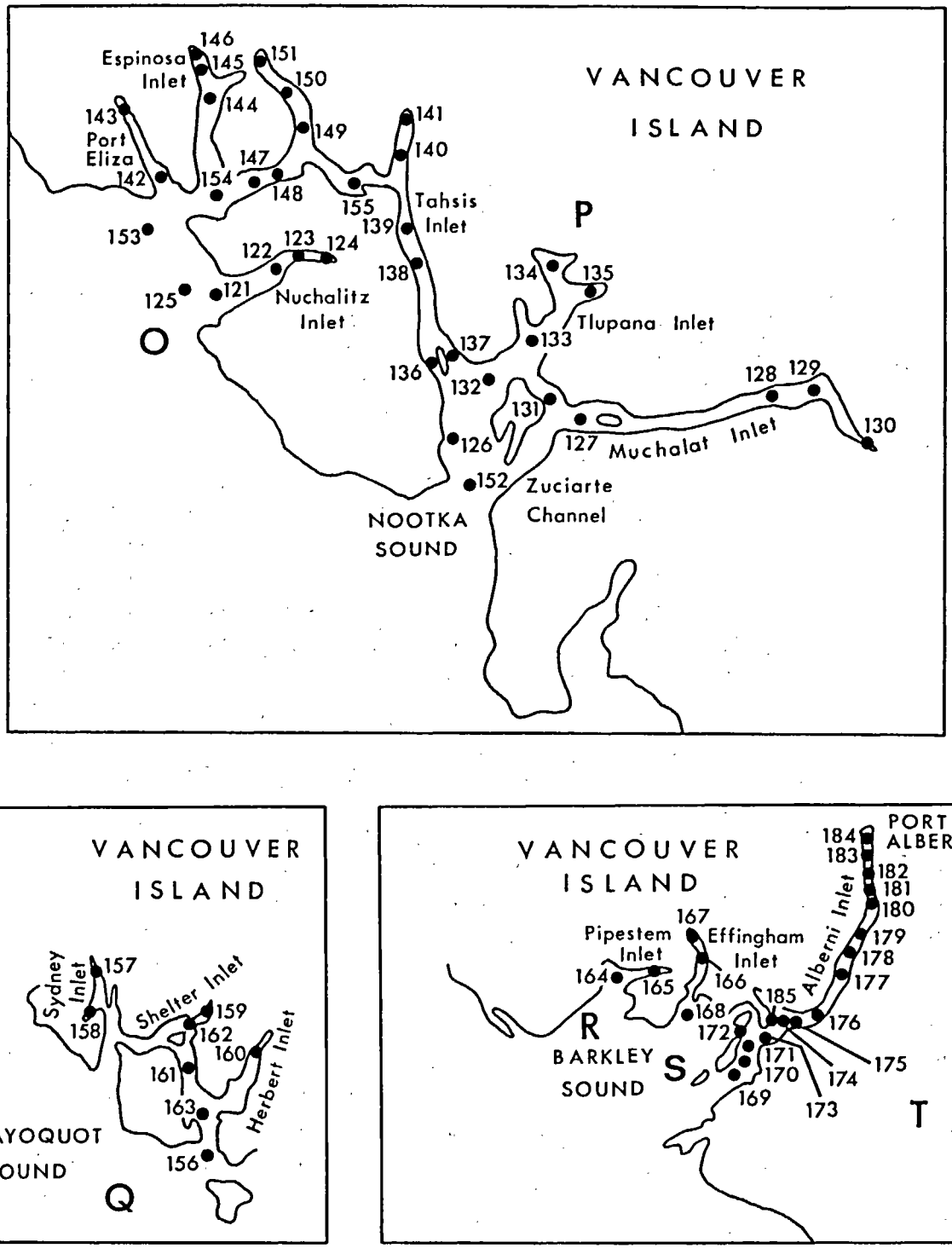

Fig. 4 Concluded

Table 3 Maximum tsunami water levels and currents on the British Columbia Coast for sources: 1a: 1964 Alaska earthquake, 1b: 1964 Alaska earthquake intensified by 25%, 2: May 1960 Chile earthquake, 3: Shumagin, 4: Kamchatka.

Location Number	Inlet System	Source Region					Source Region				
		1a	1b	2	3	4	1a	1b	2	3	4
		Water Level (m)					Current Speed (m/s)				
1	A	0.6	0.7	0.0	0.6	0.2	1.15	1.32	0.02	1.13	0.41
2	A	0.7	0.9	0.0	0.8	0.3	0.13	0.15	0.00	0.12	0.05
3	A	0.8	0.9	0.0	0.8	0.3	0.12	0.13	0.00	0.11	0.04
4	A	0.8	1.0	0.0	0.8	0.3	0.09	0.10	0.00	0.08	0.03
5	A	1.1	1.3	0.0	0.9	0.4	0.04	0.04	0.00	0.04	0.01
6	A	0.8	1.0	0.0	0.9	0.3	0.08	0.10	0.00	0.09	0.03
7	A	0.9	1.0	0.0	0.9	0.3	0.05	0.06	0.00	0.06	0.02
8	A	0.9	1.1	0.0	0.9	0.3	0.04	0.04	0.00	0.04	0.01
9	A	1.6	1.8	0.0	1.6	0.3	0.59	0.69	0.01	0.64	0.11
10	A	1.7	1.9	0.0	1.7	0.4	1.11	1.27	0.02	0.83	0.20
11	A	1.9	2.1	0.0	1.9	0.4	1.08	1.25	0.01	0.84	0.19
12	A	2.3	2.6	0.0	2.1	0.5	0.14	1.36	0.02	1.13	0.26
13	A	3.0	3.5	0.0	2.6	0.6	0.18	0.20	0.00	0.20	0.04
14	A	3.0	3.5	0.0	3.0	0.7	0.10	0.11	0.00	0.12	0.03
15	A	1.2	1.3	0.0	1.1	0.3	0.22	0.26	0.00	1.29	0.07
16	A	1.3	1.5	0.0	1.5	0.5	0.50	0.57	0.01	0.44	0.08
17	A	1.6	1.9	0.0	1.0	0.2	0.30	0.36	0.00	0.32	1.08
18	A	1.4	1.7	0.0	0.9	0.2	0.12	0.15	0.00	0.14	0.04
19	A	1.4	1.7	0.0	0.9	0.2	0.39	0.49	0.01	1.42	0.10
20	A	1.3	1.6	0.0	0.9	0.2	1.87	2.30	0.02	1.69	0.37
21	A	1.9	2.4	0.0	1.7	0.3	0.50	0.62	0.01	0.47	0.10
22	A	2.0	2.5	0.0	1.8	0.3	0.51	0.63	0.01	0.48	0.11
23	A	2.1	2.7	0.0	1.9	0.3	0.17	0.21	0.00	0.16	0.04
24	A	2.3	2.9	0.0	2.1	0.4	0.49	0.60	0.01	0.46	0.11
25	A	1.6	2.0	0.0	1.4	0.3	1.01	1.15	0.03	0.96	0.36
26	A	1.8	2.2	0.0	1.5	0.4	0.08	0.09	0.00	0.08	0.02
27	A	1.8	2.2	0.0	1.5	0.4	0.05	0.06	0.00	0.05	0.02
28	A	2.5	3.1	0.0	2.2	0.4	0.23	0.28	0.00	0.20	0.04
29	A	2.7	3.3	0.0	2.2	0.4	0.33	0.41	0.01	0.33	0.07
30	A	2.8	3.4	0.0	2.4	0.5	0.07	0.09	0.00	0.09	0.02
31	A	1.6	1.9	0.0	1.1	0.2	0.44	0.54	0.01	0.36	0.08
32	A	1.6	1.9	0.0	1.1	0.2	0.44	0.54	0.01	0.36	0.08
33	A	2.8	3.4	0.0	1.9	0.3	0.30	0.35	0.00	0.26	0.06
34	A	3.2	4.0	0.0	2.2	0.4	0.17	0.22	0.00	0.19	0.03

Table 3 Continued

Location Number	Inlet System	Source Region					Source Region				
		1a	1b	2	3	4	1a	1b	2	3	4
		Water Level (m)					Current Speed (m/s)				
35	A	3.3	4.1	0.0	2.3	0.4	0.23	0.29	0.00	0.25	0.04
36	A	0.9	1.1	0.0	0.8	0.2	—	—	—	—	—
37	A	0.8	1.0	0.0	0.8	0.3	—	—	—	—	—
38	A	2.1	2.3	0.0	2.0	0.4	—	—	—	—	—
39	A	1.6	1.8	0.0	1.3	0.3	—	—	—	—	—
40	B	0.7	0.8	0.0	0.7	0.2	0.31	0.35	0.03	0.39	0.12
41	B	1.8	2.2	0.0	1.7	0.3	1.29	1.52	0.04	1.25	0.26
42	B	1.5	1.7	0.0	1.2	0.3	0.94	1.10	0.07	1.40	0.29
43	B	0.7	0.8	0.0	0.6	0.2	0.14	0.16	0.02	0.11	0.05
44	B	1.9	2.3	0.0	1.7	0.3	0.53	0.61	0.02	0.77	0.12
45	B	2.3	2.7	0.0	1.8	0.3	—	—	—	—	—
46	C	—	—	—	—	—	—	—	—	—	—
47	D	1.8	1.9	0.1	2.0	0.7	0.28	0.31	0.03	0.39	0.11
48	D	1.9	2.0	0.1	2.0	0.7	0.12	0.13	0.01	0.24	0.07
49	D	2.1	2.2	0.2	2.4	0.7	0.24	0.29	0.03	0.54	0.16
50	E	1.4	1.7	0.3	3.5	0.8	0.70	0.84	0.05	0.81	0.36
51	E	2.4	2.9	0.4	4.3	1.3	0.73	0.86	0.17	1.22	0.42
52	E	2.5	3.1	0.1	3.3	0.7	0.47	0.57	0.03	0.62	0.11
53	E	1.1	1.3	0.1	1.0	0.2	0.05	0.06	0.00	0.08	0.03
54	E	1.1	1.4	0.1	1.5	0.5	0.30	0.36	0.01	0.46	0.10
55	E	1.2	1.5	0.1	1.4	0.4	0.12	0.15	0.01	0.18	0.06
56	E	1.8	2.2	0.2	2.3	0.7	0.04	0.05	0.00	0.05	0.03
57	E	1.2	1.5	0.2	2.5	0.8	0.04	0.04	0.01	0.05	0.03
58	E	1.2	1.4	0.1	1.9	0.4	0.02	0.03	0.00	0.03	0.02
59	E	1.1	1.2	0.1	1.0	0.4	0.25	0.27	0.04	0.28	0.17
60	E	1.3	1.6	0.1	1.3	0.4	—	—	—	—	—
61	E	1.7	1.9	0.0	1.6	0.3	—	—	—	—	—
62	F	2.0	2.3	0.1	3.0	0.4	0.19	0.22	0.01	0.17	0.07
63	F	1.5	1.8	0.2	2.2	0.6	0.03	0.03	0.01	0.05	0.01
64	F	1.2	1.5	0.2	2.0	0.3	0.48	0.58	0.07	0.79	0.25
65	F	2.7	3.3	0.3	4.2	3.1	0.27	0.33	0.03	0.28	0.27
66	F	1.7	2.1	0.1	1.9	0.6	0.84	1.02	0.04	0.67	0.26
67	F	2.0	2.4	0.2	1.1	0.8	1.10	1.34	0.06	1.15	0.30
68	F	1.6	2.0	0.2	2.4	0.7	0.78	0.97	0.07	0.67	0.35
69	F	2.0	2.5	0.2	2.8	0.9	0.74	0.92	0.07	0.82	0.43
70	F	1.6	1.9	0.1	1.9	0.4	0.46	0.55	0.02	0.26	0.15
71	F	1.8	2.1	0.1	2.0	0.6	0.83	1.00	0.05	0.78	0.37
72	F	1.8	2.2	0.1	2.8	0.7	0.97	1.18	0.12	1.24	0.58

Table 3 Continued

Location Number	Inlet System	Source Region					Source Region				
		1a	1b	2	3	4	1a	1b	2	3	4
		Water Level (m)					Current Speed (m/s)				
73	F	5.9	7.2	0.3	4.0	3.4	0.54	0.66	0.04	0.35	0.36
74	F	1.0	1.3	0.1	1.2	0.5	—	—	—	—	—
75	F	3.7	4.4	0.4	5.6	1.5	0.16	0.20	0.03	0.47	0.13
76	F	2.2	2.5	0.3	3.3	1.5	0.14	0.17	0.02	0.24	0.14
77	I	1.9	2.2	0.1	3.1	1.3	0.75	0.89	0.03	0.83	0.21
78	I	1.8	2.1	0.1	2.7	1.2	0.63	0.73	0.03	0.80	0.19
79	I	2.3	2.8	0.1	2.8	1.5	1.16	1.43	0.10	1.73	0.52
80	I	2.2	2.7	0.1	2.4	1.2	0.57	0.69	0.03	0.83	0.17
81	I	2.5	3.0	0.1	3.3	1.1	0.60	0.72	0.04	0.85	0.18
82	I	3.1	3.6	0.2	5.0	1.5	0.08	0.09	0.01	0.11	0.04
83	I	4.7	5.6	0.2	5.3	1.6	0.16	0.18	0.01	0.15	0.05
84	I	5.9	7.2	0.3	9.2	5.1	0.13	0.15	0.01	0.19	0.16
85	I	1.8	2.2	0.1	2.3	1.2	—	—	—	—	—
86	J	3.4	4.1	0.4	4.6	3.5	0.89	1.09	0.16	1.16	0.90
87	J	7.6	9.3	0.4	8.4	2.2	1.31	1.64	0.25	1.66	0.81
88	J	1.2	1.4	0.2	1.2	0.4	0.03	0.03	0.01	0.04	0.01
89	J	4.9	6.0	0.4	5.0	1.3	—	—	—	—	—
90	K	0.1	0.1	0.0	0.1	0.0	0.07	0.09	0.01	0.13	0.08
91	K	0.1	0.1	0.0	0.1	0.0	0.06	0.07	0.01	0.09	0.08
92	K	0.1	0.1	0.0	0.1	0.0	0.01	0.01	0.00	0.01	0.01
93	K	0.3	0.3	0.0	0.5	0.2	0.39	0.45	0.04	0.56	0.20
94	K	0.0	0.1	0.0	0.0	0.0	0.01	0.01	0.00	0.01	0.01
95	K	0.3	0.3	0.0	0.6	0.3	—	—	—	—	—
96	K	0.1	0.1	0.0	0.1	0.1	—	—	—	—	—
97	L	1.7	2.1	0.5	7.2	2.4	1.09	1.37	0.14	1.79	1.39
98	L	1.9	2.1	0.5	7.2	2.4	1.18	1.48	0.11	1.66	1.51
99	L	2.2	2.5	0.5	6.1	2.5	1.16	1.40	0.11	2.35	1.40
100	L	2.7	3.5	0.4	6.7	4.0	0.94	1.11	0.19	2.46	0.89
101	L	3.0	3.7	0.4	5.4	3.6	0.67	0.84	0.10	1.68	1.24
102	L	3.1	3.9	0.3	5.5	4.2	1.03	1.25	0.18	2.65	1.83
103	L	3.9	4.7	0.5	9.1	7.2	2.77	3.13	0.57	5.76	4.30
104	L	—	—	—	—	—	—	—	—	—	—
105	L	3.5	3.9	0.5	8.5	4.2	1.26	1.42	0.30	2.50	1.55
106	L	3.8	4.3	0.7	7.9	4.8	1.41	1.65	0.22	2.84	1.16
107	L	3.3	3.7	0.7	8.1	4.4	2.60	2.92	0.42	4.71	3.00
108	L	0.7	0.9	0.1	1.2	0.8	0.18	0.21	0.04	0.26	0.17
109	L	0.3	0.4	0.0	0.8	0.4	0.29	0.33	0.02	0.23	0.33
110	L	0.7	0.8	0.1	1.0	0.9	0.26	0.30	0.03	0.25	0.28

Table 3 Continued

Location Number	Inlet System	Source Region					Source Region				
		1a	1b	2	3	4	1a	1b	2	3	4
		Water Level (m)					Current Speed (m/s)				
111	L	1.2	1.4	0.1	1.3	1.1	0.06	0.07	0.01	0.14	0.06
112	L	2.1	2.3	0.2	3.4	2.3	1.22	1.35	0.18	2.27	1.25
113	L	2.5	2.7	0.3	6.1	2.8	2.04	2.29	0.29	3.72	2.02
114	L	5.3	6.1	0.8	9.6	6.1	9.47	12.76	0.90	21.42	9.65
115	L	—	—	—	—	—	—	—	—	—	—
116	L	2.7	3.2	0.4	7.0	3.7	—	—	—	—	—
117	M	3.0	3.7	0.4	5.5	2.3	2.08	2.40	0.45	2.99	2.32
118	M	4.2	5.0	0.7	5.7	3.7	0.37	0.43	0.09	0.97	0.50
119	N	8.6	10.1	1.2	13.0	4.6	0.80	0.98	0.13	2.29	1.04
120	N	1.3	1.6	0.3	3.9	1.7	—	—	—	—	—
121	O	2.1	2.6	0.3	3.3	1.2	0.76	0.91	0.17	1.93	0.98
122	O	3.3	3.8	0.6	4.4	1.7	0.56	0.62	0.12	1.22	0.40
123	O	0.2	0.2	0.0	0.2	0.1	0.02	0.03	0.01	0.04	0.02
124	O	0.2	0.2	0.0	0.2	0.1	0.00	0.00	0.00	0.01	0.00
125	O	1.9	2.4	0.3	2.9	1.1	—	—	—	—	—
126	P	1.7	2.1	0.2	2.9	2.3	0.74	0.91	0.06	1.76	1.06
127	P	2.4	3.0	0.2	4.5	1.8	1.33	1.64	0.13	2.66	0.47
128	P	5.9	7.3	0.4	10.6	1.6	0.33	0.40	0.04	0.86	0.18
129	P	6.1	7.5	0.4	10.8	1.70	0.13	0.16	0.02	0.36	0.09
130	P	6.5	8.0	0.4	11.1	2.2	0.22	0.26	0.03	0.68	0.24
131	P	1.9	2.3	0.2	3.0	1.8	1.25	1.53	0.11	2.59	0.80
132	P	1.6	2.0	0.2	4.2	1.8	0.71	0.88	0.06	1.69	0.81
133	P	2.2	2.7	0.2	8.4	3.3	1.14	1.40	0.08	3.53	1.54
134	P	3.5	4.1	0.3	10.3	6.0	0.51	0.63	0.03	1.65	0.87
135	P	3.7	4.3	0.3	11.1	6.4	0.42	0.53	0.03	1.89	0.77
136	P	2.1	2.6	0.2	4.7	2.8	0.51	0.60	0.07	1.85	0.86
137	P	1.8	2.2	0.1	3.5	2.1	1.31	1.62	0.24	2.30	0.64
138	P	1.8	2.1	0.3	2.3	1.2	0.75	0.88	0.11	1.42	0.54
139	P	1.9	2.2	0.3	2.7	1.3	0.31	0.36	0.04	0.75	0.25
140	P	1.9	2.3	0.3	2.9	1.2	0.10	0.12	0.02	0.31	0.12
141	P	2.0	2.3	0.3	3.10	1.30	0.06	0.08	0.02	0.21	0.08
142	P	1.6	1.9	0.1	3.6	0.9	1.25	1.48	0.20	1.87	1.19
143	P	2.9	3.3	0.5	4.7	2.8	0.49	0.55	0.10	1.18	0.60
144	P	3.8	4.6	0.3	5.2	1.8	0.52	0.63	0.06	1.21	0.38
145	P	4.5	5.4	0.4	6.8	2.2	0.45	0.54	0.05	1.11	0.34
146	P	4.7	5.6	0.4	7.6	2.3	0.36	0.43	0.04	0.91	0.27
147	P	2.2	2.7	0.1	3.4	1.0	0.66	0.82	0.09	1.15	0.61
148	P	2.1	2.7	0.1	3.5	1.0	0.73	0.89	0.10	1.30	0.68

Table 3 Concluded

Location Number	Inlet System	Source Region					Source Region				
		1a	1b	2	3	4	1a	1b	2	3	4
		Water Level (m)					Current Speed (m/s)				
149	P	2.7	3.4	0.3	4.4	2.2	0.48	0.56	0.05	0.97	0.43
150	P	3.4	4.2	0.4	5.3	2.6	0.59	0.68	0.07	1.21	0.53
151	P	3.9	4.8	0.4	6.1	2.9	0.25	0.30	0.03	0.51	0.23
152	P	1.6	1.9	0.2	3.6	2.0	—	—	—	—	—
153	P	1.2	1.6	0.1	3.1	0.9	—	—	—	—	—
154	P	2.2	2.7	0.2	3.2	1.3	—	—	—	—	—
155	P	2.4	3.0	0.3	5.5	2.7	—	—	—	—	—
156	Q	0.8	0.9	0.1	1.4	0.6	0.65	0.74	0.09	1.31	0.73
157	Q	1.8	2.3	0.3	3.8	1.4	0.10	0.12	0.03	0.41	0.12
158	Q	1.7	2.2	0.3	3.1	1.2	0.07	0.08	0.02	0.21	0.08
159	Q	1.1	1.4	0.1	2.8	1.0	0.05	0.06	0.01	0.18	0.05
160	Q	0.8	0.9	0.1	1.5	0.6	0.03	0.04	0.00	0.07	0.02
161	Q	0.7	0.8	0.1	0.9	0.4	0.29	0.33	0.05	0.35	0.16
162	Q	1.0	1.4	0.1	2.5	0.9	—	—	—	—	—
163	Q	0.8	0.9	0.1	1.1	0.3	0.00	0.00	0.00	0.00	0.00
164	R	2.2	2.7	0.4	7.6	2.9	0.46	0.55	0.11	3.70	1.25
165	R	3.0	3.6	0.4	5.2	2.3	0.18	0.22	0.06	0.95	0.43
166	S	2.3	3.1	0.3	4.5	1.2	0.22	0.25	0.02	0.33	0.17
167	S	2.6	3.3	0.3	4.1	1.5	0.13	0.14	0.02	0.25	0.14
168	S	2.0	2.5	0.2	3.1	0.9	—	—	—	—	—
169	T	2.7	3.0	0.2	2.4	1.4	0.74	0.89	0.07	0.93	0.29
170	T	2.7	3.1	0.3	2.5	1.4	0.80	0.94	0.08	1.02	0.30
171	T	2.7	3.1	0.3	2.6	1.3	1.14	1.33	0.12	1.48	0.46
172	T	2.3	2.6	0.2	3.3	1.0	1.53	1.73	0.13	2.16	1.04
173	T	2.8	3.2	0.3	2.9	1.0	0.99	1.19	0.12	1.46	0.65
174	T	3.4	4.2	0.4	3.7	1.1	0.72	0.93	0.16	1.43	0.93
175	T	3.8	4.7	0.5	4.1	1.4	0.52	0.67	0.12	1.06	0.69
176	T	4.1	5.1	0.6	4.6	1.8	0.29	0.38	0.07	0.63	0.40
177	T	3.3	4.1	0.3	3.9	2.2	0.40	0.48	0.05	0.58	0.20
178	T	3.5	4.3	0.3	3.9	2.2	0.80	0.95	0.11	1.51	0.57
179	T	4.1	5.1	0.4	3.5	1.4	1.15	1.28	0.12	2.47	0.98
180	T	4.2	5.4	0.4	3.8	1.1	0.65	0.79	0.06	1.48	0.61
181	T	4.2	5.3	0.4	3.8	1.2	0.74	0.89	0.08	1.56	0.64
182	T	5.3	6.3	0.5	6.8	2.5	1.65	2.01	0.22	3.46	1.34
183	T	5.7	6.8	0.5	7.5	3.0	1.11	1.35	0.15	2.39	0.86
184	T	6.2	7.4	0.6	8.3	3.6	0.93	1.17	0.12	2.14	0.67
185	T	3.0	3.4	0.3	3.0	1.1	—	—	—	—	—

Table 4 Travel times (h:min) from the epicentre to the location on the coast. These times are based on the instant when the water level deviates by ±10 cm from the undisturbed value at that location. For travel times, sources 1a and 1b (Table 3) are designated as source 1.

Location Number	Source Region			
	1	2	3	4
1	2:59	19:50	3:31	7:08
2	3:05	19:59	3:37	7:14
3	3:08	19:59	3:40	7:17
4	3:11	20:05	3:43	7:20
5	3:23	19:59	3:55	7:29
6	3:14	20:08	3:46	7:23
7	3:20	19:56	3:52	7:26
8	3:20	19:56	3:52	7:26
9	2:59	19:32	3:31	7:05
10	2:59	19:32	3:31	7:05
11	3:02	19:35	3:34	7:08
12	3:05	19:38	3:37	7:11
13	3:14	19:47	3:46	7:20
14	3:11	19:47	3:43	7:23
15	2:56	19:29	3:28	7:02
16	2:59	19:32	3:28	7:08
17	3:14	19:44	3:46	7:20
18	3:08	19:41	3:40	7:14
19	3:08	19:41	3:40	7:17
20	3:11	19:44	3:43	7:17
21	3:17	20:08	3:52	7:26
22	3:20	19:59	3:52	7:29
23	3:20	19:59	3:52	7:29
24	3:23	20:02	3:58	7:32
25	3:29	20:23	4:01	7:41
26	3:33	20:17	4:10	7:47
27	3:38	20:17	4:10	7:47
28	3:29	20:05	4:01	7:35
29	3:32	20:08	4:04	7:38
30	3:38	20:11	4:10	7:44
31	3:08	19:41	3:40	7:14
32	3:08	19:44	3:40	7:17
33	3:41	20:14	4:13	7:47
34	3:50	20:23	4:22	7:56
35	3:47	20:23	4:19	7:59
36	2:50	19:26	3:25	6:59
37	3:11	20:05	3:43	7:20

Table 4 Continued

Location Number	Source Region			
	1	2	3	4
38	3:02	19:38	3:34	7:11
39	3:02	19:35	3:34	7:08
40	3:17	19:53	3:49	7:26
41	3:32	20:11	4:01	7:41
42	3:38	20:20	4:10	7:47
43	3:44	20:32	4:13	7:56
44	3:32	20:14	4:04	7:44
45	3:35	20:17	4:07	7:47
46	1:59	18:11	2:25	6:08
47	1:53	17:47	2:16	5:53
48	1:53	17:47	2:16	5:56
49	1:56	17:50	2:19	5:59
50	3:05	18:23	3:25	7:02
51	3:14	18:35	3:34	7:11
52	3:32	18:53	3:43	7:20
53	3:20	18:44	3:37	7:11
54	3:29	18:50	3:46	7:17
55	4:02	19:26	4:19	7:53
56	4:14	19:38	4:31	8:05
57	3:50	19:11	4:07	7:38
58	3:50	19:11	4:04	7:38
59	3:56	20:20	4:28	8:03
60	3:35	19:32	4:04	7:44
61	3:41	19:38	4:13	7:50
62	4:08	19:23	4:22	7:56
63	3:59	19:11	4:13	7:47
64	4:05	19:20	4:22	7:56
65	3:41	18:53	3:52	7:29
66	3:35	18:47	3:46	7:23
67	3:29	18:41	3:40	7:17
68	3:17	18:35	3:34	7:11
69	3:20	18:35	3:37	7:11
70	3:11	18:29	3:28	7:05
71	3:11	18:29	3:28	7:05
72	3:17	18:35	3:34	7:11
73	3:26	18:44	3:43	7:20
74	3:20	18:32	3:31	7:03
75	3:23	18:44	3:43	7:20
76	3:14	18:41	3:34	7:11

Table 4 Continued

Location Number	Source Region			
	1	2	3	4
77	3:29	18:26	3:43	7:14
78	3:35	18:32	3:49	7:20
79	3:35	18:35	3:52	7:23
80	3:41	18:35	3:55	7:23
81	3:41	18:38	3:55	7:26
82	3:41	18:41	3:55	7:29
83	3:44	18:44	4:04	7:35
84	3:47	18:47	4:07	7:38
85	3:33	18:32	3:52	7:23
86	3:23	18:23	3:40	7:14
87	3:35	18:35	3:52	7:26
88	3:44	18:44	3:58	7:35
89	3:26	18:29	3:43	7:20
90	3:59	18:59	4:13	7:47
91	4:02	19:02	4:13	7:50
92	4:11	19:14	4:25	7:59
93	3:44	18:41	3:58	7:32
94	4:17	19:41	4:31	8:08
95	3:41	18:38	3:58	7:29
96	4:08	19:11	4:22	7:56
97	2:44	17:26	2:58	6:35
98	2:47	17:26	2:58	6:38
99	2:50	17:29	3:01	6:41
100	2:56	17:38	3:07	6:47
101	3:05	17:44	3:16	6:56
102	3:05	17:47	3:19	6:56
103	3:08	17:47	3:19	6:59
104	3:11	17:50	3:22	7:02
105	2:59	17:41	3:10	6:50
106	3:02	17:41	3:13	6:53
107	3:05	17:44	3:16	6:56
108	3:17	17:56	3:28	7:05
109	3:17	17:56	3:28	7:05
110	3:20	17:59	3:34	7:08
111	3:33	18:17	3:52	7:26
112	2:41	17:20	2:52	6:32
113	2:41	17:23	2:55	6:32
114	2:50	17:29	3:01	6:41
115	2:53	17:32	3:04	6:44

Table 4 Continued

Location Number	Source Region			
	1	2	3	4
116	2:59	17:38	3:10	6:50
117	2:44	17:20	2:55	6:35
118	2:50	17:26	3:01	6:41
119	2:50	17:20	3:01	6:41
120	2:44	17:14	2:55	6:35
121	2:59	17:20	3:13	6:47
122	3:03	17:29	3:19	6:56
123	3:29	17:44	3:34	7:08
124	3:23	17:44	3:34	7:08
125	2:56	17:17	3:10	6:44
126	3:11	17:26	3:25	6:59
127	3:17	17:32	3:28	7:02
128	3:26	17:41	3:40	7:11
129	3:26	17:41	3:40	7:14
130	3:29	17:44	3:43	7:14
131	3:17	17:32	3:28	7:02
132	3:14	17:32	3:28	7:02
133	3:17	17:35	3:31	7:05
134	3:23	17:38	3:37	7:08
135	3:23	17:38	3:37	7:11
136	3:17	17:32	3:31	7:02
137	3:17	17:32	3:29	7:02
138	3:20	17:41	3:34	7:08
139	3:20	17:41	3:34	7:08
140	3:20	17:41	3:31	7:05
141	3:20	17:41	3:34	7:03
142	2:59	17:20	3:10	6:47
143	3:05	17:29	3:16	6:53
144	3:05	17:26	3:13	6:53
145	3:05	17:26	3:16	6:53
146	3:05	17:26	3:16	6:53
147	3:02	17:23	3:16	6:50
148	3:02	17:26	3:16	6:50
149	3:05	17:29	3:22	6:53
150	3:08	17:29	3:19	6:56
151	3:08	17:32	3:19	6:56
152	3:11	17:26	3:22	6:56
153	2:56	17:17	3:07	6:44
154	3:02	17:23	3:16	6:47

Table 4 Concluded

Location Number	Source Region			
	1	2	3	4
155	3:08	17:29	3:22	6:56
156	3:38	17:41	3:43	7:17
157	3:32	17:41	3:43	7:17
158	3:32	17:41	3:43	7:14
159	3:35	17:44	3:46	7:17
160	3:53	17:53	3:58	7:29
161	3:47	17:47	3:49	7:23
162	3:32	17:41	3:43	7:17
163	3:44	17:47	3:52	7:20
164	3:47	17:41	3:55	7:26
165	3:53	17:47	4:01	7:35
166	4:11	17:59	4:13	7:44
167	4:11	18:02	4:16	7:50
168	4:05	17:53	4:07	7:41
169	3:53	17:44	3:58	7:32
170	3:53	17:44	4:01	7:35
171	3:53	17:47	4:01	7:35
172	3:56	17:50	4:04	7:35
173	3:56	17:50	4:04	7:38
174	3:59	17:50	4:07	7:41
175	3:59	17:53	4:07	7:41
176	3:59	17:53	4:07	7:41
177	4:05	17:56	4:13	7:44
178	4:05	17:59	4:13	7:47
179	4:08	18:02	4:16	7:50
180	4:11	18:02	4:19	7:53
181	4:11	18:05	4:19	7:53
182	4:17	18:08	4:22	7:56
183	4:17	18:08	4:25	7:56
184	4:17	18:11	4:25	7:59
185	3:59	17:50	4:04	7:38

Table 5 Summary of extreme tsunami amplitudes.

Location	Maximum Tsunami Height	Source Area
North Coast	3.5 m near the head of Khutzeymateen Inlet	Alaska
	3 to 3.5 m throughout Hastings Arm (north end of Observatory Inlet)	Alaska
	3.5 to 4 m near Stewart	Alaska
North Central Coast	3.5 to 4.5 m west of Princess Royal Island	Shumagin
	4.2 m in Cousins Inlet	Shumagin
	7.2 m at the head of Spiller Channel	Alaska
	5.6 m at the head of Laredo Sound	Shumagin
	3.3 m at the head of Surf Inlet	Shumagin
South Central Coast	3.3 to 9.2 m at the heads of Rivers and Moses Inlets	Shumagin
	6 to 9.3 m in Smith Inlet (increasing toward the head)	Alaska
Northwest coast of Vancouver Island	5.5 to 7.2 m in Quatsino Sound	Shumagin
	up to 9 m in Neroutsos Inlet	Shumagin
	8 to 8.5 m in Quatsino Narrows	Shumagin
	3.4 m at the head of Holberg Inlet	Shumagin
	6 to 7 m in Forward Inlet	
	5 to 6 m in Klaskino Inlet	Shumagin
	> 10 m at the head of Quoukinsh Inlet	Shumagin
Central Coast of Vancouver Island	3.5 to 4.5 m in Nuchalitz Inlet	Shumagin
	4.5 to > 10 m in Muchalat and Tlupana Inlets (increasing toward the heads)	Shumagin
	3.5 to 4.5 m at south end of Tahsis Inlet	Shumagin
	3 m at the head of Tahsis Inlet	Shumagin
	3.6 to 7.6 m in Port Eliza and Espinosa Inlets	Shumagin
	3.5 m in Nootka Sound	Shumagin
Southern Coast of Vancouver Island	3 to 4 m in Sydney Inlet	Shumagin
	4 to 8 m in Pipestem and Effingham Inlets	Shumagin
	3 to 8 m in Alberni Inlet (increasing toward the head)	Shumagin

Table 6 Summary of extreme tsunami wave current speeds.

Location	Maximum Tsunami Current	Source Area
North Coast	2.3 m/s at entrance to Observatory Inlet	Alaska
North Central Coast	currents less than 2 m/s	n/a
South Central Coast	currents less than 2 m/s	n/a
Northwest Coast of Vancouver Island	2.5 to 4.7 m/s in Quatsino Narrows	Shumagin
	2.5 to > 5 m/s near Port Alice on Neroutsos Inlet	Shumagin
	3 m/s at entrance to Forward Inlet	Shumagin
	3 m/s at entrance to Klaskino Inlet	Shumagin
	2 m/s in Quoukinsh Inlet	Shumagin
Central Coast of Vancouver Island	2.7 m/s at entrance to Muchalat Inlet	Shumagin
	2.5 to 3.5 m/s near entrance to Tlupana Inlet	Shumagin
	2.3 m/s at south end of Tahsis Inlet	Shumagin
Southern Coast of Vancouver Island	3.7 m at entrance to Pipestem Inlet	Shumagin
	2 to 3.5 m in Alberni Inlet	Shumagin

REFERENCES

Dunbar, D., P.H. LeBlond, and T.S. Murty. 1989. Maximum tsunami amplitudes and associated currents on the coast of British Columbia. *Science of Tsunami Hazards*, 7(1): 3–44.

Dunbar, D., P.H. LeBlond, and T.S. Murty. 1990. Evaluation of tsunami amplitudes for the Pacific coast of Canada. *Progress in Oceanography*, (in press).

THE HISTORICAL APPROACH TO THE STUDY OF TSUNAMIS

RESULTS OF RECENT UNITED STATES STUDIES

James F. Lander
Cooperative Institute for Research in Environmental Science
University of Colorado, Boulder, Co 80309

Abstract

An essential element in developing an appropriate response to a tsunami hazard is a detailed knowledge of the effects of prior tsunamis. From this the design tsunami can be selected to be used with the contemporary coastal zone development and variables such as possible tide stages and time of day and date effects. Warning systems, education, insurance, emergency planning (including evacuation, and search and rescue), modeling and engineering options may be combined to mitigate the hazard.

An analysis of the historical tsunami record from Hawaii, Alaska, the United States West Coast and the Puerto Rico/Virgin Islands area shows the hazard to be quite different among these areas and among localities within each region. Although the quality of the compiled historical record for United States tsunamis has been substantially improved, further improvements can be made.

Introduction

There are at least two reasons why a detailed tsunami history is needed: (1) to test predictive models through hindcasting, and 2) to be able to design appropriate mitigation responses to the tsunami hazard. The history needs a balance of quantitative and descriptive elements to understand not only what happened but why. Before a tsunami mitigation plan can be devised, the hazard at each locality must be understood in detail - a fundamental step not always taken. A reasonably complete history can identify the design tsunami or tsunamis for an area and identify unique features of the hazard.

The utility of historical data in formulating a mitigation plan rests on the assumption that the history is long enough and complete enough to include a tsunami from the most hazardous source and that subsequent tsunamis will approximate those which have occurred historically. In some cases there may be adequate geophysical reasons to suspect that worse events could occur than are in the record. These cases are probably rare and must be treated with another set of estimates and assumptions.

The effects from the historical data must also be considered with the changes in land use, possible tide stages, and time of day and date. In addition, coastal zone land use is constantly changing and mitigation plans must monitor these changes.

Figure 1 lists the kinds of data that would be useful in devising a mitigation plan. The mitigation plan may consist of a mix of local, regional, and Pacific-wide warning systems in conjunction with plans for evacuation, and treating secondary hazards. Land use regulations, hazard education, insurance, modeling, and engineering defenses may also be appropriate responses. Search and rescue should be an integral part of the response plan as there are numerous references in the historical record of people being rescued many hours after a tsunami.

The historical record of United States tsunamis is unique to each area and even within areas. This complicates modeling and mitigation planning. The rest of this paper will look at some of these problems.

Hawaii

Hawaii has had far more known tsunami fatalities (291) than all of the rest of the United States and territories combined (about 190 fatalities). However, the hazard is not distributed equally throughout the islands. Figure 2 shows this distribution. The Island of Hawaii has suffered nearly 87% of the fatalities including all deaths relating to local tsunamis. Hilo alone accounts for 61% of all of the fatalities. Note that there were only 2 fatalities due to the 1975 local tsunami compared with 47 for the similar 1868 event. This reflects the depopulation of the southern coast which once supported a much larger population at a subsistence level but currently lacks attractions for a cash economy. (The number of fatalities used here are from a recent re-evaluation by Cox (1987) which showed that accounts overestimated the total fatalities in Hawaii by 94.

Hawaii is affected more by remote-sourced tsunamis than any other place in the world. Figure 3 shows the distribution of all tsunamis with 1 meter or more amplitude. The predominance of tsunami sources from the northwest Pacific and South America are clear. The two smaller tsunamis not part of this trend are interesting discoveries resulting from the compilation of United States Tsunamis (Lander and Lockridge, 1989). The earliest listed tsunami for Hawaii had been given as occurring in 1813-1814 but questions raised in the preparation of United States Tsunamis led Cox (in press) to refine the date to between December 18 to 23, 1812 with a high probability of its originating from the December 21, 1812 Santa Barbara earthquake and tsunami. The 1901 remote-sourced tsunami (see Figure 3) had been associated with either of two major earthquakes off Sanriku, Japan since it occurred even though the observed arrival time did not fit either event. The travel times do fit for a magnitude 7.9 earthquake in the Tonga Island reported by Gutenberg (1956) although no reports of a tsunami are known for that area at that date.

The history of tsunamis in Hawaii is relatively complete but substantial improvements can be made by adding data, especially for nineteenth century remote-sourced tsunamis.

DATA NEEDED FOR MITIGATION PLANNING

A. *Historical Data on the Source of Tsunamis*

Source (earthquake, volcanic, landslide,...)
Location
Size (earthquake and tsunami magnitudes)
Date/Time
Source area (aftershock zone, area of uplift)
Seismic gaps
Recurrence rate (rate of strain increase or sedimentation rates)

B. *Historical Data on Coastal Effects*

Time interval between earthquake and 1st wave arrival
Wave heights and areas of inundation
Tide stage
Time history of wave - largest, period, 1st motion
Effects - damage, fatalities, casualties (why?)

C. *Current Situation*

Changes in use of coastal areas
State of awareness (education, emergency plans)
Special factors and secondary hazards

Figure 1.

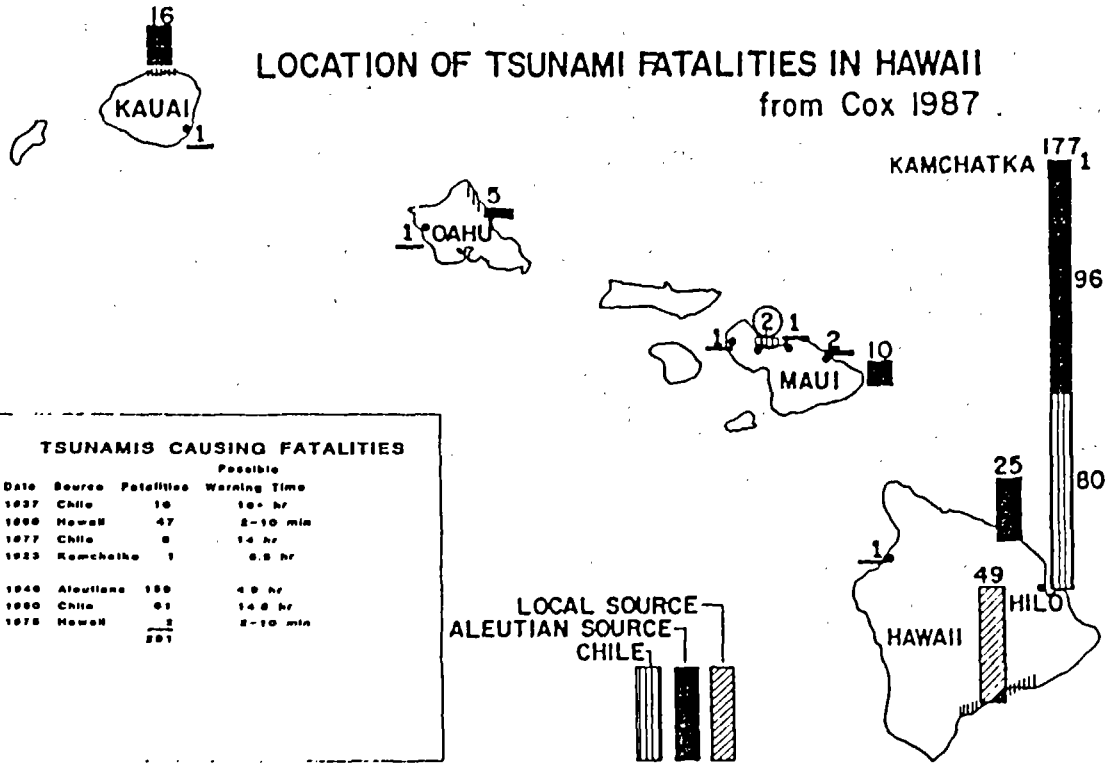

Figure 2

Alaska

The tsunami history of Alaska presents some special problems. For example Russian settlers on Kodiak reported the tsunami of 1788, one of the earliest reported on United States shores. However, there are almost no reports of earthquakes or tsunamis from the sparsely populated Aleutian Islands before seismographs came into general use in 1900. This area has the shortest recorded history of tsunamis in the United States. Also, the early records that still exist are in old Russian and difficult for American scholars to access.

The Russian settlers brought with them the Julian calendar. Tsunami dates recorded on the Julian calendar were later converted to the Gregorian calendar by adding eleven days for events in the 18th century and twelve days for 19th century dates. This resulted in an error of one day due to the effect of changing time in traveling east and west (now compensated for by the International Date Line). Several tsunami dates have been corrected for the one day error. However, the dates of two events, May 15, 1868, and August 29, 1878, are still in doubt and may be Julian, Gregorian, or Gregorian-plus-one dates.

Another complicating factor is the regional high tidal ranges of up to 9 meters which mask most tsunamis. Small tsunami waves arriving near high tide are more dangerous than larger waves at low tide. Few remote-sourced tsunamis have been observed in Alaska except on tide gages and none have caused damage. However, Alaska is the source of the more destructive tsunamis affecting both Hawaii and the United States West Coast.

Destructive tsunamis may arise from volcanic eruptions, from tectonic deformations associated with earthquakes, or from submarine and subaerial landslides with or without earthquake triggers. Submarine and subaerial landslides generated tsunamis are common in the Gulf of Alaska and southeastern Alaska but are rare elsewhere in the United States. The Prince William Sound earthquake of 1964 illustrates some of these hazards. It caused the most destructive tsunami in Alaska's history. In addition to the main tectonic tsunami, the earthquake generated at least nine local tsunamis due to submarine landslides. The action of glaciers and glacial outwash had deposited poorly sorted materials at angles up to 30^{0} to 35^{0}. These collapsed giving rise to local tsunamis arriving within a few minutes of the earthquake.

Figure 4 shows the fatalities from the 1964 tsunami by locale and by a three-class system. In Class I there was no opportunity to take evasive action. Whether a person survived or not-and many did survive-did not depend on one's own actions. Class II victims experienced a natural warning from the earthquake and could have saved themselves by prompt action. Others needed a communicated warning (Class III). Most of the Class II fatalities occurred when people tried to save their property, mainly boats, between tsunami waves. They knew without a formal warning that a tsunami was in progress. The highest water typically occurred at high tide several hours after the first tsunami wave. One fatality at Seward occurred about four hours after the initial wave due to a combination of high tide and the tsunami. Note that 70% to 80% of the fatalities were due to local submarine slump tsunamis and probably could not have been avoided. Also, although aware of the existence of the tsunami, over twenty people in Class II were killed. However, many

TSUNAMI AMPLITUDES IN HAWAII - 1 METER OR GREATER
1812-1988

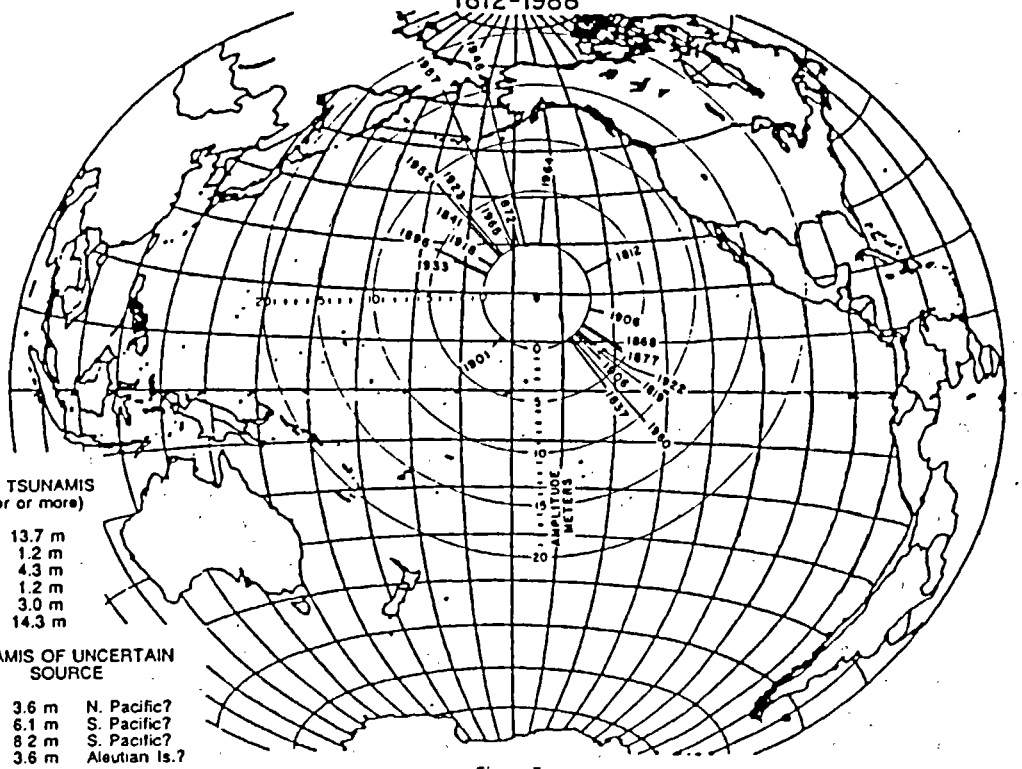

LOCAL TSUNAMIS
(1 meter or more)

1868	13.7 m
1908	1.2 m
1919	4.3 m
1951	1.2 m
1952	3.0 m
1975	14.3 m

TSUNAMIS OF UNCERTAIN SOURCE

1860	3.6 m	N. Pacific?
1868	6.1 m	S. Pacific?
1869	8.2 m	S. Pacific?
1878	3.6 m	Aleutian Is.?

Figure 3

FATALITIES IN ALASKA FROM 1964 TSUNAMI

LOCAL SUBMARINE LANDSLIDE WAVE VICTIMS

LOCALITY	FATALITIES	TIME AFTER EARTHQUAKE	COMMENTS
VALDEZ	32	25 SEC	28 ON DOCK
CHENEGA	23	4-10 MIN	1 RESCUED
WHITTIER	13	SEVERAL MIN	
PORT NELLIE JUAN	3		
CRAB BAY	1	SEVERAL MIN	
PORT NEWELL	1		
ANDERSON BAY	1	25 SEC	

MAIN TSUNAMI VICTIMS

SEWARD	13	75 SEC (LOCAL) - 25 MIN (MAIN)	1 FATALITY 4 HRS LATER
KODIAK	9	SEVERAL HRS	30 MIN WARNING OF 1st WAVE
KALSIN BAY	6	SEVERAL HRS	
KAGUYAK	3	ABOUT 3 HRS	2 RESCUED
POINT WHITSHED		2ND WAVE	IN CABIN
SITKALIDAK			HERMIT
CAPE ST. ELIAS		1 HR	INJURED COAST GUARDSMAN

CLASS I No Evasive Action	70-80 %	74
CLASS II & III Evasive Action Possible Some Warnings given	20-30 %	22
Numbers Killed by Each Wave not known		12

Figure 4

hundreds more heeded the natural or communicated warning and spent the night on high ground.

Alaska's glaciated, steep-sided fjords have sometimes given rise to large, local tsunamis from subaerial landslides, notably at Lituya Bay and Disenchantment Bay. Fatalities have occurred from this cause; subaerial landslides will continue to be a hazard. These are Class I situations and warnings are not possible.

West Coast of the United States

Although the recorded tsunami history exists for a period of 150 to 200 years on the West Coast, tsunamis there have not been studied in detail. The hazard is lower on the West Coast than for Alaska and Hawaii. Major harbors of Seattle and San Francisco are well protected by narrow entrances to wide bays; the coast of southern California is protected by a broader continental slope, offshore islands, and smaller harbors. The population is low on the outer coasts of Washington, Oregon and northern California with most communities having only a few hundred inhabitants. Thirteen tsunamis of at least 1 meter and one smaller tsunami which caused damage have been reported and are listed in Table 1. Four of these are of local or possible local origin, including the 1812 Santa Barbara, California, tsunami. This tsunami, once thought to have had an amplitude of 15 meters, is now believed to have had an amplitude of 3.5 meters. Another wave at Santa Barbara (in 1896) once thought to be the largest in their history, was actually due to astronomic tides.

Prior to 1960 no tsunami caused more than a few thousand dollars in damage on the West Coast. Since then there have been two destructive tsunamis; the 1960 Chilean tsunami which caused about $1,000,000 in damages and perhaps one fatality, and the 1964 Alaskan tsunami which caused about $12 million in damage and 16 fatalities. The damage to the West Coast was overshadowed by much more catastrophic effects elsewhere which drew most of the scientific attention.

Figure 5 shows the amplitudes of tsunamis for 1946, 1960, and 1964 tsunamis. This figure presents substantially more data than that available in earlier standard references. Much of the damage from the 1960 tsunami in southern California was due to currents set up in marinas where small pleasure and fishing craft were often moored to floating slips. This is an example of a change in use which has led to increased risk from future tsunamis. Much of the damage due to the 1964 Alaskan tsunami in San Franciso was also due to currents in marinas. In Washington, Oregon and northern Califorina, flooding following river beds and carried logs from the beaches which caused much of the damage.

The variations in amplitude along the coast from the three tsunamis is probably related to the source region orientation with respect to the West Coast shorelines. Effects similar to 1960 and 1964 could be expected from future tsunamis originating from the Peru/Chile and Shumagin, Alaska seismic gaps, respectively.

The hazard is increasing due to changing use of the coastal area including increased population, increased coastal development, increased recreational use of beaches, and increased numbers of small boats.

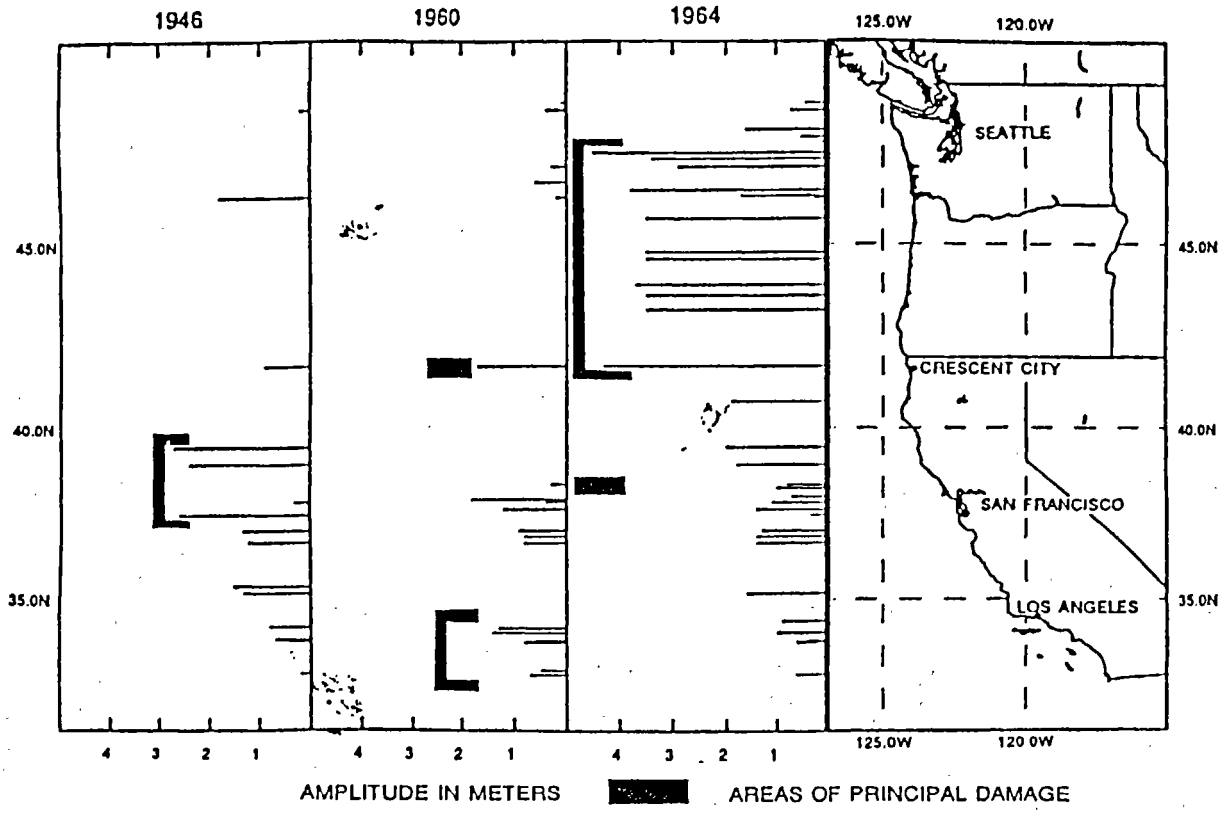

Figure 5 Tsunami amplitudes at selected localities along the west coast of the United States for the tsunamis of April 1, 1946, in the Aleutian Islands, May 22, 1960, in Chile and March 28, 1964, in the Gulf of Alaska.

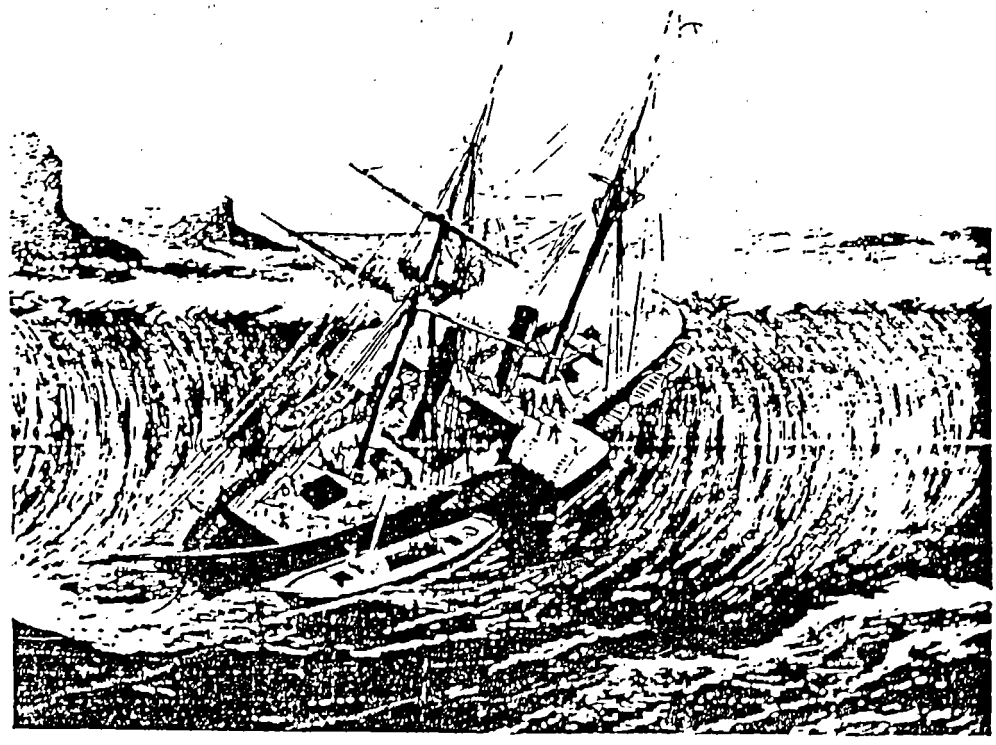

Figure 6: The Royal Mail Steamer *La Plata* anchored near the southern point of Water Island abo.' 4 km from Charlotte Amalie engulfed by the tsunami of November 18, 18[illegible] Credit: Harper's Weekly.

The history may be substantially improved using contemporary accounts, marigraphic data since 1854, and computer programs capable of calculating the expected tide stages for earlier tsunamis.

Puerto Rico/Virgin Islands

Three tsunamis in the Puerto Rico/Virgin Islands area are of interest. The first occurred on April 16, 1690. The earthquake was apparently strongest at Antigua, St. Kitts, Nevis (where the sea receded 200 meters), St. Thomas, and Guadeloupe, and was also felt at Barbados, Martinique, and St. Lucia. The sea also receded at St. Thomas. Dates of April 5, 6, 9 and 10 are also used for the event but the 16th is probably the correct Gregorian date for all of these reports.

The next reported tsunami occurred on November 18, 1867. This is a historically interesting tsunami as the United States was in the process of purchasing the islands from Denmark. The tsunami damaged one United States naval vessel and left another stranded on a reef for six months, factors which helped delayed the United States purchase for 50 years. A wave of 2.4 m washed over the wharf at Charlotte Amalie, St. Thomas. Figure 6 is a lithograph from the Harper's Weekly (January 11, 1868) depicting the plight of the Steam Packet "La Plata" which had just arrived with the King of Denmark's envoy. At St. Thomas and St. Croix about 17 people were killed including four United States sailors. Most people escaped to higher ground upon seeing the wave approach. The wave was observed throughout the lesser Antilles where some damage occurred as far as Granada more than 1.5 hours later.

The third main tsunami occurred in 1918 in the Mona Passage area on the west coast of Puerto Rico. Waves of up to 6 meters were observed and 40 people were drowned (Class I fatalities). The waves arrived almost immediately at that location; no evacuations were possible.

The November 1, 1755 Lisbon, Portugal, earthquake and tsunami produced waves of 7 m at Saba, 3.6 m at Antigua, and 4.5 m at St. Martin, and should have been observed in Puerto Rico and the Virgin Islands. However, no reports of its being observed at either place have been found.

Today the use of the coastal areas has been greatly increased for all of the Caribbean Islands. In Charlotte Amalie, St. Thomas, five to eight cruise ships arrived daily and discharge 5,000 passengers who crowd the wharfside shops. However, no warning system yet exists. The 1867 tsunami arrived 20 minutes after the earthquake was felt in the Virgin Islands and up to two hours later at other islands. Thus, there would be time for Class II and III warnings. Figure 7 shows the travel times recently prepared for Charlotte Amalie by Tom Weissert (1989).

Conclusion

The historical approach to study of tsunamis can provide insight to the nature of the problems and possible strategies for this mitigation.

The historical record is far from complete and capable of significant improvement which will increase its usefulness. Under-utilized sources include tide gage records since 1854, contemporary records including

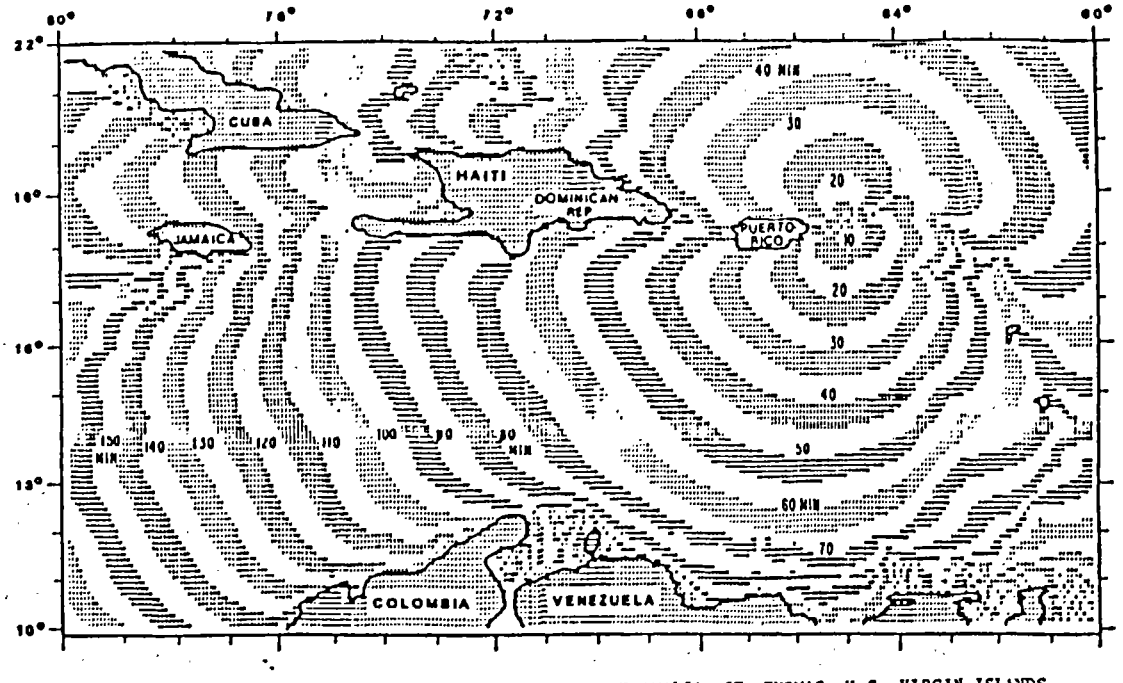

FIGURE 7: TRAVEL TIME PLOT FOR TSUNAMIS TO CHARLOTTE AMALIA, ST. THOMAS, U.S. VIRGIN ISLANDS (WEISSERT, 1989)

Table 1.

Tsunamis Affecting the West Coast of the U.S.
Damaging or at Least 1 Meter Amplitude

Date	Amplitude (M)	Locality Most Affected	Source
1812	3.5	Gaviota (S. Calif.) Negligible Damage	S. California
1859	4.6	Half Moon Bay (C. Calif.) Schooner Damaged	Unknown
1862	1.2	San Diego (S. Calif.)	S. California
1868 (Aug.)	1.8	San Pedro (S. Calif.)	Chile
1868 (Oct.)	4-5	San Francisco (C. Calif.)	N. California
1877	3.6	Gaviota (S. Calif.)	Peru-Chile
1878	2.0	Wilmington (S. Calif.) Unspecified Damage	Chile?
1896	1.5	Santa Cruz (C. Calif.) Dike Destroyed, Ship Damaged	Japan
1927	1.8	Surf and Avila (S. Calif.)	S. California
1946	2.7	Santa Cruz (S. Calif.) Some Damage, 1 Killed	Aleutian Is.
1952	1.4	Crescent City and Avila (N. and S. Calif.)	Kamchatka
1957	1.0	San Diego (S. Calif.) Minor Damage	Aleutian Is.
1960	1.7	Crescent City and Los Angeles (N. and S. Calif.) $1,000,000 in Damage, 1 Killed?	Chile
1964	4.3	Crescent City (N. Calif.) $12,000,000 in Damange, 16 Killed	Gulf of Alaska
1975	0.4	Catalina Is. (S. Calif.) $2,000 in Damage	Hawaii

newspapers, and official archives, and computer programs to provide "predicted" tide levels at the time of historic tsunamis.

REFERENCES

Breve og dokumenter fre Vertindien 1674-98 (West Indian Letters and Documents 1674-98) Letters dated April 8, 1690 from the Governor to the Board of Directors, Copenhagen.

Cox, Doak C., Fatalities due to Tsunamis and other Causes associated with the Alaska Earthquake, March 22-28, Table 1 in Weller in National Academy of Sciences Committee on the Alaskan Earthquake, The Great Alaskan Earthquake 1964, Human Ecology, National academy of Sciences, Washinton DC 1972, p.227.

Cox, Doak C., Tsunami Casualties and Mortality in Hawaii, Joint Institute for Marine and Atmospheric Research, University of Hawaii, Honolulu, June 1987, 53 p.

Cox, Doak C., "On the Probable Tsunami Observed at Hookena, South Kona, Hawaii, Early in the Second Decade of the 1800's," University of Hawaii, Draft, April 1989.

Cox, Doak C. and Joseph Morgan, Local Tsunamis and Possible Local Tsunamis in Hawaii, HIG-77-14, Hawaii Institute of Geophysics, November 1977, 118 p.

Cox, Doak C. and George Pararas-Carayannis, Catalog of Tsunamis in Alaska, SE-1, United States Department of Commerce, National Oceanic and Atmospheric Administration, March 1976, 43 p.

Deville, Ch. Sainte-Claire, "Sur le tremblement de terre du 18 Novembre, 1867 aux Antilles," Extrait des Comptes rendus des seances de l'Academie des Sciences, Tome LXV, seance du 30, Decembre, 1867, Institut Imperial de France, Academie des Sciences, Paris.

Grauzinis, V.J., J.W. Joy, and R.R. Putz, "The Reported California Tsunami of December, 1812", unpublished manuscript, 120 p.

Gutenberg, B., "Great Earthquakes, 1896-1903," Transactions of the American Geophysical Union, Vol. 37, 1956, p. 603-614.

Harpers Weekly, "The Late Earthquake at St. Thomas," New York, Vol. XII, No. 578, January 25, 1868, p. 1.

Heaton, Thomas H. and Stephen H. Hartzell, "Earthquake Hazards on the Cascadia Subduction Zone," Science, American Association for the Advancement of Science, Washington, D.C., 1987, Vol. 236, p. 162-168.

Hogan, O.W., W. W. Whippe, and C. Lundy, "Tsunamis of 27 and 28 March, 1964, State of Washington Coastline," United States Army Corps of Engineers, Seattle, Washington, unpublished file report, 1964, 29 p.

Ii, John Papa, Fragments of Hawaiian History, Honolulu, Bishop Museum Press, 1959, 183 p. (originally published in the Hawaiian language newspaper, Kuokua, in the 1860's).

Iida, Kumiji, Doak C. Cox and George Parasas-Carayannis, Preliminary Catalog of Tsunamis Occurring in the Pacific Ocean, University of Hawaii, Honolulu, 1967, 274 p.

Kisslinger, Gerald, and John W. Davies, Untitled manuscript catalog of Alaskan earthquakes, Geophysical Institute, University of Alaska, Fairbanks, 1987.

Lander, James F. "Impact of Tsunamis on the United States and Associated Territories," International Tsunami Symposium Proceedings, Vancouver, B.C. Canada 1987, United States Department of Commerce, NOAA, Pacific Marine Environmental Laboratory, 1988, p 49-55.

Lander, James F. "An Analysis of Tsunami Fatalities in the United States" International Conference on Natural and Man-Made Hazards in Coastal Zones, Abstract, Ensenada, Baja, Mexico, 1988, p. 60.

Lander, James F. "Observations of Tsunamis on the West Coast of the United States," Proceedings of the 21 Joint UJNR Panel on Wind and Seismic Effects, Joint Meeting, National Institute of Standards and Technology (in press), 1989.

Lander, James F. and Patricia A. Lockridge, United States Tsunamis (including United State possessions) 1690-1988, Publication 41-2, United States Department of Commerce, NOAA, National Geophysical Data Center, July, 1989, 269 p.

Magoon, O.T., "Structural Damage by Tsunamis," 1965 Proceedings American Society of Civil Engineers Specialty Conference on Coastal Engineering, , Santa Barbara, California, 1965, p. 35-38.

McCulloch, D.S., "Evaluating Tsunami Potential," in Evaluating Earthquake Hazards in the Los Angeles Region, United States Geological Survey Professional Paper 1360, United States Geological Survey, Reston, Virginia, 1985, p. 375-413.

Miller, Don J., Giant Waves in Lituya Bay, Alaska, United States Geological Survey Professional Paper 354-C, United States Government Printing Office, Washington, D.C., 1960, 83 p.

National Academy of Sciences Committee on the Alaska Earthquake, The Great Alaska Earthquake of 1964, Human Ecology, National Academy of Sciences, Washington, D.C., 1970, 510 p.

National Academy of Sciences Committee on the Alaska Earthquake, The Great Alaska Earthquake of 1964, Geology, Part A, National Academy of Sciences, Washington, D.C., 1970, 834 p.

National Academy of Sciences Committee on the Alaska Earthquake, The Great Alaska Earthquake of 1964, Oceanography and Coastal Engineering, National Academy of Sciences, Washington, D.C., 1972, 556 p.

O'Brien, M. P., Preliminary Report on Seismic Sea Waves from Aleutian Earthquake of April 1, 1946, Technical Report HE 116207, Wave Project, Fluid Mechanics Laboratory, University of California at Berkeley, April, 1946, 10 p.

Paiewonsky, Isidors, "History Corner" in the Daily News, St. Thomas, Virgin Islands, a series of articles dated July 30, 1979; August 6, 1979; August 13, 1979; August 20, 1979; August 27, 1979; November 5, 1979; November 9, 1979; November 12, 1979; November 19, 1979; November 26, 1979; December 3, 1979; December 10, 1979; December 17, 1979; December 24, 1979; and November 2, 1981.

Pararas-Carayannis, George and Jeff Calebaugh, Catalog of Tsunamis in Hawaii, SE-4, United States Department of Commerce, National Oceanic and Atmospheric Administration, March 1977, 77 p.

Reid, Harry Fielding and Stephen Taber, "The Porto Rico Earthquakes of October-November, 1918," Bulletin of the Seismological Society of America, Vol. IX, No. 4, December 1919a, p. 94-127.

Reid, Harry Fielding and Stephen Taber, "The Virgin Islands Earthquakes of 1867-1868," Bulletin of the Seismological Society of America, Vol. 10, No. 1, 1920, p. 9-30.

Robson, G. R., "An Earthquake Catalogue for the Eastern Caribbean 1530-1960," Bulletin of the Seismological Society of America, Vol. 54, No. 2, April 1964, p. 785-832.

Soloviev, S.L. and Ch.N. Go, A Catalogue of Tsunamis on the Western Shore of the Pacific Ocean, Academy of Sciences of the USSR, "Nauka" Publishing House, Moscow, 1974, 310 p. Translation by Canada Institute for Scientific and Technical Information, National Research Council, Ottawa, Ontario, Canada K1A 0S2, 1984, 439 p.

Soloviev, S.L. and Ch.N. Go, A Catalogue of Tsunamis of the Eastern Shore of the Pacific Ocean, Academy of Sciences of the USSR, "Nauka" Publishing House, Moscow, 1975, 204 p. Translation by Canada Institute for Scientific and Technical Information, National Research Council, Ottawa, Ontario, Canada K1A 0S2, 1984, 285 p.

Taylor, Charles E., Leaflet from the Danish West Indies originally published by William Dawson and Sons, London, 1888, reprinted by Negro University Press, a division of Greenwood Press, Inc., New York, 1970.

Von Huene, Roland and Doak C. Cox, "Locally Generated Tsunamis and Other Local Waves," in The Great Alaskan Earthquake of 1964, Oceanography and Coastal Engineering, National Academy of Sciences, Washington, D.C., 1972, p. 211-221.

Weissert, Thomas P. "A Preliminary Report on Tsunami Travel Time Charts for the Caribbean" (in preparation).

Wilson, Basil W. and Alf Trum, "Runup Heights of the Major Tsunami on North American Coasts," in The Great Alaskan Earthquake of 1964; Oceanography and Coastal Engineering, National Academy of Sciences, Washington, D.C., 1972, p. 138-180.

A Program to Acquire Deep Ocean Tsunami Measurements in the North Pacific

F.I. Gonzalez*
E.N. Bernard*
H.B. Milburn*

Abstract: Deep ocean tsunami measurements are needed to provide open ocean boundary conditions for testing numerical models in hindcast studies, and for improving our understanding of tsunami generation and propagation. Jacob (1984) has identified a portion of the Aleutian Trench which includes the Shumagin Island group as a seismic gap (the Shumagin Gap); he has computed estimates which indicate that the probability of a great earthquake occurrence (M_W > 7.8) is significantly higher for this region than any other in the U.S. Because tsunamigenic earthquakes along a major portion of the seismically active Aleutian trench threaten Hawaii and the U.S. west coast, and because a large tsunami is possible in the event of a great earthquake in the Shumagin Gap, this region has become the focus of a long-term monitoring program by the Pacific Marine Environmental Laboratory (PMEL) of the National Oceanic and Atmospheric Administration (NOAA).

Introduction

Theoretical and numerical modeling capabilities in the field of tsunami research have far outstripped the observational database. In 1981, the National Science Foundation (NSF) sponsored a study of tsunami research needs; this study concluded that the highest need was "to design and install instruments to measure tsunami along the coastline and in the open ocean" (Bernard and Goulet, 1981). Again, a more recent review of tsunami research requirements found that the highest priority should be given to

*NOAA/PMEL, 7600 Sand Point Way, N.E., Seattle, WA. 98115

"a significant effort ... within the tsunami community to gather meaningful field data related to the generation and propagation of a tsunami" (Raichlen, 1985).

Most existing tsunami data have been acquired in harbors by standard tide gauges which employ stilling wells. As a consequence, a clear analysis of a particular tsunami event is difficult for a number of reasons: the inaccuracies of the record induced by the non-linear transfer function of the stilling well; the lack of deep ocean amplitude, period and direction measurements to provide initial and/or boundary conditions for the problem; and the contamination of the record by sometimes very complex bay-harbor-inlet oscillations forced by the incident tsunami.

The most recent example of the inadequacy of tide gauge data for tsunami research has been documented by Okada (1985) for a record obtained at Fukaura, Japan during the 1983 Japan Sea tsunami. His estimates of the errors induced by the stilling well non-linearities indicate that the actual tsunami amplitude was at least double that of the recorded amplitude.

The lack of deep ocean data, which could provide verification as well as initial and boundary conditions for numerical simulations, has serious consequences as well. Conflicting model results, which can occur for any number of reasons, including differences in physics and/or computational techniques, may remain unresolved because the necessary data are not available. Two examples of such instances are cited here.

The first example is of two similar studies which assessed the threat of Alaskan tsunamis to the U.S. west coast (Houston, et. al., 1975 and Brandsma, et. al., 1977). Both used similar, but somewhat different, model physics and computational approaches, and both were faced with a lack of adequate observational data to verify their models. Both were thus forced to attempt model verification by hindcasting the 1964 Alaskan tsunami and comparing their results with the only record available, that of Van Dorn (1969). While the best available, this record was nonetheless poorly suited for model verification, since it was collected on the southwest side of very distant (6500 km) Wake Island in 800 feet of offshore water. Thus, since the source was to the northeast of Wake, near Kodiak, the incident waves first interacted with the island before being recorded; furthermore, the tsunami signal was quite weak (approximately 6 cm) since most of the energy propagated

southeast, toward the U.S. west coast and away from the observation point. Finally, although each of the studies obtained relatively good agreement between computed and observed intial wave amplitude at Wake Island, seriously conflicting results were obtained for the corresponding estimates of tsunami leading wave amplitudes along the U.S. west coast - estimates computed by Houston, et. al. were greater than those of Brandsma, et. al. by factors of two to six.

The second example is similar. Kowalik and Murty (1984) simulated a tsunami generated by a source near the Shumagin Island group in the Aleutian Island chain. They found that most of the wave energy was focused almost due south, thus, evidently, posing a greater threat to the Hawaiian Island chain rather than the U.S. west coast; in contrast, a similar simulation by Houston, et. al. (1975) indicated that most of the energy in such an event would, in fact, be directed toward the U.S. west coast. Again, each used somewhat different model assumptions and numerical techniques.

The Pacific Tsunami Observational Program (PacTOP)

PacTOP, a program designed to obtain research quality tsunami data which would help resolve theoretical and modeling issues such as those cited in the examples above, has been initiated by NOAA's Pacific Marine Environmental Laboratory. The goal of PacTOP is to acquire high quality tsunami measurements during the

generation,
deep ocean propagation, and
coastal amplification

of one or more tsunami events.

In 1986, a start was made on acquiring deep ocean tsunami records. As for any oceanographic field program, the primary experimental design problems that had to be addressed were appropriate instrumentation and optimal siting.

Instrumentation

Over the last 15 years, technological advances have improved our ability to monitor pressure fluctuations on the ocean bottom

(Vitousek and Miller, 1970; Filloux, 1971; Irish and Snodgrass, 1972; Filloux, 1980; Filloux, 1982). PMEL has concentrated on the development of a deep ocean Bottom Pressure Recorder (BPR) system specifically designed for long-term tsunami monitoring. Since the open ocean tsunami signal can be as small as 1 cm, the BPR must be characterized by high sensitivity; since typical tsunami periods are in the range 5 - 90 minutes, BPR sampling rates must be 60 seconds or less; and since individual tsunami events occur relatively infrequently, the BPR must possess sufficient storage to accomodate the 1-year deployment cycles envisioned for a long-term monitoring program such as PacTOP.

In 1982, a BPR was deployed in the equatorial region. The instrument employed a Paroscientific 0-7000m quartz crystal pressure transducer mated to a Sea Data Model 635-7H recorder. Average values were recorded every 56.25 seconds (64 samples per hour); this averaging time provided a theoretical sensitivity of 0.5 mm static load of water pressure. The unit was deployed for a period of 5 months in 3751 m of water, successfully detecting a very small tsunami (maximum amplitude 0.5 cm) in the process. Bernard and Milburn (1985), provide a more detailed description of the instrumentation, as well as an analysis and interpretation of the data. All of the deployments described below utilized BPRs of the same essential design.

Siting

Clearly, logistics and expense prohibit blanket coverage of a region as enormous as the Pacific ocean. With limited resources available, one is forced to develop a deployment strategy based on identification of regions with high tsunamigenic potential, and a consideration of logistic and programmatic constraints.

Over the years, geophysicists, using plate tectonic theory as a basic framework, have identified a number of regions with high seismic potential (seismic gaps), particularly around the Pacific rim (Kelleher, 1970; Kelleher, 1972; Kelleher, et. al., 1973). In particular, Jacob (1984) has concluded that three Alaskan regions - the Shumagin, Unalaska and Yakataga Seismic Gaps - have a significant probability of experiencing a great (M_W > 7.8) earthquake in the next two decades. More recently, Nishenko (1986) has indicated that the 1938 Alaskan earthquake region may also

possess similar seismic potential. Because of these findings, the U.S. Geological Survey (USGS) and Lamont-Doherty Geological Observatory maintain a relatively dense seismic network in these regions (Beaven, et. al., 1986; Savage, et. al., 1986).

Thus, for a number of reasons, the Shumagin and Unalaska Seismic Gaps and the 1938 Alaska earthquake regions, shown as stippled areas in Figure 1, were chosen as the focus of PacTOP efforts. The most important of these reasons were as follows:

(1) High seismic potential - as indicated by geophysical studies,
(2) High tsunamigenic potential - suggested by the presence of a number of Alaskan tsunamis in the historical record,
(3) U.S. threat - as indicated by the historical record and numerical simulations cited above,
(4) Favorable PMEL logistics - because of significant NOAA ship activity in this region,
(5) Seismic instrumentation - because of USGS/Lamont-Doherty interest in the region.

In August of 1986, four BPRs were deployed in a "4-gauge star" directional array approximately 450 km southwest of the Shumagin Islands. Two months later, a fifth BPR was deployed approximately 500 km west of the Oregon coast. These locations are shown in Figure 1. The array site was chosen to take advantage of the data, especially the atmospheric pressure measurements, collected routinely by environmental buoy 46003 of the NOAA Data Buoy Center (NDBC). The west coast BPR is situated near the great circle connecting the Shumagin Island region with Crescent City, which sustained enormous damage during the 1964 Alaska tsunami.

Future plans

One new BPR will be constructed, and the west coast BPR will be recovered before the Summer, 1987 field season. These two will then be deployed in the potential Shumagin source regions (see Figure 1) in order to acquire data during generation, should a tsunami occur. Resources and logistics permitting, the four BPRs in the array will also be recovered, refurbished, and redeployed as an array in deep water.

Negotiations are presently being conducted with the U.S. Corps of

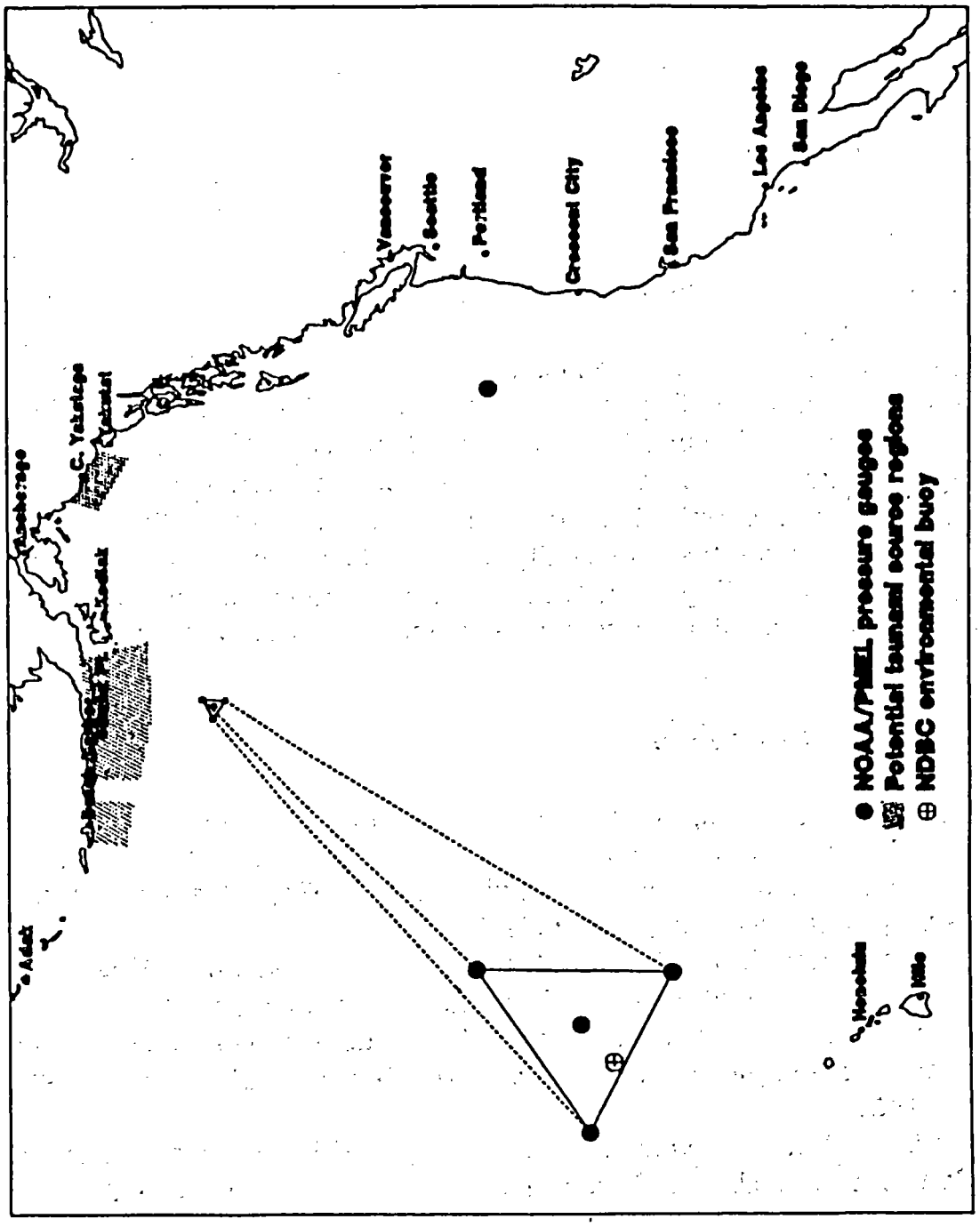

Fig. 1. - BPR sites and Potential Tsunami Source Regions

Engineers with regards to possible tsunami data collection at a selected number of sites maintained on the U.S. west coast by the Coastal Data Information Program (CDIP) (Seymour, et. al., 1985) and by the Field Wave Gaging Program (FWGP) in Hawaii (Hemsley,

1984). In contrast to typical tide guage installations, stations maintained by the CDIP and FWGP are bottom-mounted pressure guages at shallow water, exposed coastal sites. Suitably modified, these gauges would provide excellent coastal amplification data in the event of a tsunami.

Summary

The goal of the Pacific Tsunami Observation Program (PacTOP) is to acquire high quality field data during generation, deep ocean propagation, and coastal amplification of tsunamis; emphasis is on the Shumagin Seismic Gap and vicinity. In the first year of PacTOP, five BPRs were deployed which would provide the deep ocean propagation measurements. During the second year, two BPRs will be deployed in the potential generating region. During the second year, there is also the possibility that participation in PacTOP by the U.S. Corps of Engineers could provide measurement capability for coastal amplification of tsunamis along the U.S. west coast and Hawaii.

Appendix. - References

Beaven, J., K. Hurst, R. Bilham and L. Shengold, 1986. A Densely Spaced Array of Sea Level Monitors for the Detection of Vertical Crustal Deformation in the Shumagin Seismic Gap, Alaska,*Journal of Geophysical Research*, 91, 9067-9080.

Bernard, E.N. and R. Goulet, 1981. Tsunami Research Opportunities, National Science Foundation, Washington, D.C.

Bernard, E.N. and H.B. Milburn, 1985. Long-Wave Observations Near the Galapagos Islands, *Journal of Geophysical Research*, 90, 3361-3366.

Brandsma, M., D. Divoky and L. Hwang, 1977. Tsunami Atlas for the Coasts of the United States, Tetra Tech Report No. TC-486, 235 pp.

Filloux, J.H., 1971. Deep Sea Observations from the Northeastern Pacific, *Deep Sea Research*, 18, 275-284.

Filloux, J.H., 1980. Pressure Fluctuations on the Open Ocean Floor Over a Broad Frequency Range: New Program and Early Results, *Journal of Physical Oceanography*, 10, 1949-1971.

Filloux, J.H., 1982. Tsunami Recorded on the Open Ocean Floor,

Geophysical Research Letters, 1, 25-28.

Hemsley, J.M., 1984. U.S. Army Corps of Engineers Field Wave Gaging Program, *Proceedings of the 19th International Conference on Coastal Engineering*, ASCE, Houston, Texas, 1, 304-315.

Houston, J.R., R.W. Whalin, A.W. Garcia and H.L. Butler, 1975. Effect of Source Orientation and Location in the Aleutian Trench on Tsunami Amplitude Along the Pacific Coast of the Continental United States, U.S. Army Engineer Waterways Experiment Station Research Report H-75-4, 48 pp.

Irish, J.D. and F.E. Snodgrass, 1972. Quartz Crystal multi-purpose oceanographic sensors - I. Pressure, *Deep Sea Research*, 19, 165-169.

Jacob, K.H., 1984. Estimates of Long-Term Probabilities for Future Great Earthquakes in the Aleutians, *Geophysical Research Letters*, 11, 295-298.

Kelleher, J.A., 1970. Space-time seismicity of the Alaska-Aleutian Seismic Zone, *Journal of Geophysical Research*, 75, 5745-5756.

Kelleher, J.A., 1972. Rupture Zones of Large South American Earthquakes and Some Predictions, *Journal of Geophysical Research*, 78, 2547-2585.

Kelleher, J.A., L.R. Sykes, and J. Oliver, 1973. Possible Criteria for Predicting Earthquake Locations and their Applications to Major Plate Boundaries of the Pacific and Caribbean, *Journal of Geophysical Research*, 78, 2547-2585.

Kowalik, Z. and T.S. Murty, 1984. Computation of Tsunami Amplitudes Resulting from a Predicted Major Earthquake in the Shumagin Seismic Gap, *Geophysical Research Letters*, 11, 1243-1246.

Nishenko, S.P., 1986. Recent Advances in Earthquake Forecasting: Impact on Tsunami Research and Planning, *EOS Transactions, American Geophysical Union* (Abstract), 67, 1003.

Okada, M., 1985. Response of Some Tide-wells in Japan to Tsunamis, *Proceedings of the International Tsunami Symposium*, Sidney, B.C., Canada, 208-213.

Raichlen, F. (Chairman), 1985. Report of Tsunami Research Planning Group, National Science Foundation, Washington, D.C.

Savage, J.C., M. Lisowski and W.H. Prescott, 1986. Strain Accumulation in the Shumagin and Yakataga Seismic Gaps, Alaska, *Science*, 231, 585-587.

Seymour, R.J., M.H. Sessions and D. Castel, 1985. Automated Remote Recording and Analysis of Coastal Data, *Journal of Waterway, Port, and Coastal Engineering*, 111, 388-400.

Van Dorn, W.G., 1969. A Model Experiment on the generation of the Tsunami of March 23, 1964 in Alaska, *Proceedings of the International Symposium on Tsunamis and Tsunami Research.*

Vitousek, M. and G. Miller, 1970. An Instrumentation System for Measuring Tsunamis in the Deep Ocean, in *Tsunamis in the Pacific Ocean,* W.M. Adams, Ed., East-West Center, Honolulu, 239-252.

TSUNAMI OBSERVATIONS USING OCEAN BOTTOM PRESSURE GAUGE

M. Okada and M. Katsumata
Meteorological Research Institute, Tsukuba 305, Japan

Introduction

Some seismologists in Japan pointed out about fifteen years ago that a large earthquake may occur off the Tokai District, south of Honshu, in the near future and cause serious damage in the area near the origin. The Japan Meteorological Agency (JMA) has been improving the system processing, in real time, data on earthquakes, tsunami and other geophysical events. Under these circumstances the Permanent Ocean Bottom Seismograph System was developed and installed off Cape Omaezaki in 1978 by the Meteorological Research Institute (MRI). This OBS system has four seismographs and one pressure gauge, which may detect the crustal movement precursors of the large earthquake. JMA has been routinely operating this system for eleven years and observing seismic events and ocean tides. Another OBS system has been deployed off Boso Peninsula, Kanto District since 1986. This system has four seismographs and three pressure gauges.

The anchored buoy OBS or the pop-up OBS could be used to observe in the sea areas. However, we cannot use these instruments on a real time basis. The OBS system with signal transmission in real time over long cable lines, is much more expensive than the anchored buoy or pop-up OBS, but we risked adopting the telemetering system by submarine cable, for the purpose of earthquake prediction and tsunami warning.

System and Stations

Figure 1 indicates the concept of OBS laid off Cape Omaezaki in August 1978. Four apparatuses are linked in series to the shore monitoring stations by submarine coaxial cable, by which the signals are transmitted in real time. Electric power is supplied through the same cable by a DC constant current and its circuit is completed through a ground electrode, then to the one buried on the beach at Omaezaki. The pressure gauge which moniors sea level changes is kept in the terminal apparatus.

The OBS system off Boso Peninsula is very similar to the one at Omaezaki except that pressure and temperature are observed at two intermediate apparatus as well as at the terminal one.

Signals from both OBSs are monitored at the shore station, Omaezaki and Katsuura, and telemetered to the National Tsunami Warning Center in JMA over telephone lines.

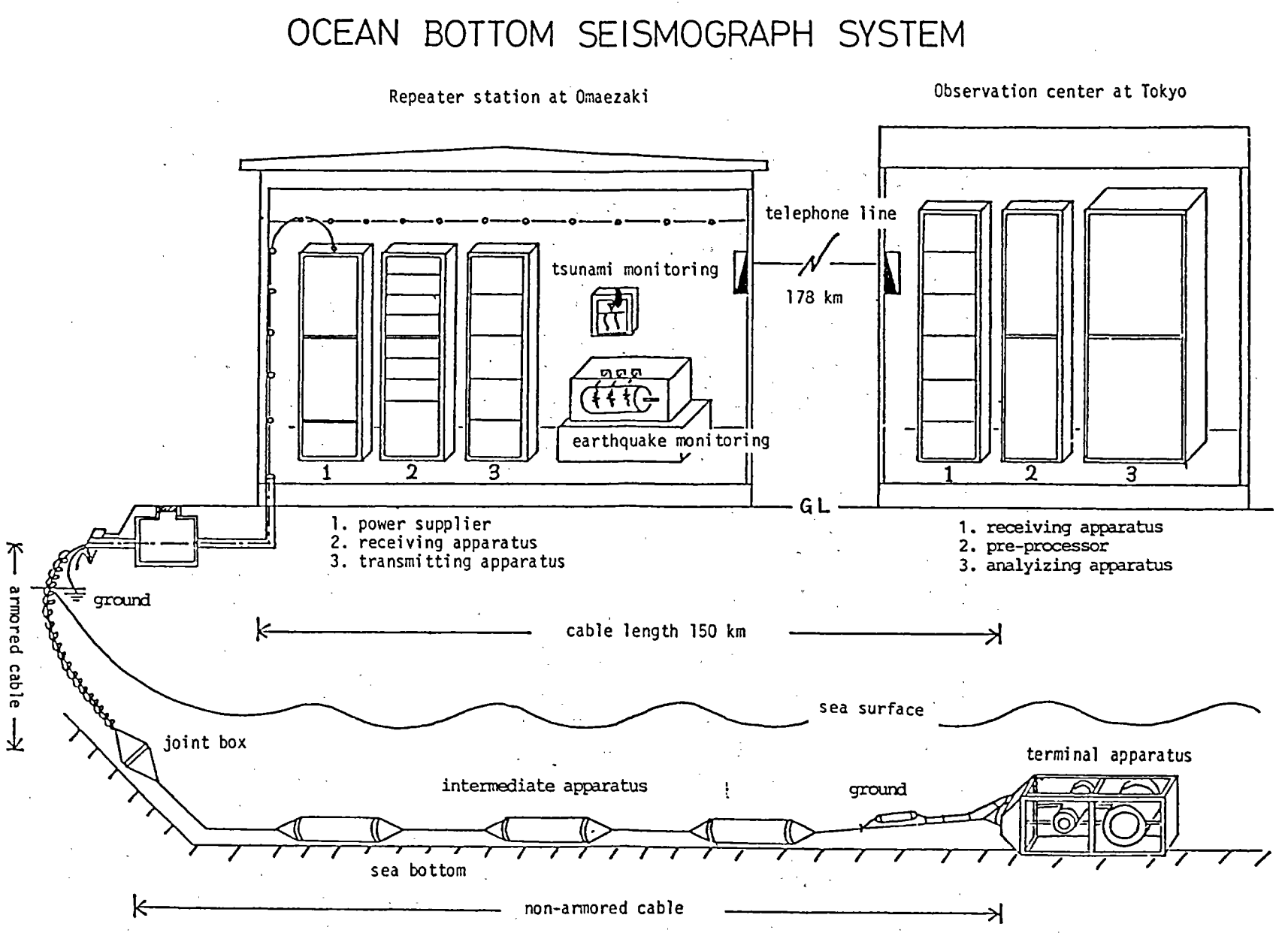

Fig.1. Ocean bottom seismograph system off Cape Omaezaki. Seismographs are kept in the intermediate apparatus and the terminal one and the pressure gauge (tsunami meter) is store in the terminal one at the depth of 2202m.

There, a large amount of data, including the data from OBSs, is processed by the Earthquake Phenomena Observation System (EPODS).

The locations of the OBS stations are shown in figure 2 and the positions of pressure gauges are listed in table 1. The lengths of submarine cables are about 150km and 120km for Omaezaki and Boso system, respectively. The cable routes were determined by selecting gentle bathymetry.

Table 1 - Locations of Ocean Bottom Pressure Gauge

Station	Latitude	Longitude	Depth
TK1	33° 45.90'N	137° 35.38'E	2,202m
BS1	34° 39.21'N	140° 58.68'E	4,011m
BS2	34° 44.95'N	140° 45.49'E	2,098m
BS3	34° 47.97'N	140° 30.70'E	1,912m

Sensor Algorithm

We use the quartz sensor, model 2813B, made by Hewlett Packard Co., Ltd., in USA, of which the block diagram is shown in figure 3. Let f_S and f_r be the resonant frequencies of quartz pressure transducer, QTP, and quartz temperature compensator which is stored in closed case, QTC, respectively. Then f_S and f_r are given as follows:

$$f_S=4,992,000+19.8Ts-2.0D$$
$$f_r=5,000,000+20.0Tr$$

Here, Ts and Tr are the temperature of QPT and QTC, respectively, and D is water depth in meters. Non-linearity due to temperature is negligible, since it is used in deep water where the temperature is fairly stable. Output frequency f is

$$f=f_r-f_S=8,000+20.0(Tr-0.,99Ts)+2.0D$$

and it depends not only on pressure but also on temperature. Thermally induced changes of output frequency are mostly derived from the difference between Tr and Ts generated by environmental water temperature fluctuations. Hence, this sensor is not good for sea level measurement in the shallow water where temperature fluctuates. If water temperature changes suddenly, the output data fluctuates for about one hour.

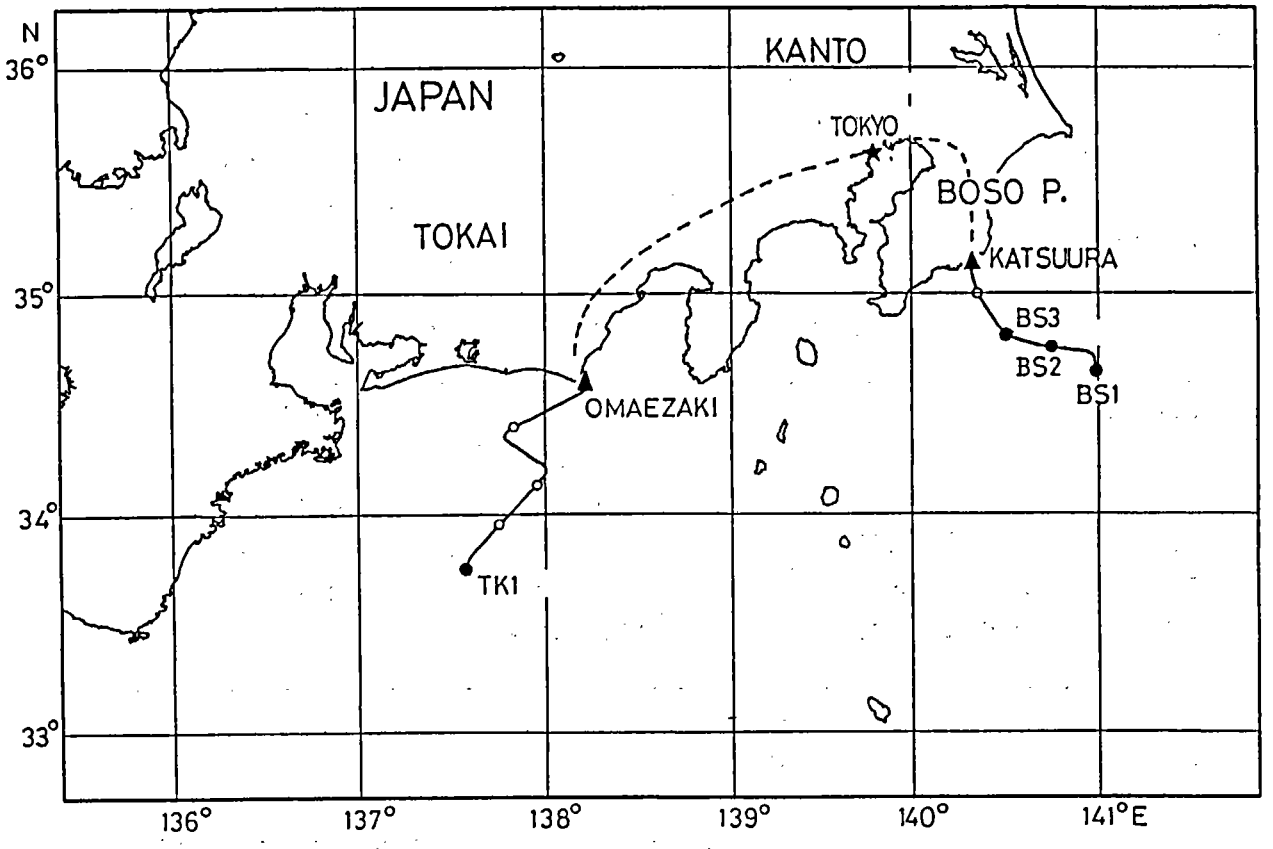

Fig.2. Cable routes and stations of ocean bottom seismograph network. Seismographs are laid at the open and closed circles and tsunami-meter are installed at the closed circles.

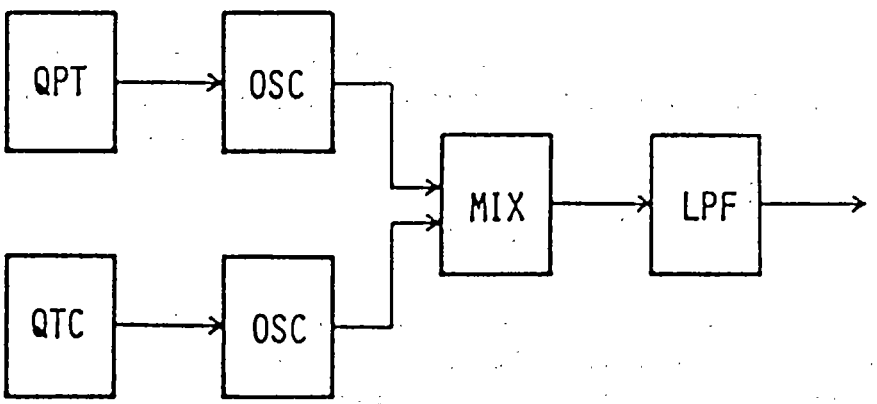

Fig.3. Block diagram of the pressure sensor. QPT:quartz pressure transducer. QTC:quartz temperature compensator. OSC:oscillator. MIX:mixer. LPF:low pass filter.

Frequency of output is determined by measuring mean time interval of pulses, about 8000 pulses for low gain and 160,000 pulses for high again. The resolution is 1cm in sea level change for low gain and 0.5mm for high gain.

The pressure response to sea surface wave depends on the wave length and water depth. The ratio of pressure head at bottom in meters of water to surface wave height is

$$R=\mathrm{sech}(2\ h/L).$$

Here h and L are water depth and wave length. Figure 4 shows an example of frequency response for TK1. We cannot expect to observe waves shorter in period than a few minutes.

Records

In the record of ocean bottom pressure gauge we can find not only sea level changes, due to tides and tsunami, but also thermally induced fluctuations and pressure variations caused by sea bottom motions.

Figure 5 prepared with EPOS shows a typical feature. The record at BS1 station indicates ocean tide fairly well, however the ones at BS2 and BS3 are somewhat disturbed by thermally induced noise, since BS2 and BS3 are half depth of BS1 and thermal fluctuation is larger.

Figure 6 represents the pressure variation caused by seismic bottom motion. Vertical ground motion generates pressure wave traveling in water with the acoustic speed and being reflected by the surface and the bottom. The seismic wave may disturb the low gain record of 1Hz sampling, but high gain of the 20 second interval has little sensitivity to ground motion.

A large earthquake occurred near the Aleutian Islands on May 7, 1986, and a small tsunami of about 20cm in total amplitude was observed at many tide stations along the Japan Islands. We can find the fluctuation of tsunami on the record of BS tsunami meter shown in figure 7. The amplitude is smaller and the ground motion noise is larger, as water gets deeper.

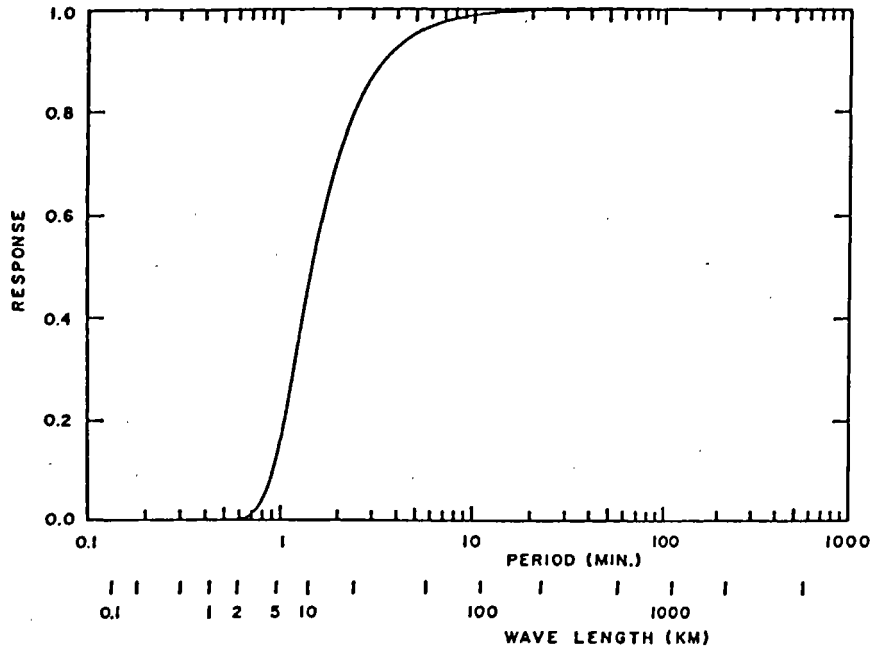

Fig.4. Frequency response of pressure at 2,200m deep to surface sea wave.

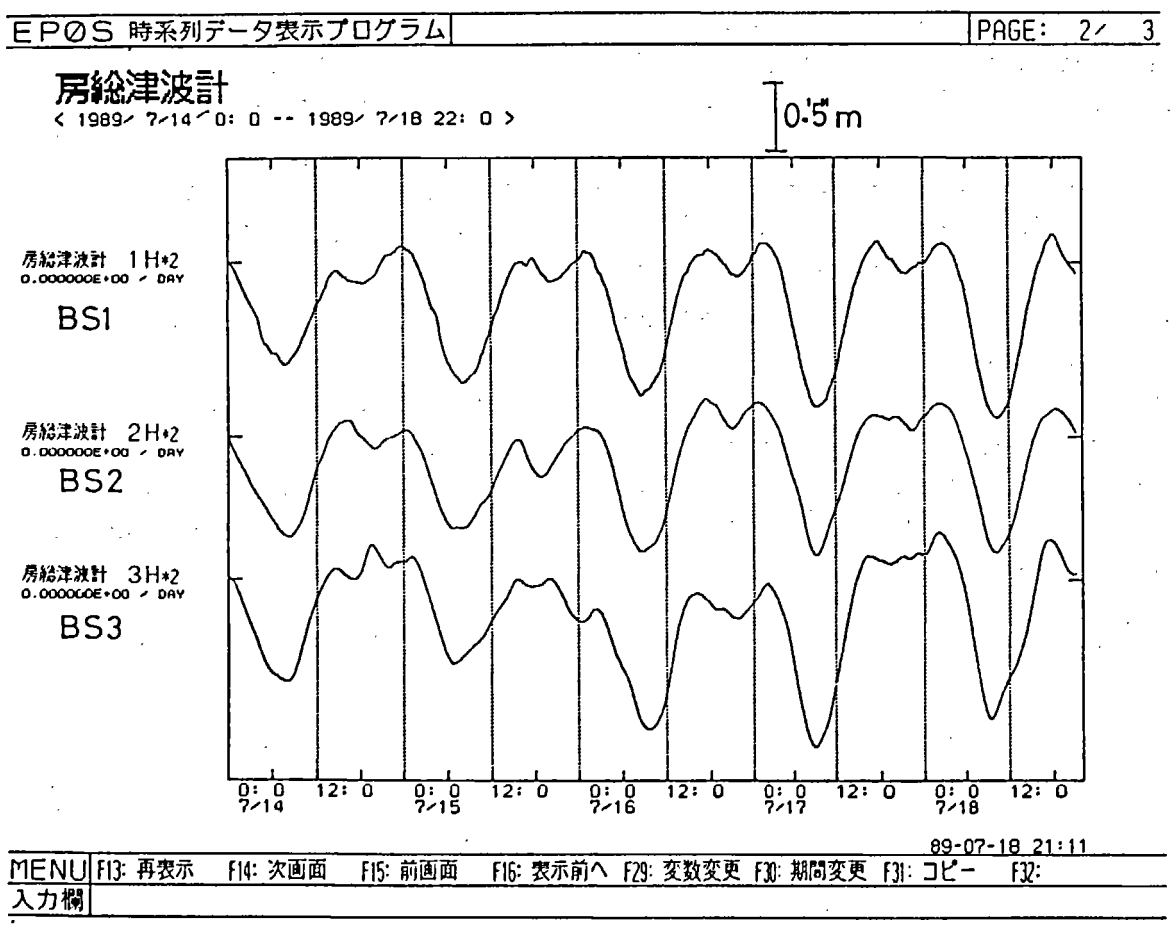

Fig.5. Example of pressure gauge records processed by Earthquake Phenomena Observation System (EPOS). Upper middle and lower are the records at BS1, BS2 and BS3, respectively.

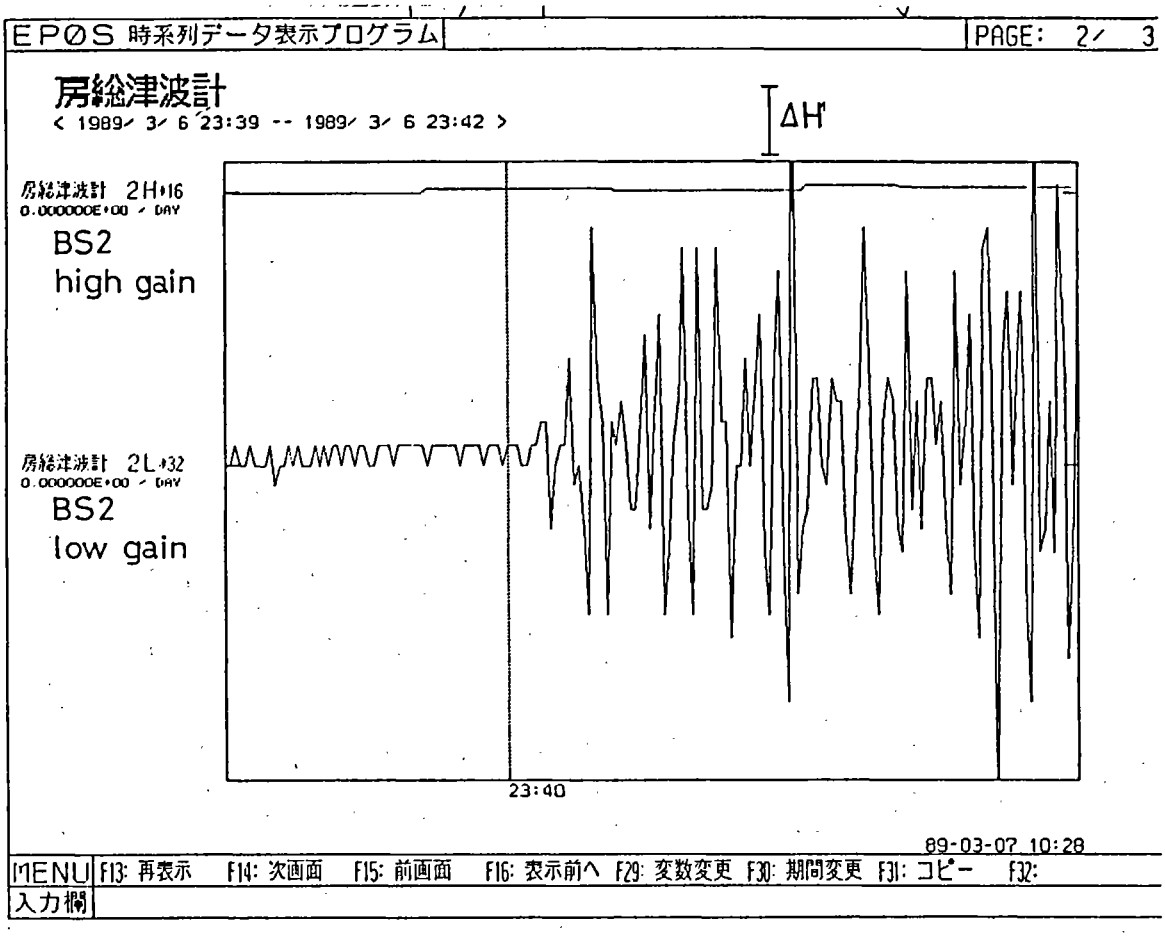

Fig.6. Example of seismic wave recorded by the bottom pressure sensor. Pressure change is induced by vertical ground motion. Upper and lower are high gain (0.05 Hz sampling) and low gain (1 Hz sampling) at BS2. ΔH is 6.25cm for high gain and 3.125cm for low gain.

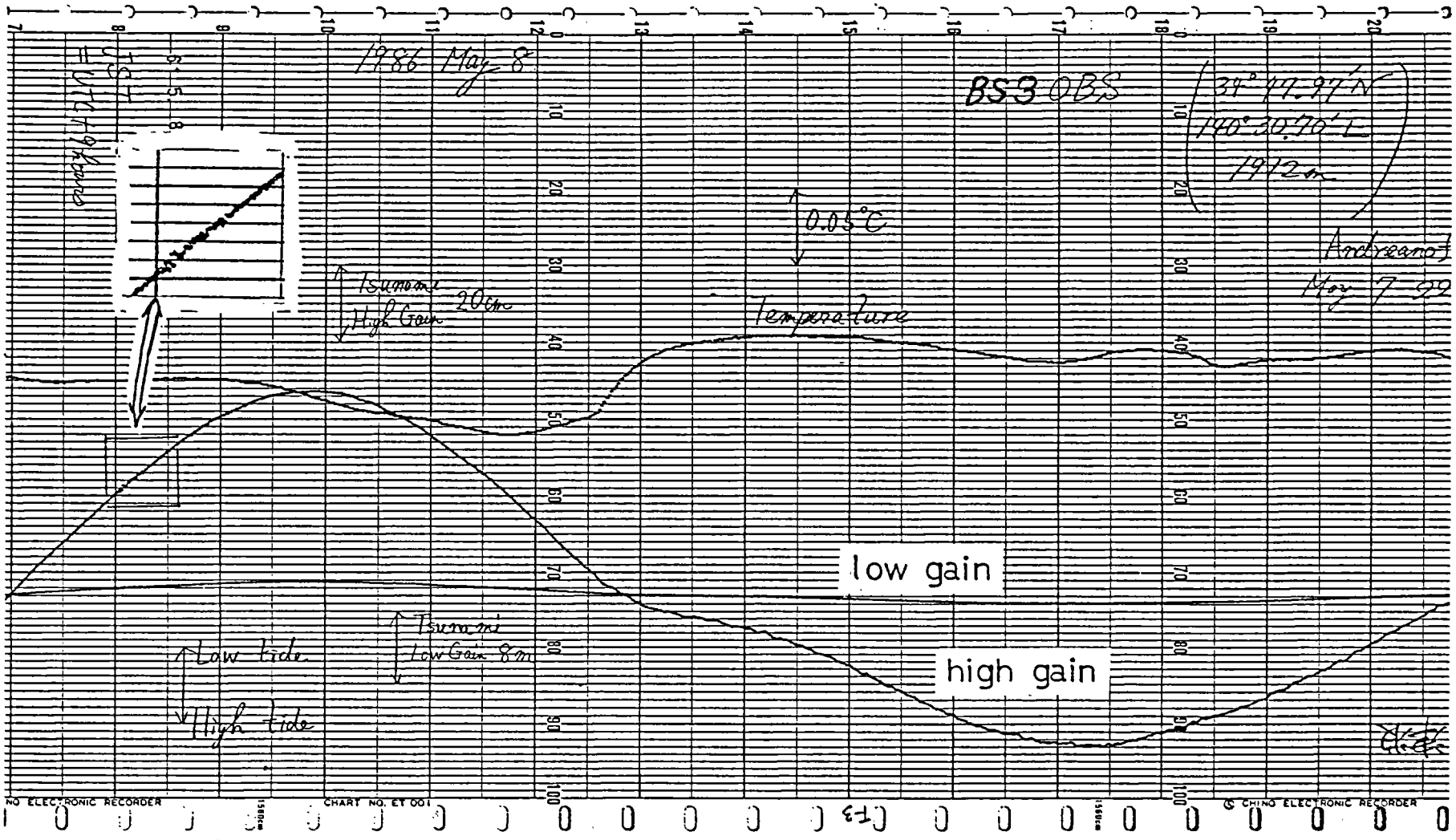

Fig.7. Small tsunami accompanying the earthquake of M7.5 occurred near the Aleutian Islands. Noise induced by ground motion is also recorded.

THE COASTAL TSUNAMI WARNING STATION "MEGA"

G.S. Rybin

The coastal tsunami warning station "Mega" was designed for the automatic system of tsunami warning developed at the Soviet Far East.

The station design and operation just meets the requirements of the tsunami determination which occur infrequently. In order to justify the costs the equipment at the station has been designed to provide, besides tsunami detection, automatic oceanographic observations in the coastal zone. To provide this additional function the following oceonographic parameters are measured:

- Sea level to +5 cm, -5 cm in the range of up to 20 m (hourly mean, 24-hour minimum and maximum);
- Sea water temperature to + 0, 05°C;
- Sea water conductivity to 0,006 Cm/m; (The observed values of sea water temperature and conductivity are also used for sea water density and sea level computations).
- Wind wave components averaging over ten minutes (mean wave period from 2 to 30 sec, average and maximum amplitude). The station comprises of two basic units: the submarine measuring unit and the land based unit. Both units are connected with each other by four core cables (the operating state is supplied by two core cables), of up to 6 km length for both power supply and data transmission. The communication cable is made of a three core geophysical wire and a telephone cable. The cables are coupled in a hermetic junction box. The submarine unit can be set up to 15 m depth. The land based unit is supplied with a built-in microcomputer to provide the control of the complex, data processing and output, built-in numeric display; video monitor, teletype, analog data recorder, and standard interface C2 for data transmission to the master center over the communications channels. In a waiting mode by the station operation can transmit the information each 1,3 or 6 hours, in the warm mode. Tsunami, each ten minutes.

To increase the reliability of the tsunami detection the following special algorithms of data processing are suggested:

- Filtering one second readings for tolerance and overshootings exceeding 3 (3.3 of the value of the standard deviation);
- Filtering one minute readings using Bourterwort's algorithm;
- Detecting the tsunami by comparing the first and second derivatives with the accepted for a given place's limits;

- Defining the dangerous phenomenon associated with the exceedance of the lower and upper limits of sea level;

- Overall there is no problem with the minimum false alarms because the final decision about their emergency message is taken either by an operator guided by the diagram on the display or by the system master center from the summation of the available data. The principal task of the station is not to miss a tsunami. The control test of the proposed algorithms showed 4 minutes of tsunami detection lag compared to the real records of tsunami.

The improved reliability of the station performance is provided by the following special measures:

- Two hydrostatic pressure sensors have been installed, one of which could be contacted with the atmosphere by means of a pneumatic wire;

- Two communication lines are provided operating in a different freguency spectrum;

- Special algorithms (time diagram of data transmission) has been developed for transmitting sea level data by codes and by frequency-modulated signals. Also, there is a failure analyzer which transmits the signal from the sea level sensors to the communication lines for continuous emission in case the control module fails;

-Continuous-attentive monitoring of processors are provided for hardware and software, for switching the processors, and for restarting the programme;

-Electric power is supplied from the electric circuit with a wide range of voltage from 170 to 250 vt. In the absence of electric power, 24 vt storage battery is used.

In 1989, the prototype stations were tested at the laboratory and in the field. In due time eight to ten such stations will be deployed in the Pacific.

TPC-1 REUSE AND GLOBAL SEISMOLOGY

Junzo Kasahara
Earthquake Research Institute, University of Tokyo
1,1,1 Yayoi, Bunkyo, Tokyo 113, Japan

Abstract

Recently many submarine cables which have been used over two decades will be replaced or are planned to be repalced by new optical fiber cables. The TPC-1 (Trans Pacific Cable-1) submarine cable connecting Japan-Guam-Hawaii is one of these. The current TPC-1 was replaced by the new TPC-3 in June, 1989. Since the new one has 7,560 channels of telecommunication in contrast to 138 channels of the current one, all of TPC-1 channels were transferred to the new one. By this reason, TPC-1 will be retired soon.

The feasibility study for the POSEIDON project has found that the reuse of the present TPC-1 with its own seismic cable would be the most practical and cost-efficient way to realize the global seismic network in the oceanic region. We call this the TPC-1 geoscience cable project. In the first stage, only Japan-Guam segment will be used.

The TPC-1 geoscience cable system is composed of sensor units, a transmission station, a terminal station, a power feed station, and a data center. The sensor units will include two seismometer units and one geophysical unit. The seismic unit will include conventional velocity type seismometers, very broadband seismometers, and a hydrophone. The frequency band of the broadband seismometer will be from 0.003 to 30 Hz which is similar to GEOSCOPE or IRIS. The resolution level will be slightly lower than those. The geophysical unit will be equipped with identical seismic sensors as the seismic unit and with other geophysical sensors such as pressure gauge, electropotential meter, magnetometers, water current meters and quartz thermometer. This unit will branch from the main cable. To obtain high resolution, the current analog telemetry method should be converted to the digital method. The whole data will be telemetered to the data center in Tokyo.

The remaining life of TPC-1 is estimated to be long. The installation of TPC-1 geoscience cable system might greatly contribute, not only to global seismology, but also to tsunami measurements and other deep ocean geoscience projects.

This paper describes the outline of TPC-1 project at Earthquake Research Institute, University of Tokyo, Japan.

1. Optical fiber cable technology and TPC-1

Many submarine cables such as TPC-1 and HAW contribute to international communication linkages. The TPC-1, which is one of those submarine cables, runs from Japan through Guam to Hawaii and HAW runs from Hawaii to the west coast of the US.

In July 1987, KDD, which is a Japanese international telecommunication company, announced that Hawaii-Japan telecommunication cables using coaxial cable technology will be replaced by a new optical fiber cable, called TPC-3 (Figure 1). TPC-3 has 7,560 telephone channels in contrast to 138 channels of the current TPC-1. The use of TPC-3 began in June 1989. For this reason, TPC-1 has been planned to be retired in September 1990.

The feasibility studyh for the POSEIDON project has found that the reuse of the current TPC-1 would be the most practical and cost-effective way to realize the GDSN (Global Digital Seismic Network) in the ocean.

In addition to the seismic use, there is a plan to use TPC-1 for other geoscience observations such as deep sea tsunami measurements, magmeto-telluric measurements, ocean bottom temperature measurements, bottom water current measurements and other geoscience measurements. In this sense, the TPC-1 cable could be the trans ocean geoscience cable.

Many other new optical fiber cables are now either under construction or in the planning. HAW-4 is currently under construction. HAW-4 and TPC-3 will serve as communication links between Japan and USA.

2. Outline of TPC-1 project

The TPC-1 project aims to convert the current telecommunication TPC-1 cable to geoscience cable system. In the first stage, only Japan-Guam segment of TPC-1 will be used because of the unknown release time of Guam-Hawaii segment. The Japan-Guam segment will be equally owned and used by the University of Tokyo as Japanese representative, and IRIS (Incorporated Research Institutions for Seismology), and/or JOI (Joint Oceanographic Institutions), as USA representatives. The geoscience cable system will be composed of five major portions: sensor stations, a power feed station, a transmission station, a terminal station and a data center. These will be described in the following sections.

2 - 1 Power feed station, transmission and terminal stations, and data center (Fig. 2)

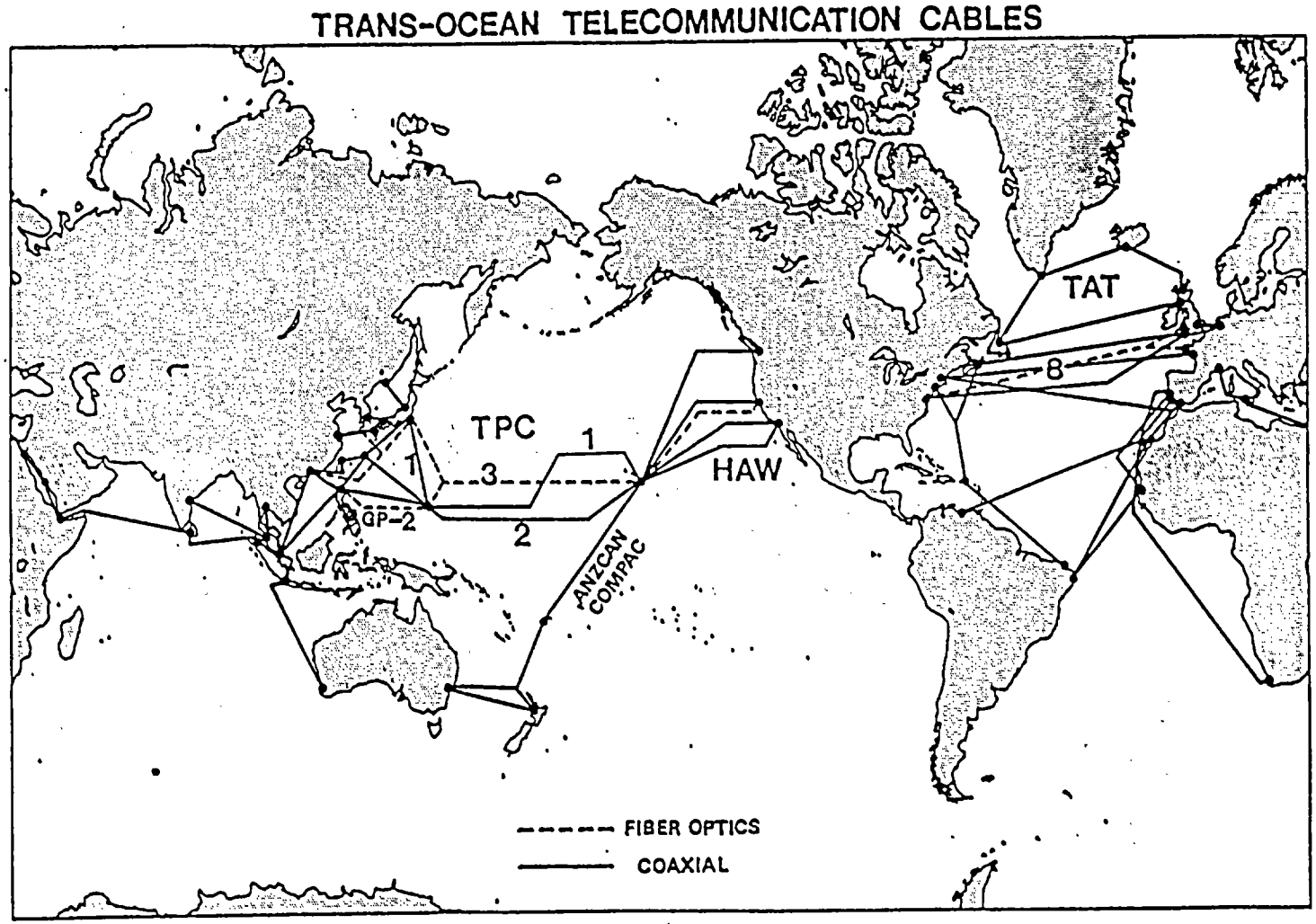

Figure 1
Trans-ocean telecommunication cables in the world. Cables using coaxial technology by solid line and ones using optical fiber technology by dotted line.

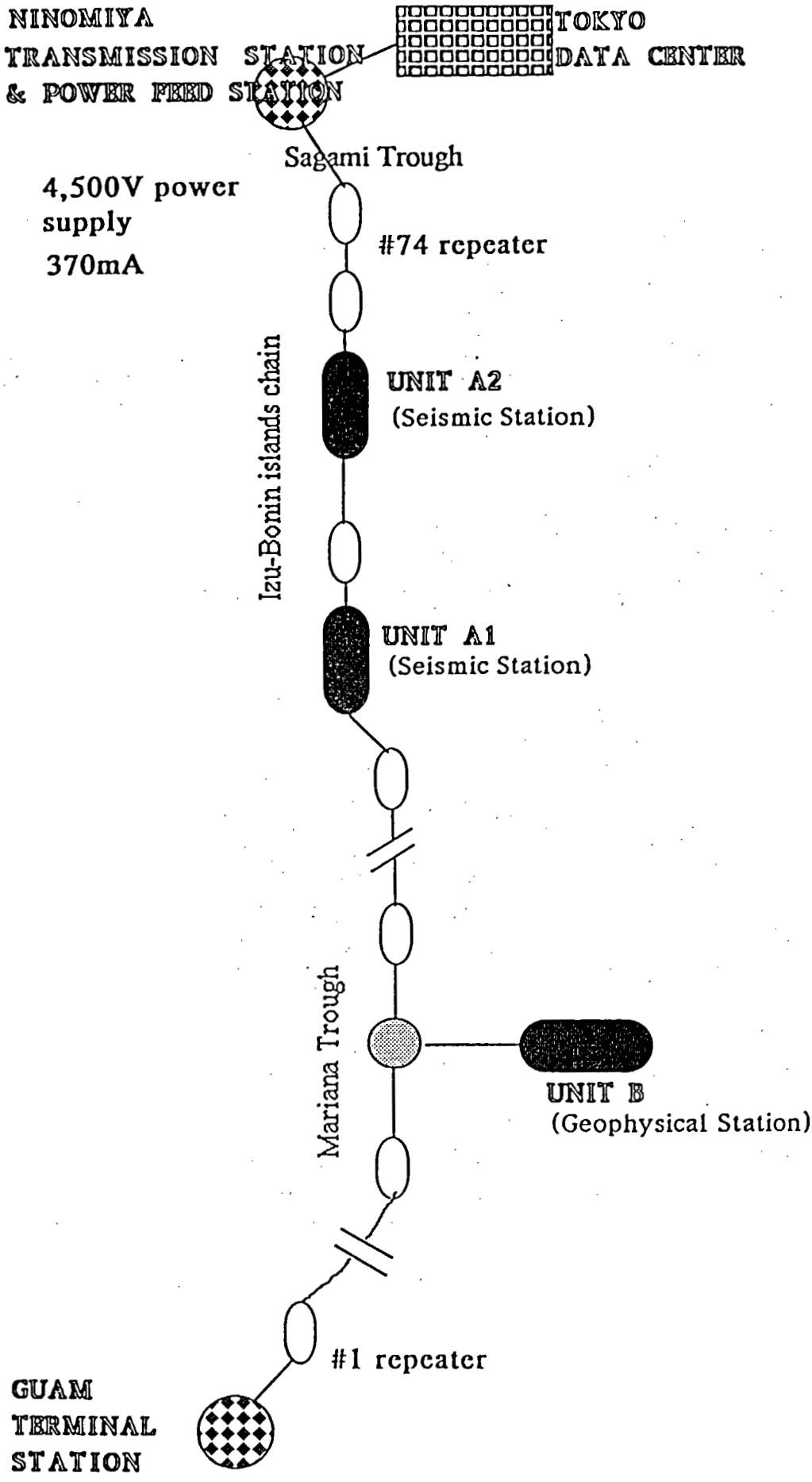

Figure 2

A plan of TPC-1 geoscience cable. Units A1 and A2 are seismic stations and unit B is a geophysical station. In this plan, power is supplied by the Ninomiya station in Japan.

The installation of seismic units into the present telecommunication cable requires an adjustment for the power feed to the cable. The current supply voltage of 4,500 V should be raised according to the power dissipation in each geoscience unit. However, the maximum voltage is limited to 6,000 V. On the other hand, the supply current should be kept to be constant as 370mA. Ninomiya (Japan), or Guam could be the power feed station, and either one could be the ground station. In contrast to the Japan-Guam segment case, in the current TPC-1 Guam-Hawaii segment, both Guam and Hawaii stations are power feed stations. In the middle of the total cable length, the cable is grounded to the sea water.

To meet the broad frequency band and the wide dynamic range specifications, the data telemetry system should be modified from current analog telemetry to digital telemetry. The transmission capacity of one voice channel corresponds to 7,200 Baud. If one voice channel is used for 3 component seismometer outputs, we can get 100Hz even for 24 bit on one data length. Other geoscience data need only slow data rate. Since TPC-1 has 138 channels, there are enough channels besides the seismic sensor unit.

By the terminal equipments at the landing station, geoscience data and DC voltage are separated. The telemetered signals are transferred to the commercially available digital telephone line.

At the data center in Tokyo, the telemetered geoscience data are received. Broadband seismic data are edited in the standard FDSN format. The broadband seismic data obtained by the TPC-1 will become a part of FDSN data set.

2 - 2 Sensor station

Sensor stations

Since University of Tokyo has not received the go sign for the Guam-Hawaii segment of TPC-1, the current TPC-1 project is limited to the use of the Japan-Guam segment. Two seismic unit and one geophysical units are being considered (Figure 3). By using the above, four principal measurements are planned, that is, seismic, tsunami, electromagnetic, and ocean bottom environmental studies. The quartz pressure gauge is a tsunami sensor. For electromagnetic measurements, an electrical potentiometer, a proton-magnetometer, and a three-components fluxgate magnetometer will be used. For the ocean bottom environmental study, bottom current meters, a Doppler current meter, a quartz thermometer, and a salinity meter will be used.

Seismic sensor (Figure 4)

Two seismic units will be installed along Izu-Bonin islands. Three kinds of seismic sensors are considered, such as conventional velocity type seismometers, broadband seismometers and a hydrophone. A velocity type seismometer has been successfully used

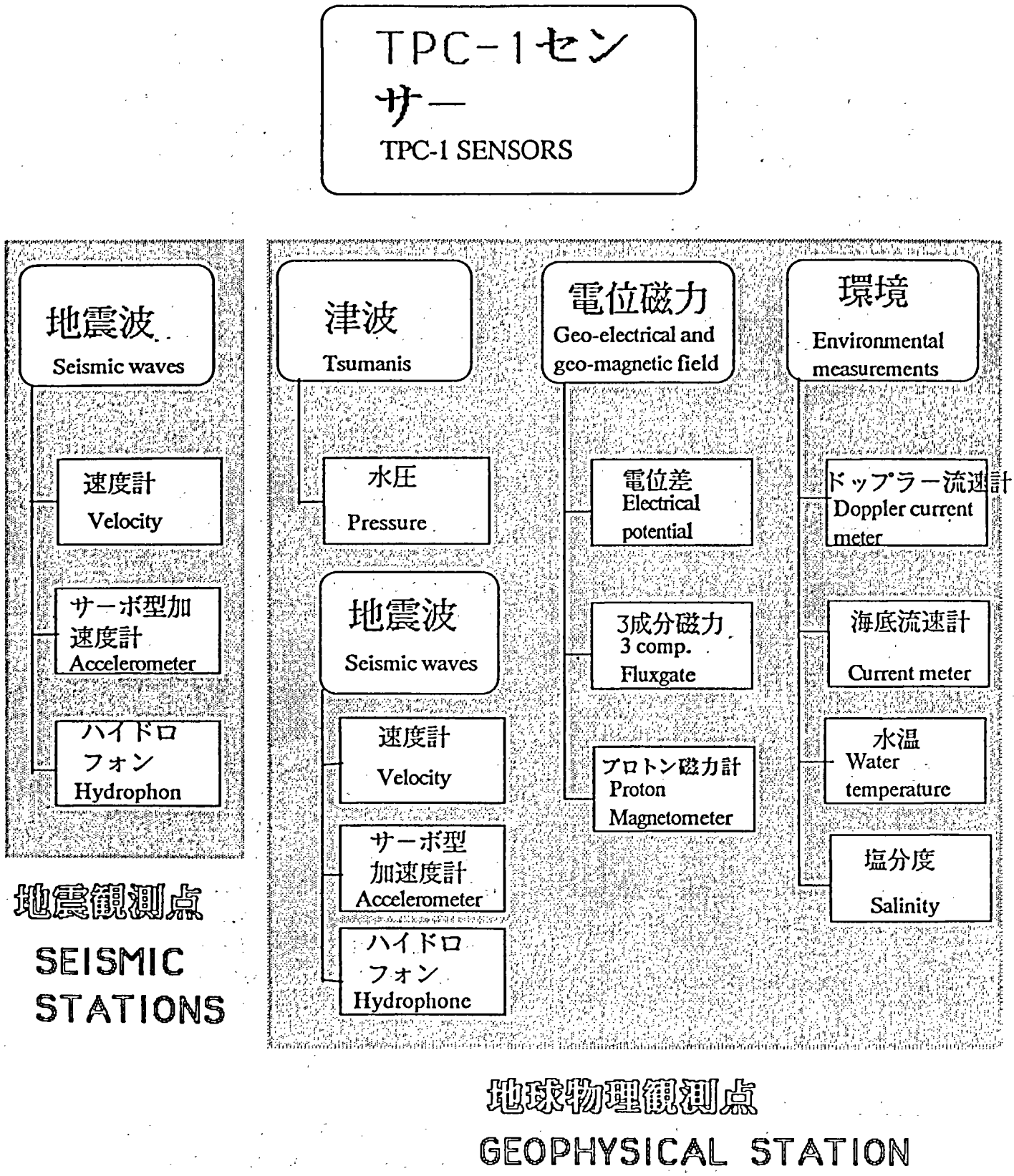

Figure 3
TPC-1 sensor assembly plan for seismic and geophysical stations.

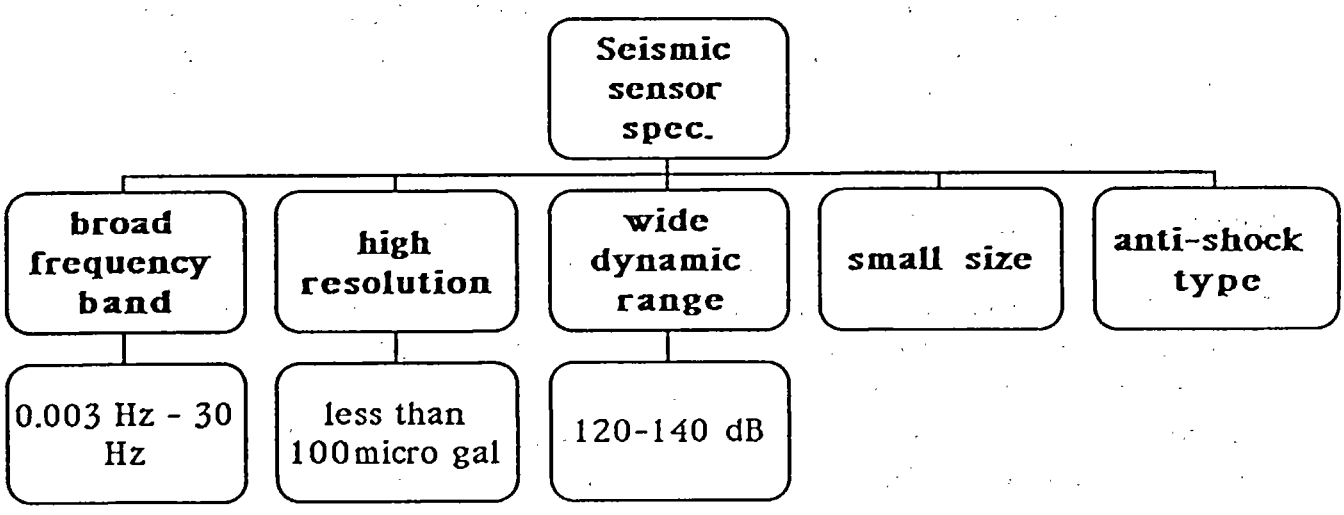

Figure 4
Seismic sensor specification.

by pop-up ocean bottom seismometers and it proved its high reliability. High frequency pressure components of a seismic wave can be detected by hydrophone. A broadband seismometer is quite new. One of the objectives of the TPC-1 project is to observe distant earthquakes. It is necessary to detect the long period component of an earthquake with significant S/N ration. The target specifications for broadband seismometer is: a) frequency band such as 0.003 Hz to 30 Hz, b) high resolution level less than 100 micro gal in acceleration level, c) wide dynamic range similar to GEOSCOPE, namely 120-140 dB, d) small enough size in submarine repeater pressure case, and e) anti-shock type. The sensor should be strong enough during rough treatment in deployment work in the ocean. The existing long period land seismometers such as STS-1/2 VBB and Teledyne BB-13 may not satisfy such rough operation. Also, the size of existing long period land-use seismometer may cause difficulty on mounting it in the small pressure case.

Broadband seismometer

One of the candidates for the broadband seismometers is the CMG-3T made by Guralp Co. Ltd. This instrument needs very precise vertical and horizontal axial controls at initial setting. There is no field experiences for long range ocean bottom observation. The other candidate is an aerospace precision accelerometer for INS (Inertia Navigation System) used in aircraft. The aerospace accelerometer is small enough and it is shock resistant. The dynamic range for the precision accelerometer has roughly an order of 100 dB to 120 dB. By using two different kinds of precision accelerometer (two JA-5V and one QA-1400 manufactured by JAE (Japan Aeronautical Electric Co. Ltd.) and Sundstrand Data and Control, Co. Ltd., repectively, it was found that its resolution level is around 100 micro gal over 30 seconds to 30 Hz (Katao et al., 1989). The comparison of outputs from three kinds of aerospace accelerometers showed precise matching of wave forms within the above frequency band and signal level. Figure 5 shows a comparison of outputs among two JA-5V accelerometers and a 2 Hz conventional velocity type seismometer. All seismometers are horizontally set. It is seen that both accelerometer records are almost identical. Figure 6 shows integrated wave forms of accelerometer outputs. Integrated accelerometer wave forms which correspond to velocity components show very low frequency initial onset of S wave even though this event occurred locally. The quite important nature of wave forms was lost in the 2 Hz velocity type seismometer record. The high pass, higher than 2 Hz, filtered and integrated outputs of accelerometers are very similar to the velocity seismometer records. The noise level in the low-frequency band can be reduced by the use of a pair of sensor units.

An accelerometer can also be used as an inclinometer because it responds to gravitational force, if the DC components are recorded. Aerospace accelerometers can also be used without gimbals. However, in the long period range, the temperature

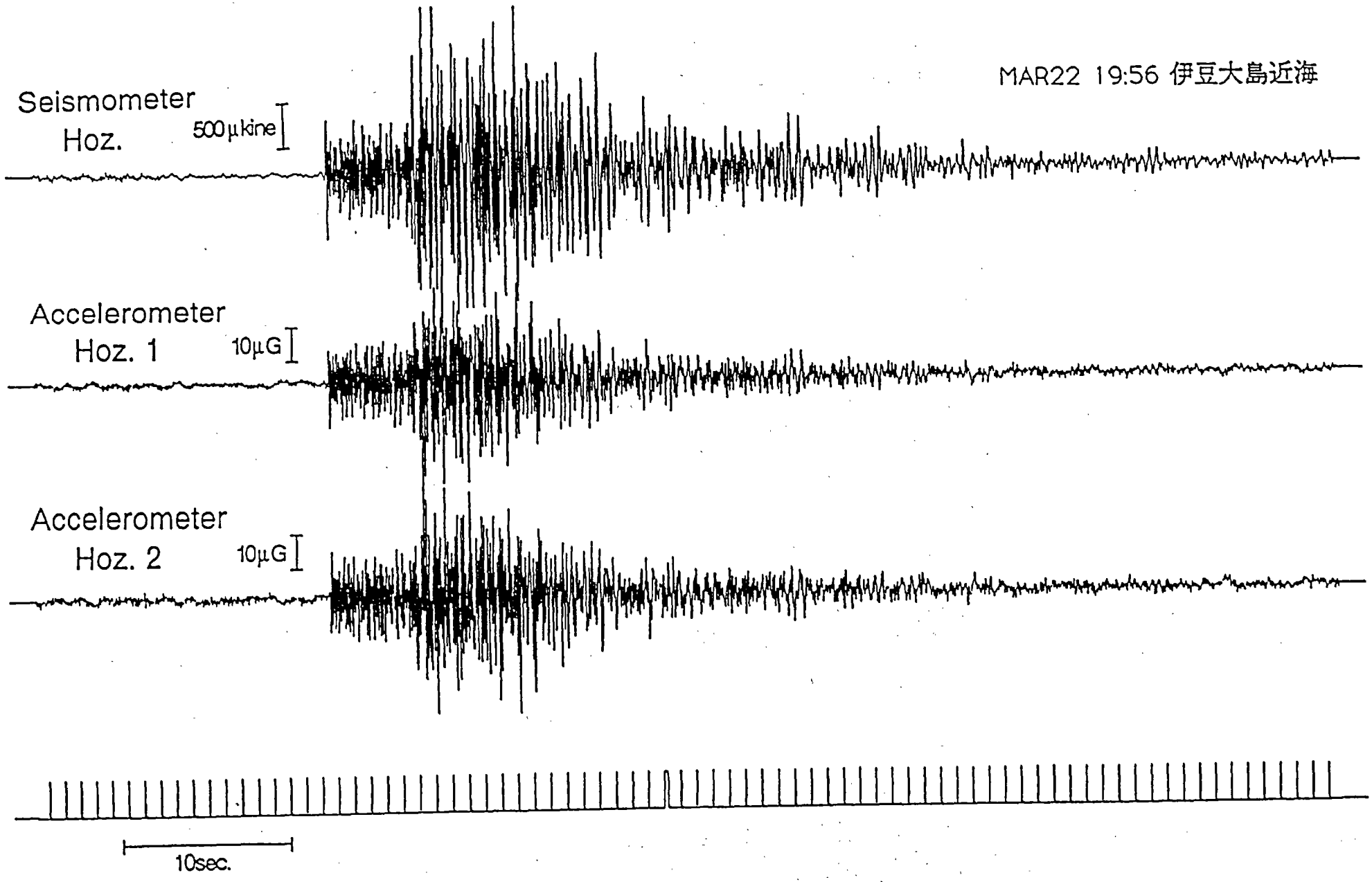

Figure 5
Comparison of two accelerometer (JA-5V) outputs and one 2 Hz velocity seismometer output (top) observed at Abratsubo Observatory. All are horizontal components. Bottom is second mark.

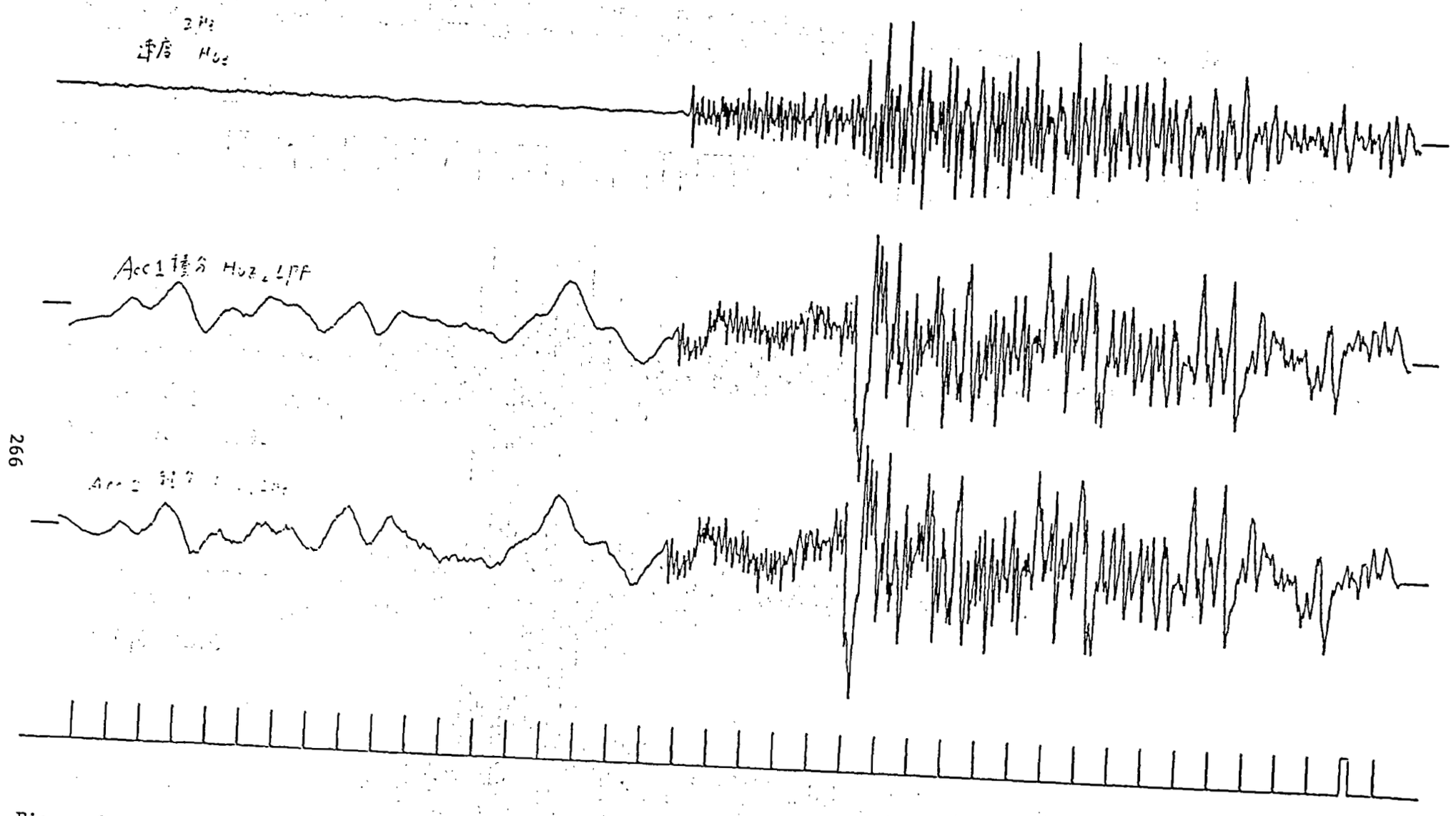

Figure 6
Integrated acceleration records for seismograms shown in Figure 5 with velocity seismometer record. 0.1 Hz high pass filter applied to two accelerometer records. Note the low frequency onset of S wave seen in integrated accelerometer records, in contrast to velocity meter records.

dependence might be one of the most important factors. It might be necessary to measure ambient temperature at the same time for the purpose of the temperature correction. The greater difficulty in the observation of the long period component is the natural excitement on the ocean floor. There have been very few noise spectral studies of ocean bottom noise. Some measurements (Sutton et al., 1988; Webb, 1988) showed the general tendency of ocean floor seismic noise: one high peak in several seconds, minimum in several ten seconds, and sharp increase at lower than several ten seconds. It may change from place to place and from time to time. At this moment, we do not know how extensive this disturbance of the broadband seismic measurements is and if this disturbance is significant, or how we can reduce the noise. One of the possible ways is to use an array of measurement and the f-k domain filter. In this case, we should modify the system design for seismometers significantly.

The shape of the seismic unit is very similar as the repeater used by SD cable system. The deployment of the seismic unit is the same as the repair works at the occasion of cable failure (Figure 7).

Geophysical station (Figure 4)

The geophysical unit will be installed as a branch from the main cable because of minimizing induced electromagnetic field by the main cable. The geophysical unit will contain a seismic unit, a pressure gauge, an electro-potentiometer, magnetometers, water current meters, a quartz thermometer and a salinity meter. Sensor elements in the geophysical unit, such as electro-potentiometer, hydrophone, water current meter, pressure gauge, and quartz thermometer, should be exposed in the sea water. The main cable uses very high voltage (4,500V). This high voltage should be insulated. From the view point of safety, the geophysical unit should be protected against any damages due to any water leakage by these sensors. Therefore, the branching unit needs a special device to avoid exposure of high voltage to sea water if any water leakage occurs.

Since the size of an electro-potentiometer is large and the weight is heavy, it cannot be handled the same way as the repeater deployment. The deployment of the geophysical unit must be handled separate by using the "Branching technique." The operation by TPC-3 branching near the Marcus island is the first deployment by Branching Technology.

2 - 3 Objectives of the TPC-1 geoscience cable system

Figure 8 shows the objectives for the TPC-1 geoscience cable. These are our major objectives, that is, earthquake study, tsunamis, electromagnetics, and ocean bottom environmental study. In seismic measurements, we study earthquake occurrence along the Izu-Bonin and Mariana subductions, seismic tomography of Pacific Ocean and

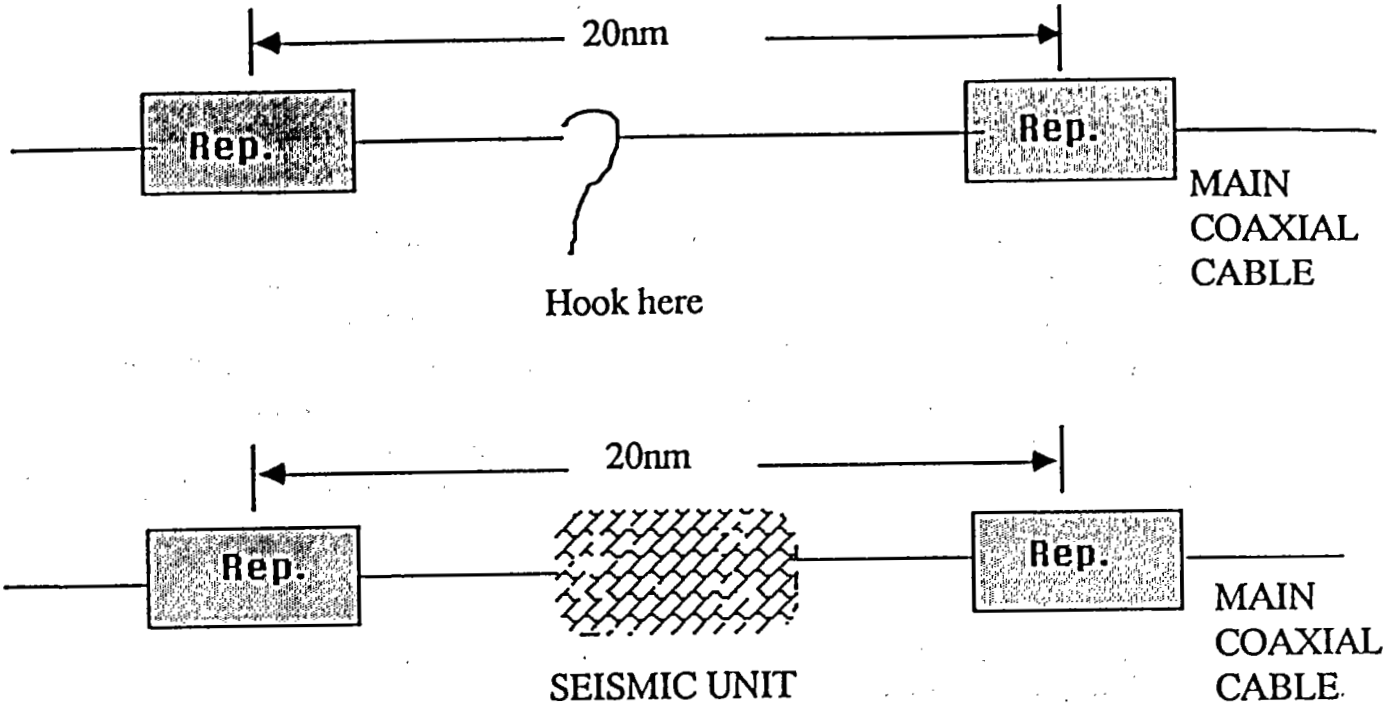

Deployment of seismic unit= Cable reparing operation

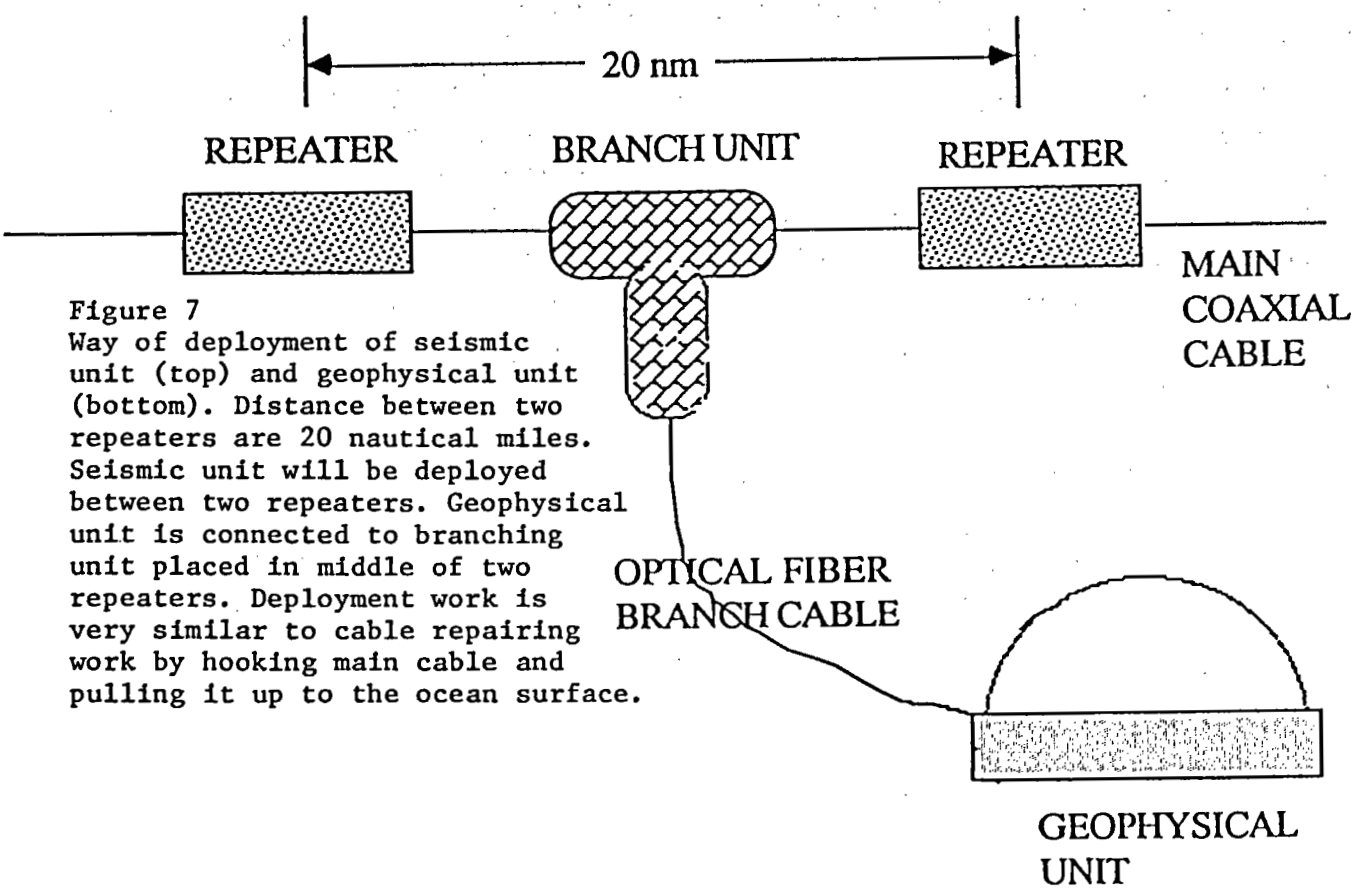

Figure 7
Way of deployment of seismic unit (top) and geophysical unit (bottom). Distance between two repeaters are 20 nautical miles. Seismic unit will be deployed between two repeaters. Geophysical unit is connected to branching unit placed in middle of two repeaters. Deployment work is very similar to cable repairing work by hooking main cable and pulling it up to the ocean surface.

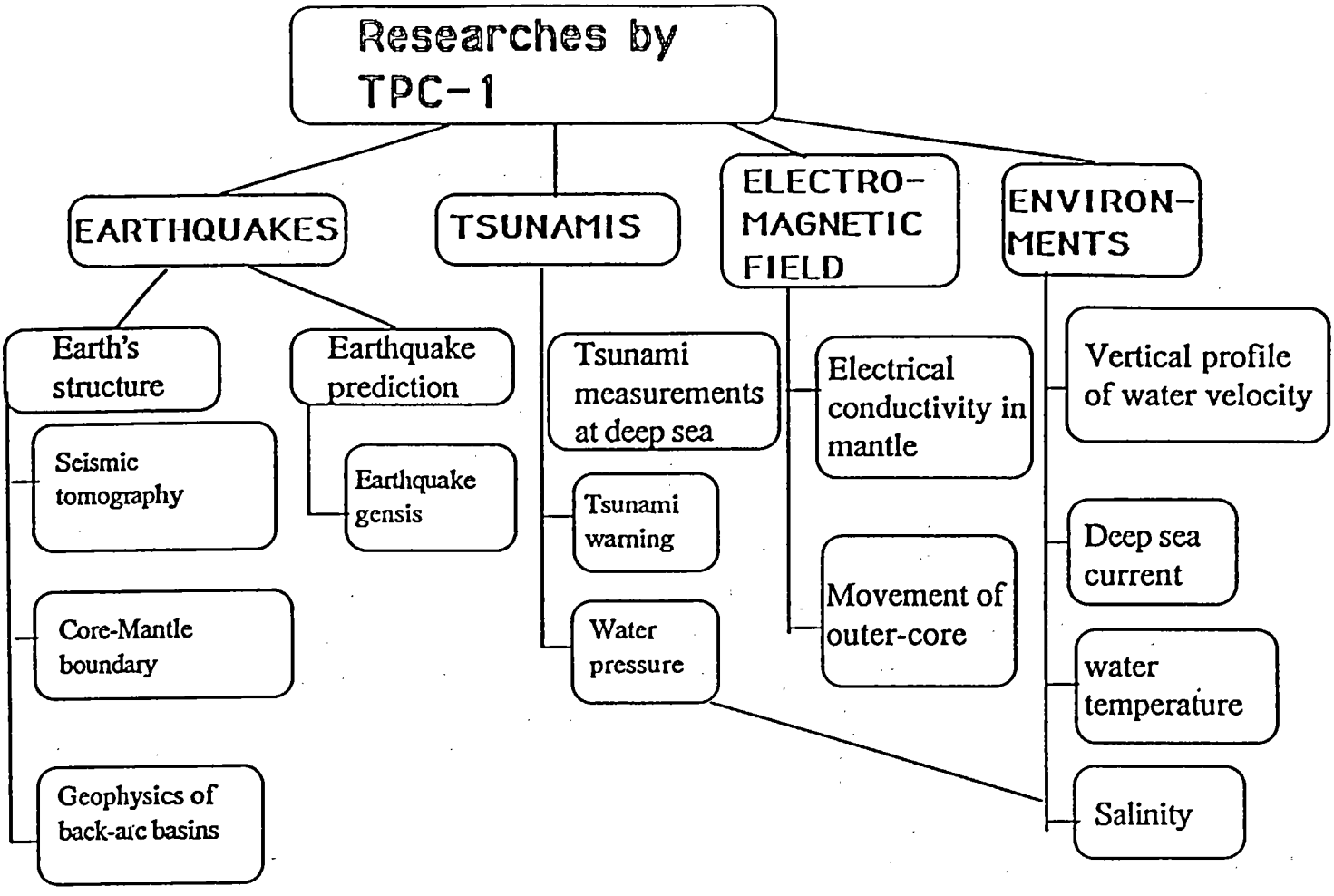

Figure 8
Research objectives of TPC-1 geoscience cable project. There are four major targets: earthquakes, tsunami, electromagnetic field and environments.

Philippine Sea (Figure 9), and mantle-core boundary study. In electromagnetic measurements, we study electrical conductivity anomalies in the mantle, and core dynamics (Figurte 10). In tsunami measurements, we study deep sea tsunami propagation (Figure 11). Since we can detect tsunami waves earlier than in Japan for those in the southern Pacific, we can predict the possible tsunami heights along the Japanese coast. However, the sensitivity of tsunami meter needs as much as 0.1 cm because the tsunami height in the deep sea is quite low even in case of tsunami caused by significant earthquakes.

3. Estimation of the TPC-1 Failure and Accidents (Figure 12)

Since this project needs a large amount of money, it should be necessary to estimate the possibility of failure of the TPC-1 during several observation periods.

3 - 1 Possibility of failure due to electronic tube

It will be a question how long can the retired cable work in the future. The telecommunication authorities explained that the retirement does not mean the end of cable life, but simply it means the necessity of a large amount of communication channels and inefficiency of operational cost-performance compared to that of a new cable. However, the construction costs of a new cable with a length of 3,000 km is too huge in costs to build it with University funds.

The high reliability of the system ensures a residual life for more than several years; at least for 10 years.

There are two major factors which control the life of the system. The one is failure due to electronic tubes used in repeaters. The other one is failure of the cable line due to natural as well as human causes, intentionally or accidentally.

The failure of the electronic tubes are mainly due to two causes, the one is "random failure," which depends mostly on mechanical manufacturing characteristics, the other one is "wear out" of the thermo-ionic emission. Both possibilities were estimated as very low.

3 - 2 Cable line troubles (Table 1)

Almost all troubles of the submarine cable system have occurred in the cable lines. The TPC-1 Japan-Guam segment experienced five cable troubles during a 25-year service period since its deployment. The causes were either natural or human activities in the shallow water area. In the future, we may not be able to escape from such kind of cable line troubles. However, the frequency of occurrence is infrequent, roughly once every five years. Since the TPC-1 has sufficient amount of spare parts, including repeaters and cables, we will be able to repair the cable and then maintain its

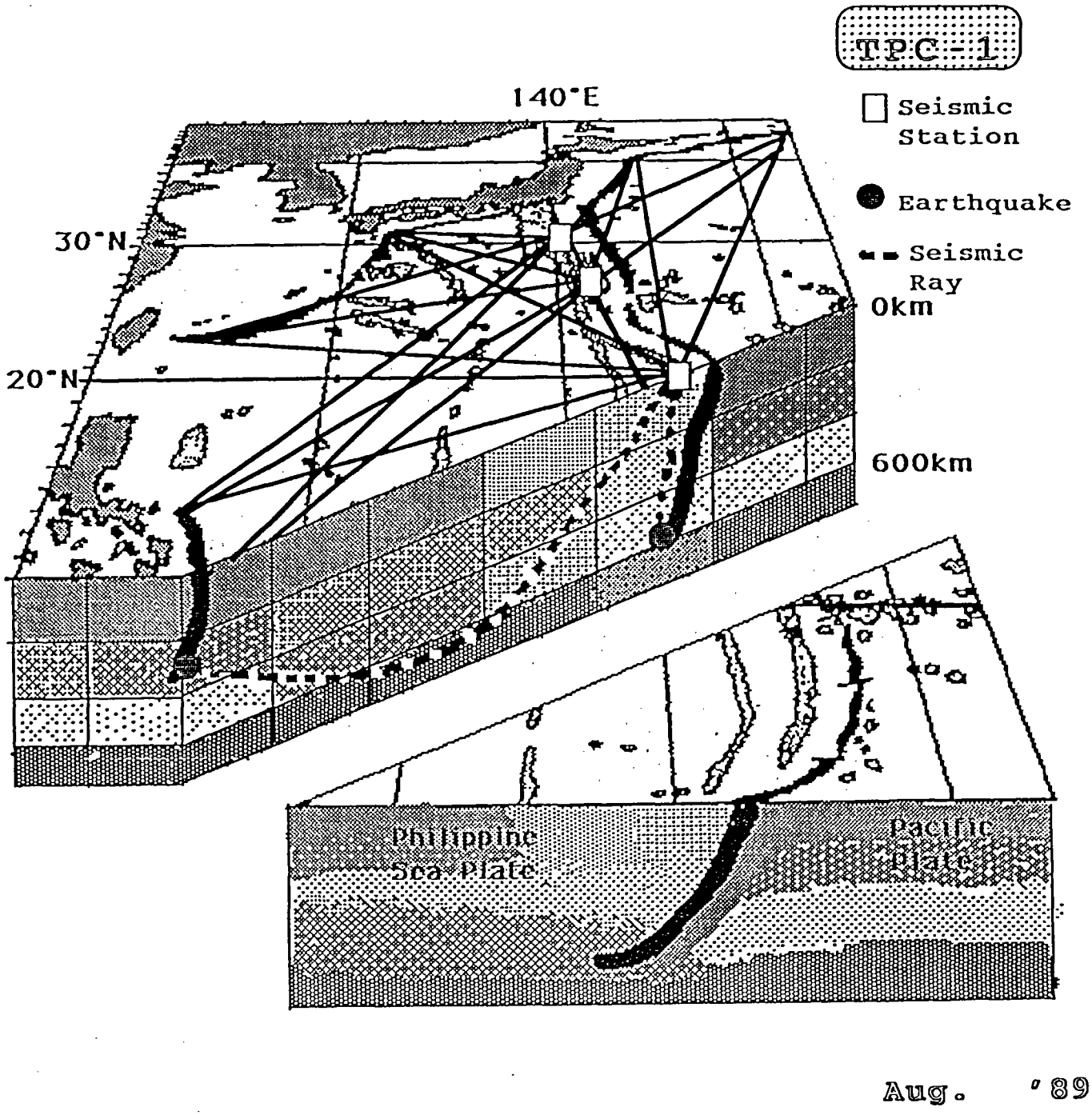

Figure 9
Illustration of tomographic study application using broadband seismometers. Three seismic stations can observe earthquakes occurring in the Philippine Sea and Japan-Kuril subduction zone.

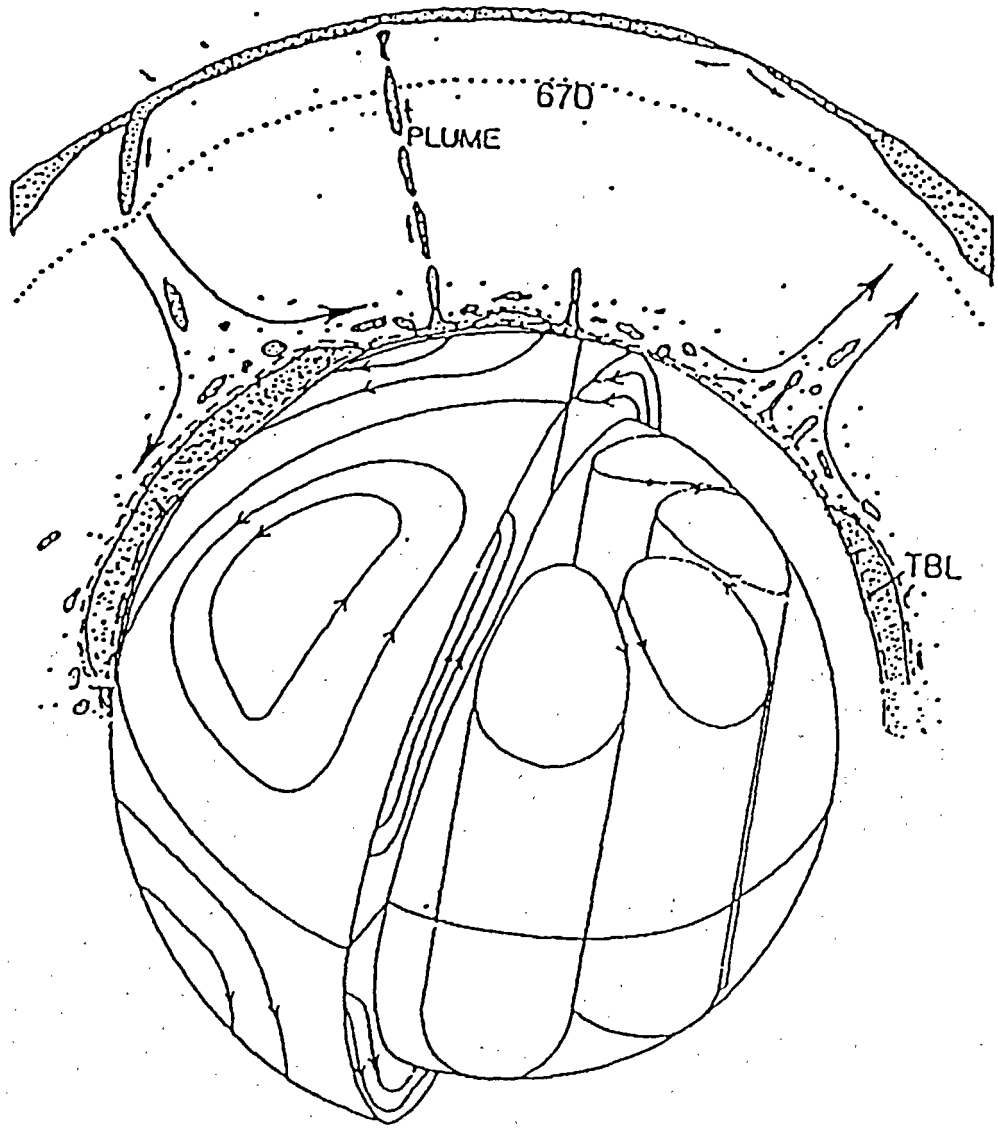

Figure 10
Illustration of core dynamic study using very long period electromagnetic observations.

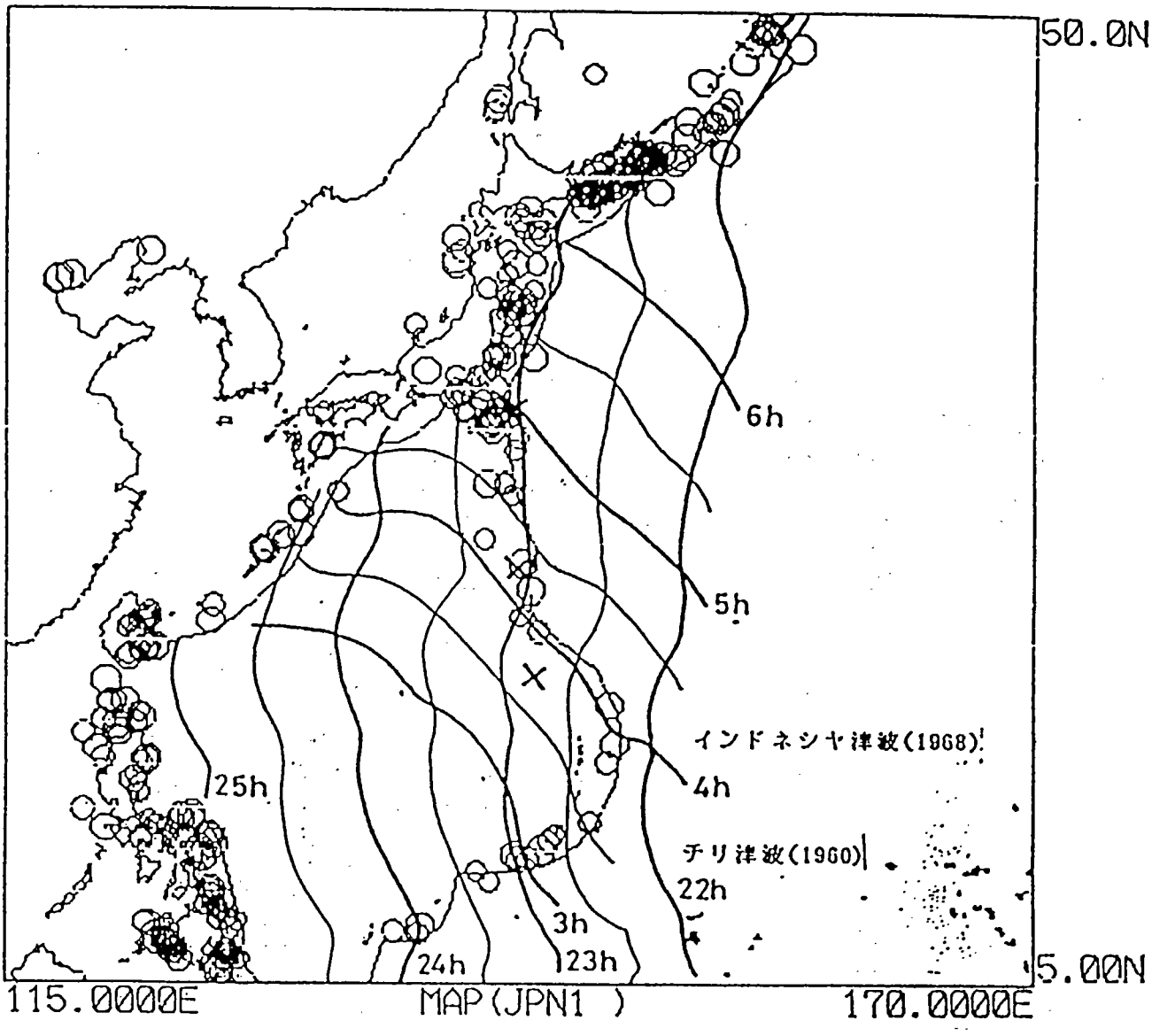

Figure 11
Tsunami wave travel time estimates for the Chilean Earthquake (1960) and the Indonesian earthquake (1968). Cross (X) showing the proposed site for a geophysical station. This station can observe tsunamis earlier than arrivals to Japanese coast.

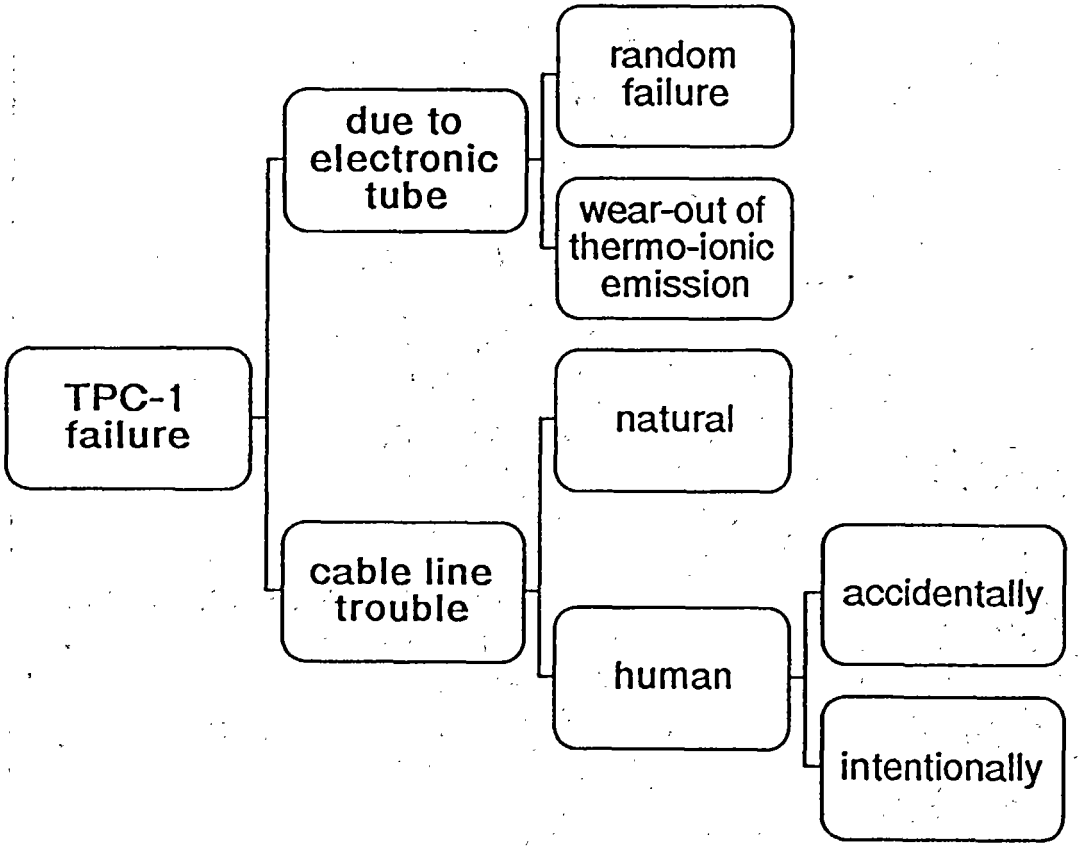

Figure 12
Causes of cable failures.

System	Section	Construction	Stopped	Service Life	Comments
SB	Washington-Alaska	1956	1977	22	Frequent Cable Failures
	TAT-1	1956	1976	20	TAT-7 started
	Hawaii-1	1957		31<	In operation
	TAT-2	1959	1982	23	TAT-7 started
	Florida-Puerto Rico	1960		28<	In operation
SD	Florida-Jamaica-Canal Zone	1963	1988	25<	In operation
	TAT-3	1963		25?	TAT-8 started
	TPC-1	1964		24<	In operation
	Guam-Phillipine	1964		24<	In operation
	Hawaii-2	1964		24<	In operation
	Florida-ST. Thomas	1964		24<	In operation
	Oahu-Tie-Cable	1964	1987	23	
	TAT-4	1965	1986	21	Frequent cable failure due to trolling
	ST. Thomas-Dominica	1965		23<	In operation

Table 1
Operational summary of submarine telecommunication cables. In this table, new optical fiber cables are not shown.

transmission capability for many years in extended service period. The cable itself is very stable on the deep sea floor and will keep its high quality for a long period. There are many actual examples of extended service periods. For example, HAW-1 (SB system) has been in operation for over 31 years, and the Florida-Jamaica-Canal zone has been in operation for over 25 years.

4. Conclusions

The motivation for terminating TPC-1 services will be classified into three categories: 1) increase of failure rate, 2) outdated technology and 3) termination of planned service period. The termination of the present Japan-Hawaii cable, TP:C-1, falls into categories (2) and (3), not (1). The factor (2) means that the existing cable with a small number of channels will be replaced by a new optical cable using advanced technology and having a large number of channels. The timing of TPC-1 retirement will be in September 1990. By reusing TPC-1 after its retirement, we can realize a part of GDSN system in Bonin an Mariana region.

Two seismic units and one geophysical unit will be connected to the current TPC-1. The seismic unit will have conventional seismometers, a hydrophone and broadband seismometers with wide dynamic ranges, and the geophysical unit will have several sensors, such as a pressure gauge, an electro-potentiometer, magnetometers, bottom current meters, and others. It is necessary to have a power feed station, a transmission station, a terminal station, and a data center for this system.

After examining the remaining life of TPC-1, the author is confident that TPC-1 will maintain the current high reliability for more than several years after its retirement from the commercial telecommunication services.

In conclusion, we will be able to realize a part of global geoscience system in the ocean region by reuse of TPC-1 and it seems as the most inexpensive way to meet these objectives.

References

Katao, H., J. Kasahara and S. Koresawa, "Experiment of Broadband Seismic Observation Using Small Size Servo-Accelerometer." Abstract of Fall annual meeting, Seism. Soc. Japan, p.244, 1989.

Sutton, G.H., N. Barstow and J.A. Carter, "Particle Motion Pressure Relationships of Ocean Bottom Noise at 3900m Depth: 0.001 to 10 Hz." Seism. Soc. Am.," 59, p.48, 1988.

Webb, S.C., "Long Period Acoustic and Seismic Measurements and Ocean Floor Currents," J. Ocean Engineering, submitted, 1988.

TSUNAMIS OF THE 21st CENTURY

George Pararas-Carayannis
International Tsunami Information Center

Tsunamis are disasters that repeat themselves with frequency. Repetition of such tsunami events means that they occur in cycles - short, medium, long and super-long. Each tsunamigenic region of the world appears to have its own cycle and pattern in producing tsunamis that range in size from small to the large and highly destructive events.

For some places in the world, tsunamis follow cycles of occurrence which are fairly regular. However in other geographical regions, the tsunami disaster cycles appear to be irregular or intermittent, displaying varying periodicity. Only short-term tsunami prediction is presently of any usefulness and can be made on the basis of seismic parametersafter an earthquake has occurred. Such short-term prediction of a few hours of the arrival of a tsunami can be given for areas that are 1-1 1/2 hours travel time away.

The ability to forecast or predict tsunamis with any degree of accuracy is limited. Long-term tsunami prediction is based primarily on statistical methods of earthquake prediction at identified seismic gaps. Medium-term prediction is also based on statistical recurrence and is of limited value. However, destructive tsunamis do not always happen in forecasted seismic-gap regions. Often such was the case with the 1975 tsunami in the Philippines, the 1979 tsunami in Colombia, and the 1983 tsunami in the Sea of Japan. All these events occurred in unexpected areas. No tsunami warnings were issued for these events that could have been of any value to the threatened population. Thus many lives were lost.

Presently, it is not possible to predict when these big earthquakes will strike again and whether they will produce large or small tsunamis. In some instances, it may not even be possible to issue an operational warning.

Where will the big tsunamis of the 21st Century occur and what causes their varying periodicity? Although most of the large tsunamigenic earthquakes occur in geological cycles which may be considered regular or rhythmical, conditions that are exogenous or random cause time variations in their recurrence, so this is the problem in prediction. Because of the scarcity of the historical data for large tsunamigenic earthquakes, only

statistical methods of extremes can be used to obtain statistical recurrence values. Similarly, because the epicenters of most of the large tsunamigenic earthquakes are in the ocean, it is difficult to measure other geophysical and geochemical precursory phenomena that would give clues as to event recurrence. But based on currently available information, each known tsunamigenic region of the world could be assigned its own recurrence frequency or recurrence cycle. Even though each destructive tsunami has its own unique pattern and own time and impact variables, certain general principles seem to apply to most of them, which may be described by what I call the "law of tsunami disaster cycles." Let me explain.

In my talk yesterday I questioned the validity of such a statistical approach as the seismic gap theory, and today I am going to explain why it may not be valid for tsunami prediction. In my opinion, the 30-year time interval which is the criterion for establishing a seismic gap may be too short of an interval for our predictions of tsunamis, particularly for certain geographical regions of the globe. I propose a new theory for our use which we may call the "tsunami gap theory." The criteria for the development of the tsunami gap designations will not be uniform but will differ from region to region. According to this approach, the time path of variables of each future tsunami could be established, or at least estimated statistically for each potential tsunamigenic area by using historical and geophysical data, and the same historical and geophysical criteria could be projected to form predictive schemes relating to other seismic tsunami parameters.

This type of historical and statistical analysis, if properly executed, can establish tsunami gap regions and can lead to better forecasts of future destructive events. The centerpiece of this proposed approach is what I call "historical tsunami determinism." The basic premise of the proposed process is that tsunamis follow certain patterns, although these are not uniform for all regions. What I refer to is not a qualitative historical information, but a more accurate quantitative measurement and catalogue of all the meaningful tsunami disaster parameters, including seismic and geophysical precursory phenomena. This may be somewhat difficult to do and we may have to establish a new methodology for doing it. Also it will require the development of an extensive tsunami data base which should include, not only historical information, but other extensive data and catalogues as for example - data on focal mechanisms, power spectra, seismic moments of previous events on specific broadband seismic signatures. Developing such historical and geophysical data bases would require a great deal of effort. However, we could standardize the development of such data bases, and we could agree conceptually on the methodology and the development of such historical tsunami determinism, and we could integrate this knowledge into real-time operational

assessment of the tsunami risk for warning purposes.

There should not have been surprise by the occurrence of the 1975 Philippine tsunami or the 1979 Colombian tsunami, or the 1983 Sea of Japan tsunami. There is historical and geologic precedents for all these events, and their occurrence should have been expected. Similarly, source and impact regions of future tsunamis could be forecasted for the remainder of this century and for the 21st Century, by utilizing these proposed extensive historical and geophysical databases.

Forecasting of future tsunamis on the medium or longer term may be possible. Just as with earthquakes, prolonged periods of quiescence of a region that has been historically tsunamigenic (using the tsunami gap hypothesis and criteria) may be signaling the eventual occurrence of another destructive tsunami. Many such areas exist presently in the Pacific and elsewhere, and the location of these regions can be identified. If we develop the proper criteria of historic tsunami determinism, we can also assign a time frame for tsunami recurrence. This can be done not only for areas of established seismic gaps but for areas where seismic gaps have not been identified, or for which a different recurrence time frequency applies.

The data exists, but its proper analysis has not been undertaken. A total of 482 tsunamis have been reported in the 20th Century alone, with at least 133 having a runup greater than 1.5 meters. We know that Japan, the West Coast of South America, Alaska, the Aleutian Islands, Kamchatka, and the Kuril Islands are potential tsunami generating areas. We know that these are the boundaries of major tectonic plates. But what about all the other subplates of the inland seas that have produced also the big destructive tsunamis and for which we have not established seismic gaps?

Where in the Pacific Ocean can we expect the big tsunamis in the 21st Century other than the areas mentioned? Let us be more specific. There are many tsunamigenic regions that have shown high density of seismic energy release and where large future tsunamis can be expected. For example, one such area is a segment of the Peruvian coastal region between 8.5^{0} S and 14^{0} S. This is a region of extremely high seismic energy release and site of large but infrequent historical tsunamis. Other parts of the South American seismic belt are tsunami gap regions and these regions in the 17th, 18th and 19th Centuries produced several destructive tsunamis, destroying such towns in Chile as Arica, Antofagasta and Valparaíso. There is also a great potential for another destructive tsunami on the Pacific side of Colombia, in the vicinity of the State of Narino. The west coast of Mexico can be expected to experience larger tsunamis. Large destructive tsunamis can be expected again in the Moro Gulf in the Philippines, in the

Celebes and Sulu Sea, in the Java Sea and elsewhere in the South West Pacific.

A lot can be said about the potential of such future tsunamis, but to make reasonable predictions about the time and place of future events, the criteria of the proposed historical determinism must be utilized. These criteria have not been as yet developed and I propose that we develop them. As a starting point, we need to develop a uniform and standardized program of tsunami, seismic and geologic data collection. A wealth of such data already exists but this data is not properly organized, is not uniformly collected, and of course it is not readily available. Therefore, standards must be established for the collection of such data and a tsunami data base must be organized on a regional basis initially, and shared on a global scale at a later time. Finally, the methodology of historical tsunami determinism as I described earlier for real-time operational use must be established.

8. LIST OF PARTICIPANTS

CANADA

Dr. M. El-Sabh
Department d'Oceanographie
Universite de Quebec a Rimouski
300, allee des Ursulines Rimouski
Quebec G5L 3A1

Dr. T. Murty
Institute of Ocean Sciences
Deptartment of Fisheries and Oceans
P.O. Box 6000
Sidney, B.C. V8L 4B2

Mr. W. Rapatz
Institute of Ocean Sciences
Department of Fisheries and Oceans
P.O. Box 6000
Sidney, B.C. V8L 4B2

CHILE

Lt. Cdr. H. Gorziglia
Instituto Hidrografico de la Armada
Errazuriz 232, Playa Ancha
Valparaiso

Dr. E. Lorca
Instituto Hidrografico de la Armada de Chile
Casilla 324
Valparaiso

CHINA

Prof. C. Bao
National Research Center for
Marine Environmental Forecasts
No. 8 Dahusi, Haidan Division
Beijing, 100081

Mr. Y. Hauting
State Oceanic Administration
1 Fuxingmenwai Ave.
Beijing, 100880

DEMOCRATIC PEOPLE'S REPUBLIC OF KOREA

Mr. Jae Song Ryom
National Oceanographic Commission
State Hidrometeorological Service
P. O. Box 100
Pyongyang

FIJI

Mr. G. Prasad
National Agency for
Development Mineral Resources
Suva

FRANCE (POLYNESIE FRANCAISE)

Dr. J. Talandier
Laboratoire de Geophysique
B.P. 840
Papeete, Tahiti

Dr. Dr. Raymond
Laboratoire de Geophysique
B.P. 840
Papeete, Tahiti

Dr. O. Hyvernaud
Laboratoire de Geophysique
B.P. 840
Papeete, Tahiti

GREECE

Dr. Th. Carambas
University of Thessaloniki
Dept. Civil Engineering
GR-54006, Thessaloniki

Dr. P. Dimitriou
University of Thessaloniki
Geophysical Laboratory
P.O. Box 352-1
GR-54006 Thessaloniki

ITALY

Dr. S. Tinti
Dipartimento di Fisica
Setorre di Geofisica
University of Bolonga
Viale Berti Pichat 8
40127 Bologna

JAPAN

Dr. K. Abe
General Education Department Nippon Dental Univ.
Niigata Branch
Hamaura-cho 1-8
Niigata City, 951

Mr. K. Fujima
Dept. Civil Engineering
National Defence Academy
1-10-20 Hashirimizu
Yokosuka, Kanagawa 239

Dr. R. Geller
Geophysical Institute
University of Tokyo,
Faculty of Science
Yayoi 2-11-16
Bunkyo-ku, Tokyo 113

Mr. F. Imamura
Dept. of Civil Engineering
Faculty of Engineering
Tohoku University, Aoba
Sendai, 980

Mr. S. Iwasaki
Hisatsuka Branch of Oceanographic Studies
National Research Center for Disaster Prevention
9-2 Nijigahama, Hiratsuka
Kanagawa, 254

Dr. K. Kajiura
Shin-Nipon Metocean Consulting Co.,Ltd
4-13-9 Akazutsumi
Setagava-ku
Tokyo 113

Mr. M. Katsumata
Seismology and Volcanology Division
Meteorological Research Institute
1-1 Nagamine, Tsukuba-shi
Ibaraki-ken, 305

Dr. H. Matsutomi
Akita University,
Department of Civil Engineering
Faculty of Mining
1-1 Tegata Gakuen-cho
Akita-Shi, 010

Dr. K. Minoura
Institute of Geology and Paleontology
Faculty of Sciences
Tohoku University
Sendai, 980

Dr. H. Murakami
Dept. Civil Engineering
Technical College
University of Tokushima
Minami-josamjima
Tokushima, 770

Dr. Sh. Nakamura
Shirahama Oceanographic Observatory
DPRI, Kyoto University
Katada-Hatasaki,
Shirahama, Wakayama 649-22

Dr. M. Okada
Seismological and Volcanological Division
Meteorological Research Institute
1-1 Nagamine, Tsukuba-shi
Ibaraki-ken 305

Dr. N. Shuto
Dept. of Civil Engineering
Faculty of Engineering
Tohoku University
Aoba, Sendai, 980

Dr. Y. Tsuji
Earthquake Research Institute
University of Tokyo
Yayoi 1-1-1, Bunkyo-ku
Tokyo 113

Mr. H. Watanabe
Tohoku Head Office
Japan Weather Association
2-1-2, Ichibancho
(Chogin Bld.)
Sendai, 980

MEXICO

Prof. A. Sanchez
Direc. Gnl. de Oceanografia Naval
Secretaria de Marina
C. Vincente Guerrero No.133-
Altos, Fracc. Bahia,
C.P.22880
Ensenada, B.C.

NEW ZEALAND

Mr. G. Elder
Civil Defence Commissioner
Ministry of Civil Defence
P.O. Box 5143,
Auckland

REPUBLIC OF KOREA

Prof. Hui Soo An
Dept. Earth Science
College of Education
Seoul National University
San 56-1, Shinlim-dong,
Kwanak-ku
Seoul, 151

Prof. Byung Ho Choi
Sung Kyun Kwan University
Suwon Campus
Chonchon-Dong, Suwon-city

Mr. Jong Yul Chung
Director
Research Institute of
Oceanography
Seoul National University
Seoul 151-740

Mr. Kim Sang-Jo
Central Meteorological Office
1 Songwol-Dong, Changno-Gu
Seoul 110

UNITED STATES OF AMERICA

Dr. E. Bernard
NOAA/PMEL
7800 Sand Point Way, NE,
Seattle, WA 98115-0070

Mr. G. Burton
Pacific Tsunami Warning Center
91-270 Ft. Weaver Road
Ewa Beach, HI 96706

Dr. S. Farreras
CICESE Oceanology Division
P. O. Box 4844
San Ysidro, CA 92073

Dr. F. Gonzalez
NOAA
Pacific Marine Environmental
Laboratory
7800 Sand Point Way, NE,
Seattle, WA 98115-0070

Mr. R. Hagemeyer (Chairman ICG/ITSU)
Director, Pacific Region
NWS - NOAA
P.O. Box 50027
Honolulu, HI 96850

Dr. G. Hebenstreit
SAIC
1710 Goodridge Dr.
P.O. Box 1303
McLean, VA 22102

Mr. J. Lander
University of Colorado
NOAA, E/GC-1
325 S. Broadway
Boulder CO 8032

Dr. G. Pararas-Carayannis (Chairman)
Director, ITIC
P.O. Box 50027
Honolulu, HI 96850-4993

Dr. K. Satake
Seismological Lab. 252-21
California Institute of Technology
Pasadena, CA 91125

Mr. Th. Sokolowski (Rapporteur)
Alaska Tsunami Warning Center
910 South Felton St.
Palmer, AK 99845

Mr. D. Sigrist
NOAA
National Weather Service HQ
Silver Spring, Maryland 20910

Prof. C. Synolakis
Univ. of Southern California
Dept. of Civil Engineering 0242
Los Angeles, CA 90089

UNION OF SOVIET SOCIALIST REPUBLICS

Prof. A. Alekseev
Computing Center
pr. Lavrentieva, 6
830090 Novosibirsk

Dr. Yu. Aleshkov
ul. Morskoy Pekhoty 8-II-149
198302 Leeningrad

Dr. V. Belokon
Far East University
ul. Sukhanova, 8
690600 Vladivostok

Dr. V. Berdin
USSR State Committee for Hydrometeorology
per P. Morozova, 12
1233376 Moscow

Dr. L. Chepkunas
Institute of Earth's Sciences
pr. Lenina, 88
249020 Obninsk

Dr. L. Chubarov
Computing Center
Akademagorodok
660036 Krasnoyarsk

Dr. V. Davletshin
Institute of Hydrotechtonics
322690 Dneprodzerzhinsk

Dr. S. Dotsenko
Marine Geological Institute
ul. Lenina, 38
335005 Sevastopol

Dr. Yu. Egorov
Shipbuilding Institute
ul. Lotsmanskaya, 3
190008 Leningrad

Dr. A. Fatyanov
Computing Center
pr. Lavrentieva, 6
633090 Novosibirsk

Dr. M. Garber
Far East Research
Hydrometeorological Institute
ul.Dzerzhinskogo, 24
690600 Vladivostok

Dr. Ch. Go
Institute of Marine Geology and Geophysics
ul. Nauki, 5
693002 Yuzhno-Sakhalinsk

Dr. V. Gusiakov
Computing Center
pr. Lavrentieva, 6
630090 Novosibirsk

Dr. V. Ivanov
Institute of Marine Geology and Geophysics
ul. Nauki, 5
693002 Yuzhno-Sakhalinsk

Dr. V. Ivanov
VNII Geoinformsystem
Varshavskoye Shosse, 8
117105 Moscow

Dr. A. Ivaschenko
Institute of Marine Geology and Geophysics
ul. Nauki, 5
693002 Yuzhno-Sakhalinsk

Dr. V. Kaistrenko
Institute of Marine Geology and Geophysics
ul. Nauki, 5
693002 Yuzhno-Sakhalinsk

Dr. K. Klevanny
State Hydrological Institute
2 Liniya, 23
199053 Leningrad

Dr. E. Kulikov
State Oceanographic Institute
Kropotkinsky per., 6
119034 Moscow

Dr. B. Kusnetzov
Sakhalin Tsunami Center
ul. Zapadnaya, 78
693000 Vuzhno-Sakhalinsk

Dr. I. Kuzminykh
USSR State Committee for Hydrometeorology
per. Pavlika Morozova, 12
123376 Moscow

Dr. B. Levin
Institute of Mining
Moskovskaya oblast
140004 Lyubertsi-4

Dr. An. Marchuk
Computing Center
pr. Lavrentieva, 6
630090 Novosibirsk

Dr. R. Mazova
Politechnical Institute
ul. Minina, 24
603600 Gorky

Dr. A. Metalnikov
USSR State Committee for Hydrometeorology
per. Pavlika Morozova, 12
123376 Moscow

Dr. V. Mitrophanov
Inst. of Marine Geology and Geophysics
ul. Nauki, 5
693002 Yuzhno-Sakhalinsk

Dr. V. Novikov
Computing Center
Akademgorodok
660036 Krasnoyarsk

Dr. A. Poplavsky
Inst. of Marine Geology and Geophysics
ul. Nauki, 5
693002 Yuzhno-Sakhalinsk

Dr. N. Plink
Leningrad Hydrometeorological Institute
Malookhotinsky pr., 98
195196 Leningrad

Dr. A. Rabinovich
Inst. of Marine Geology and Geophysics
ul. Nauki, 5
693002 Yuzhno-Sakhalinsk

Dr. G. Rybin
USSR State Committee for Hydrometeorology
per. Pavlika Morozova, 12
123376 Moscow

Prof. I. Salezov
Institute of Geology,
ul. Zhelyabova, 8/4
252057 Kiev

Prof. Yu. Shokin
Computing Center
Akademgorodok
660036 Krasnoyarsk

Mr. K. Simonov
Computing Center
Akademgorodok
660036 Krasnoyarsk

Dr. O. Soboleva
Computing Center
pr. Lavrentieva, 6
630090 Novosibirsk

Dr. A. Sudakov
Computing Center
Akademgorodok
660036 Krasnoyarsk

Dr. S. Sukhinin
Institute of Hydrodinamics
pr. Lavrentieva, 13
630090 Novosibirsk

Dr. I. Tikhonov
Inst. of Marine Geology and Geophysics
ul. Nauki, 5
693002 Yuzhno-Sakhalinsk

Mr. V. Titov
Computing Center
pr. Lavrentieva, 6
630090 Novosibirsk

Dr. V. Yakovlev
Institute of Hydromechanics
ul. Zhelyabova, 8/4
252057 Kiev

Dr. A. Zakharova
Institute of Earth's Sciences
pr. Lenina, 88
249020 Obninsk

Dr. Yu. Zayakin
Tsunami Station
ul. Sovetskaya, 21
683000 Petropavlovsk
Kamchatsky

Dr. M. Zhaleznyak
Institute of Cybernetics
pr. Glushkova, 22
252207 Kiev

Dr. T. Zheleznyak
Institute of Earth's Science
pr. Lenina, 88
249020 Obninsk

II. SECRETARIAT

Dr. A. Tolkachev
Senior Assistant Secretary IOC
Intergovernmental
Oceanographic Commission
Unesco
7, Place de Fontenoy
75700, Paris
France

tel: (1) 45 68 39 78
tlx: 204 461 Paris
fax: (33 1) 40 56 93 16
tlm: IOC.SECRETARIAT
tlg: Unesco, Paris

Dr. K. Kitazawa
Assistant Secretary IOC
(same address as above)
tel: (1) 45 68 39 89
(same fax, tlx, tlm, tlg
as above)

CONT'D ON INSIDE OF BACK COVER

No.	Title	Languages
64	Second IOC-FAO Workshop on Recruitment of Penaeid Prawns in the Indo-West Pacific Region (PREP), Phuket, Thailand, 25-31 September 1989	E
65	Second IOC Workshop on Sardine/Anchovy Recruitment Project (SARP) in the Southwest Atlantic, Montevideo, Uruguay, 21-23 August 1989	E
66	IOC *ad hoc* Expert Consultation on Sardine/Anchovy Recruitment Programme, La Jolla, California, USA, 1989	E
67	Interdisciplinary Seminar on Research Problems in the IOCARIBE Region, Caracas, Venezuela, 28 November - 1 December 1989	E
68	International Workshop on Marine Acoustics. Beijing, China, 26-30 March 1990	E
69	IOC Workshop on Sea-Level Measurements in the Antarctica, Leningrad, USSR, 28-31 May 1990	E